

THESIS FOR THE DEGREE OF DOCTOR OF PHILOSOPHY

Engineering Cytosolic Acetyl-CoA Metabolism in *Saccharomyces cerevisiae*

Combining metabolic engineering and adaptive laboratory evolution

YIMING ZHANG



Department of Biology and Biological Engineering  
CHALMERS UNIVERSITY OF TECHNOLOGY  
Gothenburg, Sweden 2015

Engineering Cytosolic Acetyl-CoA Metabolism in *Saccharomyces cerevisiae*

Combining metabolic engineering and adaptive laboratory evolution

YIMING ZHANG

@YIMING ZHANG, 2015

ISBN: 978-91-7597-147-6

*Doktorsavhandlingar vid Chalmers tekniska högskola*

Ny serie nr: 3828

ISSN: ISSN 0346-718X

Systems and Synthetic Biology Group  
Department of Biology and Biological Engineering  
Chalmers University of Technology  
SE-412 96 Göteborg  
Sweden  
Telephone +46 (0) 31-772 1000

Cover illustration:

A simple illustration for possible roles of the mutated proteins in the evolved Pdc negative strains.  
For more details, refer to Figure 14B.

Printed by Chalmers Reproservice

Göteborg, Sweden 2015

# PREFACE

This dissertation serves as a partial fulfilment of the requirement to obtain the degree of doctor of philosophy at Department of Biology and Biological Engineering, Chalmers University of Technology, Sweden. The research was carried out in Systems and Synthetic Biology group under the supervision of Professor Jens Nielsen. This study combines metabolic engineering and adaptive laboratory evolution to establish a non-ethanol producing yeast strain as a cell factory. The research was funded by the doctoral scholarship program of China Scholarship Council (China), the Chalmers Foundation, Vetenskapsrådet, FORMAS and European Research Council (Grant no. 247013).

Yiming Zhang

January 2015

# Abstract

A *Saccharomyces cerevisiae* strain carrying deletions in all three pyruvate decarboxylase genes (also called Pdc negative yeast) represents a non-ethanol producing platform strain for biochemical production. However, it cannot grow on glucose as the sole carbon source due to the lack of cytosolic acetyl-CoA for lipid biosynthesis. Its growth inability on glucose could be restored through directed evolution, which was explained by an in-frame internal deletion in *MTH1* (*MTH1*- $\Delta T$ ). The *MTH1*- $\Delta T$  allele resulted in reduced glucose uptake, which may attenuate the repression of respiratory metabolism. However, it was not clear what mechanism could provide the cells with sufficient precursors for cytosolic acetyl-CoA. Here we investigated this using a Pdc negative strain with *MTH1*- $\Delta T$ , IMI076. Our results identified a route relying on Ach1 that could transfer acetyl units from mitochondria to the cytoplasm. Based on the results a new model was proposed, in which acetyl units are shuttled from the mitochondria to the cytoplasm in the form of acetate. In addition, a collection of Pdc negative strains was constructed and one of them was adaptively evolved on glucose via serial transfer. Three independently evolved strains were obtained, which can grow on glucose as the sole carbon source at maximum specific rates of  $0.138 \text{ h}^{-1}$ ,  $0.148 \text{ h}^{-1}$ ,  $0.141 \text{ h}^{-1}$ , respectively. Several genetic changes were identified in the evolved Pdc negative strains by genome sequencing. Among these genetic changes, 4 genes were found to carry point mutations in at least two of the evolved strains: *MTH1*, *HXT2*, *CIT1*, and *RPD3*. Reverse engineering of the non-evolved Pdc negative strain through introduction of the *MTH1*<sup>81D</sup> allele restored its growth on glucose at a maximum specific rate of  $0.05 \text{ h}^{-1}$  in minimal medium with 2% glucose. The non-synonymous mutations in *HXT2* and *CIT1* may function in the presence of mutated *MTH1* alleles and could be related to an altered central carbon metabolism in order to ensure production of cytosolic acetyl-CoA in the Pdc negative strain.

In connection with biobased chemical production, it is necessary to engineer the metabolism of cell factories such that the raw material, typically sugars, can be efficiently converted to the product of interest. Although IMI076 could grow on glucose, it was still inefficient at conversion of pyruvate to cytosolic acetyl-CoA. To increase cytosolic acetyl-CoA supply from pyruvate, pyruvate formate lyase and its activating enzyme from *Escherichia coli* were expressed with two different cofactors, ferredoxin or flavodoxin, and their reductase, respectively, and it was found that the co-expression of either of these cofactors had a positive effect on growth under aerobic conditions, indicating increased activity of PFL. The positive effect on growth was manifested as a higher final biomass concentration and a significant increase in transcription of formate dehydrogenase genes (*FDHs*). Among the two cofactors reduced flavodoxin was found to be a better electron donor than reduced ferredoxin.

**Key words:** yeast, acetyl-CoA, central carbon metabolism, mitochondria, pyruvate decarboxylase, genomic DNA sequencing, reverse engineering, adaptive evolution, hexose transporter, citrate synthase, histone deacetylase; ferredoxin, flavodoxin, ferredoxin/flavodoxin NADP<sup>+</sup> reductase, aerobic growth, metabolic engineering.

# LIST OF PUBLICATIONS

The thesis is based on the following publications, referred to as Paper I to IV in the text:

- I. **Ach1 is involved in shuttling mitochondrial acetyl units for cytosolic C2 provision in Pdc negative *Saccharomyces cerevisiae***  
Yun Chen\*, Yiming Zhang\*, Verena Siewers, Jens Nielsen.  
Submitted for publication.
- II. **Adaptive mutations in sugar metabolism restore growth on glucose in a pyruvate decarboxylase negative yeast strain**  
Yiming Zhang, Martin KM Engqvist, Anastasia Krivoruchko, Björn M Hallström, Yun Chen, Verena Siewers, Jens Nielsen.  
Submitted for publication.
- III. **Functional pyruvate formate lyase pathway expressed with its cofactors in *Saccharomyces cerevisiae* at aerobic growth**  
Yiming Zhang, Anastasia Krivoruchko, Yun Chen , Verena Siewers, Jens Nielsen.  
Submitted for publication.
- IV. **Microbial acetyl-CoA metabolism and metabolic engineering (Review)**  
Anastasia Krivoruchko, Yiming Zhang, Verena Siewers, Yun Chen, Jens Nielsen.  
*Metabolic Engineering*, March 2015; 28: 28–42.

\* Equal contribution

Additional publications during doctoral research not included in this thesis:

- V. **Improving heterologous protein secretion in aerobic conditions by activating hypoxia induced genes in *Saccharomyces cerevisiae***  
Lifang Liu, Yiming Zhang, Zihe Liu, Verena Siewers, Dina Petranovic, Jens Nielsen.  
Submitted for publication.

# **CONTRIBUTION TO MANUSCRIPTS**

A summary of my contribution to each of the publications listed is provided below:

- I. Designed research; performed the research; analyzed the data; assisted in the manuscript preparation.
- II. Designed research; performed the research; analyzed the data; wrote the manuscript.
- III. Designed research; performed the research; analyzed the data; wrote the manuscript.
- IV. Assisted in the manuscript preparation.
- V. Designed and performed part of the research; analyzed the data; assisted in the manuscript preparation.

# LIST OF FIGURES AND TABLES

<b>Figure 1. Overview of acetyl-CoA metabolism in yeast (Adapted from [6]).</b> .....	3
<b>Figure 2. Addition of succinate improves the growth of the strain IMI076</b> .....	19
<b>Figure 3. The growth of the strain IMI076 (<i>Pdc<sup>-</sup> MTH1-ΔT</i>) relies on Ach1.</b> .....	20
<b>Figure 4. Complementation with the intact <i>ACH1</i> but not the truncated version restores growth of an <i>ach1</i> mutant.</b> .....	21
<b>Figure 5. Growth assays of IMI076 (A) and CEN.PK 113-5D (B) upon addition of UK-5099</b> .....	22
<b>Figure 6. A model of Ach1 transferring acetyl units from the mitochondria to the cytosol</b> .....	23
<b>Figure 7. Bipartite strategy for gene deletion.</b> .....	24
<b>Figure 8. Work flow of Pdc negative strain construction.</b> .....	25
<b>Figure 9. Adaptive evolution process of the Pdc negative strain E1</b> .....	25
<b>Figure 10. Reverse engineering strategy for <i>MTH1<sup>8ID</sup></i> integration into <i>MTH1</i> locus of the E1 strain</b> .....	28
<b>Figure 11. Growth profiles of reverse engineered strains M81-11 and M81-33 (two transformants, <i>ura3-52 his3-Δ1 pdc1Δ pdc5Δ pdc6Δ mth1::MTH1<sup>8ID</sup></i>) in minimal medium with 2% glucose. All measurements are mean +/- standard error of three biological replicates.....</b>	29
<b>Figure 12. Transcription analysis of HXTs (<i>HXT1-7</i>) in two M81 strains and wild type strain CEN.PK 113-11C.....</b>	30
<b>Figure 13. Mapping and analysis of mutations in Mth1 (A), Hxt2 (B), Cit1 (C) and Rpd3 (D)</b> .....	31
<b>Figure 14. A cartoon representation of homology protein models generated for Hxt2 (A), Cit1 (B) and Rpd3 (C)</b> .....	32
<b>Figure 15. Predictions on the secondary structure of Mth1 protein</b> .....	33
<b>Figure 16. A simple illustration for the possible roles of the mutated proteins in the evolved pdc negative strains</b> .....	36
<b>Figure 17. Growth comparisons of the strains with and without the PFL pathway</b> .....	38
<b>Figure 18. Growth comparisons of YZ10, YZ11, YZ12 and YZ13 in minimal medium using shake flasks</b> .....	39
<b>Figure 19 Expression analysis of introduced genes in YZ12 (A) and YZ13 (B)</b> .....	40
<b>Figure 20. Expression analysis of <i>FDH1</i> and <i>FDH2</i> in YZ10-1, YZ11-1, YZ13-2 and YZ13-6.</b> .....	41
<b>Table 1. Point mutations in evolved Pdc negative strains.</b> .....	27
<b>Table 2. Strain properties of YZ10, YZ11, YZ12 and YZ13.</b> .....	39

# ABBREVIATIONS AND SYMBOLS

TCA: tricarboxylic acid

GYC: glyoxylate cycle

$\mu_{\max}$ : maximum specific growth rate

$Y_{Pyr}$ : pyruvate yield on glucose as the substrate

$Y_{Gly}$ : glycerol yield on glucose as the substrate

Chr: chromosome

## Yeast nomenclature

Gene name consist of three letters and up to three numbers in italic, e.g.*PDC1*, *acs1*;

Wild type gene name is written with upper letters in italic, e.g.*PDC1*, *ACSI*;

Recessive gene name is written with lower letters in italic, e.g.*pdc1*, *acs1*;

Mutant alleles are named with a dash and a number in italic, e.g.*ura3-52*;

Deleted gene with the genetic marker used for deletion, e.g.*pdc1Δ*, *pdc1::loxP*;

The protein product of the gene is written with an upper letter at the first letter and two lower letters in normal font, e.g.Pdc1, Acs1;

Exception case for gene name: *MATa*, *MATα*, *MTH1-ΔT*;

Genes with amino acid sequence change is written with gene name and changed amino acid with its position, e.g.*MTH1<sup>81D</sup>*.

# TABLE OF CONTENTS

PREFACE .....	iii
Abstract .....	iv
LIST OF PUBLICATIONS .....	v
CONTRIBUTION TO MANUSCRIPTS.....	vi
LIST OF FIGURES AND TABLES .....	vii
ABBREVIATIONS AND SYMBOLS .....	viii
TABLE OF CONTENTS .....	ix
Chapter 1 Introduction .....	1
1 Yeast <i>Saccharomyces cerevisiae</i> as a cell factory .....	1
1.1 Acetyl-CoA metabolism in yeast .....	3
1.1.1 Acetyl-CoA use in the TCA cycle and glyoxylate cycle .....	3
1.1.2 Acetyl-CoA use in the PDH bypass.....	6
1.1.3 Acetyl-CoA use in fatty acid and sterol metabolism .....	8
1.1.4 Acetyl-CoA transport between subcellular organelles .....	8
1.1.5 Acetyl-CoA in protein acetylation .....	9
1.2 Non-ethanol producing strain for biochemical production .....	10
1.2.1 Pyruvate decarboxylase .....	10
1.2.2 Pyruvate decarboxylase negative strain .....	11
1.3 Metabolic engineering and adaptive evolution in strain development.....	13
Chapter 2. Overview of the thesis .....	15
Chapter 3. Results and discussion .....	18
3.1 ACH1 compensates cytosolic acetyl-CoA in Pdc negative strain.....	18
3.2 Growth recovery through adaptive evolution and reverse metabolic engineering.....	24
3.3 Functional bacterial pyruvate formate lyase expressed in pdc negative strain .....	37
Chapter 4. Conclusions and perspective .....	42
Acknowledgments .....	44
References .....	45



# Chapter 1 Introduction

## 1 Yeast *Saccharomyces cerevisiae* as a cell factory

The yeast *Saccharomyces cerevisiae* (also called budding yeast, Brewer's yeast, or Baker's yeast, referred to as yeast in this thesis except when otherwise specified) has been used in food and beverage fermentation by human beings since ancient times. As an important model microorganism for eukaryotes, yeast has been intensively studied in molecular and cell biology, genetics and systems biology, much like *Escherichia coli* as the model for prokaryotes. Due to its robustness and tolerance towards industrial conditions, as well as its Generally Regarded As Safe (GRAS) feature, yeast has been exploited as an important cell factory for industrial production of chemical compounds [1]. With the development of metabolic engineering and synthetic biology [2], yeast is already used for production of various bio-compounds, ranging from large volume fermentation products, like bioethanol, big volume fermentation products like succinic acid, to small volume fermentation product of several pharmaceuticals, like human insulin [3, 4].

With the requirements for sustainable solutions to provide fuels, chemicals and pharmaceuticals, now there is increasing focus on cell factories, as they may serve as one of the pillars underlying a sustainable society [5]. As a very important cell factory already widely used for production of biofuels, chemicals and pharmaceuticals, there is much interest in developing platform strains of yeast that can be used for production of a whole range of different products.

Yeast can efficiently convert the raw material into precursor metabolites, and these precursor metabolites are then further converted into the products of interest. One of these precursor metabolites is **acetyl-CoA**, which used as precursor for the production of a wide range of valuable products, like 1-butanol, polyhydroxybutyrate, isoprenoids, polyketides, alkanes, alkenes, fatty alcohols and waxes etc.[6]. Most of these products are produced from synthetic pathways that are reconstructed and generally positioned in the cytosol as this will minimize secretion issues of the bio-products. In previous studies, it has been suggested that cytosolic acetyl-CoA availability is a limiting factor for bio-compound production probably due to the low activity and high-energy input requirements of the acetyl-CoA synthetase in yeast. Different successful strategies have been performed and evaluated to increase the production of several bio-compounds by enhancing cytosolic acetyl-CoA supply [7].

In yeast, acetyl-CoA metabolism (as described in Chapter 1.1) is highly compartmentalized and it cannot be transported across different subcellular organelles

readily. Cytosolic acetyl-CoA is generated via the pyruvate dehydrogenase (PDH) bypass, which involves three enzymes, pyruvate decarboxylase (PDC), acetaldehyde dehydrogenase (ALD) and acetyl-CoA synthetase (ACS). By over-expressing the native acetaldehyde dehydrogenase gene *ALD6* and a mutant acetyl-CoA synthetase gene *ACS<sub>SE</sub><sup>L64IP</sup>*, the production of amorphadiene increased by up to 4 fold [8]. A similar strategy was also used for  $\alpha$ -santalene production with co-overexpression of a gene encoding alcohol dehydrogenase (*ADH2*), which converts ethanol to acetaldehyde [9]. Combination with over-expression of pathways draining cytosolic acetyl-CoA towards the product resulted in additional production increases [8, 9]. Furthermore, when the pathways competing for cytosolic acetyl-CoA were blocked by deleting the peroxisomal citrate synthase gene *CIT2* or/and cytosolic malate synthase gene *MLS1*, even higher production of  $\alpha$ -santalene was achieved [9, 10]. These strategies have also been successfully applied in the production of 1-butanol [11], poly-(R)-3- hydroxybutyrate (PHB) [12], and biodiesel [13].

Besides the engineering strategies of the native pathways to increase cytosolic acetyl-CoA supply, several other strategies have been applied for different pathways for production of 1-butanol, biodiesel and PHB, such as the fungal phosphoketolase pathway [14, 15], bacterial pyruvate formate lyase pathway [16], ATP-citrate lyase pathway [17] and a bacterial PDH pathway [18].

## 1.1 Acetyl-CoA metabolism in yeast

Acetyl-CoA serves as a crucial intermediate metabolite in the metabolic network of *S. cerevisiae*, and its metabolism is highly compartmentalized as this metabolite is produced and used in the cytosol, mitochondria, peroxisomes and the nucleus (**Figure 1**). Acetyl-CoA is a key precursor metabolite for the synthesis of important cellular constituents such as fatty acids, sterols, and amino acids as well as the donor of acetyl unit for protein acetylation [19]. Besides these important functions it is also a precursor for many other biomolecules, such as polyketides, isoprenoids, 1-butanol and polyhydroxyalkanoids, which encompass many industrially relevant chemicals.

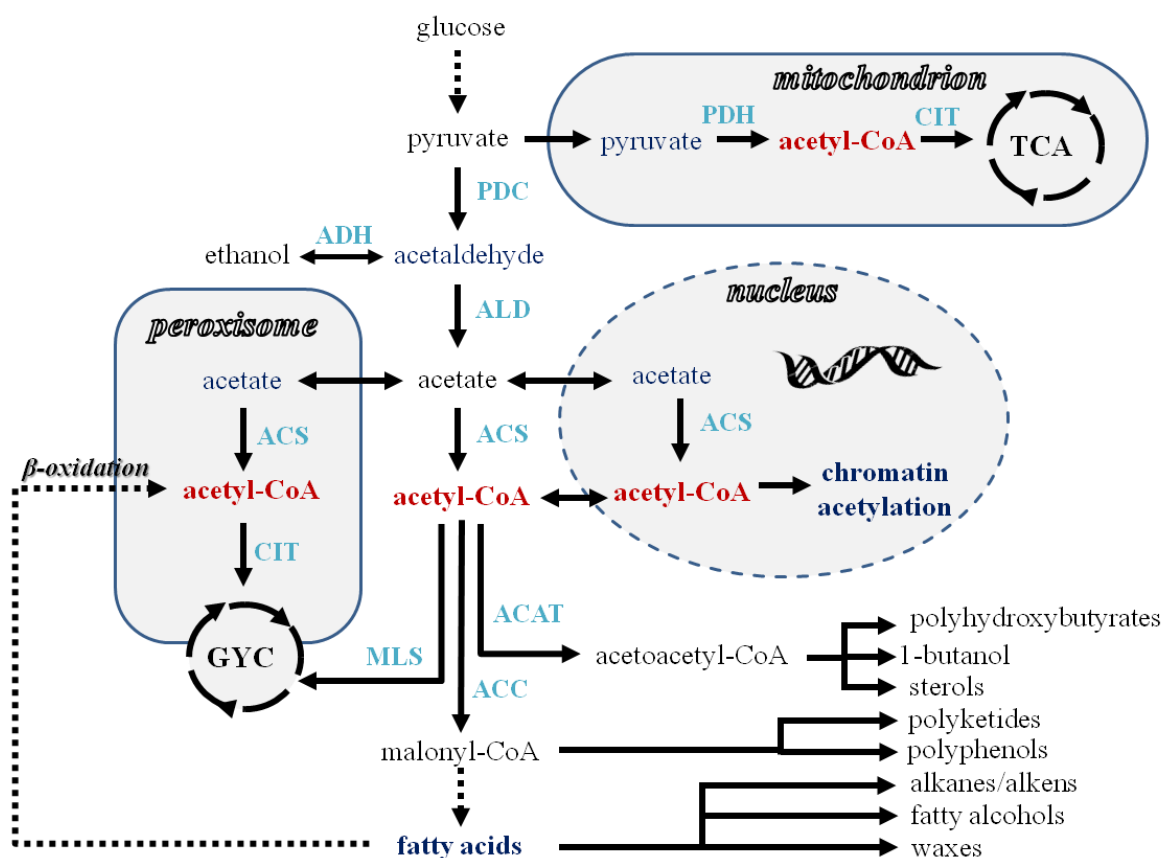


Figure 1. Overview of acetyl-CoA metabolism in yeast (Adapted from [6]).

### 1.1.1 Acetyl-CoA use in the TCA cycle and glyoxylate cycle

Acetyl-CoA is the key substrate for the TCA cycle, which plays a very important role in catabolism under glucose limited aerobic conditions. Acetyl-CoA used in the TCA cycle is generated by the pyruvate dehydrogenase complex (PDHC) from pyruvate, which is synthesized either in the cytosol via glycolysis from sugars, or from malate via malic enzyme located in the mitochondria. Acetyl-CoA is incorporated into the TCA cycle in a

step catalyzed by citrate synthase (CS), existing in two mitochondrial isoforms Cit1 [20] and Cit3 [21]. Citrate synthase (CS) condenses acetyl-CoA with oxaloacetate, yielding citrate, which is the first and generally considered to be the flux controlling reaction of the TCA cycle. Similarly to the TCA cycle, the glyoxylate cycle also begins with the condensation of acetyl-CoA and oxaloacetate, catalyzed by a peroxisomal CS isoform, Cit2. Another reaction involving acetyl-CoA in the glyoxylate cycle is catalyzed by malate synthase (MLS) encoded by *MLSI* [22], in which acetyl-CoA condenses with glyoxylate to form malate. The peroxisomal acetyl-CoA is formed directly from acetate by acetyl-CoA synthase.

PDHC is one of the largest and most complicated protein complexes known so far, and in yeast it consists of three main catalytic components termed and a fourth component. The three components are pyruvate dehydrogenase (encoded by *PDA1* and *PDB1*), dihydrolipoamide acetyltransferase (encoded by *LAT1*), dihydrolipoamide dehydrogenase (encoded by *LPD1*). The fourth component is called protein X (encoded by *PDX1*), and it is responsible to bind and position dihydrolipoamide dehydrogenase to dihydrolipoamide acetyltransferase [23-25]. In the irreversible reaction catalyzed by the PDH complex, pyruvate is converted to acetyl-CoA, CO<sub>2</sub> and NADH, with the participation of five cofactors (thiamin pyrophosphate, lipoic acid, flavin adenine dinucleotide, coenzyme A and NAD<sup>+</sup>). The PDH complex is regulated both at the transcriptional level, via the expression of its subunit gene *LPD1*, and post-transcriptional level, via the phosphorylation and dephosphorylation of its subunit Pda1 by a concerted activity of two kinases and two phosphatases [26-28].

CS has three isoforms in *S. cerevisiae*, encoded by *CIT1*, *CIT2*, *CIT3*. *CIT1* encodes the major functional isoform with an N-terminal mitochondrial targeting sequence[29-31]. *CIT2* encodes a peroxisomal isoform [32], with 81% identity with *CIT1* at the protein level and 74% identity at the DNA level. Its C-terminal signaling tripeptide SKL was found to be necessary and sufficient for directing Cit2 to the peroxisomes, which was called as the peroxisomal targeting sequence (PTS). However, the truncated Cit2 without the PTS resulted in a mislocalized form in the mitochondria, suggesting the presence of an additional signal sequence related with mitochondrial targeting [29], which was identified at its N-terminus in a later study [30]. *CIT3* encodes a minor functional isoform with an N-terminal mitochondrial targeting sequence as well [21], with 48% and 59% identity with *CIT1* at the protein level and DNA level, respectively, and with 47% and 61% identity with *CIT2*, respectively. Cit3 functions not only as a mitochondrial citrate synthase, but also as a methylcitrate synthase, which condenses propionyl-CoA and oxaloacetate to form 2-methylcitrate [33].

*CIT1* expression is regulated by carbon sources, and repressed by glucose and further repressed by glucose and glutamate [34]. Like other TCA enzymes and those of electron

transport chain, its derepression was found to be regulated by the heme activator protein (HAP) system [35]. In the *CIT1* upstream sequence, three regulatory elements have been identified, one responsible for glucose repression, one for derepression [36], and an R box element [37] first identified as a binding site for the retrograde (RTG) transcription complex Rtg1-Rtg3 [38]. With detailed analysis of *CIT1* expression on different carbon sources, it was found that *CIT1* expression is dependent on *HAP* genes in cells with robust mitochondrial function, whereas its expression is dependent on *RTG* genes in cells with compromised mitochondrial respiratory capacity. Thus it was proposed that these different patterns were due to the requirement of sufficient glutamate for cell growth with reduced respiratory capacity [37].

*CIT2* expression is also regulated by carbon sources, like *CIT1* expression [34]. In the *CIT2* upstream sequence, two R box elements were identified as the binding sites of the Rtg1-Rtg3 complex [38, 39], as mentioned above in the *CIT1* upstream sequence, which appears to be activated in a Rtg2-dependant fashion [40]. It was suggested that *CIT2* expression might be regulated by communication between the mitochondria and the nucleus, since its elevated transcription was observed in cells with dysfunctional mitochondria [41].

Disruption of *CIT1* results in several changes in the TCA cycle, such as its metabolite levels, decreases in enzyme levels and activities, reduced mitochondrial respiration of citrate and isocitrate, and inability to grow on acetate [42, 43]. The growth ability of a *cit1Δ* mutant on acetate could be restored by expressing the native Cit1, an inactive but a structurally unchanged Cit1 mutant [42], a mislocalized mitochondrial form of Cit2 [44], or additional Cit3 [21], but not by the cytosolic form of Cit1 [44]. One hypothesis for the growth inability on acetate was the dysfunction of the TCA cycle. It was also proposed that Cit1 with the normal conformation (even at an inactive state) is required for the formation of a TCA cycle enzyme complex in order to maintain  $\alpha$ -ketoglutarate dehydrogenase complex activity.

MLS has two functional isoforms identified in *S. cerevisiae*, encoded by *MLS1* [22] and *DAL7* (or *MLS2*) [45], and Mls1 turned out to be the one responsible for the reaction in the glyoxylate cycle. Both proteins have the tripeptide targeting sequence SKL at their C termini, therefore it was predicted that they were localized in the peroxisomes. However, Mls1 seems to have dual localizations in the cytosol and peroxisomes. The two different localizations of Mls1 were first noticed when yeast was grown on ethanol or oleic acid, respectively [46], and later different distributions between the cytosol and the peroxisomes were also observed in different yeast mutants [10], indicating the possible presence of some regulatory mechanisms for its subcellular distribution which are still unclear.

*MLS1* expression is also regulated by the carbon sources, the common response for genes involved in non-fermentative metabolism. In *MLS1* upstream sequence, two sites were identified as upstream activating sites (UASs), which could explain the transcriptional regulation of *MLS1* [47]. Both UASs turned out to be functional Carbon Source Responsive Elements (CSREs), which were found to be responsible for the transcriptional regulation of genes involved in acetyl-CoA generation and consumption (in the glyoxylate cycle and the subsequent gluconeogenesis), *ACSI* [48], *ICLI* [49], *MLS1* [47], *FBPI* [50] and *PCK1* [51].

### 1.1.2 Acetyl-CoA use in the PDH bypass

The PDH bypass is another important part in the metabolism of acetyl-CoA, especially cytosolic acetyl-CoA, consisting of pyruvate decarboxylase (PDC), acetaldehyde dehydrogenase (ALD) and acetyl-CoA synthetase (ACS). PDC converts pyruvate to acetaldehyde, and then acetaldehyde is converted to acetate by ALD, followed by the reaction catalyzed by ACS. The direct reaction for cytosolic acetyl-CoA biosynthesis is catalyzed by ACS. Two ACS isoforms were identified in yeast, encoded by *ACSI* and *ACS2*. These two isoforms differ from each other in a number of ways, *e.g.* enzymatic properties, subcellular localizations and immunological properties, and they were first recognized as ‘aerobic’ ACS and ‘anaerobic’ ACS, respectively [52-54].

The ‘aerobic’ and ‘anaerobic’ isoform were identified to be encoded by *ACSI* and *ACS2* [55], respectively. Although the tripeptide VKL at the C terminus of Acs1 suggested its possible location in the peroxisomes, the experimental data about its subcellular localization seems quite complex and unclear, either in the mitochondria [56], peroxisomes [10], cytoplasm or nucleus [57]. Acs1p could be dually distributed in the cytosol and the peroxisomes based on its known functions [10], *e.g.* C<sub>2</sub> carbon source (ethanol or acetate) assimilation related with the glyoxylate cycle, lipid biosynthesis. The Acs2 is 73.6% similar and 57.0% identical to Acs1. Acs2 was identified as the ‘anaerobic’ isoform, since ACS activity seemed to be derived exclusively from *ACS2* in anaerobic, glucose limited chemostat cultures [58]. However, it was not appropriate to call Acs2 as ‘anaerobic’ ACS, since *ACS2* is not only expressed under anaerobic conditions but also in aerobic conditions [58]. Acs2 is thought to be localized in the cytosol due to no obvious targeting sequences at its terminus, which was also supported by a recent study [19].

Earlier enzyme assays and northern hybridization results revealed that *ACSI* expression was regulated by carbon sources, *i.e.* repressed by glucose and induced by C<sub>2</sub> carbon [59, 60]. In the *ACSI* upstream sequence, several transcriptional regulatory elements were identified, *i.e.* a CSRE, a binding site for the transcriptional factor Adr1, two distinct upstream repression sites (URS) and three binding sites for the pleiotropic factor Abf1 [48, 60]. Under derepressed conditions, the CSRE and Adr1 binding site were responsible

for the *ACS1* activation, which contributed to 45% and 35%, respectively. The activating function of Adr1 on *ACS1* transcription was further confirmed by its over-expression under both repressed and derepressed conditions. The negative function of the two URS1 was not affected under repressed or derepressed conditions. However, when a URS1-binding transcriptional factor encoding gene *UME6* was disrupted, significant *ACS1* expression was observed under repressed and derepressed conditions, and at least one functional Abf1 binding site was required for activated expression of *ACS1* under repressed conditions, but not under derepressed conditions. Therefore, it was proposed that Abf1 activates *ACS1* expression under repressed conditions, and that there could be a functional balance between the pleiotropic factor Abf1 and the general repressor Ume6. However under derepressed conditions, the positive control of two UAS elements (the CSRE and the Adr1 binding site) overruled the negative control of Ume6, and the activation of Abf1 was negligible.

*ACS2* was considered to be constitutively expressed, since it was expressed in both aerobic and anaerobic conditions, and under aerobic conditions its expression did not show substantial differences on fermentable carbon sources (glucose) and non-fermentable carbon sources (ethanol) [58, 61]. In the upstream sequence of *ACS2*, a significantly similar region to the inositol/cholin-responsive element (ICRE) and three putative Abf1 binding sites were identified [61]. ICREs were previously identified as UASs of structural genes for membrane lipid biosynthesis, *e.g.* *FAS1*, *FAS2*, *INO1* [62], which interact with transcriptional factors, Ino2p/Ino4p (positive regulator) and Opi1p (negative regulator). The derepressed regulation of the ICRE obtained from *ACS2* was confirmed when it was inserted upstream of the reporter gene *lacZ*, and the activated expression caused by the ICRE was completely abolished in an *ino2Δ* null mutant, but no response in an *opi1Δ* null mutant. Abf1 binding sites were found in the upstream sequence of *ACS1* as well, and could contribute to the constitutive expression of *ACS2*, since Abf1 is required for the transcriptional activation of several house-keeping genes.

Although Acs1 and Acs2 belongs to the AMP-forming ACS family, which is usually post-transcriptionally regulated by acetylation of lysine in a conserved region [63-65], their acetylated regulation has not been identified yet. Amino acid alignments indicated that the reversible acetylation site is Lys675 in Acs1, and Lys637 in Acs2, respectively. In *Salmonella enterica*, when the lysine residue is acetylated in ACS, the adenylating activity of ACS is blocked in the first step, but the thioester-forming activity is not affected in the second step, and the deacetylation of inactive ACS is catalyzed by the NAD<sup>+</sup>-dependent protein deacetylase Sir2.

The *ACS1* disruption resulted in a prolonged lag phase in batch cultures with glucose [10, 55, 58], which might be explained by the 20-fold lower affinity of Acs2 for acetate compared with that of Acs1, or the possible involvement of Acs1 in chromatin regulation

[19]. However, these *acs1Δ* mutants were reported to behave quite differently in acetate or ethanol media. The ACS2 disruption did not affect growth on acetate or ethanol, but resulted in growth inability on glucose due to the *ACS1* repression by glucose, since the *acs2Δ* mutant could grow in glucose limited chemostat cultures [10, 55, 58]. The double deletion *acs1 asc2Δ* mutant is not viable, which indicated that ACSs are indispensable for the survival of yeast cells.

### 1.1.3 Acetyl-CoA use in fatty acid and sterol metabolism

Acetyl-CoA is converted to malonyl-CoA by acetyl-CoA carboxylase (ACC) in the first and rate limiting step in fatty acid biosynthesis. During fatty acid degradation acetyl-CoA is generated via beta-oxidation in the peroxisomes, and is then consumed by the glyoxylate cycle as described above [66].

Two ACCs have been identified in *S. cerevisiae*, encoded by *ACC1* (or *FAS3*) and *HFA1*, which are localized in the cytosol and mitochondria, respectively [67, 68]. The localization of the two ACC isoforms indicates that they are responsible for fatty acid biosynthesis in different subcellular compartments. The *ACC1* expression is regulated by transcriptional factors, *e.g.* *Ino2*, *Ino4*, *Opi1*, which are also responsible for the regulation of phospholipid metabolism [69], as reviewed in [70]. *In vitro* studies revealed that Acc1 can be rapidly phosphorylated and inactivated by mammalian carboxylase kinases, *e.g.* AMP-activated protein kinase (AMPK) [71, 72]. One phosphorylation site at Ser1157 first identified by phosphoproteome analysis and another putative site at Ser659 have been suggested to be the targets of Snf1, a member of AMPK family in yeast [73]. A recent study has revealed that Acc1 is under the post transcriptional regulation of Snf1, in order to maintain an appropriate distribution of acyl-chains of different length [74].

In sterol biosynthesis, two acetyl-CoA molecules are condensed into one acetoacetyl-CoA molecule in the first step. The reaction is catalyzed by acetoacetyl-CoA thiolase (ACAT), encoded by *ERG10* in *S. cerevisiae* [75].

### 1.1.4 Acetyl-CoA transport between subcellular organelles

Acetyl-CoA metabolism is highly compartmentalized in *S. cerevisiae*, as well as in other fungi, and it cannot travel freely between different subcellular organelles [76]. Three transport systems have been proposed for the acetyl-CoA transportation between these organelles in fungi, *i.e.* the carnitine/acetyl-carnitine shuttle, C<sub>4</sub> dicarboxylic acid synthesis from acetyl-CoA via the glyoxylate cycle (as discussed above), and acetyl-CoA re-generation from citrate by ATP citrate lyase (ACL) in the cytosol [77]. Two of them have been identified in *S. cerevisiae* except ACL [78].

Carnitine cannot be synthesized *de novo* in *S. cerevisiae* [79], but extracellular carnitine can be transported into the cells by a plasma membrane transport protein Hnm1 [80, 81]. In *S. cerevisiae*, besides the carnitine transporter Hnm1, four other enzymes have been identified to be involved in the carnitine/acetyl-carnitine shuttle, encoded by *YAT1*, *YAT2*, *CAT2*, *CRC1*, respectively. *YAT1*, *YAT2* and *CAT2* encode carnitine acetyltransferases (CATs), which catalyze the reversible reactions of acetyl group transfer between coenzyme A and carnitine. The intermediate acetyl-carnitine can cross the membranes of the mitochondria or the peroxisomes as the transportable molecule. Mitochondrial and peroxisomal Cat2 has been identified as the main CAT [82], Yat1 as a second one associated with the outer mitochondrial membrane [83], and Yat2 as a third one which mostly contributes when cells are grown on ethanol [84]. Crc1 is identified as a carnitine acetyl-carnitine translocase in the inner mitochondrial membrane [85].

### 1.1.5 Acetyl-CoA in protein acetylation

Besides serving as a crucial node in the network of carbon metabolism, acetyl-CoA plays an important part in regulatory network, *i.e.* protein acetylation as acetyl donor. Protein acetylation at  $\alpha$ - or  $\epsilon$ -amino groups during post-translational modification processes has been found to be important for regulation in both eukaryotes and prokaryotes [86, 87]. Histone acetylation affects chromatin structure and regulates gene transcription via different interactions [88]. Non-histone protein acetylation modulates cellular signaling at multiple levels, *e.g.*mRNA stability, protein localization, protein interaction, protein degradation or protein function [89, 90]. A number of histone acetyltransferases (HATs) and histone deacetylases (HDACs) have been identified in *S. cerevisiae*, which are responsible for the acetylation and de-acetylation of histone and non-histone proteins, but for most of them, their functions as transcriptional regulators are still under investigation [91].

It has been suggested that the nucleocytosolic acetyl-CoA abundance directly regulates the dynamic acetylation and deacetylation of proteins. Acs2 and Acs1 are required for histone acetylation as one major source and a secondary source of acetyl-CoA [19]. Decreased activity of Acc1, which consumes acetyl-CoA for *de novo* synthesis of fatty acids, resulted in increased histone acetylation and altered transcriptional regulation [92]. Using a continuous culture system termed the yeast metabolic cycle (YMC), Tu *et al.* found that acetyl-CoA drives the transcriptional growth program by promoting the acetylation of histones at growth related genes in yeast [93, 94], and they predicted that ‘intracellular acetyl-CoA fluctuations might represent a distinctive gauge of cellular metabolic state that could be decoded by way of dynamic acetylation and deacetylation reactions’ [95].

## 1.2 Non-ethanol producing strains for biochemical production

When yeast is grown on glucose under aerobic conditions, the majority of the glycolytic flux is directed towards ethanol due to the so-called Crabtree effect. Ethanol is usually the main by-product when yeast serves as a cell factory for biochemical production. In order to efficiently convert glucose to the desired products, a non-ethanol producing yeast strain would be an interesting platform for the production of biochemicals. An obvious strategy to eliminate ethanol production is to simply remove alcohol dehydrogenase (ADH) activity to prevent conversion of acetaldehyde to ethanol. However, yeast contains a very large number of ADH enzymes besides the major isoform Adh1 [96], and many of the specific product pathways may also rely on ADH activity, e.g. 1-butanol biosynthesis. It is therefore inherently difficult to eliminate ethanol production in yeast. The only strategy that has worked so far is removing pyruvate decarboxylase (PDC) activity through deletion of all three genes that encode this activity.

### 1.2.1 Pyruvate decarboxylase

Pyruvate decarboxylase converts pyruvate, the end product of glycolysis to CO<sub>2</sub> and acetaldehyde, the direct precursor of ethanol. In *S. cerevisiae*, PDC is encoded by three structural genes, *PDC1*, *PDC5* and *PDC6* [97-99]. Pdc1 is the major PDC isoform, while Pdc5 and Pdc6 are two minor isoforms.

*PDC1* was cloned and identified from isolated mutants with no or reduced PDC activities [100]. *PDC1* is strongly expressed in actively fermenting yeast cells. Disruption of *PDC1* resulted in decreased activity, suggesting the presence of a second PDC gene [97], which was later identified as *PDC5* [98, 101]. Pdc5 is found to be 88% identical with Pdc1, and also function during glycolytic fermentation. However, *PDC5* is expressed only in the absence of *PDC1* or under thiamine limitation [102]. Both *PDC1* and *PDC5* are under *PDC* auto-regulation, which means they could substitute each other. The auto-regulation has been observed for other genes, e.g. histone encoding genes. Pdc6 was identified using low-stringency Southern blot analysis [99]. *PDC6* expression is induced by nonfermentable carbon sources (ethanol) and also dramatically induced under conditions of sulfur limitation. Disruption of *PDC6* did not change the phenotype or the enzyme activity, as well as disruption of *PDC6* in a *pdc1Δ* mutant or a *pdc5Δ* mutant.

Disruption of both *PDC1* and *PDC5* resulted in undetectable PDC activity and impaired growth in complex medium with glucose [98]. However, deletion of only *PDC1* and *PDC5* can lead to mutants with increased *PDC6* expression, in which *PDC6* was spontaneously fused under *PDC1* promoter via recombination [103]. Thus, triple deletion is necessary for a non-ethanol producing yeast strain.

## 1.2.2 Pyruvate decarboxylase negative strain

Although *pdc* triple deletion mutants (*pdc1Δ pdc5Δ pdc6Δ*, also called Pdc negative strains) have the potential to be non-ethanol producing platform for biochemical production, they cannot grow on glucose as the sole carbon source [104].

When C<sub>2</sub> carbon was supplemented, the Pdc negative strain could grow in glucose-limited chemostat cultures using minimal medium, but not in batch cultures. When glucose was fed instead of the glucose-C<sub>2</sub> carbon mixture or C<sub>2</sub> carbon into the chemostat cultures, the cells of the Pdc negative strain were washed out [104]. With excess glucose pulsed into the steady chemostat cultures, a small increase in glycolytic flux was observed in the Pdc negative strain as well as pyruvate excretion, which was not caused by a decreased flux from pyruvate to the TCA cycle, since PDH activity did not show a strong decrease after a glucose pulse [105]. The growth requirements of C<sub>2</sub> carbon supplementation indicated that the growth defect of Pdc negative strain on glucose was due to the lack of cytosolic acetyl-CoA for biosynthesis of cellular biomolecules, especially lipids [78]. However, addition of carnitine does not restore growth of a Pdc negative strain in chemostat cultures using glucose as sole carbon source. In addition, by over-expressing threonine aldolase (encoded by *GLY1*), the growth of the Pdc negative strain on glucose could be restored, since that Gly1 releases acetaldehyde from threonine, which can be converted to acetyl-CoA via acetate in the cytosol.

Interestingly, the Pdc negative strains are sensitive to high glucose even when supplemented with a C<sub>2</sub> carbon source or with *GLY1* over-expression [78, 106]. van Maris *et al.* performed directed evolution of a Pdc negative strain on glucose [107]. During the evolution, the Pdc negative strain RWB837 was evolved in a glucose-limited chemostat culture supplemented with gradually reduced ethanol for five consecutive steps, yielding the C<sub>2</sub>-independent Pdc negative strain RWB837\*. Subsequently, RWB837\* was evolved in shake flasks using minimal medium with gradually increased glucose by serial transfer, yielding the ‘C<sub>2</sub>-independent, glucose-tolerant, and pyruvate-hyperproducing’ strain TAM. The TAM strain could grow on glucose as the sole carbon source, with a maximum specific growth rate of 0.20 h<sup>-1</sup> in minimal medium with 10% glucose. The transcriptome analysis revealed a number of changes in TAM compared to the wild type strain CEN.PK 113-7D, *e.g.* over-representation of Mig1 regulated genes, down-regulation of *HXT* genes, up-regulation of *GLY1* (but still low enzyme activity). The pyruvate-hyperproducing capacity of TAM makes it an important platform strain for industrial production of pyruvate or pyruvate-derived chemicals, without producing ethanol.

In a later study, an *MTH1* allele with a 225 bp internal deletion (*MTH1*- $\Delta T$ ) was identified in the TAM strain, and was found to be responsible for growth recovery of the Pdc negative strain on glucose [108].

Mth1 functions as a negative transcriptional regulator in the glucose signaling pathway together with other regulators, *i.e.* Snf3, Rgt2, Std1, Rgt1. Mth1 or its paralog Std1 interacts with Rgt1, which also interacts with other transcription factors, *e.g.* Cyc8, Tup1, and binds the promoters of hexose transporter genes [109, 110]. Besides the *MTH1*- $\Delta T$  allele, several other *MTH1* alleles have been identified in selections of glucose or catabolite repression suppressors using other glucose sensitive mutants [111-115]. The *MTH1* alleles seemed to be able to resolve the glucose sensitive problem in these mutants. Previous studies have shown that these *MTH1* alleles reduced glucose transport by repressing the transcription of several hexose transporter genes (*HXTs*) [107, 111, 113, 114], as well as over-expression of *MTH1* [108]. It has been proposed that *MTH1*- $\Delta T$  resulted in a decreased degradation of Mth1 [108], which could be related to putative PEST sequences (usually present in proteins with short intracellular half-life) and a target site for phosphorylation by casein kinase Yck1 [116], which are situated inside the deleted region. The decreased degradation of Mth1 resulting from the *MTH1*- $\Delta T$  allele, could prevent the phosphorylation of Rgt1, which was required for its release from the promoters of several hexose transporters [110], and therefore repress the transcription of hexose transporter genes even during growth on high glucose.

However, when introducing the *MTH1*- $\Delta T$  allele into an un-evolved Pdc negative strain, the growth rate ( $\mu_{\max}=0.10 \text{ h}^{-1}$ ) was slower in minimal medium with 2% glucose, compared to the TAM strain ( $\mu_{\max}=0.20 \text{ h}^{-1}$ ), indicating the possible presence of additional advantageous genetic changes in the TAM strain besides *MTH1*- $\Delta T$ .

## **1.3 Metabolic engineering and adaptive evolution in strain development**

Traditionally in industry, microorganisms that naturally produce a desired molecule were identified and then improved through classical strain engineering based on mutagenesis and screening. This has been an efficient approach and has resulted in low-cost production processes for many different chemicals, *e.g.* penicillin, citric acid and lysine . This approach is usually referred to as adaptive laboratory evolution (referred to as adaptive evolution in this thesis except when otherwise specified), experimental engineering, or evolutionary engineering [117]. However, this type of strain development typically leads to a slow, incremental increase in strain performance, especially in the later stages of strain improvement. Moreover, the unknown mechanisms underlying strain improvement precludes the rapid transfer of relevant traits among different strains or species.

With the introduction of genetic engineering and methods for detailed analysis of cellular metabolism it became possible to use a more directed approach to improve cell factories, generally referred to as metabolic engineering [118]. Today metabolic engineering has evolved into a research field that encompasses detailed metabolic analysis with the objective to identify targets for metabolic engineering and the implementation of metabolic engineering strategies for improvement and/or design of novel cell factories [119]. With help from synthetic biology, another research field that originally aimed at reconstruction of small, artificial biological systems (*e.g.* assembling a new biological regulon or oscillators for gene expression regulation in response to a specific input), metabolic engineering offers tremendous opportunities to create novel cell factories that are tailor made for efficient production of fuels and chemicals [120-122]. However, this rational strategy is not always perfect since it is based on existing knowledge. Especially in the case of synthetic pathway introduction, when designing and building non-native pathways, it needs to be optimized for strain fitness and biochemical production, which is not only related to the metabolic fluxes but also associated with regulation systems, which is always complicated and not well characterized yet.

Recently, with impressive progresses achieved in systems biology and bioinformatics, rapid, affordable, high throughput techniques for genome, transcriptome, proteome, and metabolome analysis become accessible for adaptively evolution, and whole genome sequencing is found to be superior to other analytical techniques, since the genetic changes can be immediately and exactly reconstructed in native strains [123]. Therefore it is possible to link the phenotypes with the genotypes. Using ‘reverse’ metabolic engineering, or ‘inverse’ metabolic engineering, the genetic changes responsible for the changes in phenotypes can be identified [124-127], which will elucidate underlying mechanisms for improved performance of adaptively evolved strains. As reviewed in

[117], through microbial adaptive evolution, interactions between these mutations identified by genome sequencing are very common, and adaptive mutations frequently target regulatory mechanisms. And it is pointed out that ‘principles of systems-level optimization underlie the genetic changes seen in adaptive evolution, and with a systems-level understanding, these optimization principles can be harnessed for the purposes of metabolic engineering’ [117].

Therefore, adaptive evolution harnesses the biology power for metabolic engineering [128], which could be finally applied in the development and performance improvement of cell factories

## Chapter 2. Overview of the thesis

The objective of this study is to develop a non-ethanol producing platform strain of *S. cerevisiae* as a cell factory, which can convert glucose to cytosolic acetyl-CoA for biochemical production.

A Pdc negative strain has the potential to be a non-ethanol producing strain for biochemical production. However, it cannot grow on glucose as the sole carbon source and requires supplementation of acetate or ethanol to the medium in order to meet the requirement for acetyl-CoA in the cytosol (needed for biosynthesis of fatty acids and ergosterol). Therefore, such a strain cannot directly serve as a platform cell factory for acetyl-CoA derived products. This limitation was partially solved by evolving the Pdc negative strain, resulting in a glucose tolerant and C<sub>2</sub> independent mutant TAM [129]. Its mechanisms for growth recovery were identified to be related to an in-frame internal deletion in *MTH1*. The *MTH1*-ΔT allele resulted in reduced glucose uptake, which may attenuate the repression on respiratory metabolism. However, it is not addressed what mechanism could provide the cells with sufficient precursors for the synthesis of cytosolic acetyl-CoA. In addition, the Pdc negative strain with the *MTH1*-ΔT allele does not efficiently convert pyruvate to acetyl-CoA in the cytosol.

For the reasons above, all reactions related with acetyl-CoA and C<sub>2</sub> carbon were filtered from the latest Genome Scale Metabolic Model of *S. cerevisiae* [130] for the possible routes to supply cytosolic acetyl-CoA in Pdc negative strains. One route was identified to be the source of cytosolic acetyl-CoA in Pdc negative strains (Paper I). In addition, adaptive evolution of Pdc negative strains on glucose was performed using serial transfer, and genome sequencing results revealed several genetic changes in evolved strains (Paper II). With all the findings, possible mechanisms were proposed for growth recovery of evolved Pdc negative strains on glucose, which would be useful for the fundamental understanding of acetyl-CoA metabolism in yeast, as well as yeast strain development for biochemical production as cell factories. Finally, the pyruvate formate lyase pathway was introduced into the reverse engineered Pdc negative strain with the *MTH1*-ΔT allele, which further increased the cytosolic acetyl-CoA supply and therefore increased the final biomass.

### **PAPER I. Ach1 is involved in shuttling mitochondrial acetyl units for cytosolic C2 provision in Pdc negative *Saccharomyces cerevisiae***

In yeast, acetyl-CoA is compartmentalized and not directly transported between these subcellular compartments. As described before, with the acetyl-carnitine or glyoxylate shuttle, acetyl-CoA produced in the peroxisome or the cytoplasm can be transported into the cytoplasm or the mitochondria. However, it is still unclear whether acetyl-CoA

generated in the mitochondria can be exported to the cytoplasm. Here we investigated this using a Pdc negative, non-fermentative strain, and aimed at identifying the mechanism responsible for the exchange of acetyl units between the mitochondrial matrix and the cytoplasm in *S. cerevisiae*. Our results identified a route relying on Ach1 that could transfer acetyl units from mitochondria to the cytoplasm. Based on our results we propose a new route in which acetyl units are shuttled from the mitochondria to the cytoplasm in the form of acetate.

### **PAPER II. Adaptive mutations in sugar metabolism restore growth on glucose in a pyruvate decarboxylase negative yeast strain**

In this study, a collection of Pdc negative strains was constructed and one of them was adaptively evolved in glucose medium via serial transfer in three independent cell lines, yielding three independently evolved strains. The evolved Pdc negative strains can grow in minimal medium with glucose as the sole carbon source at maximum specific rates of  $0.138\text{ h}^{-1}$ ,  $0.148\text{ h}^{-1}$ ,  $0.141\text{ h}^{-1}$ , respectively. Several genetic changes were identified in the evolved Pdc negative strains by genomic DNA sequencing, including 4 genes carrying point mutations in at least two of the evolved strains: a transcription factor gene of the glucose-sensing signal transduction pathway *MTH1*, a hexose transporter gene *HXT2*, a mitochondrial citrate synthase gene *CIT1*, and a histone deacetylase gene *RPD3*. Reverse engineering of the parental Pdc negative strain through introduction of the *MTH1*<sup>81D</sup> allele restored its growth on glucose. The non-synonymous mutations in *HXT2* and *CIT1* may function in the presence of the mutations in *MTH1* and could be related to the cytosolic acetyl-CoA supply in Pdc negative strains.

### **Paper III. Functional pyruvate formate lyase pathway expressed with its cofactors in *Saccharomyces cerevisiae* at aerobic growth**

In connection with establishing yeast platforms for production of fuels and chemicals it is necessary to engineer their metabolism such that the raw material can be efficiently converted to the product of interest. Many industrially interesting products are biosynthesized from acetyl-CoA [6] and there is therefore much interest in efficient conversion to acetyl-CoA. In yeast, acetyl-CoA metabolism is compartmentalized into three main compartments, the mitochondria, the cytosol and the peroxisome, and cytosolic acetyl-CoA is generally preferred for efficient production of heterologous products [6]. Naturally cytosolic acetyl-CoA is converted from acetaldehyde with ATP consumed, which translates to a yield loss in the overall conversion of glucose to the product of interest. There is therefore much interest in heterologous pathways which are more efficient than the endogenous pathway.

An alternative pathway is pyruvate formate lyase (PFL), and PFL is characterized as an enzyme functional at anaerobic conditions, since its active form is sensitive to oxygen. In this study, PFL gene and its activating enzyme gene from *E. coli* were expressed in a Pdc negative yeast with a mutation in the transcriptional regulator Mth1, IMI076 (Pdc<sup>-</sup> *MTH1-ΔT ura3-52*). Two different cofactors were co-expressed with the PFL pathway as electron donors, reduced ferredoxin or reduced flavodoxin, respectively, which were found to have positive effects on growth under aerobic conditions, i.e. a higher final biomass concentration and a significant increase in transcription of formate dehydrogenases (FDHs). Among the two cofactors reduced flavodoxin was found to be a better electron donor for the PFL pathway than reduced ferredoxin.

## Chapter 3. Results and discussion

### 3.1 Ach1 compensates cytosolic acetyl-CoA in Pdc negative strain

As mentioned before, a Pdc negative strain cannot grow on glucose as the sole carbon source due to the lack of cytosolic acetyl-CoA, and the *MTH1*- $\Delta T$  allele could restore its growth on glucose which resulted in reduced glucose uptake. However, the source of cytosolic acetyl-CoA is still a mystery in a Pdc negative strain with *MTH1*- $\Delta T$  allele. Using the latest Genome Scale Metabolic Model of *S. cerevisiae* [130], 57 reactions were found related with C<sub>2</sub> compound metabolism, including 34 reactions directly related with acetyl-CoA metabolism and transport, and 23 more reactions involved in metabolism of other C<sub>2</sub> compounds such as ethanol, acetaldehyde and acetate.

Without carnitine supplemented, there could be two possible routes to provide cytosolic acetyl-CoA in a Pdc negative strain, after analyzing the possible roles of these 57 reactions in cytosolic acetyl-CoA supply. One possible route is catabolizing threonine via threonine aldolase (encoded by *GLY1*) to release acetaldehyde, which can be converted to acetyl-CoA via acetate in the cytosol. A previous study has revealed that *GLY1* over-expression in a Pdc negative strain can circumvent the essential biosynthetic role of pyruvate decarboxylase when cultured in glucose limited chemostat conditions [106]. However, the possibility of the route involving Gly1 for cytosolic acetyl-CoA supply was excluded due to its low affinity for threonine and the relatively low intracellular threonine concentration when yeast is grown on excess glucose [129].

The other potential route is converting acetyl-CoA to acetate in the mitochondria, followed by transport of acetate across the mitochondrial membranes to the cytosol, and conversion of acetate into acetyl-CoA by cytosolic acetyl-CoA synthetase (ACS). One gene product, encoded by *ACH1*, is associated with both acetyl-CoA and acetate in the mitochondria, although its functions are not conclusive yet. Ach1 was originally proposed as an acetyl-CoA hydrolase to catalyze the scission of acetyl-CoA into acetate and CoA [131-134], like many other acetyl-CoA hydrolases found in mammalian tissues [135, 136]. The exact catalytic role of this enzyme was questioned by the observations of its role in acetate but not ethanol utilization [133]. It was proposed that this enzyme may have a novel function concerning acetyl-CoA metabolism, but it was only recently that Fleck and Brock characterized Ach1 as a CoA transferase involved in mitochondrial acetate detoxification, not just wasting energy by hydrolyzing acetyl-CoA [137]. In their study Ach1 showed the highest specific activity for the CoA transfer from succinyl-CoA *in vitro*. However, the substrate promiscuity of this enzyme did not exclude its transferase activity on other CoAs. We therefore proposed that this enzyme can transfer CoA unit from acetyl-CoA to succinate, forming acetate and succinyl-CoA.

To test our assumptions, we first evaluated the effects of succinate supplementation in a Pdc negative strain IMI076 carrying *MTH1* with an internal deletion (*MTH1-ΔT*) [108] and a wild type strain CEN.PK113-5D [138]. The cultivations were performed in minimal medium with 2% glucose using Bioscreen C. When 0.5 g/L succinate was added to the medium, there was no obvious growth difference for the wild type, but it was clear that external succinate supplementation shortened the lag phase for IMI076 (**Figure 2A**). This was further confirmed by culturing IMI076 in shake flasks supplemented with 0.5 g/L succinate. As shown in **Figure 2B**, the lag phase was shortened by about 22 h. This result was consistent with increased rates of glucose consumption and pyruvate accumulation (data not shown).

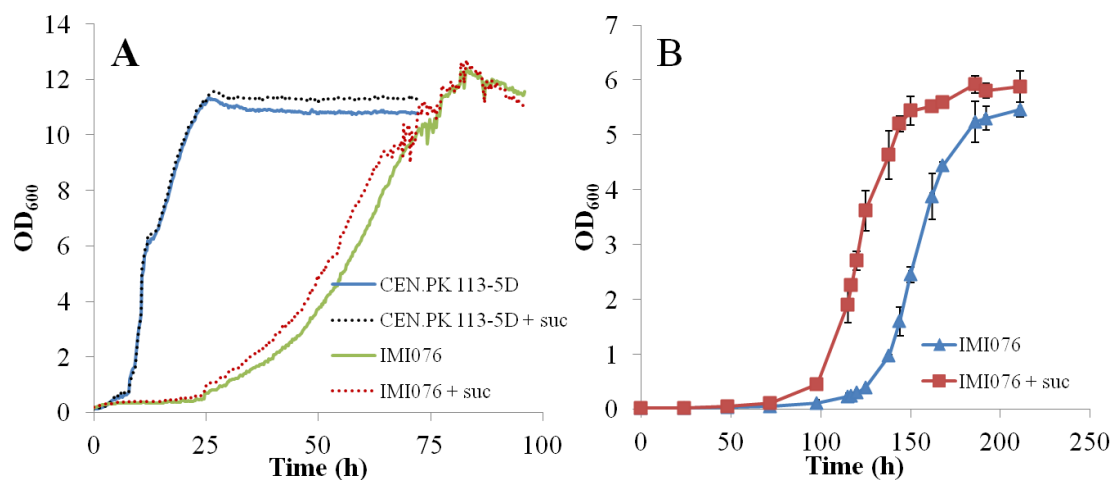


**Figure 2. Addition of succinate improves the growth of the strain IMI076 (Pdc<sup>-</sup> *MTH1-ΔT*) in minimal medium with glucose as the sole carbon source using Bioscreen (A) and shake flask (B).**

To test if Ach1 is a key player in channeling acetyl units from the mitochondria to the cytosol, *ACH1* was replaced with a functional *URA3* cassette in IMI076, yielding YACH01. As control, IMI076 was transformed with an empty plasmid pSP-GM1 [139] containing the same *URA3* cassette, yielding YACH00.

As shown in **Figure 3A**, when cultured on synthetic dextrose (SD) plates supplemented with uracil (SD+ura), no big growth difference between IMI076 and YACH00 was observed, but significantly impaired growth of YACH01. When ethanol was supplemented, all strains with or without *ACH1* deletion grew well on glucose with no difference (**Figure 3A**). These results suggested that *ACH1* is important for its growth on glucose as the sole carbon source. The spot assay results of the Pdc negative strains could be affected by the SD+ura agar plate used, since it could contain threonine or other C<sub>2</sub> contaminations as speculated by Oud *et al.* [108]. To exclude any potential C<sub>2</sub> contamination in the medium, the strains were cultured in liquid minimal medium with glucose as the sole carbon source. Cells of IMI076 and YACH01 were harvested during

exponential phase and washed twice after pre-cultured in minimal ethanol media, and then inoculated to the minimal glucose media. IMI076 grew normally as described before [139], with a specific growth rate of about  $0.07 \text{ h}^{-1}$ , whereas YACH01 could not grow on glucose as the sole carbon source (**Figure 3B**).

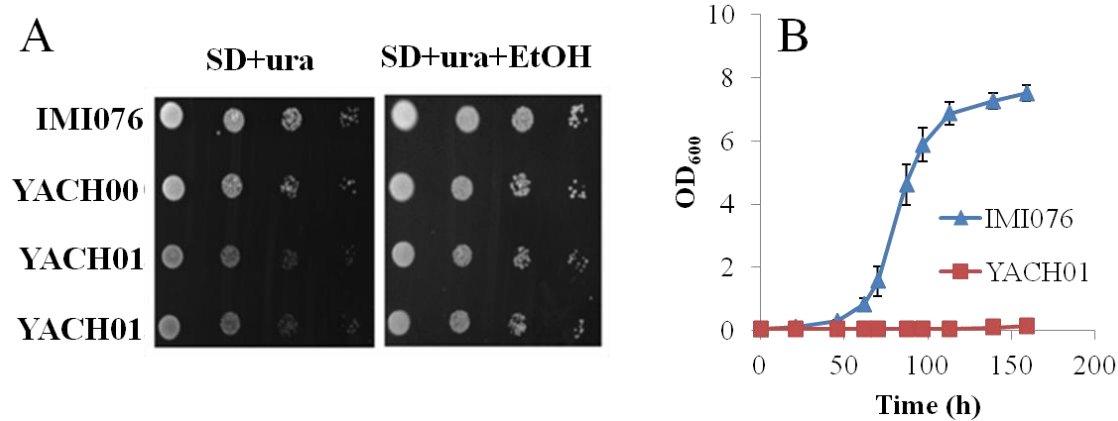


**Figure 3. The growth of the strain IMI076 (*Pdc<sup>-</sup> MTH1-ΔT*) relies on Ach1.** A) Spot assays on synthetic media with glucose or glucose plus ethanol. The plates were incubated at 30 °C and recorded photographically 4 days after inoculation. B) Growth assays in liquid minimal media with glucose as the sole carbon source. Cells were precultured in minimal media with ethanol, and washed twice before inoculation into minimal glucose media. Data are mean +/- standard error of three biological replicates.

The inability of growth on glucose as the sole carbon source that resulted from *ACH1* disruption points to this enzyme being essential for the cytosolic acetyl-CoA supply, which might be transferred from the mitochondria. To further confirm this hypothesis we performed complementation of the *ach1* deletion strain with the wild-type gene and a truncated version of *ACH1* (*tACH1*), respectively. The truncated version of Ach1 is mislocalized in the cytoplasm due to the absence of its N-terminus [134]. *ACH1* and *tACH1* were reintroduced into the *ach1* mutant YACH01 by chromosomal integration, yielding YACH02 and YACH03, respectively. Growth assays of the two resulting strains revealed that complementation with the intact *ACH1* gene could restore growth of the *ach1* mutant, but not the truncated *ACH1* (**Figure 4**). The maximum specific growth rate of the strain YACH02 was increased by 52% compared with the strain IMI076, which may be ascribed to increased *ACH1* expression in YACH02, in which *ACH1* was expressed under the strong constitutive promoter *TEF1*.

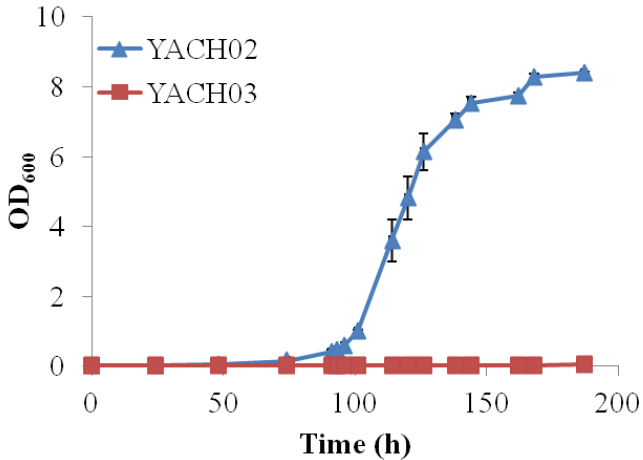


**Figure 4. Complementation with the intact *ACH1* but not the truncated version restores growth of an *ach1* mutant.** Cells were precultured in defined minimal media with ethanol, and then washed twice with sterile water before inoculation into glucose media. All measurements are mean +/- standard error of three biological replicates.

To further validate the hypothesis that the cytosolic acetyl-CoA in IMI076 is likely to come from mitochondrial acetyl-CoA, we therefore cultivated it in absence or presence of UK-5099. The compound UK-5099, an analogue of alpha-cyanocinnamate is a specific and potent inhibitor of the mitochondrial pyruvate carrier [140, 141]. In yeast, the pyruvate uptake into the mitochondria is reduced by more than about 70% with 0.2 mM UK-5099 supplemented, compared to that without inhibitor in yeast [141]. Mitochondrial acetyl-CoA is exclusively converted from pyruvate, catalyzed by the pyruvate dehydrogenase complex. Therefore in the presence of UK-5099, inhibiting mitochondrial pyruvate uptake will limit the availability of acetyl units in this compartment, which will further restrict the supply of cytosolic acetyl-CoA and therefore affect the growth of cells.

As shown in **Figure 5A**, when 0.2 mM UK-5099 dissolved in DMSO was added to the culture during the exponential growth phase, a significant decrease in growth was observed, compared with the control experiment with same amount DMSO but no inhibitor added. Furthermore, there was no significant effect on the growth of the wild type strain CEN.PK 113-5D when supplemented with 0.2 mM UK-5099 (**Figure 5B**). The maximum specific growth rate of the strain IMI076 showed a big decrease upon the addition of UK-5099, from  $0.066 \text{ h}^{-1}$  to  $0.018 \text{ h}^{-1}$ . These observations clearly shows that the flux of mitochondrial pyruvate uptake is limiting the growth of the Pdc negative strain, which again supports the hypothesis that cytosolic acetyl-CoA is derived from mitochondrial acetyl-CoA, which is related to Ach1.

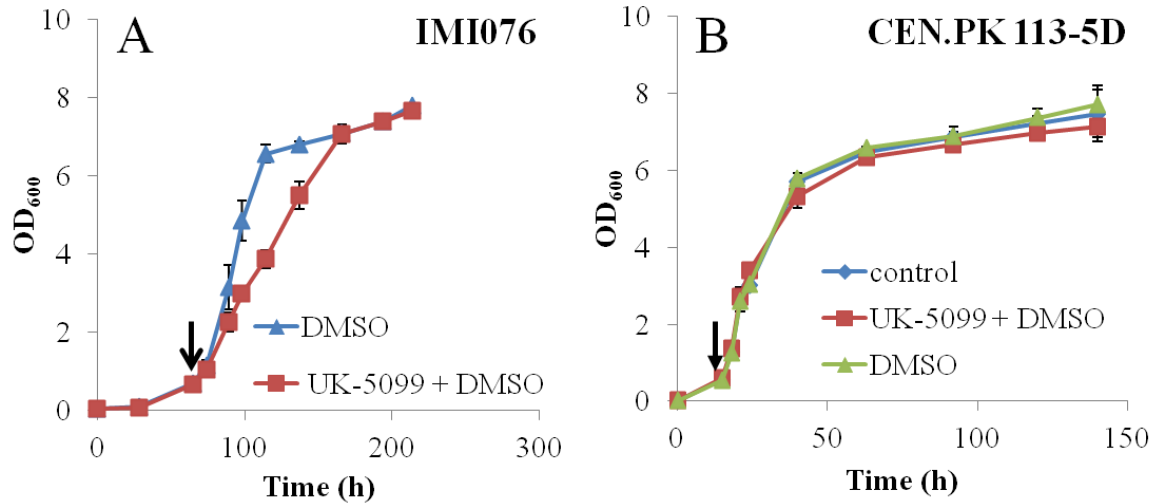


**Figure 5. Growth assays of IMI076 (A) and CEN.PK 113-5D (B) upon addition of UK-5099 in minimal medium with glucose as the sole carbon source. Arrows represent the addition of UK-5099 dissolved in DMSO or DMSO without UK-5099. All measurements are mean +/- standard error of three biological replicates.**

To summarize, inspired by the function as a CoA transferase and the promiscuity of this enzyme on its substrates, we hypothesized that Ach1 could transfer CoA from acetyl-CoA to succinate. The succinate supplementation results showed that addition of succinate improves growth of the strain IMI076, but has no impact on the growth of the wild type strain (**Figure 2**). When *ACH1* was disrupted in IMI076, the growth on glucose was interrupted (**Figure 3**), clearly indicating that Ach1 plays an important role in the growth of the Pdc negative strain on glucose. Moreover, the complementation of the *ACH1* gene under control of the strong *TEF1* promoter, not only rescued the growth on glucose but resulted in slightly faster growth than the IMI076 strain (**Figure 4**), further confirming that Ach1 is involved in cytosolic acetyl-CoA supply. It is also found that a truncated version of Ach1 localized in the cytosol could not rescue growth of IMI076 with *ach1* deletion, and that inhibition of the mitochondrial pyruvate carrier reduces growth of IMI076, which further confirmed that the cytosolic acetyl-CoA comes from the mitochondria.

Based on these results we propose a new route for acetyl-CoA transfer in the Pdc negative strains. Here *S. cerevisiae* uses acetate instead of citrate to transfer acetyl units from the mitochondria to the cytosol. This alternative shuttle route has been reported in other eukaryotes, *e.g. Trypanosoma brucei* [142]. As shown in **Figure 6**, when cells grow on glucose, acetyl-CoA produced in the mitochondria can be converted to acetate potentially through the reversible CoA transferase Ach1. Acetate can cross the mitochondrial membrane and be converted into acetyl-CoA in the cytosol. It has been reported that Ach1 is repressed by glucose, since its expression level increased in late exponential phase compared to the early exponential phase [132]. In IMI076, the *MTH1*-

$\Delta T$  allele would lead to an attenuated glucose uptake and therefore result in derepressed *ACH1* expression. The mitochondrial localization of Ach1 allows for the acetyl units shuttled from the mitochondria to the cytosol when cells are grown on glucose. This is consistent with the results in a previous study, that most Ach1 was distributed in the mitochondria by immunofluorescence microscopy [134]. The novel function of Ach1 involved in acetyl unit export from the mitochondria is not contradicting with its function in acetate detoxification as suggested earlier [133, 137], since the CoA transfer is likely a reversible reaction.

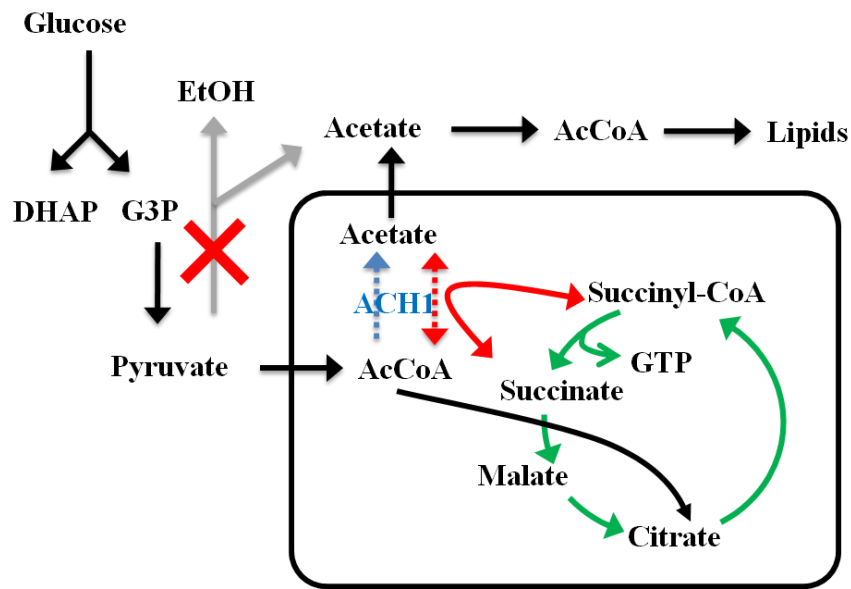


**Figure 6. A model of Ach1 transferring acetyl units from the mitochondria to the cytosol.** In a Pdc negative strain, intramitochondrial acetyl-CoA derived from pyruvate by activation of pyruvate dehydrogenase, can be converted into acetate by acetate:succinyl-CoA transferase Ach1. The acetate formed in the mitochondria crosses the membranes to the cytosol, and then is converted to acetyl-CoA for production of lipids and amino acids.

### 3.2 Growth recovery through adaptive evolution and reverse metabolic engineering

To construct Pdc negative strains, *PDC1*, *PDC5*, and *PDC6* were consecutively deleted using a bipartite strategy [143] as shown in **Figure 7**, in two different background strains, CEN.PK 113-5D (*MATa ura3-52*) and CEN.PK 110-10C (*MATa his3-Δ1*) [138].

Combined with strain crossings and tetrad segregations, a collection of triple deletion mutants was constructed carrying different auxotrophic markers: *ura3-52*, *his3-Δ1* or *ura3-52 his3-Δ1*, as shown in **Figure 8**, which will allow for synthetic gene introduction using up to two marker genes.

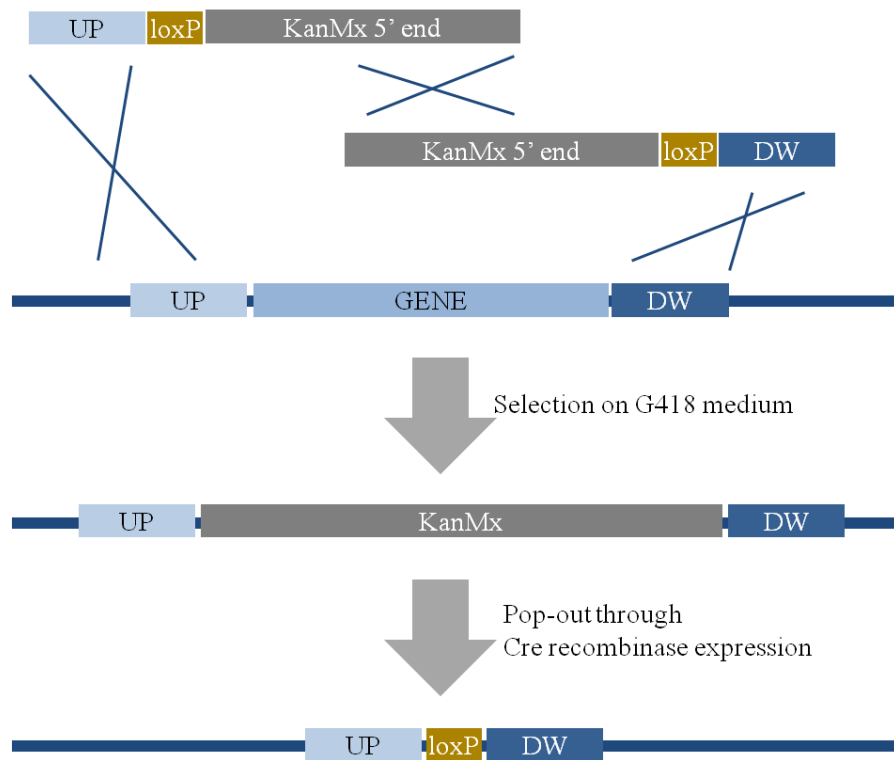


**Figure 7. Bipartite strategy for gene deletion.** Sequences upstream and downstream of the individual genes and two overlapping fragments of the *kanMX* resistance marker cassette flanked by *loxP* sites were PCR amplified. The two fused PCR fragments for each gene deletion were transformed into yeast using the lithium acetate method [144]. After each gene deletion, the *kanMX* marker cassette was looped out via Cre recombinase mediated recombination between the two flanking *loxP* sites using plasmid pUC47 or pUG62 as described previously [145].

In order to gain more insights into the possible evolving mechanisms of Pdc negative strains, adaptive evolution of a Pdc negative strain CEN.PK YMZ-E1 (*MATa ura3-52 his3-Δ1 pdc1Δ pdc5Δ pdc6Δ*), E1 for short, was performed in glucose medium via serial transfer. Afterwards, the genetic changes in the evolved Pdc negative strains were identified using genomic DNA sequencing.

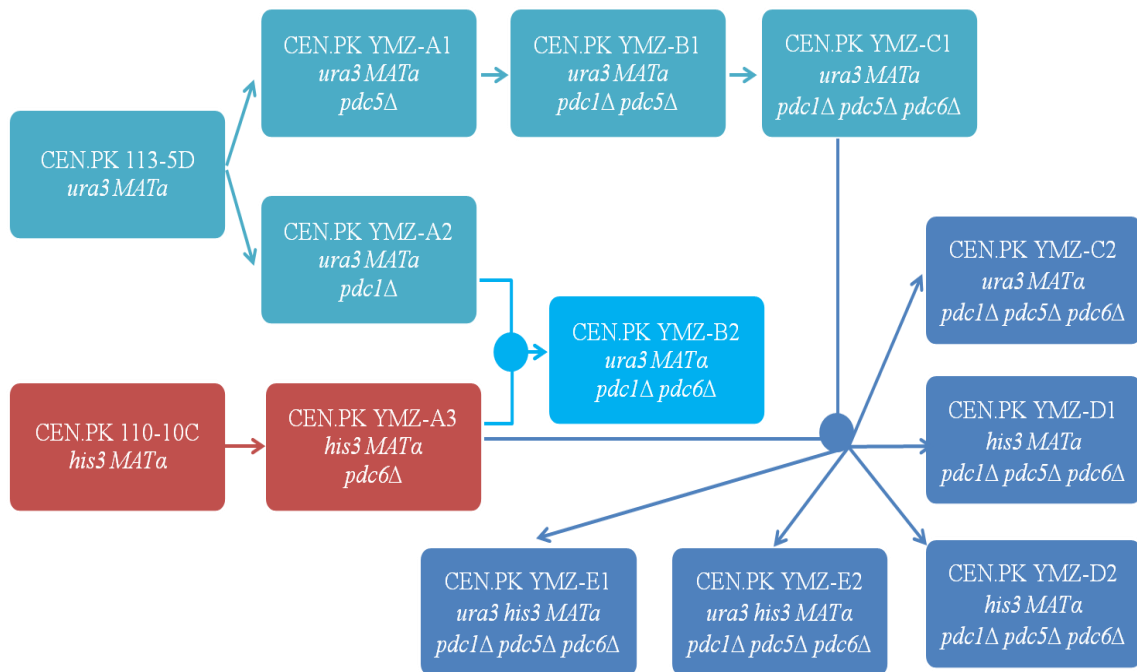


**Figure 8. Work flow of Pdc negative strain construction.** *PDC1*, *PDC5*, and *PDC6* were consecutively deleted in two different background strains CEN.PK 113-5D (*MATa ura3-52*) and CEN.PK 110-10C (*MATa his3-Δ1*). A collection of Pdc negative strains was obtained using a combination of consecutive deletions with strain crossings and tetrad dissections. The closed circles represent strain crossings.

The adaptive evolution of E1 towards growth on glucose as the sole carbon source was performed in three independent culture lines in 100 mL shake flasks with 20 mL medium at 30 °C, which involved three phases (Figure 9).

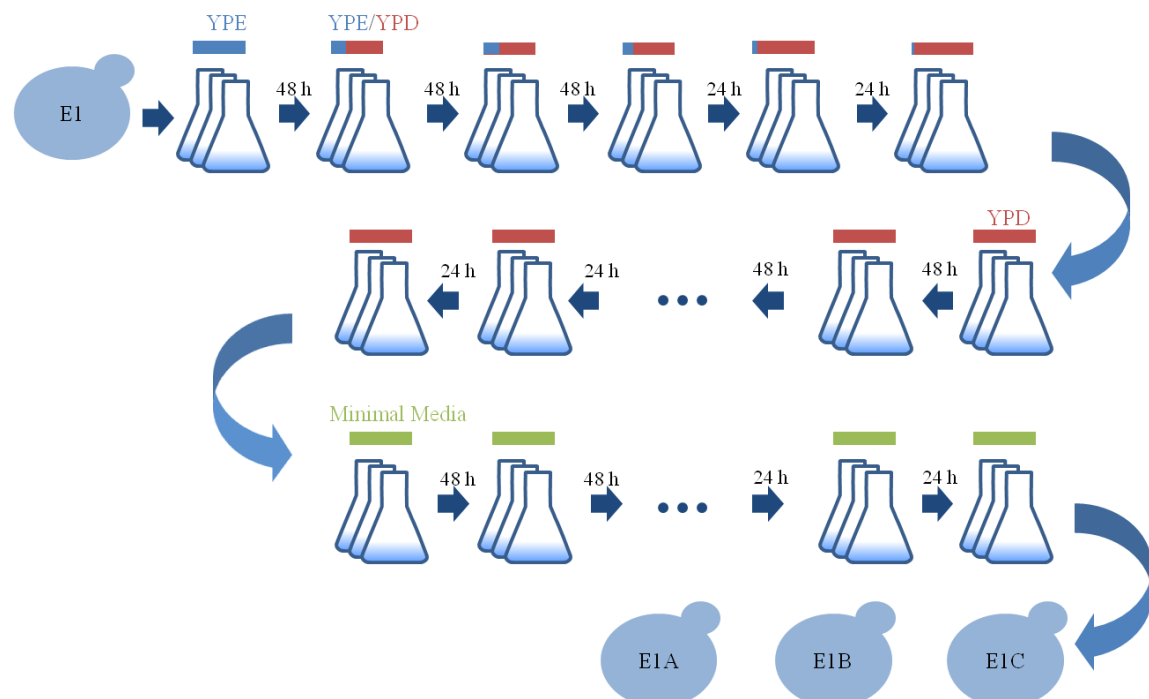


**Figure 9. Adaptive evolution process of the Pdc negative strain E1.**

First, E1 was evolved in YPD medium with gradually reduced ethanol concentration for glucose tolerance. Then the glucose tolerant strains were further evolved in YPD media for faster growth. Finally the fast-growing and glucose tolerant strains were evolved for C<sub>2</sub> source-independence and faster growth in minimal medium with 2% glucose. The evolved strains were serially transferred every 48 hours or 24 hours. The whole evolution process took 62 days. And three single clones isolates were obtained from the last three shake flasks, respectively, which were designated as CEN.PK YMZ-E1A, CEN.PK YMZ-E1B, and CEN.PK YMZ-E1C (E1A, E1B, E1C for short, respectively).

The growth of three evolved Pdc negative strains, E1A, E1B and E1C was tested in the minimal medium with 2% glucose as the sole carbon source (data not shown). In the minimal medium, the maximum specific growth rates of E1A, E1B and E1C were 0.138 h<sup>-1</sup>, 0.148 h<sup>-1</sup>, 0.141 h<sup>-1</sup>, respectively.

Cells of the parental Pdc negative strain E1 and its evolved strains (E1A, E1B, E1C) were cultured in YPD media and harvested during exponential phase for genomic DNA extraction. The sequencing was performed multiplexed on an Illumina MiSeq. The raw sequencing data of these strains were filtered and trimmed using protocols as described in [146], and the filtered reads were mapped to the reference genome of a wild type strain CEN.PK 113-7D.

The genome sequencing results (**Table 1**) identified three SNVs (Single Nucleotide Variants) in coding regions representing nonsynonymous mutations in the E1A strain; 11 SNVs in coding regions representing nonsynonymous mutations in the E1B strain; and 6 SNVs in coding regions representing nonsynonymous mutations, one chromosomal regional deletion, one mitochondrial regional deletion and one single nucleotide insertion in the E1C strain. Among all genes with SNVs, three genes, *MTH1*, *HXT2* and *CIT1*, were found to carry point mutations in all three evolved strains. And another gene, *RPD3*, was found to carry point mutations in two of the evolved strains. *MTH1* encodes a negative regulator of the glucose-sensing signal transduction pathway, as described before. *HXT2* encodes a high-affinity glucose transporter, which is usually found to function under low glucose concentrations and its transcription is repressed by high glucose and induced by low glucose [147, 148]. *CIT1* encodes a mitochondrial citrate synthase, as reviewed in Chapter 1. *RPD3* encodes a histone deacetylase, which usually functions in the form of a complex together with other proteins to regulate gene transcription, silencing and many other processes by histone deacetylation [149-151].

**Table 1. Point mutations in evolved Pdc negative strains.**

Chr	Position	E1	E1A	E1B	E1C	Nucleotide change	Effect	Gene(s)	Amino acid change	Codon change	Codon position
MT	62539	// <sup>2</sup>		DEL		Deletion of 500-600 bp the gene	chr0_JIGSAW_8452988_gene_8				
2	548654	//	SNV		A/T	Nonsynonymous	YBR157C	ICS2	L/I	Tta/Ata	123
4	825268		SNV		A/T	Nonsynonymous	YDR181C	SAS4	S/T	Tct/Act	375
4	1014480		SNV		A/C	Nonsynonymous	YDR277C	MTH1	I/S	aTt/aGt	85
4	1014492	12% <sup>1</sup>	SNV	SNV	G/T	Nonsynonymous	YDR277C		A/D	gCt/gAt	81
4	1162017	//		DEL		Deletion of ~1000 bp of gene	YDR345C	HXT3			
8	435290		SNV		A/G	Upstream: 48 bases Downstream: 200 bases	YHR169W	DBP8			
10	704204			INS	*+/A	Downstream: 359 bases	YJR152W	DAL5			
12	908162			SNV	C/G	Nonsynonymous	YLR401C	DUS3	D/H	Gat/Cat	499
13	283022		SNV		G/C	Nonsynonymous	YMR011W	HXT2	G/R	Ggt/Cgt	75
13	284197	SNV	SNV	G/A		Novel stop codon	YMR011W		W/*	tgG/tgA	466
13	704014		SNV	C/T		Nonsynonymous	YMR219W	ESC1	L/F	Ctt/Ttt	736
14	12588	25% <sup>1</sup>		T/C		Nonsynonymous	YNL330C		N/D	Aat/Gat	235
14	12704		SNV	G/A		Nonsynonymous	YNL330C	RPD3	A/V	gCg/gTg	196
14	13038		SNV	A/T		Nonsynonymous	YNL330C		F/I	Ttt/Att	85
14	278451		SNV	G/C		Nonsynonymous	YNL189W	SRP1	S/T	aGc/aCc	73
14	568887	//	SNV	G/T		Nonsynonymous	YNL032W	SIW14	S/I	aGc/aTc	132
14	624525	//	SNV	G/T		Nonsynonymous	YNR001C		P/Q	cCa/cAa	176
14	624528		SNV	T/C		Nonsynonymous	YNR001C	CIT1	H/R	cAt/cGt	175
14	624802	//	SNV	T/C		Nonsynonymous	YNR001C		M/V	Atg/Gtg	84
14	742966		//	SNV	C/A	Downstream: 150 bases Downstream: 220 bases	YNR064C, YNR063W				
16	469045	//	SNV	G/T		Nonsynonymous	YPL045W	VPS16	V/F	Gtt/Ttt	617

1: The value means the percentage reads of the mutations, ideally representing the percentage of the sequenced cells. And the mutation was excluded after sequencing of the individual gene. 2: Unfixed mutations.

Interestingly, two identical mutations occurred in more than one strain, A81D in Mth1 and W466\* in Hxt2, and two mutations affected adjacent amino acids, P176Q and H175R in Cit1.

The most interesting gene is *MTH1*, since several other *MTH1* alleles have been identified in selections of glucose or catabolite repression suppressors using glucose sensitive mutants besides *MTH1-ΔT* [111-115]. Among these *MTH1* alleles affecting glucose sensing, *e.g.* *BPC1-1*, *DGT1-1*, *HTR1-5*, *HTR1-19* and *HTR1-23*, two mutations in codon 85 (I85N, I85S) and one mutation in codon 102 (S102G) were identified. It was found that both mutations in codon 85 could alleviate glucose repression and that the S102G mutation could reinforce the mutations in codon 85 although having no effects by itself [113, 114]. Since the mutation I85S has already been confirmed to suppress glucose repression, the mutation A81D was chosen to be validated through reverse engineering in this study, to investigate if it has similar effects like other mutations.

To introduce the mutation A81D in *MTH1*, an *MTH1<sup>81D</sup>* construct was created and used to replace the native *MTH1* in the parental Pdc negative strain E1, as shown in **Figure 11**, yielding two M81 transformants, M81-11 and M81-33. They were tested for growth in glucose minimal medium. Their growth profiles in minimal medium with 2 % glucose are shown in **Figure 11**, with the maximum specific growth rates of 0.053 h<sup>-1</sup> and 0.047 h<sup>-1</sup>, respectively.

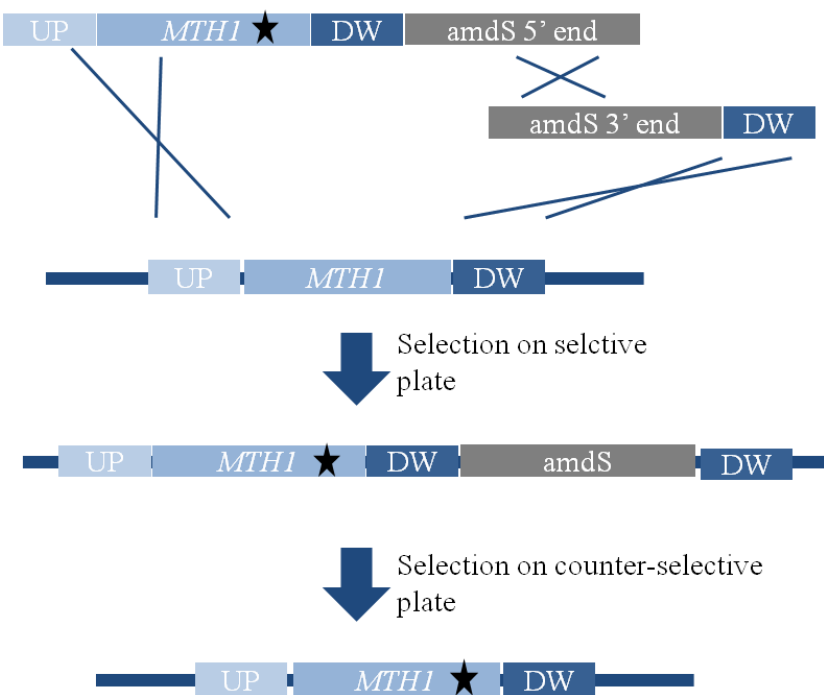


**Figure 10. Reverse engineering strategy for *MTH1<sup>81D</sup>* integration into *MTH1* locus of the E1 strain.**

The fact that  $MTH1^{81D}$  by itself could restore growth of the Pdc negative strain on glucose suggested its similar effects on glucose repression alleviation [108, 111-115]. However, the maximum specific growth rates were smaller than those of the evolved strains E1A, E1B, E1C. The  $MTH1^{81D}$  mutation contributes around 35% of the specific growth rate in the evolved E1 strains, indicating that other genetic changes are likely to contribute to the growth recovery as well.

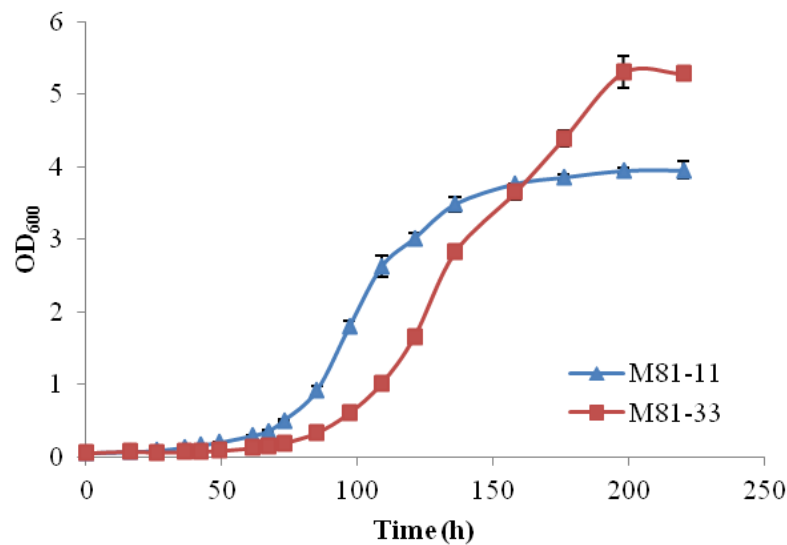


**Figure 11. Growth profiles of reverse engineered strains M81-11 and M81-33** (two transformants, *ura3-52 his3-Δ1 pdc1Δ pdc5Δ pdc6Δ mth1::MTH1<sup>81D</sup>*) in minimal medium with 2% glucose. All measurements are mean +/- standard error of three biological replicates.

In order to understand the effects of the  $MTH1^{81D}$  allele on transcription of hexose transporter genes, transcription analysis was performed on *HXT1-7* using qPCR in reverse engineered strains M81-11 and M81-33 and a wild type strain CEN.PK 113-11C [138]. Cells for RNA extraction were cultured in minimal medium and harvested during exponential growth phase ( $OD_{600} \sim 1$ ). *ACT1*, a housekeeping gene, was selected as the reference gene [152]. Since *HXT6* and *HXT7* have nearly identical sequences, they used the same pair of primers for qPCR. Therefore, the transcription analysis result for *HXT6* and *HXT7* was their sum-up.

Compared with the wild type, the expression levels of *HXT1*, *HXT3*, *HXT4* and *HXT6&7* were much lower in both M81 transformants, *i.e.* around 9 fold, 25 fold, 15 fold, and 40 fold lower, respectively (**Figure 12**). The expression level of *HXT5* did not show much difference in the M81 strains and the wild type, around 1.5 fold higher in the M81 strains. However, the expression level of *HXT2* was much higher in the M81 strains, *i.e.* around 3 fold higher, a different pattern from other *HXTs*. The different expression patterns of *HXTs* in M81 strains suggested that they were regulated by Mth1 in different ways.

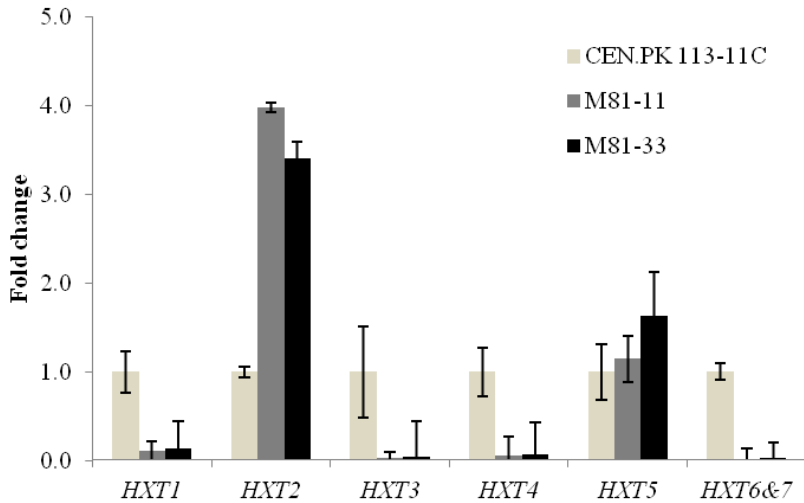


**Figure 12. Transcription analysis of HXTs (HXT1-7) in two M81 strains and wild type strain CEN.PK 113-11C.** The transcription levels of HXTs in CEN.PK 113-11C are set at 1. All measurements are mean +/- standard error of three biological replicates.

In addition, a bioinformatics approach was undertaken to gain sequence-function insight into these mutations in the four proteins. Homologous sequences were queried using the basic local alignment search tool (BLAST) of NCBI database, and then were filtered to retain only those with identity of 40% ~ 95% to the *S. cerevisiae* enzymes to reduce bias. The remaining sequences were aligned using MUSCLE [153], and the resulting alignments were used to compute the conservation of each amino acid in the *S. cerevisiae* proteins compared to the filtered BLAST results. The conservation values were used to color-code sequence representations of the *S. cerevisiae* proteins, as shown in **Figure 13**. Homology models were generated for three of the four proteins using the Swiss-Model repository [154], with the aim of gaining insights into the function of the mutations, as shown in **Figure 14**.

The BLAST search performed with Mth1 from *S. cerevisiae* yielded only 22 homologous sequences after filtering, which were orthologs of Mth1 or its homolog Std1 from unicellular fungi. Both A81 and I85 are conserved in 21 out of the 22 analyzed sequences. And A81 and I85 are positioned on an ‘island’ composed of 22 highly conserved amino acids from codon 71-91 (**Figure 13A**). The high degree of conservation of this region indicates functional or structural importance for the protein function, like the other conserved ‘island’ from codon 118 to 137 (**Figure 13A**), which is the identified target region for phosphorylation by Yck1 [116]. Since no protein crystal structures of Mth1 or homologs are available, predictions were performed for the secondary structure of the conserved ‘island’ (codon 71-91) using four prediction tools [155] (**Figure 15A**), which all indicated an alpha helix formed in this region (**Figure 15B**). The putative helix is likely initiated by the structurally rigid prolines at codon 74 and 75. Predictions for which

amino acids are exposed to the solvent and which are buried were also generated using two different tools, and both tools used predict Y77, A81, I85 and L89 to be buried away from the solvent [156] (**Figure 15A**). A helical-wheel representation was generated using the amino acids predicted to form an alpha helix (residues 75-89) (**Figure 15B**). The aim was to examine the topology of the predicted alpha-helix. The helical-wheel representation shows an amphipathic alpha helix with the buried residues Y77, A81, I85 and L89 on one side, whereas the opposite side solely has acidic and basic residues. Therefore, it is proposed that A81 and I85, together with Y77 and L89, play a structural role in anchoring a highly conserved alpha helix to the Mth1 surface via hydrophobic interactions. The A81D, I85S or I85N mutations, representing changes from non-polar to polar amino acids, would disrupt their interactions and may therefore change the secondary structure. Since the two conserved ‘islands’ are 27 residues apart, it is reasonable to speculate that the putative helix may interact with the phosphorylation site, and thus affect the Mth1 degradation [148].

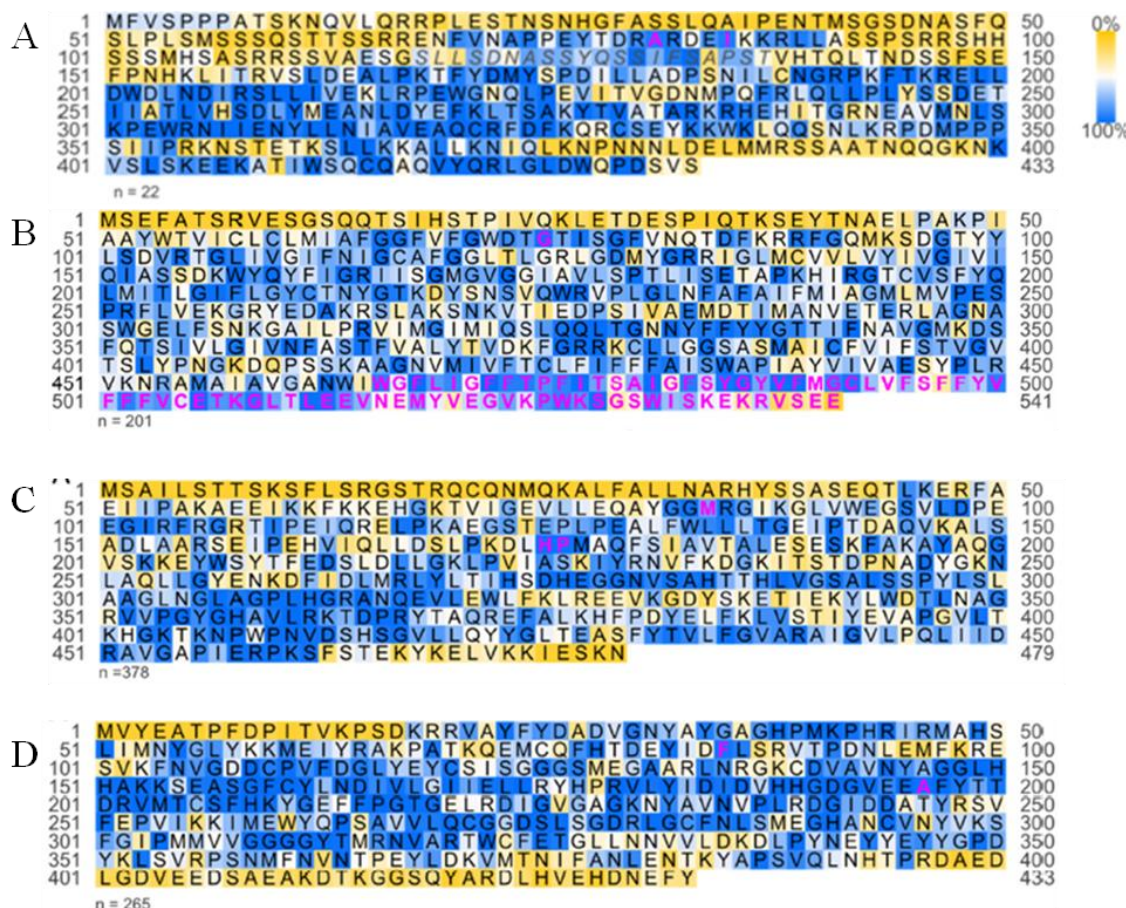


**Figure 13. Mapping and analysis of mutations in Mth1 (A), Hxt2 (B), Cit1 (C) and Rpd3 (D).** The protein sequences of *S. cerevisiae* are shown with colored conservation levels. Yellow indicates low conservation, white intermediate, and blue high. Magenta text indicates positions for non-synonymous mutations identified in this study. n presents the number of homologous sequences used in a multiple alignment. A) Gray and italic text indicates the phosphorylation region of casein kinase Yck1.

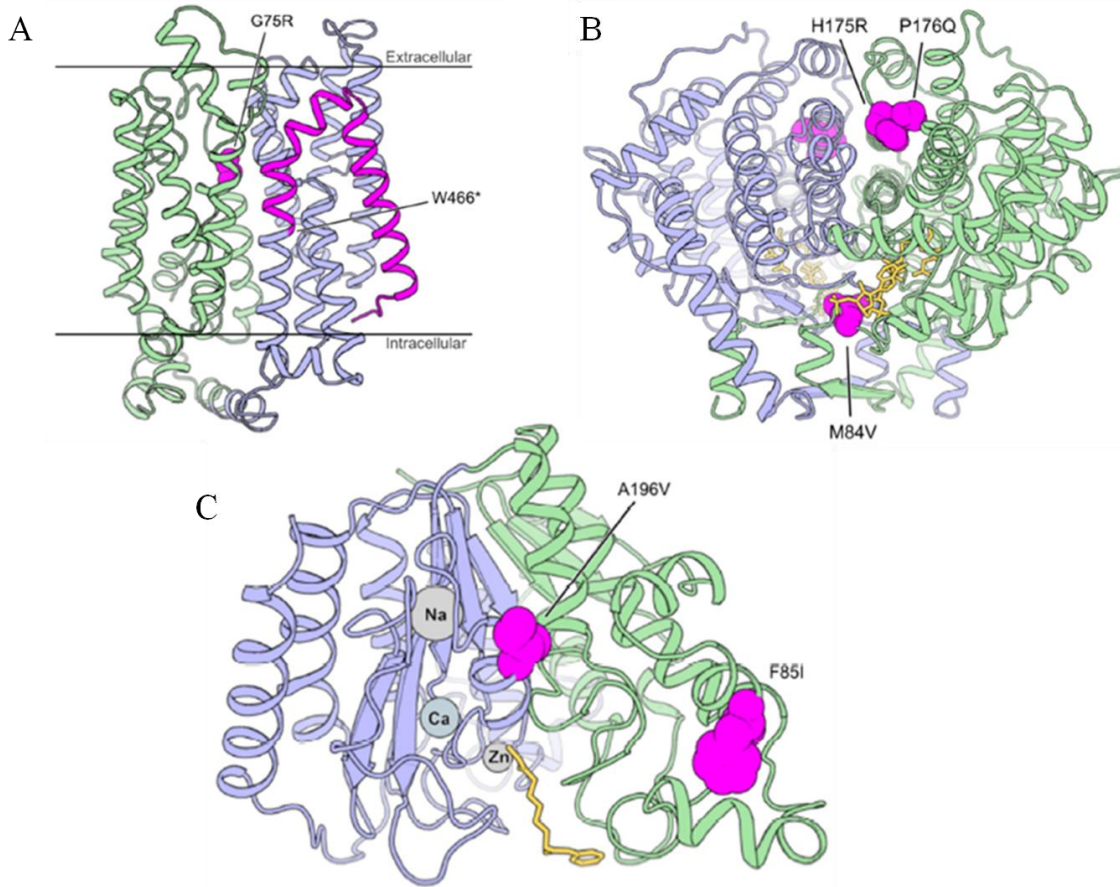


**Figure 14. A cartoon representation of homology protein models generated for Hxt2 (A), Cit1 (B) and Rpd3 (C).** A) An Hxt2 homology model generated using the crystal structure of the human glucose transporter Glut1 (PDB ID: 4PYP). The N-terminal and C-terminal domain of the peptide are shown in pale green and purple, respectively. The global position of the mutation G75R is indicated by magenta sphere representation, and the mutation W466\* by magenta coloring for the deleted protein sequence. Lines indicate the approximate boundaries of the phospholipid bilayer in which the protein performs its function. B) A Cit1 homology model generated using a crystal structure of chicken citrate synthase (PDB ID: 1AL6). The position of mutations is indicated by magenta sphere representations of the amino acids in the two polypeptides of the Cit1 homodimer shown in pale purple and pale green, respectively. The substrate oxaloacetate and the substrate analog N-hydroxyamido-CoA are shown in yellow. C) A Rpd3 homology model generated using a crystal structure of the human histone deacetylase 2 protein (PDB: 4LXZ). The N-terminal and C-terminal domain of the polypeptide are shown in pale green and pale purple, respectively. The global position of mutations is indicated by magenta sphere representations of the amino acids. The enzyme inhibitor Vorinostat co-crystallized with the enzyme is shown in yellow. Metal ions in the structure are shown in grey colors (Na: sodium ion; Ca: calcium ion; Zn: zinc ion.).

The BLAST search performed with Hxt2 resulted in 201 sequences after filtering, which come exclusively from unicellular fungi. In this dataset the G75 position is completely conserved and W466 is also highly conserved at 93% (**Figure 13B**). Furthermore in the W466\* mutant there are many amino acids with close to complete conservation that are missing due to the premature stop codon (**Figure 13B**). A homology model of Hxt2 was generated using the human glucose transporter Glut1 [157] (**Figure 14A**). G75 is positioned in the interface between the N- and C-terminal domains, with the alpha carbon facing inwards in a bundle of four helices that form the substrate channel. W466 and the

residues thereafter comprise one and a half transmembrane alpha helices situated on the outside of the protein, which forms the main constituents of the extracellular gate of the substrate channel [157]. The mutations G75R and W466\* identified in Hxt2 in evolved Pdc strains were likely to impair or completely abolish its activity to transport glucose. Therefore in evolved Pdc negative strains, the glucose transport by the mutated Hxt2 was likely to decrease, despite its transcriptional increase that resulted from the mutations in Mth1.

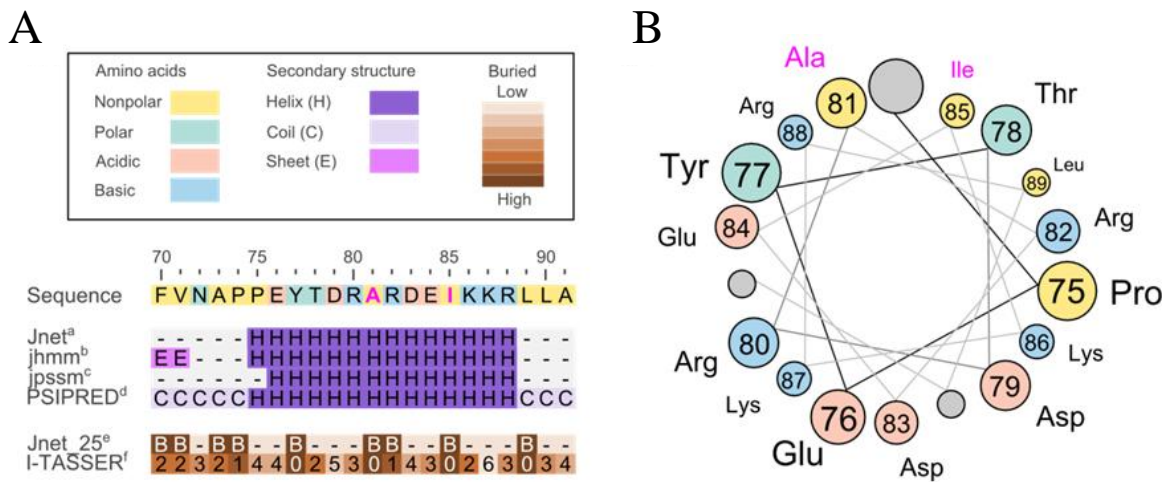


**Figure 15. Predictions on the secondary structure of Mth1 protein.** A) Analysis of the 22 amino acids from the conserved region at position 70-91 and secondary structure predictions using 6 different prediction programs [155, 156]. B) A helix wheel representation of amino acids predicted to form an alpha-helix (Codon 75-89). The amino acid types are colored as in A.

The BLAST search performed with Cit1 resulted in 378 sequences after filtering, which come from unicellular and multicellular fungi, animals and plants. Alignment results revealed that the H175R, P176Q and M84V mutations occurred at positions that are 99%, 98%, and 79% conserved, respectively (**Figure 13C**). A homology model of Cit1 was generated using the chicken citrate synthase crystal structure (**Figure 14B**). All three mutations are situated at the interface between the two polypeptides of the Cit1 homodimer. M84 may serve structural and functionally important roles, and the M84V mutation might lead to a decreased Cit1 enzyme activity due to structural perturbations around the active sites, which in turn would lead to a decrease or loss of substrate binding affinity. H175 likely helps increasing the structural rigidity, and the mutation H175R may therefore lead to incorrect or inefficient protein folding or interfere with interactions between the two monomers. P176 likely serves a structural role initiating an alpha helix, and the mutation P176Q may therefore cause the alpha helix not to form or to form later in the primary sequence, which may cause structural perturbation of several amino acids, including H175.

The BLAST search performed with Rpd3 resulted in 265 sequences after filtering, which come from unicellular and multicellular fungi, plants, animals and a range of bacteria. Analysis of these sequences revealed that the F85 position is 97% conserved and the A196 position is 98% conserved (**Figure 13D**). A homology model of Rpd3 was generated using the crystal structure of the human histone deacetylase 2 protein (**Figure 14C**). F85 is buried in between two alpha helices and a loop in the N-terminal domain, with less conserved surrounding residues. The conservation data and properties of the amino acids in this region indicate that F85 is important for the hydrophobic packing of this region and thus serves a structural role in the protein. A196 is part of an alpha helix that is situated at the interface between the N- and C-terminal domains, which is highly a conserved region. The residues are obviously very sensitive to mutations. It is possible that the two extra methyl groups introduced by the A196V mutation may cause a displacement of the conserved helix and result in decreased or abolished enzyme activity.

Based on the results and the predictions above, some possible mechanisms were proposed for the evolved Pdc negative strains.

In an unevolved Pdc negative strain, although Ach1 could channel acetyl-CoA from the mitochondria to the cytosol, it is only functional under glucose derepressed conditions. And this route can be blocked by the limited mitochondria acetyl-CoA due to the stringent regulation in *S. cerevisiae* (**Figure 16A**), e.g. the regulated activity of the PDH complex via the post-transcriptional phosphorylation of Pda1 subunits [28] or the transcriptional repression of Lpd1 subunits [27].

In the evolved Pdc negative strains, the mutations in Mth1 seemed to play the most critical role, since the allele with a single mutation *MTH1*<sup>81D</sup> alone has been proved to restore the growth of the Pdc negative strain on glucose, as well as *MTH1*- $\Delta T$  [108]. According to the predictions of the conserved ‘island’ (codon 71-91) in Mth1, A81 and I85 may play a structural role in maintaining the putative alpha helix formed within it, and thus the mutations on either site probably affect the phosphorylation region of Yck1 in another adjacent conserved ‘island’. However, a crystal structure of Mth1 would be instrumental to validate these predictions. The *MTH1* alleles seem to decrease glucose uptake transport by repressing the transcription of several *HXTs* (**Figure 12**) [111, 112, 114, 115], which was also observed in the TAM strain by van Maris *et al* [107]. Moreover, a regional deletion within *HXT3* (~1000 bp) in an evolved strain E1C would undoubtedly destroy its activity to transport glucose. A previous study suggested that the rate of glucose transport determines the strength of glucose repression [158]. With the reduced glucose uptake, the transcription of many glucose repressed genes, e.g. those encoding mitochondrial enzymes, could probably be partially derepressed despite the high extracellular glucose. Therefore, in the evolved Pdc negative strains with the

mutations in *MTH1*, it is possible that the cytosolic acetyl-CoA supply shuttled from the mitochondria via Ach1 route was no longer blocked (**Figure 16B**).

The mutations in *HXT2* seemed to make no sense in high glucose medium (2% glucose) used in this study, since its expression is usually induced by low glucose and repressed by high glucose [147, 159]. One possible explanation would be the possible complicated effects of the mutated Mth1. Transcriptional analysis of the TAM strain showed decreased transcription of *HXT1*, *HXT3*, *HXT4*, *HXT6* and *HXT7*, and increased transcription of *HXT2* and *HXT5* [107], which is consistent with our qPCR results (**Figure 12**). The mutations in Hxt2 might result in structural disruptions based on our predictions, and may therefore further reduce glucose transport in this strain.

The mutations in *CIT1* might also be connected with cytosolic acetyl-CoA supply via the Ach1 route. As shown in **Figure 16B**, Cit1 competes with Ach1 for the substrate acetyl-CoA in the mitochondria. The mutated Cit1 with potentially decreased activity, as predicted by the bioinformatics analysis of the identified mutations, might allow for more acetyl-CoA being converted to acetate by Ach1, and would therefore provide more acetate for cytosolic acetyl-CoA biosynthesis. The previous study on Ach1 suggested that C<sub>2</sub> supply in the cytosol seemed to be a limiting step for the growth of Pdc negative strains. Thus, the Cit1 mutations might further improve growth on glucose in the presence of the mutated Mth1. However, when *CIT1* was disrupted in the strain M81, the growth on glucose was significantly impaired (data not shown), since the complete disruption of *CIT1* would result in the dysfunction of the TCA cycle and hereby significantly reduce the ability to generate ATP required for growth.

Although the Rpd3 mutations were predicted to result in activity decreases, it is still too difficult to speculate about their roles in the evolved Pdc negative strains, since more and more studies suggest that histone acetylation and deacetylation regulate gene transcription in complex and comprehensive ways [160]. A previous study found that histone acetylation and deacetylation was directly related with nucleocytosolic acetyl-CoA abundance [19]. One possible speculation would be that the mutations in Rpd3 might be related to cytosolic acetyl-CoA abundance as well, but this will require further investigation.

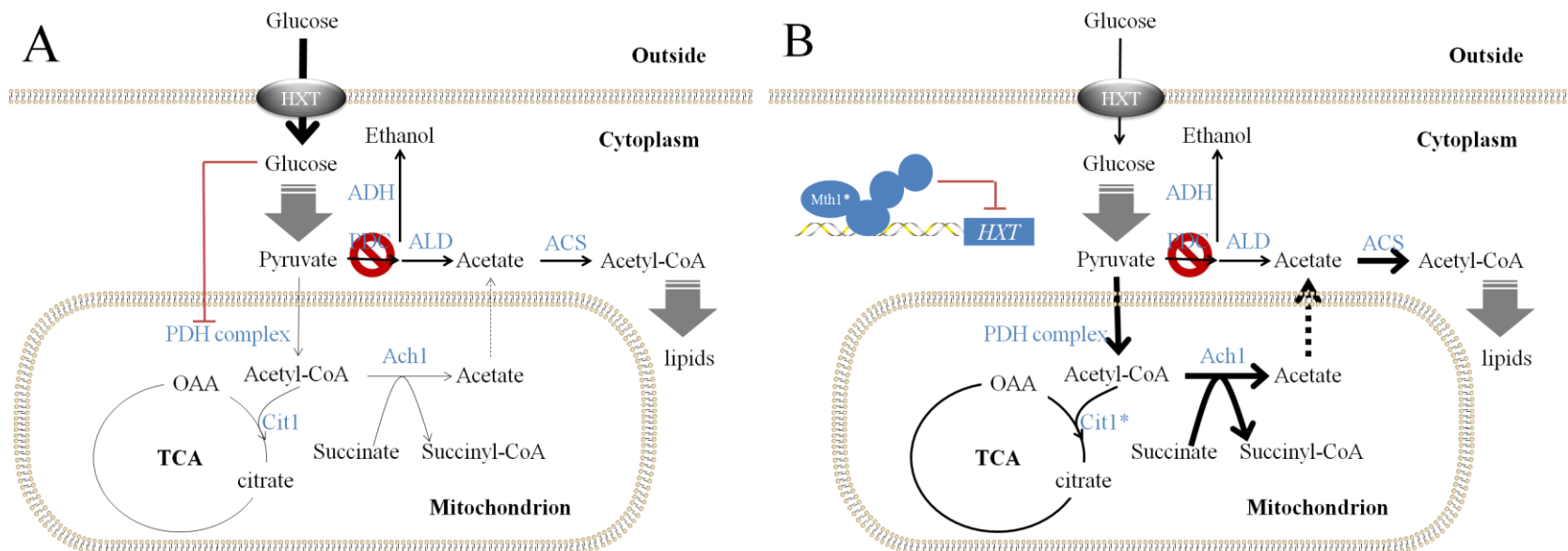


**Figure 16. A simple illustration for the possible roles of the mutated proteins in the evolved pdc negative strains.** The solid arrows represent the reactions catalyzed by the enzymes, which are indicated in blue text. The dash line represents the transportation between different subcellular organelles. The red lines with a bar at one end represent the repression or inhibition. The red circles represent the block due to *PDC* deletions. A) Simplified acetyl-CoA metabolism in the parental Pdc negative strain. The PDH complex and TCA cycle enzymes are repressed by high glucose uptake via hexose transporters (HXTs). B) Simplified acetyl-CoA metabolism in evolved Pdc negative strains with point mutated *Mth1* (*Mth1\**) and *Cit1* (*Cit1\**). Glucose uptake via HXT decreases in the presence of *Mth1\**, resulting in derepression of the PDH complex and TCA cycle enzymes. *Cit1\** with predicted decreased activity allows more mitochondria acetyl-CoA convert to acetate by *Ach1*, which can be transported to the cytosol and converted to acetyl-CoA there.

### 3.3 Functional bacterial pyruvate formate lyase expressed in a Pdc negative strain

Pdc negative strains can serve as potential non-ethanol producing platform strains for biochemical production. However, they cannot grow on glucose as the sole carbon source. Although *MTH1-ΔT* can restore its growth on glucose, its capacity for glucose consumption is limited as well as the cytosolic acetyl-CoA supply. In order to increase cytosolic acetyl-CoA supply in IMI076, an alternate synthetic pathway, pyruvate formate lyase (PFL) pathway from *E. coli*, was introduced to convert pyruvate to acetyl-CoA in the cytosol.

The PFL is activated by its activating enzyme PFL-AE with two other cofactors (or co-substrates), reduced flavodoxin and S-adenosylmethionine (SAM) [161]. The PFL-AE uses reduced flavodoxin as an electron donor and SAM as a co-substrate to generate a free radical (5'-dA<sup>·</sup>) for PFL activation [162]. In an *in vitro* study it was found that other artificial one-electron reductants can also serve as the electron donor for the PFL pathway [163]. Functional PFL pathway from *E. coli* and *Lactobacillus plantarum* has been expressed in yeast under anaerobic conditions [16, 164]. Waks and Silver coexpressed *pflA* (PFL gene) and *pflB* (PFL activating enzyme gene) in a strain with deletions in both formate dehydrogenase (FDH) genes, *FDH1* and *FDH2*, which increased formate production by 4.5 fold under anaerobic conditions [164]. Kozak *et al.* found that *pflA* and *pflB* co-expression could restore growth of an ACS deficient (*acs1Δ acs2Δ*) mutant on glucose under anaerobic conditions, by complementing cytosolic acetyl-CoA synthesis [16]. In these studies the cofactors were, however, not co-expressed even though it was speculated that there could be other cytosolic, single-electron donors replacing reduced flavodoxin to activate PFL [164].

In this study, the PFL pathway (encoded by *pflA* and *pflB*) was expressed in IMI076, or with two different cofactors and their reductase (*fdx-fpr*, *fldA-fpr*). We found that the co-expressed cofactors, especially *fldA-fpr*, facilitates the PFL pathway function at aerobic growth conditions, which could be useful for its application in yeast bioprocesses that have to be operated at aerobic conditions.

*pflA* and *pflB* from *E. coli* were codon-optimized for expression in *S. cerevisiae*, and cloned under the control of the constitutive promoters *P<sub>PGK1</sub>* and *P<sub>TEF1</sub>* respectively into the vector pSP-GM1 [139], yielding pPFL01. pSP-GM1 and pPFL01 were transformed into the background strain IMI076 respectively, yielding YZ10 and YZ11. Two transformants of each strains were picked and cultured in glucose minimal medium at aerobic growth conditions using Bioscreen C. Growth results revealed that, two YZ11 transformants (with the PFL pathway) reached a higher final biomass, compared with two YZ10 transformants (without the PFL pathway) (**Figure 17A**). No major growth difference was observed between different transformants for both strains. The growth of YZ10-1 and YZ11-1 was further confirmed by culturing in shake flasks, as shown in **Figure 17B**. However, a small improvement in final biomass concentration was observed with the PFL pathway expressed (**Figure 17**). As reported by *in vitro* studies, the activated PFL is

sensitive to oxygen and it cleaves into fragments at the activation site when exposed to oxygen [165]. Therefore, the function of the PFL pathway with constitutive expression was limited under aerobic conditions, which may explain the small increase in the final biomass concentration.

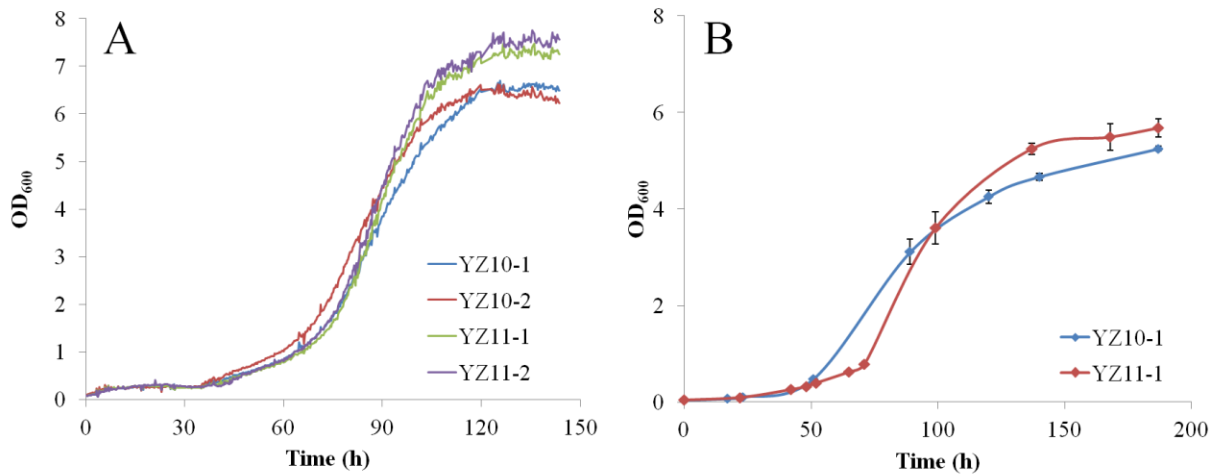


**Figure 17. Growth comparisons of the strains with and without the PFL pathway** in minimal medium using Bioscreen C (A) and shake flasks (B). A) Two YZ10 transformants YZ10-1 and YZ10-2 (without PFL pathway), and two YZ11 transformants YZ11-1 and YZ11-2 (with PFL pathway) were cultured in octuplicate, and the standard deviations (not shown here) were within 5%. B) YZ10-1 and YZ11-1 were cultured in triplicate in shake flasks.

Two cofactors and their reductase, ferredoxin (encoded by *fdx*) and ferredoxin NADP<sup>+</sup> reductase (encoded by *fpr*), and flavodoxin (encoded by *fldA*) and flavodoxin NADP<sup>+</sup> reductase (encoded by *fpr*), were introduced together with the PFL pathway (*pflA* and *pflB*) by being cloned in one plasmid to the background strain IMI076 respectively, resulting in strain YZ12 and YZ13, respectively. Three different transformants of each strain were picked and cultured using minimal medium with 2% glucose in shake flasks, to evaluate the role of the cofactors in the PFL pathway.

As shown in **Figure 18**, all transformants of YZ12 (with PFL pathway and ferredoxin) and YZ13 (with PFL pathway and flavodoxin) reached higher final biomass concentrations, compared with YZ10 (without PFL pathway) and YZ11 (with PFL pathway). However, three transformants of YZ12 and YZ13, respectively, showed different growth behavior. As shown in **Figure 18** and **Table 2**, the three transformants of YZ12 differed from each other in lag phase, maximum specific growth rate and the final biomass concentration, and those of YZ13 differed from each other in the lag phase and the maximum specific growth rate (**Table 2**), but all reached a similar final biomass concentration (**Figure 18B**).

Overall, the transformants with *fldA-fpr* co-expressed showed higher final biomass concentrations than those with *fdx-fpr*, as well as higher specific growth rates in the late growth phase. Moreover, YZ13 transformants consumed all the supplied glucose and accumulated no pyruvate in the culture (**Table 2**). Therefore, reduced flavodoxin seems to be a more efficient cofactor for the PFL pathway than reduced ferredoxin. Although reduced ferredoxin and

flavodoxin can both serve as single electron donors, some enzymes require either one or the other [166, 167]. In *E. coli*, ferredoxin does not substitute for flavodoxin for PFL activation [168], which probably explains why *fdx-fpr* co-expression did not contribute much to biomass formation.

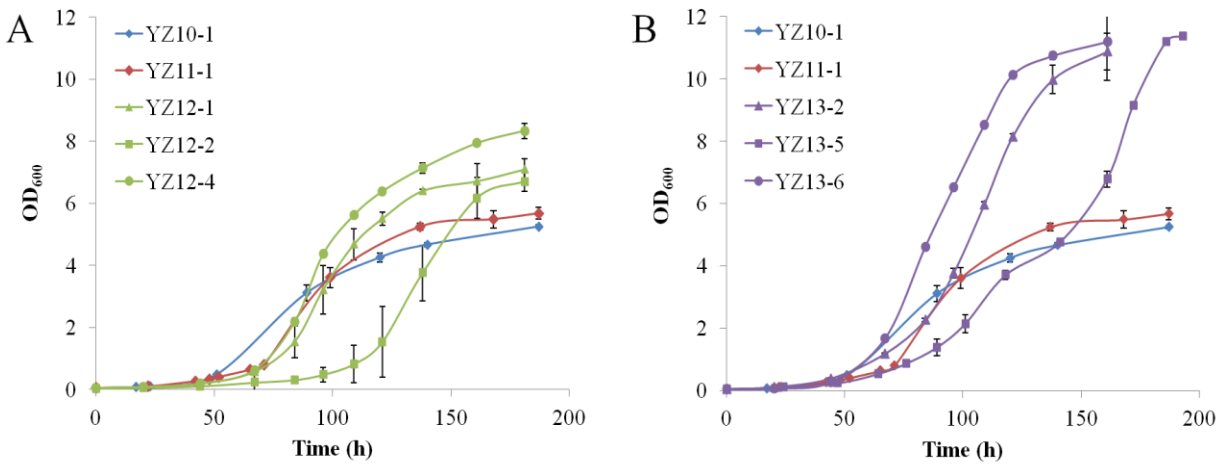


**Figure 18. Growth comparisons of YZ10, YZ11, YZ12 and YZ13 in minimal medium using shake flasks.** (A) YZ10-1 (without PFL pathway), YZ11-1 (with PFL pathway), and three YZ12 transformants (YZ12-1, YZ12-2, YZ12-4, with PFL pathway and cofactor ferredoxin); (B) YZ10, YZ11 and three YZ13 transformants (YZ13-2, YZ13-5, YZ13-6, with PFL pathway and cofactor flavodoxin).

**Table 2. Strain properties of YZ10, YZ11, YZ12 and YZ13.**

	$\mu_{\max}$ (h <sup>-1</sup> )	Y <sub>Pyr</sub> (g pyruvate / g glucose)	Y <sub>Gly</sub> (g glycerol / g glucose)	Residual glucose (g/L)	Residual pyruvate (g/L)
YZ10-1	0.055	0.326	0.023	3.97±0.34	3.72±0.04
YZ11-1	0.052	0.316	0.026	2.97±0.10	3.84±0.06
YZ12-1	0.060	0.204	0.021	3.15±0.47	3.22±0.15
YZ12-2	0.052	0.248	0.021	4.06±0.52	3.29±0.02
YZ12-4	0.068	0.255	0.012	2.36±0.07	3.29±0.08
YZ13-2	0.050	0.087	0.025	0.00±0.00	0.00±0.00
YZ13-5	0.045	0.100	0.076	0.00±0.00	0.00±0.00
YZ13-6	0.066	0.108	0.021	0.00±0.00	0.00±0.00

Due to the differences in the growth behavior of the three transformants of each type, we therefore tested gene expression of the four introduced genes via qPCR. Cells for gene expression analysis were cultured in minimal medium and harvested at several different time points during the cultivations. *ACT1* was selected as the reference gene. The results revealed that the expression levels of *pflB* and *pflA* varied up to 2-fold between three YZ12 transformants (**Figure 19A**), and up to 5-fold between three YZ13 transformants (**Figure 19B**). These results indicated that higher expression level of *pflA* or *pflB* might not be beneficial for higher final biomass

concentration. However, YZ13-5 with a relatively low expression of *fldA* showed delayed growth and a higher glycerol yield on glucose. These results suggested that the expression levels of the cofactors might be crucial for optimal function of the PFL pathway under aerobic conditions.

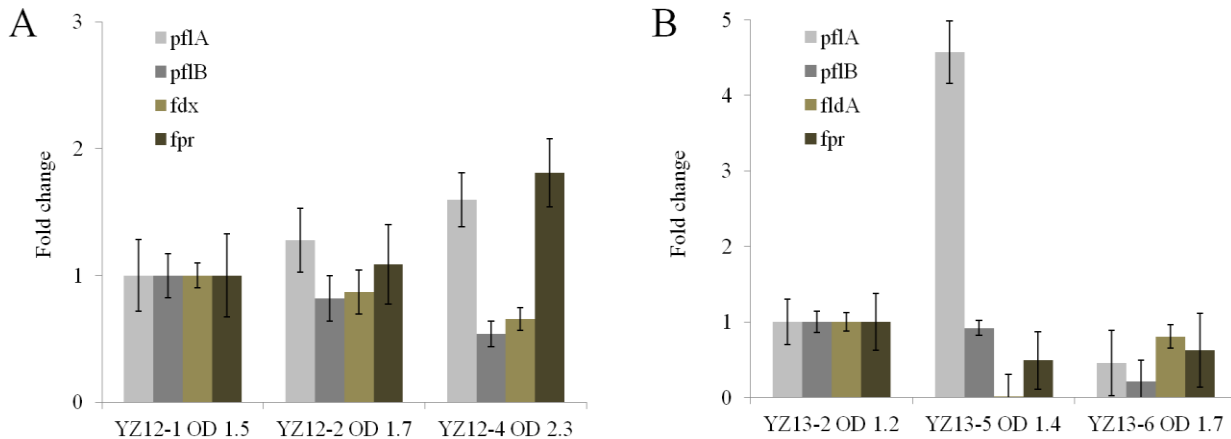


**Figure 19 Expression analysis of introduced genes in YZ12 (A) and YZ13 (B).** (A) Gene expression analysis of three YZ12 transformants. Samples were taken at OD<sub>600</sub> between 1-2.5 for the transcription analysis of 4 introduced genes (*pflA*, *pflB*, *fdx*, and *fpr*). The gene expression levels of introduced genes in YZ12-1 were set as 1. (D) Gene expression analysis of three YZ13 transformants. Samples were taken at OD<sub>600</sub> between 1-2.5 for the transcription analysis of 4 introduced genes (*pflA*, *pflB*, *fldA*, and *fpr*). The gene expression levels of introduced genes in YZ13-2 were set as 1.

However, no formate byproduct was detected at aerobic growth in our study, which was a different observation from that when the PFL pathway was expressed under anaerobic conditions [16, 164]. This might be caused by different activities of FDHs under aerobic and anaerobic conditions, which convert formate to CO<sub>2</sub>. In a previous study, it seemed that formate assimilation by FDHs was not as efficient under anaerobic conditions [164] as aerobic conditions [169], probably due to inefficient NAD<sup>+</sup> recycling in the absence of electron transport chain and oxidative phosphorylation at anaerobic growth. Therefore the transcription levels of *FDH1* and *FDH2* were measured in the different constructed strains, as shown in **Figure 20**. In YZ10-1, the FDHs expression levels increased about 5-fold. In YZ11-1, their expression levels increased about 3 fold. In YZ13-2, their expression levels did not increase when OD<sub>600</sub> increased from 1.2 to 2.3, but increased more than 25 fold when OD<sub>600</sub> reached 8.1. In YZ13-6, the expression levels increased above 20 fold when the OD<sub>600</sub> increased from 1.7 to 4.6, and above 15 fold when OD<sub>600</sub> reached 8.5.

FDHs expression is reported to be induced by methanol or formate, or with glycine as the sole nitrogen source. When the PFL pathway was expressed in an *Acs*<sup>-</sup> mutant under anaerobic glucose-limited chemostat conditions, the transcript levels of *FDH1* and *FDH2* were over 25-fold higher than those in the wild type [16]. Therefore, the small transcription increase in YZ10-1 and YZ11-1 may result from activities of some unknown reactions related with FDHs [169], whereas the large increase in the two YZ13 transformants probably resulted from a direct response to formate production.

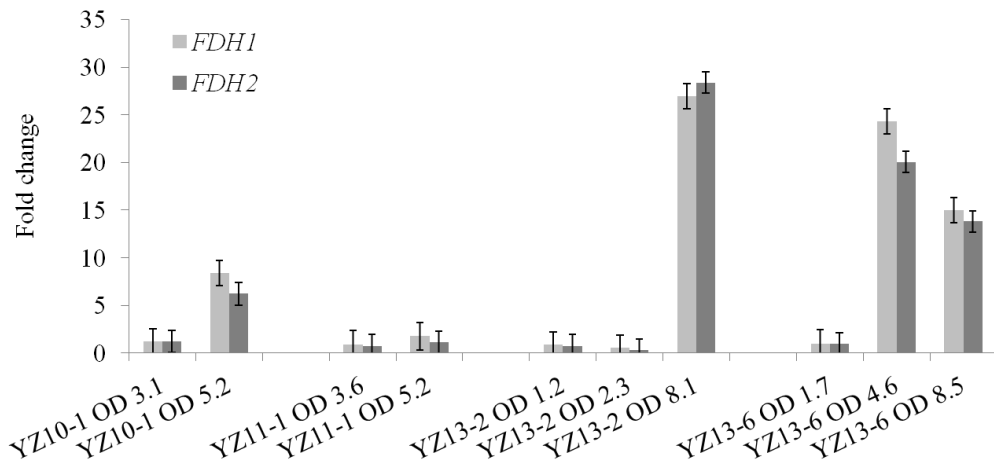


**Figure 20. Expression analysis of *FDH1* and *FDH2* in YZ10-1, YZ11-1, YZ13-2 and YZ13-6.** *FDH1* and *FDH2* expression levels of YZ13-6 at OD<sub>600</sub> 1.7 are set to 1.

*FDHs* expression results suggested that the PFL pathway may function during the late growth phase (OD<sub>600</sub> above 4), when major induced expression was observed (**Figure 20**). This was consistent with the fact that the PFL pathway with its cofactors mostly contributed to increases in the final biomass concentrations, but not always in the maximum specific growth rates (**Figure 18** and **Table 2**). It indicated that the native pathway (the route via Ach1) provided the cytosolic acetyl-CoA required for growth during the exponential growth phase, while the PFL pathway supplied additional cytosolic acetyl-CoA via pyruvate assimilation. However, it is difficult to explain why it would mainly function during the late growth phase. One hypothesis is that higher cell density in the late growth phase may result in lower dissolved oxygen concentration, which then affected PFL.

## Chapter 4. Conclusions and perspective

Yeast serves as a cell factory for production of a wild range of bio-compounds. Acetyl-CoA is an important metabolite as well as precursor for many biochemicals, *e.g.* 1-butanol, PHB, and its cytosolic supply is found to be a limiting factor for synthesis of these bioproducts. Despite many successful strategies for increased cytosolic acetyl-CoA supply, several questions related to cytosolic acetyl-CoA supply remain to be answered. We took the advantage of adaptive laboratory evolution and metabolic engineering, and investigated cytosolic acetyl-CoA supply in a non-ethanol-producing yeast strain. Based on the results and findings presented, we have advanced the understanding of cytosolic acetyl-CoA supply, and could make the following conclusions.

First, the metabolism of acetyl-CoA is highly compartmentalized, and it cannot be directly transported between these subcellular compartments. With help of glyoxylate shuttle, acetyl-CoA produced in the peroxisomes can be shuttled into the cytoplasm or the mitochondria. When carnitine is supplemented into the medium, acetyl-CoA can be transported between the cytoplasm, mitochondria and peroxisomes [77]. However, it was still unclear whether acetyl-CoA generated in the mitochondria can be exported to the cytoplasm without carnitine supplemented. Using a Pdc negative strain IMI076 (*Pdc<sup>-</sup> MTH1-ΔT ura3-52*), having a reduced glucose uptake rate due to a mutation in the transcriptional regulator *Mth1*, we identified a route relying on *Ach1* that could transfer acetyl units from mitochondria to the cytoplasm in the form of acetate. These results advance the fundamental understanding of acetyl-CoA metabolism in yeast, and could therefore be helpful for construction of yeast cell factories.

Second, with adaptive evolution in glucose medium via serial transfer, three independently evolved strains from a Pdc negative strain were obtained, which were able to grow in minimal medium containing glucose as the sole carbon source at maximum specific rates of  $0.138\text{ h}^{-1}$ ,  $0.148\text{ h}^{-1}$ ,  $0.141\text{ h}^{-1}$ , respectively. Genome sequencing identified several genetic changes that occurred during the evolution process, among which 4 genes were found to carry point mutations in at least two of the evolved strains: *MTH1*, *HXT2*, *CIT1*, and *RPD3*. Reverse engineering showed that the *MTH1<sup>81D</sup>* allele is partially responsible for restoring growth of the evolved Pdc negative strains by repressing the total transcriptions of several *HXTs*. The non-synonymous mutations in *HXT2* and *CIT1* may function in the presence of mutated *MTH1* alleles and could be related to the cytosolic acetyl-CoA in a Pdc negative strain. In connection to the *Ach1* related acetyl-CoA shuttle route, possible mechanisms were proposed for the generation of acetyl-CoA in evolved Pdc negative strains.

Last but not the least, in connection with establishing a non-ethanol producing yeast platform strain, alternative heterologous pathways can be introduced to increase cytosolic acetyl-CoA supply. In this study, pyruvate formate lyase (PFL) and its activating enzyme from *E. coli* were expressed in a Pdc negative strain, IMI076, as an alternate pathway. PFL is characterized as an enzyme functional at anaerobic conditions, since the radical in the enzyme's active form is sensitive to oxygen. In this study, the PFL pathway was expressed with two different cofactors as

electron donors, ferredoxin or flavodoxin, respectively, and it was found that the co-expression either of these cofactors had a positive effect on growth under aerobic conditions, indicating increased activity of PFL. The positive effect on growth was manifested as a higher final biomass concentration and a significant increase in transcription of formate dehydrogenases (FDHs). Among the two cofactors reduced flavodoxin was found to be a better electron donor than reduced ferredoxin.

## Acknowledgments

Looking back on the last four years, I could remember plenty of moments - exciting moments, frustrating moments, joyful moments, painful moments, exhausting moments, relaxing moments; and also people around who shared these happy moments together as well as helped me through those hard moments.

With that, first of all, I would like to sincerely thank my supervisor, Professor Jens Nielsen, for offering me this opportunity to be part of the big Sys<sup>2</sup>Bio family, giving valuable suggestions and freedom on my project, and encouraging and supporting me along the four years. His great expertise, inspiring smiles, optimistic attitudes, unbelievable efficiencies, open minded instructions are crucial for the accomplishment of my thesis. Jens, thank you very much for all your support, instructions, patience, encouragements, and suggestions along the way. What I learned from you are precise treasures for life.

My great gratitude also goes to my co-supervisors, Dr Verena Siewers and Dr. Anastasia Krivoruchko, for giving me their professional and detailed instructions, which helped to grow as a young scientists. Thank you, Verena and Anastasia, you were always there when I needed trouble-shootings. And a special acknowledgment goes to Dr Yun Chen, for inspiring discussions and great efforts to the project.

I would like to acknowledge my close collaborators, Dr Martin KM Engqvist, Dr. Björn M Hallström, Dr. Lifang Liu, Dr Zongjie Dai for their productive discussions and contributions to the project. And Professor Christer Larsson, Professor Ivan Mijakovic, Associate Professor Dina Petranovic, and Docent Joakim Norbeck are also thanked for their excellent comments in the seminars.

I would like to thank all of the administrators and research engineers, Erica Dahlin, Helena Janveden, Martina Butorac, Anna Bolling, Marie Nordqvist, Ximena Rozo Sevilla, Malin Nordvall, Suwanee Jansa-Ard, Emma Ribbenhed, Julia Karlsson, Andreas Hellström for their professional assistance in the office and in the lab.

In addition to the people mentioned above, I also would like to acknowledge many close colleagues and friends for their help and accompany. Ik-Kwon Kim, Jin Hou, Xin Chen, Mingtao Huang, Rahul Kumar, Yongji Zhou, Klaas Buijs, Guodong Liu, Jichen Bao, Yating Hu, Bouke de Jong, Shuobo Shi, David Jullesson, Mingji Li, Juan Valle, Cheng Zhang, Mark Bisschops, Jiufu Qin, Abderahmane Derouiche, Eugene Fletcher, Zhiwei Zhu, Michael Gossing, Ruifei Wang, Sterfan Tippmann, Lei Shi, Min-Kyoung Kang, Boyang Ji, Paulo Teixeira, Yongjun Wei, Clara Navarrete, Florin David, Zihe Liu, Hülya Karaca Gençer, Eduard Kerkhoven, Petri-Jaan Lahtvee, Jos éL. Martínez, Payam Ghiaci, Nina Johansson, Tao Yu, Luis Caspeta-Guadarrama, Kanokarn Kocharin and all of you in sysbio group, thank you very much for being around and always supportive.

A special acknowledgement goes to China Scholarship Council and my domestic responsibility supervisor Professor Ju Chu, for their support, caring, advices and encouragements since I planned my PhD study.

Finally, I own my deepest gratitude to my families, my parents and grandparents, for their forever and unconditional love and support. And thanks my boyfriend for being there with all my moods.

# References

1. Nielsen, J., et al., *Metabolic engineering of yeast for production of fuels and chemicals*. Curr Opin Biotechnol, 2013. **24**(3): p. 398-404.
2. Nielsen, J. and M.C. Jewett, *Impact of systems biology on metabolic engineering of *Saccharomyces cerevisiae**. FEMS Yeast Res, 2008. **8**(1): p. 122-31.
3. Hong, K.K. and J. Nielsen, *Metabolic engineering of *Saccharomyces cerevisiae*: a key cell factory platform for future biorefineries*. Cell Mol Life Sci, 2012. **69**(16): p. 2671-90.
4. Nielsen, J., et al., *Engineering synergy in biotechnology*. Nat Chem Biol, 2014. **10**(5): p. 319-22.
5. Chen, Y. and J. Nielsen, *Advances in metabolic pathway and strain engineering paving the way for sustainable production of chemical building blocks*. Curr Opin Biotechnol, 2013. **24**(6): p. 965-72.
6. Nielsen, J., *Synthetic biology for engineering acetyl coenzyme A metabolism in yeast*. MBio, 2014. **5**(6).
7. Krivoruchko, A., et al., *Microbial acetyl-CoA metabolism and metabolic engineering*. Metab Eng, 2014. **28C**(0): p. 28-42.
8. Shiba, Y., et al., *Engineering of the pyruvate dehydrogenase bypass in *Saccharomyces cerevisiae* for high-level production of isoprenoids*. Metab Eng, 2007. **9**(2): p. 160-8.
9. Chen, Y., et al., *Establishing a platform cell factory through engineering of yeast acetyl-CoA metabolism*. Metabolic Engineering, 2013. **15**: p. 48-54.
10. Chen, Y., V. Siewers, and J. Nielsen, *Profiling of Cytosolic and Peroxisomal Acetyl-CoA Metabolism in *Saccharomyces cerevisiae**. PLoS One, 2012. **7**(8).
11. Krivoruchko, A., et al., *Improving biobutanol production in engineered *Saccharomyces cerevisiae* by manipulation of acetyl-CoA metabolism*. Journal of Industrial Microbiology & Biotechnology, 2013. **40**(9): p. 1051-1056.
12. Kocharin, K., et al., *Engineering of acetyl-CoA metabolism for the improved production of polyhydroxybutyrate in *Saccharomyces cerevisiae**. AMB Express, 2012. **2**(1): p. 52.
13. de Jong, B.W., et al., *Improved production of fatty acid ethyl esters in *Saccharomyces cerevisiae* through up-regulation of the ethanol degradation pathway and expression of the heterologous phosphoketolase pathway*. Microb Cell Fact, 2014. **13**(1): p. 39.
14. Papini, M., et al., *Physiological characterization of recombinant *Saccharomyces cerevisiae* expressing the *Aspergillus nidulans* phosphoketolase pathway: validation of activity through <sup>13</sup>C-based metabolic flux analysis*. Appl Microbiol Biotechnol, 2012. **95**(4): p. 1001-10.
15. Kocharin, K., V. Siewers, and J. Nielsen, *Improved polyhydroxybutyrate production by *Saccharomyces cerevisiae* through the use of the phosphoketolase pathway*. Biotechnol Bioeng, 2013. **110**(8): p. 2216-24.
16. Kozak, B.U., et al., *Replacement of the *Saccharomyces cerevisiae* acetyl-CoA synthetases by alternative pathways for cytosolic acetyl-CoA synthesis*. Metab Eng, 2014. **21**: p. 46-59.
17. Lian, J., et al., *Design and construction of acetyl-CoA overproducing *Saccharomyces cerevisiae* strains*. Metab Eng, 2014. **24**: p. 139-49.
18. Kozak, B.U., et al., *Engineering Acetyl Coenzyme A Supply: Functional Expression of a Bacterial Pyruvate Dehydrogenase Complex in the Cytosol of *Saccharomyces cerevisiae**. MBio, 2014. **5**(5).
19. Takahashi, H., et al., *Nucleocytosolic acetyl-coenzyme A synthetase is required for histone acetylation and global transcription*. Molecular Cell, 2006. **23**(2): p. 207-217.
20. Suissa, M., K. Suda, and G. Schatz, *Isolation of the nuclear yeast genes for citrate synthase and fifteen other mitochondrial proteins by a new screening method*. EMBO J, 1984. **3**(8): p. 1773-81.
21. Jia, Y.K., A.M. Becam, and C.J. Herbert, *The CIT3 gene of *Saccharomyces cerevisiae* encodes a second mitochondrial isoform of citrate synthase*. Mol Microbiol, 1997. **24**(1): p. 53-9.
22. Hartig, A., et al., *Differentially regulated malate synthase genes participate in carbon and nitrogen metabolism of *S. cerevisiae**. Nucleic Acids Res, 1992. **20**(21): p. 5677-86.
23. Stoops, J.K., et al., *On the unique structural organization of the *Saccharomyces cerevisiae* pyruvate dehydrogenase complex*. J Biol Chem, 1997. **272**(9): p. 5757-64.
24. Stoops, J.K., et al., *Three-dimensional structure of the truncated core of the *Saccharomyces cerevisiae* pyruvate dehydrogenase complex determined from negative stain and cryoelectron microscopy images*. J Biol Chem, 1992. **267**(34): p. 24769-75.
25. Maeng, C.Y., et al., *Expression, purification, and characterization of the dihydrolipoamide dehydrogenase-binding protein of the pyruvate dehydrogenase complex from *Saccharomyces cerevisiae**. Biochemistry, 1994. **33**(46): p. 13801-7.
26. Pronk, J.T., H.Y. Steensma, and J.P. vanDijken, *Pyruvate metabolism in *Saccharomyces cerevisiae**. Yeast, 1996. **12**(16): p. 1607-1633.
27. Bowman, S.B., et al., *Positive regulation of the LPD1 gene of *Saccharomyces cerevisiae* by the HAP2/HAP3/HAP4 activation system*. Mol Gen Genet, 1992. **231**(2): p. 296-303.
28. Gey, U., et al., *Yeast pyruvate dehydrogenase complex is regulated by a concerted activity of two kinases and two phosphatases*. J Biol Chem, 2008. **283**(15): p. 9759-67.

29. Singh, K.K., G.M. Small, and A.S. Lewin, *Alternative topogenic signals in peroxisomal citrate synthase of *Saccharomyces cerevisiae**. Mol Cell Biol, 1992. **12**(12): p. 5593-9.
30. Lee, J.G., et al., *Identification of a cryptic N-terminal signal in *Saccharomyces cerevisiae* peroxisomal citrate synthase that functions in both peroxisomal and mitochondrial targeting*. Journal of Biochemistry, 2000. **128**(6): p. 1059-1072.
31. Hoosein, M.A. and A.S. Lewin, *Derepression of citrate synthase in *Saccharomyces cerevisiae* may occur at the level of transcription*. Mol Cell Biol, 1984. **4**(2): p. 247-53.
32. Lewin, A.S., V. Hines, and G.M. Small, *Citrate synthase encoded by the CIT2 gene of *Saccharomyces cerevisiae* is peroxisomal*. Mol Cell Biol, 1990. **10**(4): p. 1399-1405.
33. Graybill, E.R., et al., *Functional comparison of citrate synthase isoforms from *S. cerevisiae**. Arch Biochem Biophys, 2007. **465**(1): p. 26-37.
34. Kim, K.S., M.S. Rosenkrantz, and L. Guarente, **Saccharomyces cerevisiae* contains two functional citrate synthase genes*. Mol Cell Biol, 1986. **6**(6): p. 1936-42.
35. Rosenkrantz, M., et al., *The Hap2,3,4 Transcriptional Activator Is Required for Derepression of the Yeast Citrate Synthase Gene, Cit1*. Molecular Microbiology, 1994. **13**(1): p. 119-131.
36. Rosenkrantz, M., et al., *Distinct upstream activation regions for glucose-repressed and derepressed expression of the yeast citrate synthase gene CIT1*. Current Genetics, 1994. **25**(3): p. 185-195.
37. Liu, Z.C. and R.A. Butow, *A transcriptional switch in the expression of yeast tricarboxylic acid cycle genes in response to a reduction or loss of respiratory function*. Mol Cell Biol, 1999. **19**(10): p. 6720-6728.
38. Jia, Y.K., et al., *A basic helix-loop-helix-leucine zipper transcription complex in yeast functions in a signaling pathway from mitochondria to the nucleus*. Molecular and Cellular Biology, 1997. **17**(3): p. 1110-1117.
39. Chelstowska, A. and R.A. Butow, *RTG genes in yeast that function in communication between mitochondria and the nucleus are also required for expression of genes encoding peroxisomal proteins*. Journal of Biological Chemistry, 1995. **270**(30): p. 18141-18146.
40. Ferreira, J.R., et al., *Interaction between Rtg2p and Mks1p in the regulation of the RTG pathway of *Saccharomyces cerevisiae**. Gene, 2005. **354**: p. 2-8.
41. Liao, X.S., et al., *Intramitochondrial functions regulate nonmitochondrial citrate synthase (CIT2) expression in *Saccharomyces cerevisiae**. Mol Cell Biol, 1991. **11**(1): p. 38-46.
42. Kispal, G., et al., *Metabolic studies on citrate synthase mutants of yeast. A change in phenotype following transformation with an inactive enzyme*. Journal of Biological Chemistry, 1989. **264**(19): p. 11204-10.
43. Kispal, G., et al., *Metabolic changes in *Saccharomyces cerevisiae* strains lacking citrate synthases*. Journal of Biological Chemistry, 1988. **263**(23): p. 11145-9.
44. Velot, C., et al., *Metabolic effects of mislocalized mitochondrial and peroxisomal citrate synthases in yeast *Saccharomyces cerevisiae**. Biochemistry, 1999. **38**(49): p. 16195-204.
45. Yoo, H.S., F.S. Genbauffe, and T.G. Cooper, *Identification of the ureidoglycolate hydrolase gene in the DAL gene cluster of *Saccharomyces cerevisiae**. Mol Cell Biol, 1985. **5**(9): p. 2279-88.
46. Kunze, M., et al., *Targeting of malate synthase I to the peroxisomes of *Saccharomyces cerevisiae* cells depends on growth on oleic acid medium*. European Journal of Biochemistry, 2002. **269**(3): p. 915-22.
47. Caspary, F., A. Hartig, and H.J. Schuller, *Constitutive and carbon source-responsive promoter elements are involved in the regulated expression of the *Saccharomyces cerevisiae* malate synthase gene MLS1*. Mol Gen Genet, 1997. **255**(6): p. 619-27.
48. Kratzer, S. and H.J. Schuller, *Transcriptional control of the yeast acetyl-CoA synthetase gene, ACS1, by the positive regulators CAT8 and ADRI and the pleiotropic repressor UME6*. Mol Microbiol, 1997. **26**(4): p. 631-41.
49. Scholer, A. and H.J. Schuller, *A carbon source-responsive promoter element necessary for activation of the isocitrate lyase gene ICL1 is common to genes of the gluconeogenic pathway in the yeast *Saccharomyces cerevisiae**. Mol Cell Biol, 1994. **14**(6): p. 3613-22.
50. Niederacher, D., et al., *Identification of UAS elements and binding proteins necessary for derepression of *Saccharomyces cerevisiae* fructose-1,6-bisphosphatase*. Current Genetics, 1992. **22**(5): p. 363-70.
51. Proft, M., D. Grzesitza, and K.D. Entian, *Identification and characterization of regulatory elements in the phosphoenolpyruvate carboxykinase gene PCK1 of *Saccharomyces cerevisiae**. Mol Gen Genet, 1995. **246**(3): p. 367-73.
52. Satyanarayana, T. and H.P. Klein, *Studies on acetyl-coenzyme A synthetase of yeast: inhibition by long-chain acyl-coenzyme A esters*. Journal of Bacteriology, 1973. **115**(2): p. 600-6.
53. Satyanarayana, T., A.D. Mandel, and H.P. Klein, *Evidence for two immunologically distinct acetyl-coenzyme A synthetase in yeast*. Biochim Biophys Acta, 1974. **341**(2): p. 396-401.
54. Satyanarayana, T. and H.P. Klein, *Studies on the "aerobic" acetyl-coenzyme A synthetase of *Saccharomyces cerevisiae*: purification,*

- crystallization, and physical properties of the enzyme.* Arch Biochem Biophys, 1976. **174**(2): p. 480-90.
55. Van den Berg, M.A. and H.Y. Steensma, *ACS2, a Saccharomyces cerevisiae gene encoding acetyl-coenzyme A synthetase, essential for growth on glucose.* Eur J Biochem, 1995. **231**(3): p. 704-13.
56. Kumar, A., et al., *Subcellular localization of the yeast proteome.* Genes Dev, 2002. **16**(6): p. 707-19.
57. Huh, W.K., et al., *Global analysis of protein localization in budding yeast.* Nature, 2003. **425**(6959): p. 686-91.
58. van den Berg, M.A., et al., *The two acetyl-coenzyme A synthetases of Saccharomyces cerevisiae differ with respect to kinetic properties and transcriptional regulation.* J Biol Chem, 1996. **271**(46): p. 28953-9.
59. Devirgilio, C., et al., *Cloning and disruption of a gene required for growth on acetate but not on ethanol: the acetyl-coenzyme A synthetase gene of Saccharomyces cerevisiae.* Yeast, 1992. **8**(12): p. 1043-1051.
60. Kratzer, S. and H.J. Schuller, *Carbon source-dependent regulation of the acetyl-coenzyme A synthetase-encoding gene ACS1 from Saccharomyces cerevisiae.* Gene, 1995. **161**(1): p. 75-9.
61. Hiesinger, M., C. Wagner, and H.J. Schuller, *The acetyl-CoA synthetase gene ACS2 of the yeast Saccharomyces cerevisiae is coregulated with structural genes of fatty acid biosynthesis by the transcriptional activators Ino2p and Ino4p.* FEBS Lett, 1997. **415**(1): p. 16-20.
62. Schuller, H.J., et al., *Coordinate genetic control of yeast fatty acid synthase genes FAS1 and FAS2 by an upstream activation site common to genes involved in membrane lipid biosynthesis.* EMBO J, 1992. **11**(1): p. 107-14.
63. Starai, V.J., et al., *Sir2-dependent activation of acetyl-CoA synthetase by deacetylation of active lysine.* Science, 2002. **298**(5602): p. 2390-2.
64. Starai, V.J. and J.C. Escalante-Semerena, *Acetyl-coenzyme A synthetase (AMP forming).* Cell Mol Life Sci, 2004. **61**(16): p. 2020-30.
65. Starai, V.J., et al., *A link between transcription and intermediary metabolism: a role for Sir2 in the control of acetyl-coenzyme A synthetase.* Current Opinion in Microbiology, 2004. **7**(2): p. 115-119.
66. van Roermund, C.W., et al., *Fatty acid metabolism in Saccharomyces cerevisiae.* Cell Mol Life Sci, 2003. **60**(9): p. 1838-51.
67. Al-Feel, W., S.S. Chirala, and S.J. Wakil, *Cloning of the yeast FAS3 gene and primary structure of yeast acetyl-CoA carboxylase.* Proc Natl Acad Sci U S A, 1992. **89**(10): p. 4534-8.
68. Hoja, U., et al., *HFA1 encoding an organelle-specific acetyl-CoA carboxylase controls mitochondrial fatty acid synthesis in Saccharomyces cerevisiae.* Journal of Biological Chemistry, 2004. **279**(21): p. 21779-21786.
69. Hasslacher, M., et al., *Acetyl-CoA carboxylase from yeast is an essential enzyme and is regulated by factors that control phospholipid metabolism.* Journal of Biological Chemistry, 1993. **268**(15): p. 10946-10952.
70. Tehlivets, O., K. Scheuringer, and S.D. Kohlwein, *Fatty acid synthesis and elongation in yeast.* Biochimica Et Biophysica Acta-Molecular and Cell Biology of Lipids, 2007. **1771**(3): p. 255-270.
71. Witters, L.A. and T.D. Watts, *Yeast acetyl-CoA carboxylase: in vitro phosphorylation by mammalian and yeast protein kinases.* Biochem Biophys Res Commun, 1990. **169**(2): p. 369-76.
72. Woods, A., et al., *Yeast SNF1 is functionally related to mammalian AMP-activated protein kinase and regulates acetyl-CoA carboxylase in vivo.* J Biol Chem, 1994. **269**(30): p. 19509-15.
73. Shi, S., et al., *Improving production of malonyl coenzyme A-derived metabolites by abolishing Snf1-dependent regulation of Acc1.* MBio, 2014. **5**(3): p. e01130-14.
74. Hofbauer, H.F., et al., *Regulation of Gene Expression through a Transcriptional Repressor that Senses Acyl-Chain Length in Membrane Phospholipids.* Developmental Cell, 2014. **29**(6): p. 729-739.
75. Hiser, L., M.E. Basson, and J. Rine, *ERG10 from Saccharomyces cerevisiae encodes acetoacetyl-CoA thiolase.* Journal of Biological Chemistry, 1994. **269**(50): p. 31383-9.
76. van Roermund, C.W., et al., *The membrane of peroxisomes in Saccharomyces cerevisiae is impermeable to NAD(H) and acetyl-CoA under in vivo conditions.* EMBO J, 1995. **14**(14): p. 3480-6.
77. Strijbis, K. and B. Distel, *Intracellular acetyl unit transport in fungal carbon metabolism.* Eukaryot Cell, 2010. **9**(12): p. 1809-15.
78. Flikweert, M.T., et al., *Growth requirements of pyruvate-decarboxylase-negative Saccharomyces cerevisiae.* FEMS Microbiol Lett, 1999. **174**(1): p. 73-9.
79. van Roermund, C.W., et al., *Molecular characterization of carnitine-dependent transport of acetyl-CoA from peroxisomes to mitochondria in Saccharomyces cerevisiae and identification of a plasma membrane carnitine transporter, Agp2p.* EMBO J, 1999. **18**(21): p. 5843-52.
80. Li, Z.Y., E. Haase, and M. Brendel, *Hyper-resistance to nitrogen mustard in Saccharomyces cerevisiae is caused by defective choline transport.* Curr Genet, 1991. **19**(6): p. 423-7.
81. Aouida, M., et al., *Agp2, a member of the yeast amino acid permease family, positively regulates polyamine transport at the transcriptional level.* PLoS One, 2013. **8**(6): p. e65717.
82. Elgersma, Y., et al., *Peroxisomal and mitochondrial carnitine acetyltransferases of Saccharomyces*

- cerevisiae* are encoded by a single gene. EMBO J, 1995. **14**(14): p. 3472-3479.
83. Schmalix, W. and W. Bandlow, *The ethanol-inducible YAT1 gene from yeast encodes a presumptive mitochondrial outer carnitine acetyltransferase*. Journal of Biological Chemistry, 1993. **268**(36): p. 27428-27439.
84. Swiegers, J.H., et al., *Carnitine-dependent metabolic activities in Saccharomyces cerevisiae: three carnitine acetyltransferases are essential in a carnitine-dependent strain*. Yeast, 2001. **18**(7): p. 585-95.
85. Palmieri, L., et al., *Identification of the mitochondrial carnitine carrier in Saccharomyces cerevisiae*. Febs Letters, 1999. **462**(3): p. 472-476.
86. Jones, J.D. and C.D. O'Connor, *Protein acetylation in prokaryotes*. Proteomics, 2011. **11**(15): p. 3012-22.
87. Soppa, J., *Protein acetylation in archaea, bacteria, and eukaryotes*. Archaea, 2010. **2010**.
88. Kurdistani, S.K., S. Tavazoie, and M. Grunstein, *Mapping global histone acetylation patterns to gene expression*. Cell, 2004. **117**(6): p. 721-33.
89. Spange, S., et al., *Acetylation of non-histone proteins modulates cellular signalling at multiple levels*. International Journal of Biochemistry & Cell Biology, 2009. **41**(1): p. 185-198.
90. Yang, X.J. and E. Seto, *Lysine acetylation: Codified crosstalk with other posttranslational modifications*. Molecular Cell, 2008. **31**(4): p. 449-461.
91. Glozak, M.A., et al., *Acetylation and deacetylation of non-histone proteins*. Gene, 2005. **363**: p. 15-23.
92. Galdieri, L. and A. Vancura, *Acetyl-CoA carboxylase regulates global histone acetylation*. Journal of Biological Chemistry, 2012. **287**(28): p. 23865-76.
93. Cai, L. and B.P. Tu, *Acetyl-CoA drives the transcriptional growth program in yeast*. Cell Cycle, 2011. **10**(18): p. 3045-6.
94. Shi, L. and B.P. Tu, *Acetyl-CoA induces transcription of the key G1 cyclin CLN3 to promote entry into the cell division cycle in Saccharomyces cerevisiae*. Proceedings of the National Academy of Sciences of the United States of America, 2013. **110**(18): p. 7318-7323.
95. Cai, L. and B.P. Tu, *On acetyl-CoA as a gauge of cellular metabolic state*. Cold Spring Harb Symp Quant Biol, 2011. **76**: p. 195-202.
96. Leskovac, V., S. Trivic, and D. Pericin, *The three zinc-containing alcohol dehydrogenases from baker's yeast, Saccharomyces cerevisiae*. FEMS Yeast Res, 2002. **2**(4): p. 481-94.
97. Schaaff, I., et al., *A deletion of the PDC1 gene for pyruvate decarboxylase of yeast causes a different phenotype than previously isolated point mutations*. Curr Genet, 1989. **15**(2): p. 75-81.
98. Hohmann, S. and H. Cederberg, *Autoregulation may control the expression of yeast pyruvate decarboxylase structural genes PDC1 and PDC5*. Eur J Biochem, 1990. **188**(3): p. 615-21.
99. Hohmann, S., *Characterization of PDC6, a third structural gene for pyruvate decarboxylase in Saccharomyces cerevisiae*. Journal of Bacteriology, 1991. **173**(24): p. 7963-9.
100. Schmitt, H.D. and F.K. Zimmermann, *Genetic analysis of the pyruvate decarboxylase reaction in yeast glycolysis*. Journal of Bacteriology, 1982. **151**(3): p. 1146-52.
101. Seeboth, P.G., K. Bohnsack, and C.P. Hollenberg, *pdc1(0) mutants of Saccharomyces cerevisiae give evidence for an additional structural PDC gene: cloning of PDC5, a gene homologous to PDC1*. Journal of Bacteriology, 1990. **172**(2): p. 678-85.
102. Muller, E.H., et al., *Thiamine repression and pyruvate decarboxylase autoregulation independently control the expression of the Saccharomyces cerevisiae PDC5 gene*. FEBS Lett, 1999. **449**(2-3): p. 245-50.
103. Hohmann, S., *PDC6, a weakly expressed pyruvate decarboxylase gene from yeast, is activated when fused spontaneously under the control of the PDC1 promoter*. Curr Genet, 1991. **20**(5): p. 373-8.
104. Flikweert, M.T., et al., *Pyruvate decarboxylase: an indispensable enzyme for growth of Saccharomyces cerevisiae on glucose*. Yeast, 1996. **12**(3): p. 247-57.
105. Flikweert, M.T., J.P. van Dijken, and J.T. Pronk, *Metabolic responses of pyruvate decarboxylase-negative Saccharomyces cerevisiae to glucose excess*. Appl Environ Microbiol, 1997. **63**(9): p. 3399-404.
106. van Maris, A.J., et al., *Overproduction of threonine aldolase circumvents the biosynthetic role of pyruvate decarboxylase in glucose-limited chemostat cultures of Saccharomyces cerevisiae*. Appl Environ Microbiol, 2003. **69**(4): p. 2094-9.
107. van Maris, A.J., et al., *Directed evolution of pyruvate decarboxylase-negative Saccharomyces cerevisiae, yielding a C2-independent, glucose-tolerant, and pyruvate-hyperproducing yeast*. Appl Environ Microbiol, 2004. **70**(1): p. 159-66.
108. Oud, B., et al., *An internal deletion in MTH1 enables growth on glucose of pyruvate-decarboxylase negative, non-fermentative Saccharomyces cerevisiae*. Microb Cell Fact, 2012. **11**(1): p. 131.
109. Lakshmanan, J., A.L. Mosley, and S. Ozcan, *Repression of transcription by Rgt1 in the absence of glucose requires Std1 and Mth1*. Curr Genet, 2003. **44**(1): p. 19-25.
110. Polish, J.A., J.H. Kim, and M. Johnston, *How the Rgt1 transcription factor of Saccharomyces cerevisiae is repressed by glucose*. Genetics, 2005. **169**(2): p. 583-594.
111. Gamo, F.J., M.J. Lafuente, and C. Gancedo, *The mutation DGT1-1 decreases glucose transport and alleviates carbon catabolite repression in*

- Saccharomyces cerevisiae*. Journal of Bacteriology, 1994. **176**(24): p. 7423-9.
112. Blazquez, M.A., F.J. Gamo, and C. Gancedo, A mutation affecting carbon catabolite repression suppresses growth defects in pyruvate carboxylase mutants from *Saccharomyces cerevisiae*. FEBS Lett, 1995. **377**(2): p. 197-200.
113. Lafuente, M.J., et al., *Mth1* receives the signal given by the glucose sensors *Snf3* and *Rgt2* in *Saccharomyces cerevisiae*. Mol Microbiol, 2000. **35**(1): p. 161-72.
114. Schulte, F., et al., The *HTR1* gene is a dominant negative mutant allele of *MTH1* and blocks *Snf3*-and *Rgt2*-dependent glucose signaling in yeast. Journal of Bacteriology, 2000. **182**(2): p. 540-542.
115. Ozcan, S., et al., Glucose uptake and catabolite repression in dominant *HTR1* mutants of *Saccharomyces cerevisiae*. Journal of Bacteriology, 1993. **175**(17): p. 5520-8.
116. Moriya, H. and M. Johnston, Glucose sensing and signaling in *Saccharomyces cerevisiae* through the *Rgt2* glucose sensor and casein kinase I. Proceedings of the National Academy of Sciences of the United States of America, 2004. **101**(6): p. 1572-1577.
117. Conrad, T.M., N.E. Lewis, and B.O. Palsson, Microbial laboratory evolution in the era of genome-scale science. Mol Syst Biol, 2011. **7**: p. 509.
118. Bailey, J.E., et al., Strategies and challenges in metabolic engineering. Ann N Y Acad Sci, 1990. **589**: p. 1-15.
119. Nielsen, J., Metabolic engineering. Appl Microbiol Biotechnol, 2001. **55**(3): p. 263-83.
120. Jensen, M.K. and J.D. Keasling, Recent applications of synthetic biology tools for yeast metabolic engineering. FEMS Yeast Res, 2014.
121. Krivoruchko, A., V. Siewers, and J. Nielsen, Opportunities for yeast metabolic engineering: Lessons from synthetic biology. Biotechnol J, 2011. **6**(3): p. 262-76.
122. Nielsen, J. and J.D. Keasling, Synergies between synthetic biology and metabolic engineering. Nat Biotechnol, 2011. **29**(8): p. 693-5.
123. Oud, B., et al., Genome-wide analytical approaches for reverse metabolic engineering of industrially relevant phenotypes in yeast. FEMS Yeast Res, 2012. **12**(2): p. 183-96.
124. Bailey, J.E., et al., Inverse metabolic engineering: A strategy for directed genetic engineering of useful phenotypes. Biotechnol Bioeng, 1996. **52**(1): p. 109-21.
125. Bro, C., et al., Improvement of galactose uptake in *Saccharomyces cerevisiae* through overexpression of phosphoglucomutase: example of transcript analysis as a tool in inverse metabolic engineering. Appl Environ Microbiol, 2005. **71**(11): p. 6465-72.
126. Hong, K.K. and J. Nielsen, Recovery of phenotypes obtained by adaptive evolution through inverse metabolic engineering. Appl Environ Microbiol, 2012. **78**(21): p. 7579-86.
127. Caspeta, L., et al., Biofuels. Altered sterol composition renders yeast thermotolerant. Science, 2014. **346**(6205): p. 75-8.
128. Portnoy, V.A., D. Bezdan, and K. Zengler, Adaptive laboratory evolution--harnessing the power of biology for metabolic engineering. Curr Opin Biotechnol, 2011. **22**(4): p. 590-4.
129. van Maris, A.J.A., et al., Directed Evolution of Pyruvate Decarboxylase-Negative *Saccharomyces cerevisiae*, Yielding a C2-Independent, Glucose-Tolerant, and Pyruvate-Hyperproducing Yeast. Appl. Environ. Microbiol., 2004. **70**(1): p. 159-166.
130. Österlund, T., et al., Mapping condition-dependent regulation of metabolism in yeast through genome-scale modeling. BMC Systems Biology, 2013. **7**.
131. Lee, F.J.S., L.W. Lin, and J.A. Smith, Purification and characterization of an acetyl-CoA hydrolase from *Saccharomyces cerevisiae*. European Journal of Biochemistry, 1989. **184**(1): p. 21-28.
132. Lee, F.J.S., L.W. Lin, and J.A. Smith, A glucose-repressible gene encodes acetyl-CoA hydrolase from *Saccharomyces cerevisiae*. J. Biol. Chem., 1990. **265**(13): p. 7413-7418.
133. Lee, F.J.S., L.W. Lin, and J.A. Smith, Acetyl-CoA hydrolase involved in acetate utilization in *Saccharomyces cerevisiae*. Biochimica et Biophysica Acta - Protein Structure and Molecular Enzymology, 1996. **1297**(1): p. 105-109.
134. Buu, L.M., Y.C. Chen, and F.J.S. Lee, Functional characterization and localization of acetyl-CoA hydrolase, Ach1p, in *Saccharomyces cerevisiae*. J. Biol. Chem., 2003. **278**(19): p. 17203-17209.
135. Gergely, J., P. Hele, and C.V. Ramakrishnan, Succinyl and acetyl coenzyme a deacylases. The Journal of biological chemistry, 1952. **198**(1): p. 324-334.
136. Knowles, S.E., et al., Production and utilization of acetate in mammals. Biochemical Journal, 1974. **142**(2): p. 401-411.
137. Fleck, C.B. and M. Brock, Re-characterisation of *Saccharomyces cerevisiae* Ach1p: Fungal CoA-transferases are involved in acetic acid detoxification. Fungal Genetics and Biology, 2009. **46**(6-7): p. 473-485.
138. Entian, K.-D. and P. Kötter, 25 Yeast Genetic Strain and Plasmid Collections, in *Methods in Microbiology*, S. Ian and J.R.S. Michael, Editors. 2007, Academic Press. p. 629-666.
139. Chen, Y., et al., Enhancing the copy number of episomal plasmids in *Saccharomyces cerevisiae* for improved protein production. FEMS Yeast Res, 2012. **12**(5): p. 598-607.
140. Halestrap, A.P., The mitochondrial pyruvate carrier. Kinetics and specificity for substrates and inhibitors. Biochemical Journal, 1975. **148**(1): p. 85-96.

141. Bricker, D.K., et al., *A mitochondrial pyruvate carrier required for pyruvate uptake in yeast, Drosophila, and humans*. Science, 2012. **336**(6090): p. 96-100.
142. Rivi ère, L., et al., *Acetate produced in the mitochondrion is the essential precursor for lipid biosynthesis in procyclic trypanosomes*. Proceedings of the National Academy of Sciences, 2009. **106**(31): p. 12694-12699.
143. Erdeniz, N., U.H. Mortensen, and R. Rothstein, *Cloning-free PCR-based allele replacement methods*. Genome Research, 1997. **7**(12): p. 1174-1183.
144. Gietz, R.D. and R.A. Woods, *Transformation of yeast by lithium acetate/single-stranded carrier DNA/polyethylene glycol method*. Methods Enzymol, 2002. **350**: p. 87-96.
145. Guldener, U., et al., *A new efficient gene disruption cassette for repeated use in budding yeast*. Nucleic Acids Res, 1996. **24**(13): p. 2519-24.
146. McKenna, A., et al., *The Genome Analysis Toolkit: a MapReduce framework for analyzing next-generation DNA sequencing data*. Genome Research, 2010. **20**(9): p. 1297-303.
147. Ozcan, S. and M. Johnston, *Three different regulatory mechanisms enable yeast hexose transporter (HXT) genes to be induced by different levels of glucose*. Mol Cell Biol, 1995. **15**(3): p. 1564-72.
148. Gancedo, J.M., *The early steps of glucose signalling in yeast*. Fems Microbiology Reviews, 2008. **32**(4): p. 673-704.
149. Ruiz-Roig, C., et al., *The Rpd3L HDAC complex is essential for the heat stress response in yeast*. Mol Microbiol, 2010. **76**(4): p. 1049-62.
150. Knott, S.R., et al., *Genome-wide replication profiles indicate an expansive role for Rpd3L in regulating replication initiation timing or efficiency, and reveal genomic loci of Rpd3 function in Saccharomyces cerevisiae*. Genes Dev, 2009. **23**(9): p. 1077-90.
151. Yi, C., et al., *Function and molecular mechanism of acetylation in autophagy regulation*. Science, 2012. **336**(6080): p. 474-7.
152. Teste, M.A., et al., *Validation of reference genes for quantitative expression analysis by real-time RT-PCR in Saccharomyces cerevisiae*. BMC Mol Biol, 2009. **10**: p. 99.
153. Edgar, R.C., *MUSCLE: multiple sequence alignment with high accuracy and high throughput*. Nucleic Acids Res, 2004. **32**(5): p. 1792-7.
154. Kiefer, F., et al., *The SWISS-MODEL Repository and associated resources*. Nucleic Acids Res, 2009. **37**(Database issue): p. D387-92.
155. Cole, C., J.D. Barber, and G.J. Barton, *The Jpred 3 secondary structure prediction server*. Nucleic Acids Research, 2008. **36**: p. W197-W201.
156. Roy, A., A. Kucukural, and Y. Zhang, *I-TASSER: a unified platform for automated protein structure and function prediction*. Nat Protoc, 2010. **5**(4): p. 725-38.
157. Deng, D., et al., *Crystal structure of the human glucose transporter GLUT1*. Nature, 2014. **510**(7503): p. 121-5.
158. Reifenberger, E., E. Boles, and M. Ciriacy, *Kinetic characterization of individual hexose transporters of Saccharomyces cerevisiae and their relation to the triggering mechanisms of glucose repression*. Eur J Biochem, 1997. **245**(2): p. 324-33.
159. Ozcan, S. and M. Johnston, *Function and regulation of yeast hexose transporters*. Microbiol Mol Biol Rev, 1999. **63**(3): p. 554-69.
160. Kurdistani, S.K. and M. Grunstein, *Histone acetylation and deacetylation in yeast*. Nat Rev Mol Cell Biol, 2003. **4**(4): p. 276-84.
161. Knappe, J. and G. Sawers, *A radical-chemical route to acetyl-CoA: the anaerobically induced pyruvate formate-lyase system of Escherichia coli*. FEMS Microbiol Rev, 1990. **6**(4): p. 383-98.
162. Sawers, G. and G. Watson, *A glycyl radical solution: oxygen-dependent interconversion of pyruvate formate-lyase*. Mol Microbiol, 1998. **29**(4): p. 945-54.
163. Frey, M., et al., *Adenosylmethionine-dependent synthesis of the glycyl radical in pyruvate formate-lyase by abstraction of the glycine C-2 pro-S hydrogen atom. Studies of [2H]glycine-substituted enzyme and peptides homologous to the glycine 734 site*. J Biol Chem, 1994. **269**(17): p. 12432-7.
164. Waks, Z. and P.A. Silver, *Engineering a synthetic dual-organism system for hydrogen production*. Appl Environ Microbiol, 2009. **75**(7): p. 1867-75.
165. Wagner, A.F., et al., *The free radical in pyruvate formate-lyase is located on glycine-734*. Proc Natl Acad Sci U S A, 1992. **89**(3): p. 996-1000.
166. Sancho, J., *Flavodoxins: sequence, folding, binding, function and beyond*. Cell Mol Life Sci, 2006. **63**(7-8): p. 855-64.
167. Osborne, C., L.M. Chen, and R.G. Matthews, *Isolation, cloning, mapping, and nucleotide sequencing of the gene encoding flavodoxin in Escherichia coli*. Journal of Bacteriology, 1991. **173**(5): p. 1729-37.
168. Knoell, H.E. and J. Knappe, *Escherichia coli ferredoxin, an iron-sulfur protein of the adrenodoxin type*. Eur J Biochem, 1974. **50**(1): p. 245-52.
169. Overkamp, K.M., et al., *Functional analysis of structural genes for NAD(+) -dependent formate dehydrogenase in Saccharomyces cerevisiae*. Yeast, 2002. **19**(6): p. 509-20.

## **PAPER I**



1   **Title: Ach1 is involved in shuttling mitochondrial acetyl units for cytosolic**  
2   **C2 provision in Pdc negative *Saccharomyces cerevisiae***

3   Yun Chen<sup>1#</sup>, Yiming Zhang<sup>1#</sup>, Verena Siewers<sup>1</sup>, Jens Nielsen<sup>1,2\*</sup>

4   1 Department of Biology & Biological Engineering, Chalmers University of Technology, SE412 96  
5   Gothenburg, Sweden

6   2 Novo Nordisk Foundation Center for Biosustainability, Technical University of Denmark, DK2970  
7   Hørsholm, Denmark

8   <sup>#</sup>These authors contributed equally to this work.

9

10   \*Corresponding author:

11   Professor Jens Nielsen, Department of Biology and Biological Engineering, Chalmers University of  
12   Technology, SE-412 96 Göteborg, Sweden

13   Telephone: +46 (0)31 772 3804,

14   Fax: +46 (0)31 772 3801,

15   E-mail: nielsenj@chalmers.se

16   **Abstract**

17   Acetyl-coenzyme A (acetyl-CoA) is not only an essential intermediate in central carbon metabolism,  
18   but also an important precursor of many products of commercial interest due to its role as precursor  
19   metabolite for native or engineered pathways that can produce pharmaceuticals, chemicals or biofuels.  
20   In the yeast *Saccharomyces cerevisiae*, acetyl-CoA is compartmentalized in the cytosol,  
21   mitochondrion, peroxisome and nucleus, and cannot be directly transported between these  
22   compartments. With the acetyl-carnitine or glyoxylate shuttle, acetyl-CoA produced in peroxisomes or  
23   the cytoplasm can be transported into the cytoplasm or the mitochondria. However, whether acetyl-  
24   CoA generated in the mitochondria can be exported to the cytoplasm is still unclear. Here we  
25   investigated whether the transfer of acetyl-CoA from mitochondria to the cytoplasm can happen using  
26   a pyruvate decarboxylase negative, non-fermentative yeast strain. We found that mitochondrial Ach1  
27   can convert acetyl-CoA in this compartment into acetate, followed by crossing the mitochondrial  
28   membrane and being converted into acetyl-CoA in the cytosol. Based on our finding we propose a  
29   model in which acetate can be used to exchange acetyl units between mitochondria and the cytosol.  
30   These results will increase our fundamental understanding of intracellular transport of acetyl units, and  
31   also help to develop microbial cell factory for many kinds of acetyl-CoA derived products.

32   **Key words**

33   acetyl-CoA; central carbon metabolism; yeast; mitochondria;

34

35 **Introduction**

36 Acetyl-CoA is recognized as one of the most central molecules in the metabolism of most known  
37 organisms. It functions as a linking point of anabolism and catabolism and is involved in various  
38 acetyl transfer reactions. In addition to essential roles in carbon and energy metabolism, it plays  
39 important regulation roles in eukaryotic cells as the acetyl group is donor in post-translational protein  
40 acetylation, e.g. of histones [1]. Besides native cellular functions, the availability of nucleocytosolic  
41 acetyl-CoA has been shown to affect autophagy during yeast aging [2]. Also, acetyl-CoA metabolism  
42 and transport was reported to play an important role for full virulence in the fungal pathogen *Candida*  
43 *albicans* [3]. Furthermore, acetyl-CoA is a key precursor metabolite for a wide range of industrially  
44 important chemical products [4], and there is much interest in engineering acetyl-CoA metabolism in  
45 connection with metabolic engineering and synthetic biology of *S. cerevisiae*, e.g. by Verena, Alper,  
46 da Silva, Keasling, Smolke).

47 Of special interest, the acetyl-CoA metabolism in the yeast *Saccharomyces cerevisiae* has been well  
48 studied for both basic and applied interests [5, 6]. In this fungus acetyl-CoA is present in at least four  
49 different cellular compartments where it is either being synthesized (e.g. in nucleus) or transferred by  
50 specific shuttle systems (Fig. 1) [7]. To date, it is well acknowledged that *S. cerevisiae* exhibits two  
51 routes in parallel for the transport of acetyl units [8]. In one route acetyl units in the form of acetyl-  
52 CoA enter the glyoxylate cycle to synthesize C<sub>4</sub> dicarboxylic acids, which can be transported from  
53 peroxisomes to the cytosol or from the cytosol to mitochondria where they serve as substrate for the  
54 TCA cycle or gluconeogenesis, respectively. The other route is a carnitine-dependent route in which  
55 acetyl units in a form of acetylcarnitine, can be transported to the cytosol and/or the mitochondria.  
56 Although *S. cerevisiae* holds all components for carnitine synthesis it is not capable of *de novo*  
57 synthesis of carnitine [9] and can therefore only use the carnitine-dependent route if carnitine is  
58 provided to the growth medium.

59 Yeast has been widely used as a model organism to study intracellular transport of acetyl units in  
60 eukaryotes [10]. However, it is not clear whether acetyl group equivalents can be transported from the  
61 mitochondrial matrix to the cytosol across the acetyl-CoA-impermeable mitochondrial inner  
62 membrane [8]. It is widely accepted that almost all eukaryotes use the citrate/malate shuttle and/or  
63 citrate transporter to transfer acetyl units from the mitochondria to the cytoplasm. In this shuttle, intra-  
64 mitochondrial acetyl-CoA is converted to citrate through reaction with oxaloacetate, which can be  
65 exported to the cytosol and then converted back to acetyl-CoA by cytosolic ATP:citrate lyase.  
66 However, ATP:citrate lyase that is widely present in fungi, is absent in *S. cerevisiae* [11]. There are  
67 neither any experimental data that confirm either of the shuttle systems can be used to transfer acetyl  
68 units from the mitochondria to the cytosol. Therefore, the question remains whether acetyl-CoA  
69 formed in the mitochondrial matrix can be exported to the cytoplasm.

70 In yeast acetyl-CoA formation in the cytosol is formed via the pyruvate dehydrogenase bypass route  
71 (Fig. 1), where pyruvate is decarboxylated (by pyruvate decarboxylase, PDC) to acetaldehyde that is  
72 further converted to acetate. Since the availability of acetyl units in the cytosol is essential for the  
73 biosynthesis of lipids and certain amino acids [12], Pdc negative strains require C<sub>2</sub> compounds such as  
74 ethanol or acetate for growth [13]. Furthermore, these strains are sensitive to high glucose  
75 concentrations. These limitations were partially solved by evolving a Pdc minus strain, resulting in a  
76 glucose tolerant mutant having unknown mechanisms for provision of cytosolic acetyl-CoA [14]. In a  
77 later study, the mechanisms for growth in excess glucose were identified to be related to an in-frame  
78 internal deletion of *MTH1*, which is involved in transcriptional regulation of glucose sensing [15]. The

79 mutation in *MTH1* results in reduced glucose uptake through attenuating the expression of genes  
80 encoding hexose transporters and hereby reducing the glucose uptake rate. However, it was not  
81 identified what mechanism that ensured provision of cytosolic acetyl-CoA for lipid biosynthesis.

82 Here we aimed at identifying the mechanism responsible for the exchange of acetyl units between the  
83 mitochondrial matrix and the cytoplasm in *S. cerevisiae*. Our results identified a route relying on Ach1  
84 that could transfer acetyl units from the mitochondria to the cytoplasm. Based on our results we  
85 propose a new model in which acetate can be used to exchange acetyl units between the mitochondria  
86 and cytosolic compartments.

## 87 Materials and methods

### 88 • Materials and strain handling

89 All PCRs were performed with Phusion, DreamTaq DNA Polymerase from Thermo-Scientific  
90 (Waltham, MA, USA), or PrimeSTAR HS DNA Polymerase from Takara Bio Europe (Segeltorp,  
91 Sweden). Oligonucleotides were custom synthesized from Sigma-Aldrich (Stockholm, Sweden).  
92 *Escherichia coli* plasmid extraction, PCR product purification, and DNA gel extraction were  
93 performed with kits from Thermo-Scientific (Waltham, MA, USA). *S. cerevisiae* plasmid extraction  
94 was performed with Zymoprep Yeast Plasmid Miniprep II from Zymo Research (Nordic Biolabs,  
95 Täby, Sweden). All restriction enzymes were purchased from Thermo-Scientific (Fermentas,  
96 St.LeonRot, Germany).

97 *Escherichia coli* DH5 $\alpha$  was used for routine cloning procedures and selection and maintenance of *E.*  
98 *coli* recombinant strains was performed in LB medium containing 10 g/liter of peptone, 10 g/liter of  
99 NaCl, and 5 g/liter of yeast extract and supplemented with 100 mg/liter of ampicillin sodium salt.  
100 Solid version of this medium also included 16 g/liter of agar. Recombinant yeast strains were selected  
101 for Ura $^+$  phenotypes on Synthetic Dextrose (SD) medium containing 6.7 g/liter of yeast nitrogen base  
102 without amino acids (ForMedium), 0.77 g/liter of complete supplement mixture (CSM, lacking uracil)  
103 (ForMedium) and 20 g/liter of glucose. For KanMX marker selection the cells were cultivated in YPD  
104 medium, containing 10 g/liter yeast extract, 20 g/liter of peptone, 20 g/liter of glucose and  
105 supplemented with 200 mg/liter G-418 DiSulphate (Formedium).

106 Strains were preserved for long-term storage after overnight cultivation in selective media by adding  
107 glycerol to a final concentration of 20% and stored at -80 °C.

### 108 • Plasmid and strain construction

109 All plasmids and strains used and constructed in this study are summarized in table 1, as well as their  
110 main features and source. All primers used in this study are listed in table 2. The plasmids in this study  
111 were constructed based on the plasmid pSP-GM1 [16]. *ACH1* was amplified from CEN.PK113-5D [17]  
112 genomic DNA template using primers OEA\_UP/OEA\_DW (table 2), and cloned into pSP-GM1 under  
113 the promoter *TEF1* using *Bam*HI/*Xho*I, resulting into the plasmid pACH1 (table 1). *tACH1* (coding for  
114 the truncated version of Ach1) was amplified from CEN.PK113-5D genomic DNA template using  
115 primers OEA\_tUP/OEA\_DW, and cloned into pSP-GM1 using the same restriction sites *Bam*HI/*Xho*I,  
116 forming the plasmid ptACH1. Transformation of the plasmid pSP-GM1 into IMI076, resulting in the  
117 strain YACH00.

118 To interrupt the gene *ACH1* in strain IMI076 [15], the coding region of this gene was replaced by the  
119 functional cassette URA3. This was achieved by amplification of the upstream and downstream  
120 homologous of *ACH1* gene from yeast genome using primer pairs AHF/UAUR and UADF/AHR, and  
121 the *URA3* cassette from pSP-GM1 by primers AUF/AUR. All PCR products were fused together by  
122 primers AHF/AHR via fusion PCR, and then the linear DNA fragment was transformed into strain  
123 IMI076. Transformants were selected on SD supplemented with uracil drop-out medium and single  
124 colony isolates were confirmed to have the correct chromosomal replacement by PCR using primers  
125 DPAF/DPAR, resulting in strain YACH01.

126 Complementation of *ACH1* gene into strain YACH01 was done through integration of the *ACH1* gene  
127 under the control of the *TEF1* promoter together with KanMX marker gene into chromosome XI site  
128 No.3 (XI-3) [18]. The upstream and downstream homologous parts of the genome were amplified  
129 using primers AchIntUF/AchIntUR and AchIntDF/AchIntDR. The *ACH1* cassette was amplified from  
130 the plasmid pACH1 using primers AchIntF/AchIntR and the KanMX cassette was cloned from the  
131 vector pUG6 [19] by using primers AchIntKanF/KanInR, KanInF/AchIntKanR. The PCR products  
132 were fused together into two fragments by using primers AchIntUF/KanInR, and  
133 AchIntKanF/AchIntDR. The two overlapping cassettes were transformed into strain YACH01, and the  
134 transformants were selected on YPD supplemented with 200 mg/L G418 medium. Single colony  
135 isolates were confirmed to have the correct insert by PCR, resulting in strain YACH02. Similarly, the  
136 truncated version of *ACH1* gene was also introduced into strain YACH01 with slight difference to  
137 amplify the fragment from the plasmid ptACH1 instead of pACH1, but using the same primers, the  
138 obtained strain was named as YACH03.

139 • **Cultivation procedures**

140 Pre-cultivations were performed in defined minimal medium with 2% (v/v) of ethanol. The minimal  
141 medium consisted of 7.5 g/liter of  $(\text{NH}_4)_2\text{SO}_4$ , 14.4 g/liter of  $\text{KH}_2\text{PO}_4$ , 0.5 g/liter of  $\text{MgSO}_4 \cdot 7\text{H}_2\text{O}$ , 1  
142 ml of a vitamin solution and 1 ml of a trace metal solution, the pH was adjusted to 6.5 with NaOH  
143 before autoclaving, as described by Verduyn et al. [20]. Cells for culture inoculation were harvested  
144 by centrifugation during exponential growth phase, and washed twice using sterile water.

145 Cultivations in 100 ml shake flasks were performed in triplicates with initial  $\text{OD}_{600}$  of 0.05 using the  
146 minimal medium with 20 g/liter of glucose. Cultivation in Bioscreen C (Oy Growth Curves Ab Ltd,  
147 Finland) was performed in octuplicates at 30 °C in a micro-plate (10x10 wells) with 200 µl minimal  
148 glucose medium per well. And 20 mg/liter uracil was supplemented when required. When succinate  
149 was supplemented into the minimal medium, filter sterilized succinic acid (MERCK, Hohenbrunn,  
150 Germany) solution was added to a final concentration of 0.5 g/liter at the beginning of the cultivations.  
151 When UK-5099 was supplemented into the minimal medium, UK-5099 was first dissolved in dimethyl  
152 sulfoxide (DMSO), and then added to a final concentration of 200 nM during the exponential growth  
153 phase, while the same amount DMSO was supplemented to the control.

154 Spot assay was performed as described before [7]. Cells were grown in SD-ura medium with 2% (v/v)  
155 ethanol at 30 °C. The cells were harvested and washed twice with sterile water. After measuring the  
156  $\text{OD}_{600}$  serial dilutions with final cell concentrations of  $1 \times 10^6$ ,  $1 \times 10^5$ ,  $1 \times 10^4$ ,  $1 \times 10^3$  cells per ml  
157 were prepared. From each dilution, 4 µl were spotted on synthetic medium agarose plates with 20  
158 g/liter glucose or 20 g/liter glucose supplemented with 0.3 % (v/v) ethanol.

159 • **Analytical methods**

160 Biomass was determined by optical density measurement at 600 nm ( $OD_{600}$ ) with a GENESYS™ 20  
161 Visible spectrophotometer (Thermo Electron Scientific, Madison, USA). Samples from liquid cultures  
162 were taken at precise sampling times and filtered using syringe nylon filters with a pore size of 0.45  
163  $\mu\text{m}$  into HPLC vials and stored in a -20 °C freezer until being analyzed. HPLC analysis was performed  
164 in a Dionex UltiMate 3000 systems using a refractive index detector (RI-101 from Shodex) and a UV  
165 detector set at 210 nm (Ultimate 3000 VWD from Dionex, Sunnyvale, CA USA). The samples were  
166 analyzed using an Bio-Rad HPX 87H column (Hercules, USA), which was kept at 45 °C and 5 mM  
167  $H_2SO_4$  was used as the mobile phase with a flow rate of 0.6 ml/min. Quantitative analysis of glucose,  
168 pyruvate, glycerol, acetate and ethanol was performed by injecting a mixture of standards with known  
169 concentrations of each metabolite. Calibration curves were calculated using the peak areas of the RI  
170 detector for glucose, glycerol and ethanol and of the UV detector for pyruvate and acetate.

171 **Results**

172 • **Possible alternative routes for acetyl-CoA synthesis**

173 In yeast the production of acetyl-CoA in the cytosol is vital for the synthesis of important cellular  
174 components such as lipids and certain amino acids. A pyruvate decarboxylase (Pdc) negative strain,  
175 which lacks the cytosolic route to acetyl-CoA via acetaldehyde (Fig.1), when cells grow on glucose as  
176 the sole carbon source, is therefore a good platform strain to study alternative routes for acetyl-CoA  
177 synthesis in the cytosol. First, we searched the latest Genome Scale Metabolic Model of *S.cerevisiae*  
178 [21], and in this model 34 reactions are directly related with acetyl-CoA metabolism and transport. As  
179 C<sub>2</sub> compounds such as ethanol, acetaldehyde and acetate are also associated with acetyl-CoA  
180 production, 23 additional reactions involved in C<sub>2</sub> compounds metabolism were also included in this  
181 initial analysis.

182 When analyzing the possible role of these 57 reactions (supplementary Table 1) in providing cytosolic  
183 acetyl-CoA in a Pdc negative strain two possible routes were identified for provision of C<sub>2</sub>  
184 compounds/acetyl-CoA in the absence of carnitine. One possible route is the catabolism of threonine  
185 via threonine aldolase Gly1 to release acetaldehyde, which can be converted to acetyl-CoA via acetate  
186 in the cytosol. Although it has been shown that over-expression of *GLY1* can circumvent the essential  
187 biosynthetic role of pyruvate decarboxylase in glucose limited chemostat cultures of *S. cerevisiae* [22],  
188 Gly1 as a possible source for cytosolic acetyl-CoA production was excluded due to its low affinity for  
189 threonine and the relatively low intracellular threonine concentration when yeast is grown at excess  
190 glucose [14].

191 The other potential route is conversion of acetyl-CoA to acetate in the mitochondria followed by  
192 transport of acetate across the mitochondrial inner membrane to the cytosol where it can be converted  
193 into acetyl-CoA by cytosolic acetyl-CoA synthetase (ACS). One gene product, encoding by *ACH1*, is  
194 associated with acetyl-CoA and acetate in the mitochondria, although the functions of Ach1 are not  
195 conclusive. It was originally proposed to be an acetyl-CoA hydrolase to catalyze the scission of acetyl-  
196 CoA into acetate and CoA or being involved in acetate utilization [23-26]. Later it was, however,  
197 characterized as a CoA transferase and being involved in mitochondrial acetate detoxification [27]. In  
198 this study it showed the highest specific activity for the CoA transfer from succinyl-CoA to acetate *in*  
199 *vitro*, however, the substrate promiscuity of this enzyme did not exclude CoA transferase activity on  
200 additional substrates. We therefore proposed that this enzyme can transfer the CoA from acetyl-CoA  
201 to succinate with the formation of acetate and succinyl-CoA in a Pdc negative strain with the  
202 *MTH1* internal deletion.

203 • **Addition of succinate improves the growth of *MTH1-ΔT* strain IMI076**

204 To test our assumption, we firstly evaluated the impact of adding succinate to the medium of a Pdc  
205 negative strain IMI076 with an internal deletion of *MTH1* (*MTH1-ΔT*, see ref. [15]) and the control  
206 strain CEN.PK113-5D. The cultivations were tested in a Bioscreen C with a computer-controlled  
207 incubator/reader/shaker equipped with 8 filters from 405 nm to 600 nm. By addition of 0.5 g/liter  
208 succinate to the medium, there was no obvious difference in the growth of the control strain (Fig.2A),  
209 but it was clear that external succinate supplementation decreased the length of the lag phase for the  
210 IMI076 strain. This was further shown by the cultivation of strain IMI076 in shake flasks  
211 supplemented with succinate. As shown in Fig. 2B, the lag phase was shortened by about 22 h, and the  
212 maximum specific growth rate increased by 13%. This was consistent with observed increased rates of  
213 glucose consumption and pyruvate accumulation (data not shown).

214 • **The growth of *MTH1-ΔT* strain IMI076 relies on Ach1**

215 Next, in order to test the hypothesis that Ach1 is a key player in channeling acetyl units from the  
216 mitochondrial matrix to the cytoplasm the *ACH1* gene was deleted by replacing it with a functional  
217 *URA3* cassette in strain IMI076 (Pdc<sup>-</sup> *MTH1-ΔT ura3*, ref. [15]). As control, the parental Pdc minus  
218 strain was transformed with empty plasmid pSP-GM1 [16] containing the same *URA3* cassette,  
219 resulting in the strain YACH00.

220 As previously reported, the unevolved Pdc minus strain carrying the *MTH1-ΔT* allele (strain IMI076)  
221 grew on synthetic medium agarose plates with glucose as sole carbon source supplemented with uracil  
222 (Fig. 3A). There was no big difference in growth between this parental strain and the strain expressing  
223 a URA3 cassette (strain YACH00). However, the growth of the *ACH1* deletion strain YACH01 was  
224 significantly impaired as shown in Fig. 3A. All strains grew well on glucose supplemented with  
225 ethanol, and there was no difference between strains with or without *ACH1* deletion (Fig. 3A), clearly  
226 showing that *ACH1* is essential for growth of the IMI076 strain, clearly showing that *ACH1* is  
227 essential for growth of the IMI076 strain.

228 The growth in absence of Ach1 on plates could be an effect of the medium used for the solid growth  
229 assays, i.e. this could contain threonine or there could be C<sub>2</sub>-contamination as speculated by Oud *et*  
230 *al.*[15]. To exclude any potential C<sub>2</sub> contamination in the medium growth was also checked in liquid  
231 cultures using defined minimal medium [20]. Cells of IMI076 and the *ach1* mutant YACH01 were  
232 washed twice after pre-growth in synthetic ethanol media, and then transferred to a minimal glucose  
233 media. Strain IMI076 grew normally as before [16], with a specific growth rate of about 0.066 h<sup>-1</sup> ±  
234 0.001, whereas the *ach1* mutant YACH01 could not grow on glucose as the sole carbon source (Fig.  
235 3B).

236 • **Complementation of *ACH1* but not a truncated version restores growth of the *ach1* mutant**

237 The inability of growth on glucose as sole carbon source in absence of *ACH1* (Fig. 3B) points to this  
238 enzyme being responsible for transferring acetyl units from the mitochondria to the cytosol. To further  
239 confirm this hypothesis we performed complementation of the *ach1* deletion strain with both the wild-  
240 type gene and a truncated version of *ACH1*, where the N-terminus of Ach1 was removed which is  
241 reported to result in redirection of this protein to the cytoplasm [26]. *ACH1* with its N-terminal deleted  
242 or the entire protein coding gene was reintroduced into the *ach1* mutant by chromosomal integration.  
243 Growth assays of the resulting strains showed that complementation with the complete *ACH1* gene

244 could restore growth of the deletion mutant, whereas complementation with the truncated version  
245 could not restore growth of the *ach1* mutant (Fig. 4). The maximum specific growth rate of the *ACH1*  
246 complemented strain (YACH02) was increased by 52% compared with the control strain IMI076,  
247 which may be ascribed to increased expression in the complementation strain, where *ACH1* was  
248 expressed from the strong *TEF1* promoter.

249 • **Inhibition of the mitochondrial pyruvate carrier retards the growth of the IMI076 strain**

250 The compound UK-5099, an analogue of alpha-cyanocinnamate is known as a specific and potent  
251 inhibitor of the mitochondrial pyruvate carrier [28, 29]. Uptake of pyruvate into mitochondria in yeast  
252 is reduced by more than about 70% in presence of 0.2 mM UK-5099 compared to no presence of the  
253 inhibitor [29]. The sole source of acetyl-CoA in the mitochondria is through the oxidative  
254 decarboxylation of pyruvate, catalyzed by the pyruvate dehydrogenase complex. Reduction of  
255 mitochondrial pyruvate uptake will therefore limit the availability of acetyl units in this compartment.  
256 This will further restrict the supply of acetyl-CoA to the cytoplasm and may therefore affect cell  
257 growth. To further validate if the cytosolic acetyl-CoA in IMI076 is likely coming from mitochondrial  
258 acetyl-CoA we therefore cultivated this strain in absence or presence of UK-5099. When the cells  
259 entered the exponential growth phase 0.2 mM UK-5099 was added to the culture (Fig. 5). This  
260 resulted in a significant decrease in growth compared with the control experiment where no inhibitor  
261 was added. While there is no significant effect on the growth of the control strain (CEN.PK 113-5D)  
262 when supplemented with 0.2 mM UK-5099 (data not shown), the maximum specific growth rate of  
263 strain IMI076 decreased in presence of UK-5099, from 0.066 h<sup>-1</sup> to 0.018 h<sup>-1</sup>. These observations  
264 clearly indicate that the flux of mitochondrial pyruvate uptake is limiting cell growth, which again  
265 supports the hypothesis that cytosolic acetyl-CoA is derived from mitochondrial acetyl-CoA.

266 **Discussion**

267 A fundamental feature of most eukaryotes is the existence of different compartments and the flow of  
268 carbon metabolites between subcellular compartments. One of the key intermediates in cellular  
269 metabolism is acetyl-CoA, as it plays an essential role in carbon and energy metabolism. While acetyl-  
270 CoA metabolism has been extensively studied in the budding yeast *S. cerevisiae*, it is still not known  
271 whether acetyl-CoA produced in the mitochondria can be transported out to the cytosol. To address  
272 this fundamental question, we used a recently reported yeast strain IMI076 with a disruption of Pdc  
273 genes together with an internal deletion of *MTH1*, which enables cell growth in conditions of excess  
274 glucose [15]. Using this Pdc deficient strain (IMI076), that lacks the first step of the pyruvate  
275 dehydrogenase bypass pathway involving Pdc, acetaldehyde dehydrogenase and acetyl-CoA  
276 synthetase, and hereby exclude the normal route for acetyl-CoA biosynthesis.

277 Through analysis of a recent Genome Scale Metabolic Model we identified a putative route for acetyl-  
278 CoA biosynthesis, namely formation of acetate in the mitochondrial matrix followed by transport of  
279 acetate to the cytosol where Acs can convert it to acetyl-CoA. In this route Ach1 forms acetate from  
280 acetyl-CoA in the mitochondria. Ach1 has been long recognized as a hydrolase catalyzing the  
281 hydrolysis of acetyl-CoA to acetate and CoA [23], like many other acetyl-CoA hydrolases found in  
282 mammalian tissues [30, 31]. The exact catalytic role of this enzyme was later questioned by the  
283 observations of its role in acetate but not ethanol utilization [25]. It was also proposed that this enzyme  
284 may have a novel function concerning acetyl-CoA metabolism, but it was not until recently, when  
285 Fleck and Brock characterized Ach1 as a CoA transferase not just wasting energy by hydrolyzing  
286 acetyl-CoA [27] that new insight was provided on this enzyme.

287 Inspired by the function as a CoA transferase and the promiscuity of this enzyme on its substrates, we  
288 hypothesized that Ach1 could transfer CoA from acetyl-CoA to succinate. From the supplementation  
289 results we observed that addition of succinate improves growth of the strain IMI076, but has no impact  
290 on the growth of the control strain (Fig.2). Next, by disruption of *ACH1* in strain IMI076, the growth  
291 on glucose was abolished (Fig. 3B), which clearly indicated that Ach1 plays an important role in the  
292 Pdc deficient strain for growth on glucose. Finally, complementation with the *ACH1* gene under  
293 control of the strong *TEF1* promoter, not only rescued growth on glucose but resulted in slightly faster  
294 growth than the IMI076 strain (Fig. 4). Further confirming that Ach1 is involved in using  
295 mitochondrial acetyl-CoA was our finding that a truncated version of Ach1 that is targeted to the  
296 cytosol could not rescue growth of a *ach1* deletion in IMI076 and that inhibition of the mitochondrial  
297 pyruvate carrier reduces growth of IMI076.

298 Based on these results we propose the model of acetyl-CoA metabolism for the Pdc deficient strain  
299 shown in Fig. 6. When cells grow on glucose acetyl-CoA produced in the mitochondria can be  
300 converted to acetate potentially through reversible acetate:succinate CoA transferase Ach1. Acetate  
301 can then cross the mitochondrial membrane by passive diffusion and be converted into acetyl-CoA by  
302 the cytosolic acetyl-CoA synthetases (Acs1 and Acs2). It has been reported that Ach1 is repressed by  
303 glucose, as the expression level increased in late log phase compared to the early log phase [24].  
304 Introduction of the *MTH1-ΔT* allele into the Pdc negative strain, would, however, lead to an attenuated  
305 glucose in-flux and therefore result in decreased repression of *ACH1* expression. As shown in Fig. 6,  
306 Ach1 has to be localized in the mitochondria, making it possible to be responsible for channeling the  
307 acetyl units from the mitochondria to the cytosol under growth on glucose. This is consistent with a  
308 previous study that showed that most Ach1 was distributed in the mitochondria by  
309 immunofluorescence microscopy [26].

310 In conclusion, we here show that the yeast *S. cerevisiae* under Pdc negative and glucose derepressed  
311 conditions, uses acetate instead of citrate to transfer acetyl units from the mitochondria to the cytosol.  
312 This alternative shuttle route has been reported in other eukaryotes, e.g. in the procyclic stage of  
313 *Trypanosoma brucei* [32]. In this transfer system acetate is produced in the mitochondrial matrix from  
314 acetyl-CoA by Ach1. The alternative function of Ach1 in exporting acetyl units from the mitochondria  
315 is not contradicting with its function involved in acetate detoxification as suggested earlier [25, 27] as  
316 the CoA transfer is likely a reversible reaction. The transferase activity of Ach1 could be potentially  
317 useful for designing yeast as a microbial cell factory to produce acetyl-CoA derived products, such as  
318 the function of Ach1 in shuttling mitochondrial acetyl units for provision of cytosolic C2 resource  
319 should be considered when trying to establish a heterologous pathway for cytosolic acetyl-CoA supply.

## 320 Acknowledgements

321 We thank Jack T Pronk from Delft University of Technology for kindly providing the yeast strain  
322 IMI076. We also acknowledge our funding resources from European Research Council project  
323 INSYSBIO (Grant no. 247013), the Novo Nordisk Foundation, Vetenskapsrådet, FORMAS and  
324 Ångpanneföreningens Forskningsstiftelse.

325

326 **References**

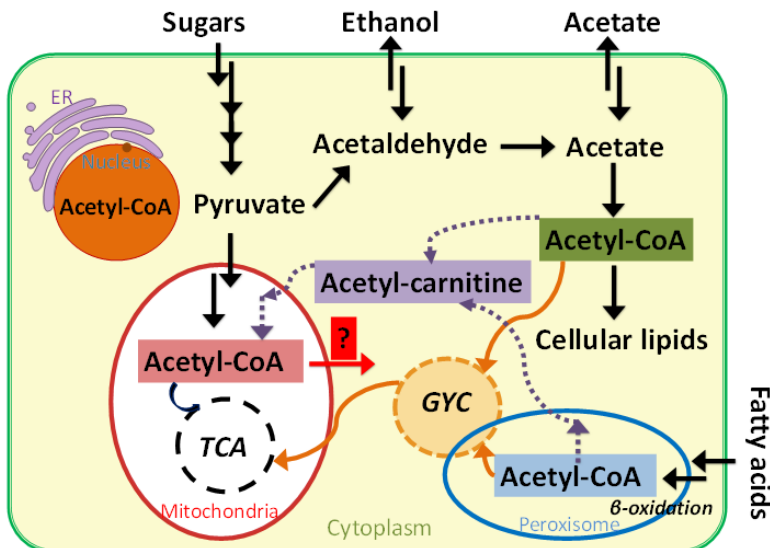
- 327 1. Takahashi, H., et al., *Nucleocytosolic acetyl-coenzyme A synthetase is required for histone*  
328 *acetylation and global transcription.* Molecular Cell, 2006. **23**(2): p. 207-217.
- 329 2. Eisenberg, T., et al., *Nucleocytosolic Depletion of the Energy Metabolite Acetyl-Coenzyme A*  
330 *Stimulates Autophagy and Prolongs Lifespan.* Cell Metabolism, 2014. **19**(3): p. 431-444.
- 331 3. Carman, A.J., S. Vylkova, and M.C. Lorenz, *Role of Acetyl Coenzyme A Synthesis and Breakdown*  
332 *in Alternative Carbon Source Utilization in Candida albicans.* Eukaryotic Cell, 2008. **7**(10): p.  
333 1733-1741.
- 334 4. Chen, Y., et al., *Establishing a platform cell factory through engineering of yeast acetyl-CoA*  
335 *metabolism.* Metab Eng, 2013. **15**(0): p. 48-54.
- 336 5. Nielsen, J., *Synthetic Biology for Engineering Acetyl Coenzyme A Metabolism in Yeast.* mBio, 2014.  
337 **5**(6).
- 338 6. Krivoruchko, A., et al., *Microbial acetyl-CoA metabolism and metabolic engineering.* Metab Eng,  
339 2014. **28C**(0): p. 28-42.
- 340 7. Chen, Y., V. Siewers, and J. Nielsen, *Profiling of cytosolic and peroxisomal acetyl-CoA metabolism*  
341 *in Saccharomyces cerevisiae.* PLoS ONE, 2012. **7**(8): p. e42475.
- 342 8. van Roermund, C.W.T., et al., *The membrane of peroxisomes in Saccharomyces cerevisiae is*  
343 *impermeable to NAD(H) and acetyl-CoA under in vivo conditions.* Embo Journal, 1995. **14**(14): p.  
344 3480-3486.
- 345 9. van Roermund, C.W., et al., *Molecular characterization of carnitine-dependent transport of acetyl-*  
346 *CoA from peroxisomes to mitochondria in Saccharomyces cerevisiae and identification of a plasma*  
347 *membrane carnitine transporter, Agp2p.* EMBO J, 1999. **18**(21): p. 5843-52.
- 348 10. Strijbis, K. and B. Distel, *Intracellular Acetyl Unit Transport in Fungal Carbon Metabolism.*  
349 Eukaryotic Cell, 2010. **9**(12): p. 1809-1815.
- 350 11. Hynes, M.J. and S.L. Murray, *ATP-Citrate Lyase Is Required for Production of Cytosolic Acetyl*  
351 *Coenzyme A and Development in Aspergillus nidulans.* Eukaryotic Cell, 2010. **9**(7): p. 1039-1048.
- 352 12. Pronk, J.T., H.Y. Steensma, and J.P. vanDijken, *Pyruvate metabolism in Saccharomyces*  
353 *cerevisiae.* Yeast, 1996. **12**(16): p. 1607-1633.
- 354 13. Flikweert, M.T., et al., *Growth requirements of pyruvate-decarboxylase-negative Saccharomyces*  
355 *cerevisiae.* FEMS Microbiology Letters, 1999. **174**(1): p. 73-79.
- 356 14. van Maris, A.J.A., et al., *Directed Evolution of Pyruvate Decarboxylase-Negative Saccharomyces*  
357 *cerevisiae, Yielding a C2-Independent, Glucose-Tolerant, and Pyruvate-Hyperproducing Yeast.*  
358 Appl. Environ. Microbiol., 2004. **70**(1): p. 159-166.
- 359 15. Oud, B., et al., *An internal deletion in MTH1 enables growth on glucose of pyruvate-*  
360 *decarboxylase negative, non-fermentative Saccharomyces cerevisiae.* Microbial Cell Factories,  
361 2012. **11**.
- 362 16. Chen, Y., et al., *Enhancing the copy number of episomal plasmids in Saccharomyces cerevisiae for*  
363 *improved protein production.* FEMS Yeast Res, 2012. **12**(5): p. 598-607.
- 364 17. Entian, K.D. and P. Kötter, *25 Yeast Genetic Strain and Plasmid Collections,* in *Methods in*  
365 *Microbiology*, I. Stansfield and M. Stark Jr, Editors. 2007. p. 629-666.
- 366 18. Mikkelsen, M.D., et al., *Microbial production of indolylglucosinolate through engineering of a*  
367 *multi-gene pathway in a versatile yeast expression platform.* Metab Eng, 2012. **14**(2): p. 104-111.
- 368 19. Guldener, U., et al., *A new efficient gene disruption cassette for repeated use in budding yeast.*  
369 Nucleic Acids Research, 1996. **24**(13): p. 2519-2524.
- 370 20. Verduyn, C., et al., *Effect of benzoic acid on metabolic fluxes in yeasts: a continuous-culture study*  
371 *on the regulation of respiration and alcoholic fermentation.* Yeast, 1992. **8**(7): p. 501-517.
- 372 21. Österlund, T., et al., *Mapping condition-dependent regulation of metabolism in yeast through*  
373 *genome-scale modeling.* BMC Systems Biology, 2013. **7**.
- 374 22. Van Maris, A.J.A., et al., *Overproduction of threonine aldolase circumvents the biosynthetic role*  
375 *of pyruvate decarboxylase in glucose-limited chemostat cultures of Saccharomyces cerevisiae.* Appl.
- 376 *Environ. Microbiol.,* 2003. **69**(4): p. 2094-2099.

- 377 23. Lee, F.J.S., L.W. Lin, and J.A. Smith, *Purification and characterization of an acetyl-CoA*  
378 *hydrolase from Saccharomyces cerevisiae*. European Journal of Biochemistry, 1989. **184**(1): p. 21-  
379 28.
- 380 24. Lee, F.J.S., L.W. Lin, and J.A. Smith, *A glucose-repressible gene encodes acetyl-CoA hydrolase*  
381 *from Saccharomyces cerevisiae*. J. Biol. Chem., 1990. **265**(13): p. 7413-7418.
- 382 25. Lee, F.J.S., L.W. Lin, and J.A. Smith, *Acetyl-CoA hydrolase involved in acetate utilization in*  
383 *Saccharomyces cerevisiae*. Biochimica et Biophysica Acta - Protein Structure and Molecular  
384 Enzymology, 1996. **1297**(1): p. 105-109.
- 385 26. Buu, L.M., Y.C. Chen, and F.J.S. Lee, *Functional characterization and localization of acetyl-CoA*  
386 *hydrolase, Ach1p, in Saccharomyces cerevisiae*. J. Biol. Chem., 2003. **278**(19): p. 17203-17209.
- 387 27. Fleck, C.B. and M. Brock, *Re-characterisation of Saccharomyces cerevisiae Ach1p: Fungal CoA-*  
388 *transferases are involved in acetic acid detoxification*. Fungal Genetics and Biology, 2009. **46**(6-7):  
389 p. 473-485.
- 390 28. Halestrap, A.P., *The mitochondrial pyruvate carrier. Kinetics and specificity for substrates and*  
391 *inhibitors*. Biochemical Journal, 1975. **148**(1): p. 85-96.
- 392 29. Bricker, D.K., et al., *A mitochondrial pyruvate carrier required for pyruvate uptake in yeast,*  
393 *Drosophila, and humans*. Science, 2012. **336**(6090): p. 96-100.
- 394 30. Gergely, J., P. Hele, and C.V. Ramakrishnan, *Succinyl and acetyl coenzyme a deacylases*. The  
395 Journal of biological chemistry, 1952. **198**(1): p. 324-334.
- 396 31. Knowles, S.E., et al., *Production and utilization of acetate in mammals*. Biochemical Journal,  
397 1974. **142**(2): p. 401-411.
- 398 32. Rivi ère, L., et al., *Acetate produced in the mitochondrion is the essential precursor for lipid*  
399 *biosynthesis in procyclic trypanosomes*. Proceedings of the National Academy of Sciences, 2009.  
400 **106**(31): p. 12694-12699.

401

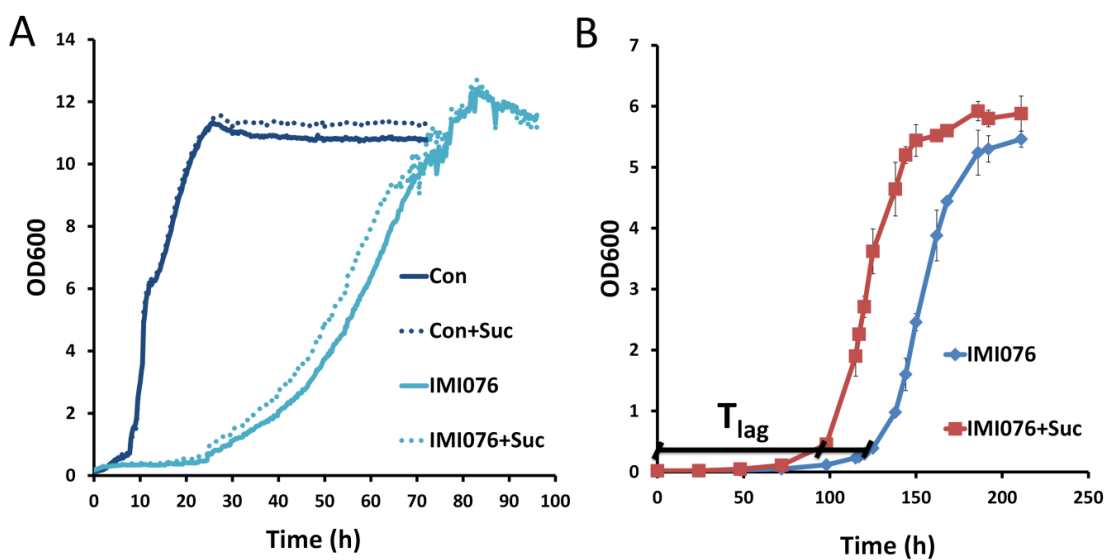
402

403



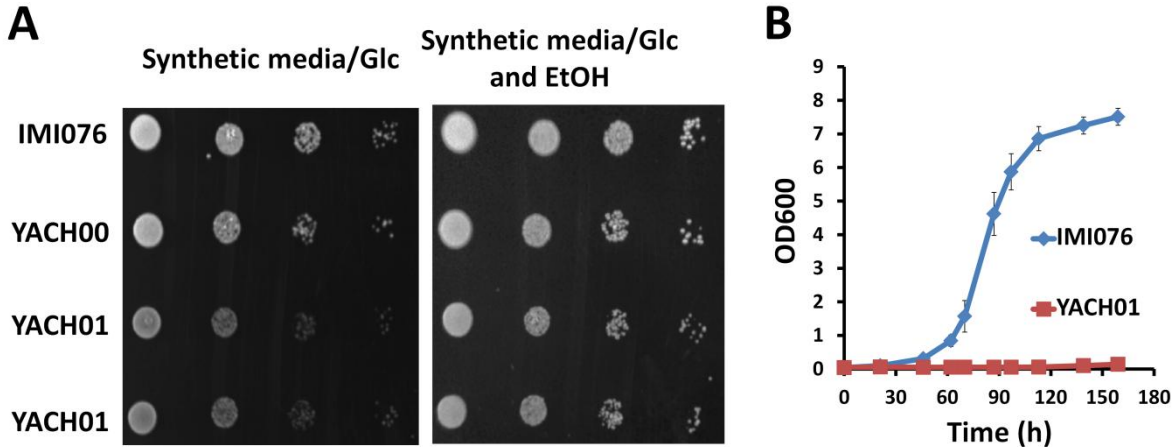
404

405 **Fig. 1 Representation of the acetyl-CoA metabolism in the yeast *S. cerevisiae*.** Acetyl-CoA in yeast  
 406 is compartmentalized in the mitochondria, peroxisomes, cytosol and nucleus. In the mitochondria  
 407 acetyl-CoA is derived from pyruvate and in the peroxisomes fatty acids can be broken down into  
 408 acetyl-CoA. In the cytosol acetyl-CoA is generated from pyruvate via acetaldehyde and acetate. With  
 409 the glyoxylate and acetyl-carnitine shuttles, peroxisomal or cytosolic acetyl-CoA can be transported  
 410 into the cytosol or the mitochondria. The question mark was the objective of this study, to evaluate  
 411 whether acetyl-CoA generated in the mitochondria can be exported to the cytoplasm. GYC, glyoxylate  
 412 cycle.

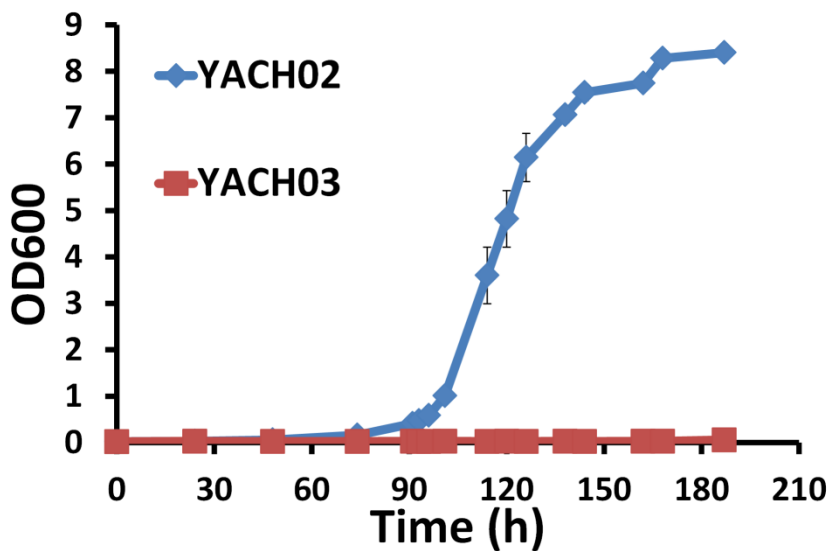


413

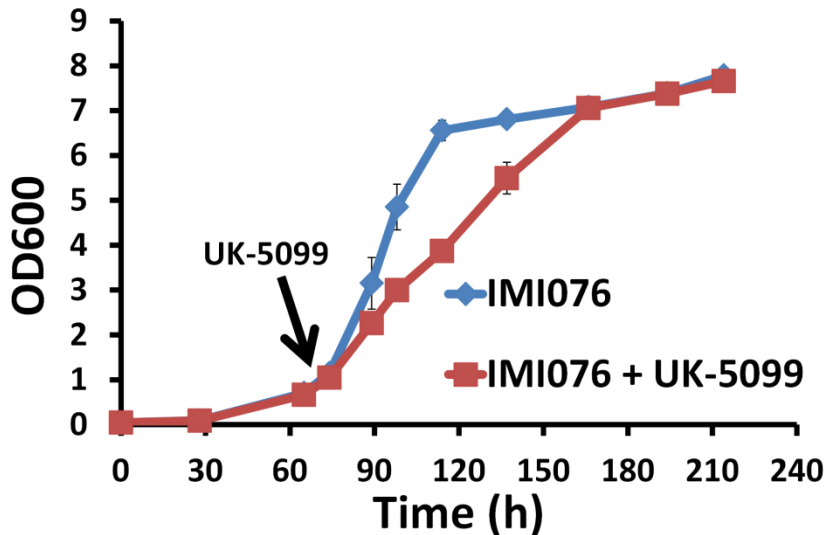
414 **Fig. 2 Addition of succinate improves the growth of strain IMI076 (Pdc<sup>-</sup> MTH1-ΔT) in bioscreen**  
 415 **(A) and shake flask (B) cultivations.** The control strain in A) was CEN.PK113-5D. Cells were grown  
 416 in defined minimal medium with 20 g/liter glucose. Supplementation with 0.5 g/liter of succinate was  
 417 performed before inoculation. Data points represent means +/- standard error of at least three  
 418 biological replicates.



420 **Fig. 3 The growth of strain IMI076 (*Pdc<sup>-</sup> MTH1-ΔT*) relies on Ach1.** A), Growth assays on solid  
421 synthetic medium with 20 g/liter glucose or 20 g/liter glucose plus 0.3% (v/v) ethanol. The plates were  
422 incubated at 30 °C and recorded photographically 4 days after inoculation. B), Growth assays in  
423 defined liquid minimal media with 20 g/liter glucose as the sole carbon source. The strains used were:  
424 IMI076 (*Pdc<sup>-</sup> MTH1-ΔT*), YACH00 (IMI076 empty plasmid pSP-GM1), YACH01 (IMI076  
425 *ach1::URA3*). Data for liquid cultures are means +/- standard error of three biological replicates.



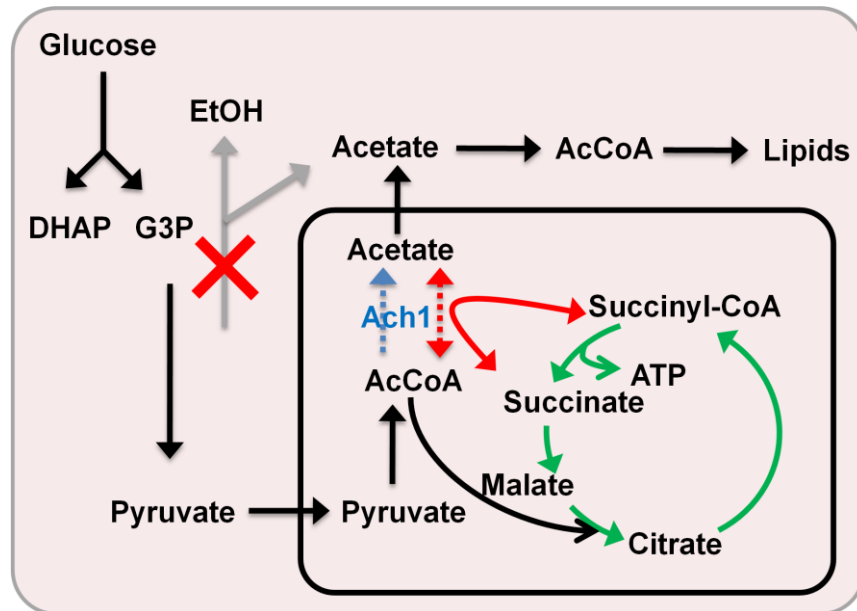
427 **Fig. 4 Complementation of *ACH1* but not its truncated version restores the growth of YACH01**  
428 (*ach1* mutant). Cells were first cultured in defined minimal medium with 2% (v/v) ethanol, and then  
429 the cells were washed twice with sterile water before inoculation of 20 g/liter glucose medium. The  
430 strains used were: YACH02 (YACH01 *ACH1 KanMX*), YACH03 (YACH01 *tACH1 KanMX*). All  
431 data points are means +/- standard error of three biological replicates.



433

434 **Fig. 5 Inhibition of the mitochondrial pyruvate transporter retards the growth of strain IMI076**  
 435 (*Pdc<sup>-</sup> MTH1-ΔT*). Cultivation was performed in defined minimal medium with 20 g/liter glucose. UK-  
 436 5099 was added when the OD<sub>600</sub> was about 1. All data points are from three biological replicates.

437



438

439 **Fig. 6 A model of Ach1 transferring acetyl units from the mitochondria to the cytosol.** During  
 440 growth on glucose under Pdc deficient conditions, intra-mitochondrial acetyl-CoA derived from  
 441 pyruvate by pyruvate dehydrogenase, can be converted into acetate by acetate:succinyl-CoA  
 442 transferase Ach1. The acetate formed in the mitochondria crosses the membrane by passive diffusion  
 443 to the cytosol, where is to be converted into acetyl-CoA for ensuring the provision of cytosolic acetyl-  
 CoA for the production of lipids and amino acids.

444

445 **Table 1- Plasmids and strains used in this work**

<b>Plasmid</b>	<b>Features</b>	<b>Source</b>
pSP-GM1	$P_{TEFI}\text{-}T_{ADH1}$ $P_{PGK1}\text{-}T_{CYC1}$ $URA3$	[16]
pACH1	$P_{TEFI}\text{-}ACH1\text{-}T_{ADH1}$ $P_{PGK1}\text{-}T_{CYC1}$ $URA3$	This work
ptACH1	$P_{TEFI}\text{-}tACH1\text{-}T_{ADH1}$ $P_{PGK1}\text{-}T_{CYC1}$ $URA3$	This work
<b>Strain</b>	<b>Genotype</b>	<b>Source</b>
CEN.PK113-5D	$MATa MAL2-8^C ura3-52$	P. Kötter, Germany
IMI076	$MATa pdc1Δ(-6, -2)::loxp pdc5Δ(-6, -2)::loxp$ $pdc6Δ(-6, -2)::loxp ura3-52 MTH1-ΔT$	[15]
YACH00	IMI076 pSP-GM1	This work
YACH01	IMI076 $ach1Δ::URA3$	This work
YACH02	IMI076 $ach1Δ::URA3 ACH1 KanMX$	This work
YACH03	IMI076 $ach1Δ::URA3 tACH1 KanMX$	This work

446

447

448 **Table 2- Oligonucleotides used in this work**

Name	Sequence (5'->3')
AHF	CAAACATACCACGATCCAAACG
AHR	GCTTACCAATCCTCCACCAC
OEA_UP	CGCCGGATCCAAAACAATGACAATTCTAATTGTTAAAGCAG
OEA_DW	TATCTCGAGCTAGTCAGCTGGTCCCAGCTG
OEA_tUP	CGCCGGATCCAAAACAATGGGAAGTTGAGATTCAACCTTTG
AchIntUF	AGTTACTTGCTCTATGCGTTGCG
AchIntUR	CATTGAAAGCTATGGTGTGCAATCAGACGCACGCTGGCG
AchIntF	ATTGACGCCAAGCGTGCCTGATTGCACACACCAGCTTCAAATG
AchIntR	CAGCGTACGAAGCTTCAGCTGGCTTCAGCGTCCAAAACCTTC
AchIntKanF	GAAGGTTTGGGACGCTCGAAGCCAGCTGAAGCTCGTACGCTG
AchIntKanR	GTATTGCTGGCTCAATCCACGTAAACTAGTGGATCTGATATCAC
KanInR	CCATGAGTGACGACTGAATCCGG
KanInF	GCAAAGGTAGCGTTGCCAATG
AchIntDF	GTGATATCAGATCCACTAGTTACGTGGATTGAGCCAGCAATAC
AchIntDR	TGAGAATCCGGACCAGCAGATAATGC
UAUR	CGATCTTCTACCCAGAACATACGCATACCTAACTCTGCTTAACAA
UADF	CGATATCAAGCTTATCGATGTAAAGAACATGCTTCAAGTTCCACACC
AUF	TTGTTAAAGCAGAGAGTTAGGTATCGTGATTCTGGGTAGAAGATCG
AUR	GGTGTGGAACTTGAAAGCATTCTTACATCGATAAGCTTGATATCG
DPAF	GCAGAGATTATGCCATCAACTACTA
DPAR	TGGTCTTCTTTCATCCATTAAACG





## **PAPER II**



# Title: Adaptive mutations in sugar metabolism restore growth on glucose in a pyruvate decarboxylase negative yeast strain

Yiming Zhang<sup>1</sup>, Martin KM Engqvist<sup>1</sup>, Anastasia Krivoruchko<sup>1</sup>, Björn M Hallström<sup>2</sup>, Yun Chen<sup>1</sup>, Verena Siewers<sup>1</sup>, Jens Nielsen<sup>1,3\*</sup>

<sup>1</sup> Department of Biology and Biological Engineering, Chalmers University of Technology, Kemivägen 10, SE-412 96 Göteborg, Sweden

<sup>2</sup> Science for Life Laboratory, KTH - Royal Institute of Technology, SE-171 21 Stockholm, Sweden

<sup>3</sup> Novo Nordisk Foundation Center for Biosustainability, Technical University of Denmark, Fremtidsvej 3, DK-2970 Hørsholm

\*Corresponding author, Email: [nielsenj@chalmers.se](mailto:nielsenj@chalmers.se), Phone: +46 (0)31 772 3804, Fax: +46(0)31 772 3801

## Abstract

A *Saccharomyces cerevisiae* strain carrying deletions in all three pyruvate decarboxylase (PDC) genes (also called Pdc negative yeast) represents a non-ethanol producing platform strain for the production of pyruvate derived biochemicals. However, it cannot grow on glucose as the sole carbon source, and requires supplementation of C<sub>2</sub> compounds to the medium in order to meet the requirement for cytosolic acetyl-CoA for biosynthesis of fatty acids and ergosterol. In this study, a collection of Pdc negative strains was constructed and one of them was adaptively evolved for improved growth in glucose medium via serial transfer. Three independently evolved strains were obtained, which were able to grow in minimal medium containing glucose as the sole carbon source at the maximum specific rates of 0.138 h<sup>-1</sup>, 0.148 h<sup>-1</sup>, 0.141 h<sup>-1</sup>, respectively. Several genetic changes were identified in the evolved Pdc negative strains by genomic DNA sequencing. Among these genetic changes, 4 genes were found to carry point mutations in at least two of the evolved strains: *MTH1* encoding a negative regulator of the glucose-sensing signal transduction pathway, *HXT2* encoding a hexose transporter, *CIT1* encoding mitochondrial citrate synthase, and *RPD3* encoding a histone deacetylase. Reverse engineering of the non-evolved Pdc negative strain through introduction of the *MTH1*<sup>81D</sup> allele restored its growth on glucose at a maximum specific rate of 0.05 h<sup>-1</sup> in minimal medium with 2% glucose. In this study, possible evolving mechanisms of Pdc negative strains on glucose was investigated by genome sequencing and reverse engineering. The non-synonymous mutations in *MTH1* alleviated the glucose repression by repressing expression of several hexose transporter genes. The non-synonymous mutations in *HXT2* and *CIT1* may function in the presence of mutated *MTH1* alleles and could be related to an altered central carbon metabolism in order to ensure production of cytosolic acetyl-CoA in the Pdc negative strain.

## Key words:

pyruvate decarboxylase, genomic DNA sequencing, yeast, reverse engineering, *MTH1*, hexose transporter, citrate synthase, histone deacetylase.

## Background

*Saccharomyces cerevisiae* is an important cell factory widely used for the production of beer, bread, wine, bioethanol, nutraceuticals, chemicals and pharmaceuticals [1-5]. When grown on glucose, the majority of the glycolytic flux is directed towards ethanol due to the so-called Crabtree effect in *S. cerevisiae*. The only strategy to eliminate ethanol production that has worked so far is removing pyruvate decarboxylase activity so that pyruvate cannot be converted to acetaldehyde, the direct precursor of ethanol [6]. In *S. cerevisiae*, pyruvate decarboxylase is encoded by three structural genes, *PDC1*, *PDC5* and *PDC6* [7-9]. However, pdc triple deletion mutants (*pdc1Δ pdc5Δ pdc6Δ*, also called Pdc negative strains) cannot grow on glucose as the sole carbon source [10]. The metabolic responses of Pdc negative strains, growth requirements, and growth recovery by threonine aldolase (encoded by *GLY1*) over-expression all suggested that the growth defect of Pdc negative strain on glucose was due to the lack of cytosolic acetyl-CoA for biosynthesis of cellular biomolecules, especially lipids.

Interestingly, the Pdc negative strains are still sensitive to high glucose concentrations even when supplemented with a C<sub>2</sub> source or with *GLY1* over-expression [6, 11]. van Maris *et al.* performed directed evolution of a Pdc negative strain on glucose, yielding the ‘C<sub>2</sub>-independent, glucose-tolerant, and pyruvate-hyperproducing’ strain TAM [12]. In the TAM strain, a *MTH1* allele with a 225 bp internal deletion (*MTH1-ΔT*) was identified, and was attributed with restoring growth of the Pdc negative strain on glucose [13]. However, when introducing the *MTH1-ΔT* allele into an un-evolved Pdc negative strain, the growth rate ( $\mu_{\text{max}}=0.10 \text{ h}^{-1}$ ) was slower in minimal medium with 2% glucose, compared to the TAM strain ( $\mu_{\text{max}}=0.20 \text{ h}^{-1}$ ), indicating the possible presence of additional advantageous genetic changes in the TAM strain besides *MTH1-ΔT*.

Mth1 functions as a negative transcriptional regulator in the glucose signaling pathway together with other regulators, *i.e.* Snf3, Rgt2, Std1, Rgt1. Several other *MTH1* alleles have been identified in selections of glucose or catabolite repression suppressors using glucose sensitive mutants [14-18]. The *MTH1* alleles seemed to be able to resolve the sensitivity to glucose in these mutants. Previous studies have shown that these *MTH1* alleles reduced glucose transport by repressing the transcription of several hexose transporter genes (*HXTs*) [12, 14, 16, 17], and that over-expression of *MTH1* had similar effects [13]. It has been proposed that *MTH1-ΔT* resulted in a decreased degradation of Mth1 [13], which could be related to putative PEST sequences (usually present in proteins with short intracellular half-life) and a target site for phosphorylation by casein kinase Yck1 [19] situated inside the deleted region. Mth1 or its paralog Std1 interacts with Rgt1, which also interacts with other transcription factors and binds the promoters of hexose transporter genes [20, 21]. The decreased degradation of Mth1 could prevent the phosphorylation of Rgt1, required for its release from the promoters of several hexose transporters [21]. The decreased degradation of Mth1 resulted from the *MTH1-ΔT* allele could therefore repress the transcription of hexose transporter genes even during growth on glucose.

In this study, a Pdc negative strain CEN.PK YMZ-E1 (*MATA ura3-52 his3-Δ1 pdc1Δ pdc5Δ pdc6Δ*) was evolved in glucose medium via serial transfer in 3 independent culture lines. Genomic DNA sequencing of these three evolved Pdc strains identified mutations in *MTH1* as

well as in *HXT2* [22], *CIT1* [23] and *RPD3* [24]. The fact that the mutated *MTH1* alleles were also identified in our evolved Pdc negative strains, indicated again that *MTH1* might be an important target for relieving high glucose repression. In order to understand the roles of these genetic changes in the evolved strains, the effects of the mutations in mutated genes, *MTH1*, *HXT2*, *CIT1* and *RPD3*, were investigated using homology analysis of their protein sequences and published crystal structure models of homologous proteins, and possible mechanisms were proposed and discussed. Although the speculations regarding the possible mechanisms in evolved Pdc negative strains still require further investigations, they may be useful and helpful for metabolic engineering strategies on Pdc negative strains.

## Results and discussion

- **Construction of Pdc negative strains**

CEN.PK 113-5D (*MAT $\alpha$  ura3-52*) and CEN.PK 110-10C (*MAT $\alpha$  his3-Δ1*) were used as background strains for the construction of Pdc negative strains (Figure 1).

*PDC1*, *PDC5*, and *PDC6* were consecutively deleted in CEN.PK 113-5D using a bipartite strategy (Figure S1), yielding CEN.PK YMZ-A1 (*MAT $\alpha$  ura3-52 pdc5Δ*), CEN.PK YMZ-A2 (*MAT $\alpha$  ura3-52 pdc1Δ*), CEN.PK YMZ-B1 (*MAT $\alpha$  ura3-52 pdc1Δ pdc5Δ*), CEN.PK YMZ-C1 (*MAT $\alpha$  ura3-52 pdc1Δ pdc5Δ pdc6Δ*). *PDC6* was deleted in CEN.PK 110-10C using the same bipartite strategy (Figure S1), yielding CEN.PK YMZ-A3 (*MAT $\alpha$  his3-Δ1 pdc6Δ*). CEN.PK YMZ-B2 (*MAT $\alpha$  ura3-52 pdc1Δ pdc6Δ*) was dissected from the diploid obtained by crossing CEN.PK YMZ-A2 and CEN.PK YMZ-A3. A collection of triple deletion mutants was dissected from the diploids obtained by crossing CEN.PK YMZ-C1 and CEN.PK YMZ-A3, which resulted in CEN.PK YMZ-C2 (*MAT $\alpha$  ura3-52 pdc1Δ pdc5Δ pdc6Δ*), CEN.PK YMZ-D1 (*MAT $\alpha$  his3-Δ1 pdc1Δ pdc5Δ pdc6Δ*), CEN.PK YMZ-D2 (*MAT $\alpha$  his3-Δ1 pdc1Δ pdc5Δ pdc6Δ*), CEN.PK YMZ-E1 (*MAT $\alpha$  ura3-52 his3-Δ1 pdc1Δ pdc5Δ pdc6Δ*), CEN.PK YMZ-E2 (*MAT $\alpha$  ura3-52 his3-Δ1 pdc1Δ pdc5Δ pdc6Δ*).

- **Adaptively evolved Pdc negative strains and their genomic sequencing results**

CEN.PK YMZ-E1 (*MAT $\alpha$  ura3-52 his3-Δ1 pdc1Δ pdc5Δ pdc6Δ*), E1 for short, was evolved in 3 independent culture lines in YPD medium with gradually reduced ethanol concentration. Once fast-growing, glucose tolerant strains were obtained in YPD media, they were further evolved for C<sub>2</sub> carbon source-independent and faster growth in minimal medium with 2% glucose.

At the end of the adaptive evolution, three independently evolved E1 strains were obtained. We refer to these as CEN.PK YMZ-E1A, CEN.PK YMZ-E1B, and CEN.PK YMZ-E1C (E1A, E1B, E1C for short, respectively). E1A, E1B, E1C could grow in minimal medium with glucose as the sole carbon source, with maximum specific growth rates of 0.138 h<sup>-1</sup>, 0.148 h<sup>-1</sup>, 0.141 h<sup>-1</sup>, respectively.

Genome sequencing of the parental strain E1 and its evolved strains (E1A, E1B, E1C) was performed to study the genetic changes that occurred during the adaptive evolution. The raw sequencing data were filtered and trimmed to remove adaptor sequences and sequence ends with a quality score below 20. The filtered reads were mapped to the CEN.PK 113-7D reference genome. In the E1A strain, three SNVs (Single Nucleotide Variants) in coding regions representing non-synonymous mutations were identified, as listed in Table S2. In the E1B strain, 11 SNVs in coding regions representing non-synonymous mutations were identified. In the E1C strain, 6 SNVs in coding regions representing non-synonymous mutations, one chromosomal regional deletion, one mitochondrial regional deletion and one single nucleotide insertion were identified.

Among all genes with SNVs, three genes, *MTH1*, *CIT1*, *HXT2*, were found to carry point mutations in all three evolved strains. And one gene, *RPD3*, was found to carry point mutations in two of the evolved strains. The mutations of the proteins encoded by the four genes are listed in Table 2. It is interesting to note that the same mutations occurred in more than one strain for two loci, A81D in Mth1 and W466\* in Hxt2, and that two mutations affected adjacent amino acids, P176Q and H175R in Cit1.

- **Integration of *MTH1*<sup>81D</sup> in non-evolved Pdc negative strain E1**

As previously reported by Oud *et al.* [13], a 225 bp in-frame internal deletion (corresponding to amino acids 57-131) in *MTH1* was identified in their evolved Pdc negative strain TAM, which was demonstrated to be responsible for relieving glucose sensitivity in the Pdc negative mutant. Among the previously identified *MTH1* alleles affecting glucose sensing, e.g. *BPC1*-1, *DGT1*-1, *HTR1*-5, *HTR1*-19 and *HTR1*-23, two mutations in codon 85 (I85N, I85S) and one mutation in codon 102 (S102G) were found, and it was also found that the S102G mutation could reinforce the mutations in codon 85 although having no effects by itself [16, 17]. Since the *MTH1*<sup>85S</sup> allele has already been confirmed to suppress glucose repression, we chose to validate the *MTH1*<sup>81D</sup> allele through reverse engineering in this study, to investigate if it has similar effects of suppressing glucose repression like other alleles.

The *MTH1*<sup>81D</sup> allele was integrated into the *MTH1* locus of the non-evolved E1 strain, resulting in strain M81. Two different M81 transformants, M81-11 and M81-33 were picked and tested for growth in glucose minimal medium. Their growth profiles in minimal medium with 2 % glucose are shown in Figure 2 with the maximum specific growth rates of 0.053 h<sup>-1</sup> and 0.047 h<sup>-1</sup>, respectively. The fact that *MTH1*<sup>81D</sup> by itself could restore the growth of the Pdc negative strain on glucose suggested it had the similar effects on glucose repression alleviation. However, the maximum specific growth rates were not as high as those of the evolved strains E1A, E1B, E1C. The *MTH1*<sup>81D</sup> mutation contributes around 35% of the specific growth rate in the evolved E1 strains, indicating there are likely other genetic changes that contribute to their growth recovery.

- **Analysis of the mutations in Mth1 and their possible effects**

Even though the N-terminal part of Mth1 appears to be important in glucose repression it is not yet clear why. To gain sequence-function insight into Mth1 protein, a bioinformatic approach was undertaken.

Alignment results of Mth1 from *S. cerevisiae* and 22 other homologous sequences of Mth1 and Std1 from unicellular fungi revealed that A81 and I85 are positioned on an ‘island’ composed of 22 highly conserved amino acids from codon 71-91 (Figure 3A). Since no protein crystal structures of Mth1 or homologs thereof are available, a secondary structure prediction was performed for the conserved ‘island’ using four prediction tools [25] (Figure 3B), which indicated an alpha helix in this region (Figure 3C). The putative helix is likely initiated by the structurally rigid prolines at codon 74 and 75, and Y77, A81, I85 and L89 are buried away from the solvent based on two prediction tools [26] (Figure 3B). Therefore, it is possible that A81 and I85, together with Y77 and L89, play a structural role in anchoring a highly conserved alpha helix to the Mth1 surface through hydrophobic interactions. The A81D, I85S or I85N mutations, representing non-polar to polar amino acid changes, would disrupt these interactions and may therefore cause structural changes in the protein.

It is interesting to note that another conserved ‘island’ from codon 118 to 137 is the identified target region for phosphorylation by Yck1 [19]. Since the two conserved ‘islands’ are 27 residues apart, it is reasonable to speculate that the putative helix may interact with the phosphorylation site, and thus affect the degradation of the protein.

- **Transcriptional analysis of hexose transporter genes**

In order to understand the effects of the *MTH1<sup>81D</sup>* allele on transcription of genes encoding hexose transporters, transcription analysis were performed on *HXT1-7* using qPCR in reverse engineered strains M81-11 and M81-33 and wild type strain CEN.PK 113-11C [27].

Compared with wild type strain, the expression levels of *HXT1*, *HXT3*, *HXT4* and *HXT6&7* were much lower in both M81 strains, i.e. around 9 fold, 25 fold, 15 fold, and 40 fold lower, respectively (Figure 4). The expression level of *HXT5* did not differ much between the wild type strain and the M81 strains. However, the expression level of *HXT2* was around 3 fold higher in the M81 strains, which was quite a different pattern from the other *HXTs*. The different expression patterns of *HXTs* in M81 strains is consistent with those in the TAM strain [12], suggesting that they are regulated by Mth1 differently, which is consistent with earlier findings [28].

According to the bioinformatic analysis and its homolog protein structure, the mutations identified in Hxt2 in evolved Pdc strains were predicted to impair or completely abolish its activity to transport glucose (Supplementary). Therefore, it is possible that the glucose transport by Hxt2 was decreased due to the identified mutations, even with an increase in its transcription level, which resulted from the mutations in Mth1.

## Possible evolving mechanisms in Pdc negative strains

Based on analysis of the possible effects of the point mutations on their corresponding proteins (Supplementary), possible mechanisms were proposed for how the evolved Pdc negative strains have acquired a faster growth phenotype.

The growth defect of a Pdc negative strain on glucose [10] was previously attributed to the lack of cytosolic acetyl units, since acetyl-CoA cannot be transported between different subcellular compartments freely and ethanol or acetate supplementation or *GLY1* over-expression could restore its growth on glucose [6, 11, 29]. However, the growth recovery of the Pdc negative strain with *MTH1*- $\Delta T$ , which does not in itself lead to cytosolic acetyl-CoA provision, indicated the presence of native pathways to cytosolic C<sub>2</sub> compounds. This was recently identified in the form of acetate, converted from mitochondrial acetyl-CoA by CoA transferase (or acetyl-CoA hydrolase, encoded by *ACH1*) (*ACH1* paper, submitted). Although Ach1 can channel acetyl-CoA from the mitochondria to the cytosol, it is only functional under glucose derepressed conditions and this route can also be blocked by limited acetyl-CoA availability due to the stringent regulation of the PDH complex in *S. cerevisiae* (Figure 5A), e.g. via post-transcriptional phosphorylation of the Pda1 subunits [30] or transcriptional repression of the Lpd1 subunits [31]. In the evolved Pdc negative strains, the mutations in Mth1 seemed to play the most critical role, since the single mutation *MTH1*<sup>8ID</sup> alone was here shown to improve the growth of a Pdc negative strain on glucose as well as the earlier reported truncation *MTH1*- $\Delta T$ . According to homology analysis of Mth1 and predictions of the conserved ‘island’ (codon 71-91), where the mutations are located, A81 and I85 may play a critical role in maintaining the alpha helix structure formed within it, and thus probably affect the phosphorylation site in another adjacent conserved ‘island’. However, a crystal structure of Mth1 would be needed to validate these predictions.

The *MTH1* alleles seem to decrease glucose uptake transport by alleviated repression of transcribing several *HXTs*, especially *HXT1* and *HXT3* [13-18], which was also found in the TAM strain (evolved Pdc negative strain, with *MTH1*- $\Delta T$  allele) by van Maris *et al* [12]. Moreover, a deletion within *HXT3* (~1000 bp) was also found in the evolved strain E1C, which would undoubtedly destroy its activity to transport glucose. A previous study suggested that the rate of glucose transport determines the strength of glucose repression [32], and the attenuated glucose uptake therefore likely resulted in a generally reduced glucose repression in the evolved strains. Thus, the transcription of many genes, which are normally repressed by glucose, could probably be partially de-repressed despite the high extracellular glucose concentration, e.g. genes encoding mitochondrial enzymes. Therefore, in the evolved strains with mutated *MTH1*, it is possible that the C<sub>2</sub> supply from the mitochondria to the cytosol via Ach1 route was no longer blocked (Figure 5B).

Hxt2, a high-affinity glucose transporter, is usually found to function under low glucose concentrations and its transcription is repressed by high glucose and induced by low glucose [33, 34]. The mutations in Hxt2 seemed to make no sense in high glucose medium (2% glucose) used in this study. One possible hypothesis would be that the effects of the mutated Mth1 might be

quite complicated. Transcriptional analysis of the TAM strain showed decreased transcription of *HXT1*, *HXT3*, *HXT4*, *HXT6* and *HXT7*, and increased transcription of *HXT2* and *HXT5*, although this might resulted from other genetic changes besides *MTH1*- $\Delta T$  [12]. Previous studies with other *MTH1* alleles revealed significant decreased transcription of *HXT1* and *HXT3*, a large increase in *HXT7* and nearly no change in *HXT2* [16, 17]. All these results suggested that *MTH1* alleles might have different effects in regulating expression of hexose transporters with low affinity compared to those with high affinity. According to previous results, the mutated *MTH1* might result in an unchanged or increased transcription level of *HXT2*, which has been confirmed by our qPCR results (Figure 4). The mutations in Hxt2 might cause structural disruptions based on our predictions (Supplementary and Figure S4), and may therefore further reduce the glucose transport.

The role of the mutated Cit1 might also be connected with C<sub>2</sub> carbon supply via the mitochondria. As seen in Figure 5, Cit1 competes with Ach1 for acetyl-CoA. The mutated Cit1 has potentially decreased activity, predicted by the analysis concerning possible effects of the identified mutations (Supplementary and Figure S5), and this might allow more acetyl-CoA being converted to acetate by Ach1, thus providing more acetate for acetyl-CoA biosynthesis in the cytosol. Since C<sub>2</sub> carbon supply in the cytosol seemed to be a limiting step for the growth of Pdc negative strains (ACH1 paper). The mutations in Cit1 might further improve the strain growth on glucose in the presence of the mutated Mth1. However, when *CIT1* was deleted in strain M81, the growth on glucose was significantly impaired (data not shown), since the complete disruption of *CIT1* would result in the dysfunction of the TCA cycle and hereby significantly reduce the ability for the cell to generate ATP required for growth.

Rpd3 usually functions in the form of a complex together with other proteins to regulate gene transcription, silencing and many other processes by histone deacetylation [35-37]. More and more studies suggest that histone acetylation and deacetylation regulate gene transcription in complex and comprehensive ways [38]. Although the mutations in Rpd3 might result in its decreased activity (Supplementary and Figure S6), it is still difficult to speculate about their role in the evolved strains. A previous study found that histone acetylation and deacetylation was directly regulated by nucleocytosolic acetyl-CoA abundance [39]. One possible speculation would be that the Rpd3 mutations might be related to cytosolic acetyl-CoA abundance, but this will require further investigation.

## Conclusions

In this study, a Pdc negative strain was adaptively evolved in glucose media via serial transfer, and evolved Pdc negative strains were shown to grow on glucose as the sole carbon source. Genomic DNA sequencing results of the parental Pdc negative strain and its corresponding evolved strains revealed four genes which carried point mutations in at least two of the evolved strains. The mutations in these four genes seemed to be related to the cytosolic acetyl-CoA supply. These findings will be useful for the fundamental understanding of acetyl-CoA metabolism in *S. cerevisiae*, as well as strain development for biochemical production as cell factories.

## Material and Methods

- **Strain construction**

*PDC1*, *PDC5* and *PDC6* were deleted using a bipartite strategy [40] (Figure S1). Sequences upstream and downstream of the individual genes were amplified using primers 1-12 listed in Table S1. Two overlapping fragments of the *kanMX* resistance marker cassette flanked by *loxP* sites were PCR amplified from plasmid pUG6 [41] using primers 13-16 listed in Table S1. The two fused PCR fragments for each gene deletion were transformed into yeast using the lithium acetate method [42]. After each gene deletion, the *kanMX* marker cassette was looped out via Cre recombinase mediated recombination between the two flanking *loxP* sites using plasmid pUC47 or pUG62 as described previously [41]. Each gene deletion was confirmed using primers 17-22 listed in Table S1.

*PDC1*, *PDC5*, and *PDC6* were consecutively deleted in two different background strains, CEN.PK 113-5D (*MATa ura3-52*) and CEN.PK 110-10C (*MATa his3-Δ1*) [27]. Together with strain crossing and tetrad segregation, a collection of triple deletion mutants was constructed carrying different auxotrophic markers: *ura3-52*, *his3-Δ1* or *ura3-52 his3-Δ1*. The mating type of these pdc negative mutants was determined using primers 35-37 listed in Table S1.

To create a Pdc-negative strain with a point mutation in *MTH1*, an *MTH1*<sup>81D</sup> construct was created and used to replace the normal *MTH1* gene in strain CEN.PK YMZ-E1 (*MATa ura3-52 his3-Δ1 pdc1Δ pdc5Δ pdc6Δ*), as shown in Figure S2, resulting in two M81 strains M81-11 and M81-33. *MTH1*<sup>81D</sup> with upstream and downstream sequences was amplified using primers 23-26, and the sequence downstream of *MTH1*<sup>81D</sup> was amplified using primers 27-28. Two overlapping fragments of the *amdSYM* marker cassette were PCR amplified from plasmid pUG-amdSYM (obtained from Euroscarf, accession number: P30669) using primers 29-32. The two fused PCR fragments for integration were transformed into CEN.PK YMZ-E1 using the electroporation method as described in [43]. The integration of *MTH1*<sup>81D</sup> and *amdSYM* was confirmed using primers 33-34. The *amdSYM* marker was looped out via selection on counter-selective plates. The replacement of *MTH1*<sup>81D</sup> was confirmed by sequencing PCR product amplified by primers 33-34.

*CIT1* was deleted in strain M81-11 using the same strategy as described in *PDC1* deletion (Figure S1), in which the *amdSYM* marker was used instead of the *kanMX* marker. Sequences upstream and downstream of the individual genes were amplified using primers 38-41 listed in Table S1. Two overlapping fragments of the *amdSYM* marker cassette were PCR amplified from plasmid pUG-amdSYM using primers 29-32 listed in Table S1. The two fused PCR fragments for integration were transformed into M81-11 using the electroporation method as described in [43]. The gene deletion was confirmed using primers 42-43 listed in Table S1

- **Medium and culture conditions**

Cultivations were performed at 30 °C in YP medium with 2% glucose (YPD) or 2% ethanol (YPE). Selections for transformants containing the *kanMX* marker were performed on YPD or

YPE plates supplemented with 200 mg/L G418 sulfate (Formedium Ltd., Hunstanton, UK). Selections for transformants carrying the *amdSYM* marker were performed on SM-Ac plates with 2% ethanol instead of glucose, and the counter selections were performed on SM-Fac plates with ethanol as carbon source, as described in [44]. A diploid resulting from two haploids of different mating type was obtained on agar plates containing a synthetic medium consisting of yeast nitrogen base (Formedium Ltd.), complete supplement mixture w/o uracil or histidine (Formedium Ltd.), and 2% (v/v) ethanol (SE-ura-his). Tetrad dissections were performed on YPE agar plates.

Cultivations for strain characterization were performed at 30 °C in triplicate in 100 mL shake flasks with 40 mL defined minimal medium. The defined minimal medium for cultivation was composed of 20 g/L glucose, 7.5 g/L  $(\text{NH}_4)_2\text{SO}_4$ , 14.4 g/L  $\text{KH}_2\text{PO}_4$ , 0.5 g/L  $\text{MgSO}_4 \cdot 7\text{H}_2\text{O}$ , 2 mL/L trace metal solution, 1 mL/L vitamin solution, with the pH adjusted to 6.5 by adding 2 M NaOH. The final concentrations of trace metal elements and vitamins were previously described in [45]. The minimal medium was supplemented with 40 mg/L uracil or 40 mg/L histidine when required.

- **Determination of biomass and extracellular metabolites**

Biomass was determined by optical density ( $\text{OD}_{600}$ ) measurement at a wavelength of 600 nm with a GENESYS™ 20 Visible spectrophotometer (Thermo Electron Scientific, Madison, USA). Glucose, ethanol, glycerol, pyruvate and formate concentrations were determined in culture supernatants by high-performance liquid chromatography (Dionex-HPLC, Sunnyvale, CA, USA) equipped with UV detector and RI detector using a Bio-Rad HPX 87H column (Bio-Rad, Hercules, CA, USA). The HPLC was operated at 45 °C with 5 mM  $\text{H}_2\text{SO}_4$  as mobile phase at a flow rate of 0.6 mL min<sup>-1</sup>.

- **Adaptive evolution of Pdc negative strain in glucose medium via serial transfer**

The adaptive evolution of CEN.PK YMZ-E1 (*MATa ura3-52 his3Δ1 pdc1Δ pdc5Δ pdc6Δ*) towards growth on glucose as the sole carbon source were performed in 3 independent culture lines in 100 mL shake flasks with 20 mL medium at 30 °C, which involved three phases (Figure S3). In the first phase, strains were cultivated in YP medium containing 1.4 % glucose and 0.6 % ethanol and then serially transferred every 48 or 24 hours using YP medium with gradually decreased ethanol concentration for 8 days. Subsequently, the strains were evolved in YPD medium for 15 days and transferred with passage every 48 or 24 hours. Finally the strains were transferred into minimal medium containing 2% glucose as the sole carbon source and evolved for increased growth by serial transfer every 48 or 24 hours for 39 days. And single clone isolates were obtained from the last shake flasks, and designated as CEN.PK YMZ-E1A, CEN.PK YMZ-E1B, and CEN.PK YMZ-E1C.

- **Genomic DNA extraction and sequencing procedures**

CEN.PK YMZ-E1 and their evolved strains were cultured in 10 mL YPE medium at 30 °C, and cells were harvested during exponential phase for genomic DNA extraction. Genomic DNA was extracted using the Genomic DNA buffer set (QIAGEN, Hilden, Germany) and QIAGEN Genomic-tip 500/G. The DNA samples were prepared for sequencing using the Illumina DNA TruSeq protocol, with an insert size of 650 bp. The sequencing was performed multiplexed on an Illumina MiSeq using the version 2 chemistry (2 x 250 bp, paired reads).

- **Analysis of genome sequencing results**

The raw sequencing data was filtered and trimmed to remove adaptor sequences and sequence ends with a quality score below 20. The filtered reads were mapped to the CEN.PK 113-7D reference genome (<http://cenpk.tudelft.nl>) using the mapper MosaikAligner version 2.1.32 (<http://code.google.com/p/mosaik-aligner/>) with a hash size of 15. Sites with potential indels were detected and realigned using the tools from the Genome Analysis Toolkit (GATK, version 2.3.9) [46], RealignerTargetCreator and IndelRealigner and potential PCR duplicates were eliminated using the MarkDuplicates tool from Picard version 1.100. (<http://picard.sourceforge.net>). The number of mappable reads after post-processing ranged from 2.9 to 5.2 million resulting in a mapped coverage spanning from approximately 50x to over 100x in the different samples. Variant calling (single nucleotide variants and small indels) was performed using GATK UnifiedGenotyper, and annotation of the detected variants was performed using SnpEff version 3.4 (<http://snpeff.sourceforge.net>). Finally, the alignments were visually inspected for all detected variants, in order to eliminate obvious false positives caused by incorrect alignments.

### **qRT-PCR procedures and gene expression analysis**

Cells were cultured in shake flasks using minimal medium with 2% glucose in triplicate, and harvested for gene expression analysis at exponential growth phase ( $OD_{600} \sim 1.0$ ) by centrifugation at -20 °C, quenched by liquid nitrogen, and stored at -80 °C for use. Total RNA was isolated using RNeasy Mini Kit (QIAGEN), which was then processed to obtain fragmented cDNA using a QuantiTect Reverse Transcription Kit (QIAGEN). 2  $\mu$ L of the synthesized cDNA (corresponding to 100 ng RNA) was used as the template for the qPCR reaction to a final reaction volume of 20  $\mu$ L, using a DyNAamo Flash SYBR Green qPCR Kit (Thermo Scientific, USA). Quantitative RT-PCR was performed on Stratagene Mx3005P (Agilent Technologies, USA). The thermocycling program consisted of one hold at 95 °C for 15 min, followed by 40 cycles of 10 s at 95 °C and 20 s at 60 °C, and a final cycle of 1 min at 95 °C, 30 s at 55 °C and 30 s at 95 °C.

Primers for real-time PCR (Table S1) were designed using Primer3 (<http://bioinfo.ut.ee/primer3-0.4.0/>) with melting temperature ( $T_m$ ) around 60 °C. *ACT1*, a housekeeping gene, was selected as the reference gene [47]. Final concentration of primers used was 0.5 mM in 20  $\mu$ L qPCR reactions. Due to nearly identical sequences of *HXT6* and *HXT7*, they used the same pair of primers for real-time PCR. Therefore, the transcription analysis result for *HXT6* and *HXT7* was their sum-up.

- **Bioinformatic analysis**

The protein sequence of each of the four *S. cerevisiae* proteins Cit1 (UniProt# P00890), Hxt2 (UniProt# P23585), Rpd3 (UniProt# P32561) and Mth1 (UniProt# P35198) was separately used to query the NCBI database with the basic local alignment search tool (BLAST). To eliminate sequences with low identity to the *S. cerevisiae* sequences, the BLAST results were filtered to retain only those with more than 40% identity to the *S. cerevisiae* enzymes. The 40% cutoff was arbitrary set and is intended to limit the analysis to sequences which can reasonably be said to have the same function as the *S. cerevisiae* enzyme. Sequences were also filtered such that anything more than 95% identical to anything else in the dataset was removed. This was done to reduce bias, should there be a large number of deposited sequences of the same gene from the same organism. The remaining sequences were aligned using MUSCLE [48]. The resulting alignment was used to compute the conservation of each amino acid in the *S. cerevisiae* proteins compared to the filtered BLAST results. The computed conservation values were used to color-code sequence representations of the *S. cerevisiae* proteins. Homology models were generated for three of the four proteins using the Swiss-Model repository [49]. For Mth1 no homology model could be made as there is no crystal structure of a homologous protein. An alternative approach was therefore used where the secondary structure of the mutated region was predicted. This prediction was used in the data analysis.

### Competing interests

The authors declare no competing financial interests.

### Authors' contributions

YZ designed and carried out the strain constructions, strain evolution, the cultivation experiments, analyzed the results and drafted the manuscript. ME performed the bioinformatics analysis on the mutations and revised the manuscript. BMH performed the genome sequencing analysis, and revised the manuscript. AK, YC, VS and JN supervised the design, revised the manuscript and coordinated the study. All authors read and approved the final manuscript

### Acknowledgements

The authors would like to acknowledge support from Science for Life Laboratory, the National Genomics Infrastructure, NGI, and Uppmax for providing assistance with genome sequencing and computational analysis. This work was performed in collaboration with Genomatica, Inc., and financially supported by Vetenskapsrådet, FORMAS, the Novo Nordisk Foundation and the European Research Council (grant no. 247013).

### Reference

1. Nielsen, J. and M.C. Jewett, *Impact of systems biology on metabolic engineering of Saccharomyces cerevisiae*. FEMS Yeast Res, 2008. **8**(1): p. 122-31.
2. Kim, I.K., et al., *A systems-level approach for metabolic engineering of yeast cell factories*. FEMS Yeast Res, 2012. **12**(2): p. 228-48.

3. Chen, Y. and J. Nielsen, *Advances in metabolic pathway and strain engineering paving the way for sustainable production of chemical building blocks*. Curr Opin Biotechnol, 2013. **24**(6): p. 965-72.
4. Jensen, M.K. and J.D. Keasling, *Recent applications of synthetic biology tools for yeast metabolic engineering*. FEMS Yeast Res, 2014.
5. Nielsen, J. and J.T. Pronk, *Metabolic engineering, synthetic biology and systems biology*. FEMS Yeast Res, 2012. **12**(2): p. 103.
6. Flikweert, M.T., et al., *Growth requirements of pyruvate-decarboxylase-negative *Saccharomyces cerevisiae**. FEMS Microbiol Lett, 1999. **174**(1): p. 73-9.
7. Schaaff, I., et al., *A deletion of the PDC1 gene for pyruvate decarboxylase of yeast causes a different phenotype than previously isolated point mutations*. Curr Genet, 1989. **15**(2): p. 75-81.
8. Hohmann, S. and H. Cederberg, *Autoregulation may control the expression of yeast pyruvate decarboxylase structural genes PDC1 and PDC5*. Eur J Biochem, 1990. **188**(3): p. 615-21.
9. Hohmann, S., *Characterization of PDC6, a third structural gene for pyruvate decarboxylase in *Saccharomyces cerevisiae**. Journal of Bacteriology, 1991. **173**(24): p. 7963-9.
10. Flikweert, M.T., et al., *Pyruvate decarboxylase: an indispensable enzyme for growth of *Saccharomyces cerevisiae* on glucose*. Yeast, 1996. **12**(3): p. 247-57.
11. van Maris, A.J., et al., *Overproduction of threonine aldolase circumvents the biosynthetic role of pyruvate decarboxylase in glucose-limited chemostat cultures of *Saccharomyces cerevisiae**. Appl Environ Microbiol, 2003. **69**(4): p. 2094-9.
12. van Maris, A.J., et al., *Directed evolution of pyruvate decarboxylase-negative *Saccharomyces cerevisiae*, yielding a C2-independent, glucose-tolerant, and pyruvate-hyperproducing yeast*. Appl Environ Microbiol, 2004. **70**(1): p. 159-66.
13. Oud, B., et al., *An internal deletion in MTH1 enables growth on glucose of pyruvate-decarboxylase negative, non-fermentative *Saccharomyces cerevisiae**. Microb Cell Fact, 2012. **11**(1): p. 131.
14. Gamo, F.J., M.J. Lafuente, and C. Gancedo, *The mutation DGT1-1 decreases glucose transport and alleviates carbon catabolite repression in *Saccharomyces cerevisiae**. Journal of Bacteriology, 1994. **176**(24): p. 7423-9.
15. Blazquez, M.A., F.J. Gamo, and C. Gancedo, *A mutation affecting carbon catabolite repression suppresses growth defects in pyruvate carboxylase mutants from *Saccharomyces cerevisiae**. FEBS Lett, 1995. **377**(2): p. 197-200.
16. Lafuente, M.J., et al., *Mth1 receives the signal given by the glucose sensors Snf3 and Rgt2 in *Saccharomyces cerevisiae**. Mol Microbiol, 2000. **35**(1): p. 161-72.
17. Schulte, F., et al., *The HTR1 gene is a dominant negative mutant allele of MTH1 and blocks Snf3-and Rgt2-dependent glucose signaling in yeast*. Journal of Bacteriology, 2000. **182**(2): p. 540-542.
18. Ozcan, S., et al., *Glucose uptake and catabolite repression in dominant HTR1 mutants of *Saccharomyces cerevisiae**. Journal of Bacteriology, 1993. **175**(17): p. 5520-8.
19. Moriya, H. and M. Johnston, *Glucose sensing and signaling in *Saccharomyces cerevisiae* through the Rgt2 glucose sensor and casein kinase I*. Proceedings of the National Academy of Sciences of the United States of America, 2004. **101**(6): p. 1572-1577.
20. Lakshmanan, J., A.L. Mosley, and S. Ozcan, *Repression of transcription by Rgt1 in the absence of glucose requires Std1 and Mth1*. Curr Genet, 2003. **44**(1): p. 19-25.
21. Polish, J.A., J.H. Kim, and M. Johnston, *How the Rgt1 transcription factor of *Saccharomyces cerevisiae* is repressed by glucose*. Genetics, 2005. **169**(2): p. 583-594.
22. Kruckeberg, A.L. and L.F. Bisson, *The HXT2 gene of *Saccharomyces cerevisiae* is required for high-affinity glucose transport*. Mol Cell Biol, 1990. **10**(11): p. 5903-13.
23. Kim, K.S., M.S. Rosenkrantz, and L. Guarente, **Saccharomyces cerevisiae* contains two functional citrate synthase genes*. Mol Cell Biol, 1986. **6**(6): p. 1936-42.

24. Vidal, M., et al., *Direct selection for mutants with increased K<sup>+</sup> transport in *Saccharomyces cerevisiae**. Genetics, 1990. **125**(2): p. 313-20.
25. Cole, C., J.D. Barber, and G.J. Barton, *The Jpred 3 secondary structure prediction server*. Nucleic Acids Research, 2008. **36**: p. W197-W201.
26. Roy, A., A. Kucukural, and Y. Zhang, *I-TASSER: a unified platform for automated protein structure and function prediction*. Nat Protoc, 2010. **5**(4): p. 725-38.
27. Entian, K.-D. and P. Kötter, *25 Yeast Genetic Strain and Plasmid Collections*, in *Methods in Microbiology*, S. Ian and J.R.S. Michael, Editors. 2007, Academic Press. p. 629-666.
28. Kim, J.H., et al., *Integration of transcriptional and posttranslational regulation in a glucose signal transduction pathway in *Saccharomyces cerevisiae**. Eukaryot Cell, 2006. **5**(1): p. 167-73.
29. Flikweert, M.T., J.P. van Dijken, and J.T. Pronk, *Metabolic responses of pyruvate decarboxylase-negative *Saccharomyces cerevisiae* to glucose excess*. Appl Environ Microbiol, 1997. **63**(9): p. 3399-404.
30. Gey, U., et al., *Yeast pyruvate dehydrogenase complex is regulated by a concerted activity of two kinases and two phosphatases*. J Biol Chem, 2008. **283**(15): p. 9759-67.
31. Bowman, S.B., et al., *Positive regulation of the LPD1 gene of *Saccharomyces cerevisiae* by the HAP2/HAP3/HAP4 activation system*. Mol Gen Genet, 1992. **231**(2): p. 296-303.
32. Reifenberger, E., E. Boles, and M. Ciriacy, *Kinetic characterization of individual hexose transporters of *Saccharomyces cerevisiae* and their relation to the triggering mechanisms of glucose repression*. Eur J Biochem, 1997. **245**(2): p. 324-33.
33. Ozcan, S. and M. Johnston, *Three different regulatory mechanisms enable yeast hexose transporter (HXT) genes to be induced by different levels of glucose*. Mol Cell Biol, 1995. **15**(3): p. 1564-72.
34. Gancedo, J.M., *The early steps of glucose signalling in yeast*. Fems Microbiology Reviews, 2008. **32**(4): p. 673-704.
35. Ruiz-Roig, C., et al., *The Rpd3L HDAC complex is essential for the heat stress response in yeast*. Mol Microbiol, 2010. **76**(4): p. 1049-62.
36. Knott, S.R., et al., *Genome-wide replication profiles indicate an expansive role for Rpd3L in regulating replication initiation timing or efficiency, and reveal genomic loci of Rpd3 function in *Saccharomyces cerevisiae**. Genes Dev, 2009. **23**(9): p. 1077-90.
37. Yi, C., et al., *Function and molecular mechanism of acetylation in autophagy regulation*. Science, 2012. **336**(6080): p. 474-7.
38. Kurdistani, S.K. and M. Grunstein, *Histone acetylation and deacetylation in yeast*. Nat Rev Mol Cell Biol, 2003. **4**(4): p. 276-84.
39. Takahashi, H., et al., *Nucleocytosolic acetyl-coenzyme A synthetase is required for histone acetylation and global transcription*. Molecular Cell, 2006. **23**(2): p. 207-217.
40. Erdeniz, N., U.H. Mortensen, and R. Rothstein, *Cloning-free PCR-based allele replacement methods*. Genome Research, 1997. **7**(12): p. 1174-1183.
41. Guldener, U., et al., *A new efficient gene disruption cassette for repeated use in budding yeast*. Nucleic Acids Res, 1996. **24**(13): p. 2519-24.
42. Gietz, R.D. and R.A. Woods, *Transformation of yeast by lithium acetate/single-stranded carrier DNA/polyethylene glycol method*. Methods Enzymol, 2002. **350**: p. 87-96.
43. Thompson, J.R., et al., *An improved protocol for the preparation of yeast cells for transformation by electroporation*. Yeast, 1998. **14**(6): p. 565-71.
44. Solis-Escalante, D., et al., *amdSYM, a new dominant recyclable marker cassette for *Saccharomyces cerevisiae**. FEMS Yeast Res, 2013. **13**(1): p. 126-39.
45. Verduyn, C., et al., *Effect of benzoic acid on metabolic fluxes in yeasts: a continuous-culture study on the regulation of respiration and alcoholic fermentation*. Yeast, 1992. **8**(7): p. 501-17.

46. McKenna, A., et al., *The Genome Analysis Toolkit: a MapReduce framework for analyzing next-generation DNA sequencing data*. *Genome Research*, 2010. **20**(9): p. 1297-303.
47. Teste, M.A., et al., *Validation of reference genes for quantitative expression analysis by real-time RT-PCR in *Saccharomyces cerevisiae**. *BMC Mol Biol*, 2009. **10**: p. 99.
48. Edgar, R.C., *MUSCLE: multiple sequence alignment with high accuracy and high throughput*. *Nucleic Acids Res*, 2004. **32**(5): p. 1792-7.
49. Kiefer, F., et al., *The SWISS-MODEL Repository and associated resources*. *Nucleic Acids Res*, 2009. **37**(Database issue): p. D387-92.
50. Deng, D., et al., *Crystal structure of the human glucose transporter GLUT1*. *Nature*, 2014. **510**(7503): p. 121-5.
51. Lauffer, B.E., et al., *Histone deacetylase (HDAC) inhibitor kinetic rate constants correlate with cellular histone acetylation but not transcription and cell viability*. *J Biol Chem*, 2013. **288**(37): p. 26926-43.

**Table 1 Strains used in this study**

Strain Name	Genotype or description
CEN.PK 113-5D	<i>MATa ura3-52</i>
CEN.PK 110-10C	<i>MATa his3-Δ1</i>
CEN.PK YMZ-A1	<i>MATa ura3-52 pdc5Δ</i>
CEN.PK YMZ-A2	<i>MATa ura3-52 pdc1Δ</i>
CEN.PK YMZ-A3	<i>MATa ura3-52 pdc6Δ</i>
CEN.PK YMZ-B1	<i>MATa ura3-52 pdc1Δ pdc5Δ</i>
CEN.PK YMZ-B2	<i>MATa ura3-52 pdc1Δ pdc6Δ</i>
CEN.PK YMZ-C1	<i>MATa ura3-52 pdc1Δ pdc5Δ pdc6Δ</i>
CEN.PK YMZ-C2	<i>MATa ura3-52 pdc1Δ pdc5Δ pdc6Δ</i>
CEN.PK YMZ-D1	<i>MATa his3-Δ1 pdc1Δ pdc5Δ pdc6Δ</i>
CEN.PK YMZ-D2	<i>MATa his3-Δ1 pdc1Δ pdc5Δ pdc6Δ</i>
CEN.PK YMZ-E1	<i>MATa ura3-52 his3-Δ1 pdc1Δ pdc5Δ pdc6Δ</i>
CEN.PK YMZ-E2	<i>MATa ura3-52 his3-Δ1 pdc1Δ pdc5Δ pdc6Δ</i>
CEN.PK YMZ-E1A	CEN.PK YMZ-E1 adaptively evolved in glucose
CEN.PK YMZ-E1B	CEN.PK YMZ-E1 adaptively evolved in glucose
CEN.PK YMZ-E1C	CEN.PK YMZ-E1 adaptively evolved in glucose
M81-11	CEN.PK YMZ-E1, <i>mth1::MTH1<sup>81D</sup></i>
M81-33	CEN.PK YMZ-E1, <i>mth1::MTH1<sup>81D</sup></i>
M81C	M81-11, <i>cit1::amdSYM</i>

**Table 2. Point mutations in evolved E1 strains**

Name	Description	Evolved strains		
		E1A	E1B	E1C
Mth1	Negative regulator of the glucose-sensing signal transduction pathway	A81/D	I85/S	A81/D
Cit1	Mitochondrial citrate synthase	P176/Q	M84/V	H175/R
Hxt2	High-affinity glucose transporter of the major facilitator superfamily	W466/*	G75/R	W466/*
Rpd3	Histone deacetylase, component of both the Rpd3S and Rpd3L complexes	85F/I	196A/V	

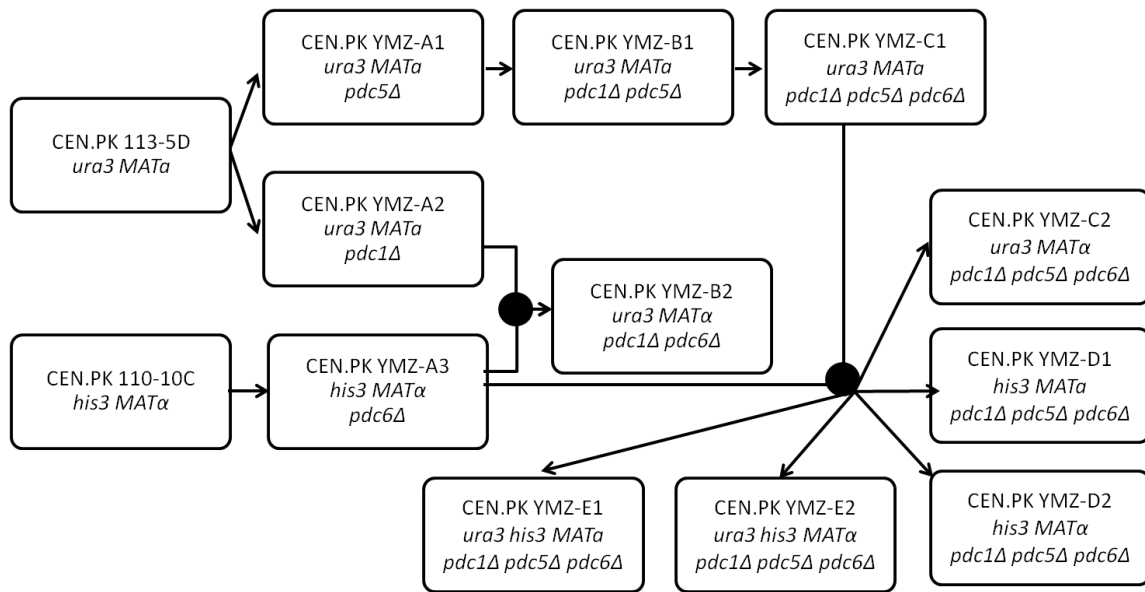


**Figure 1. Work flow of Pdc negative strain construction.** *PDC1*, *PDC5*, and *PDC6* were consecutively deleted in two different background strains CEN.PK 113-5D (*MAT $\alpha$  ura3-52*) and CEN.PK 110-10C (*MAT $\alpha$  his3-Δ1*). A collection of pdc negative strains was obtained using a combination of consecutive deletions with strain crossings and tetrad dissections. The closed circles represent crossings.

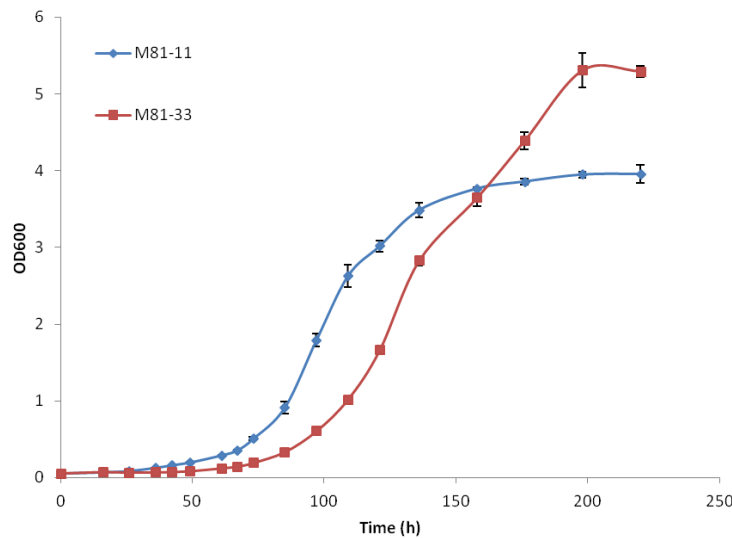


**Figure 2. Growth profiles of reverse engineered M81 strains.** M81-11 and M81-33 are two different transformants (*ura3-52 his3-Δ1 pdc1Δ pdc5Δ pdc6Δ mth1::MTH1<sup>81D</sup>*) in minimal medium with 2% glucose.

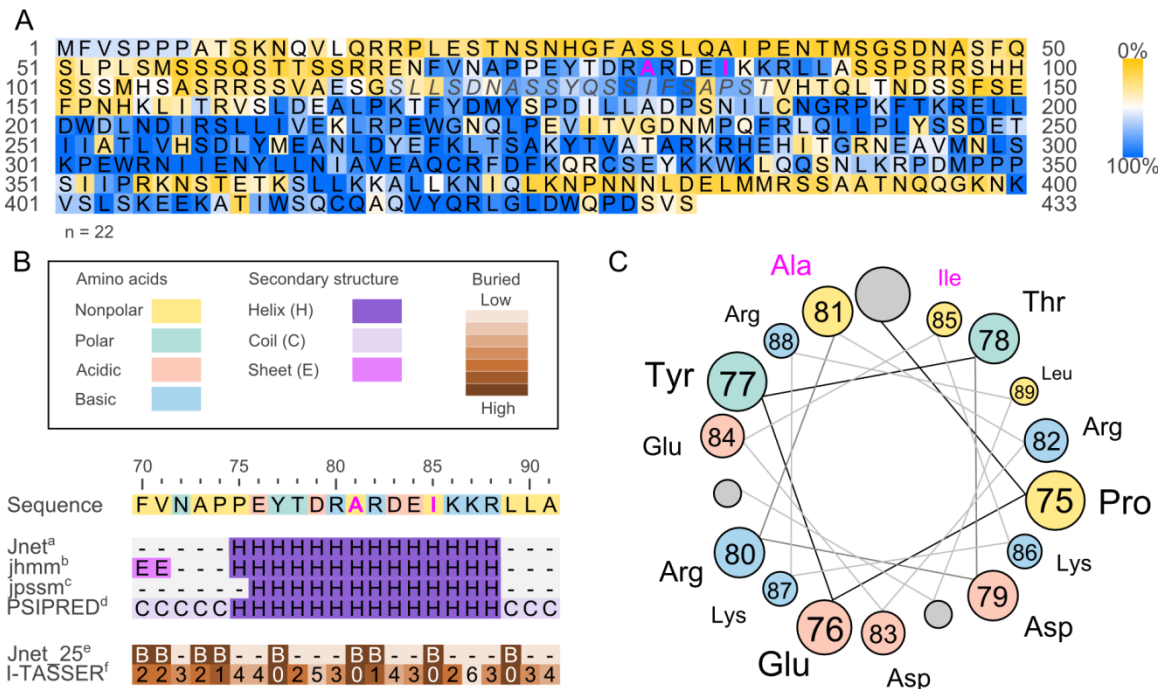


**Figure 3. Mapping and analysis of Mth1 mutations.** Magenta text indicates positions for non-synonymous mutations identified in this study. A) Result of a multiple alignment using homologous sequences (n=22). The Mth1 sequence of *S. cerevisiae* is shown with colored conservation levels. Yellow indicates low conservation, white intermediate, and blue high. Gray and italic text indicates the phosphorylation region of casein kinase Yck1. B) Analysis of the 22 amino acids from the conserved region at position 70-91 and secondary structure predictions using 6 different prediction programs [25, 26]. C) A helix wheel representation of amino acids predicted to form an alpha-helix (Codon 75-89). The amino acid types are colored as in B.

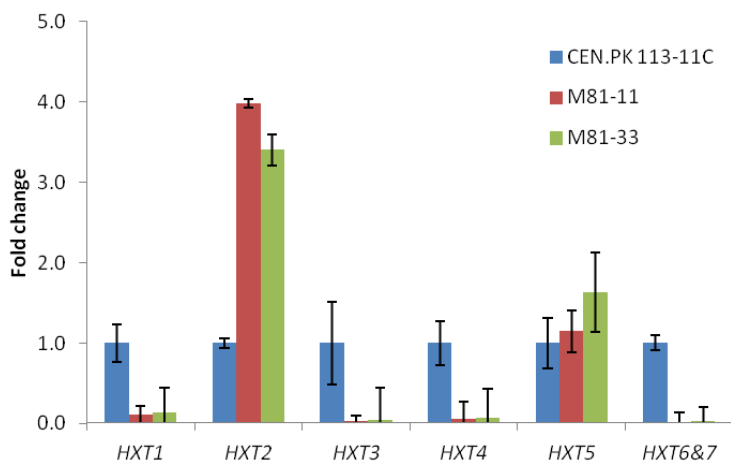
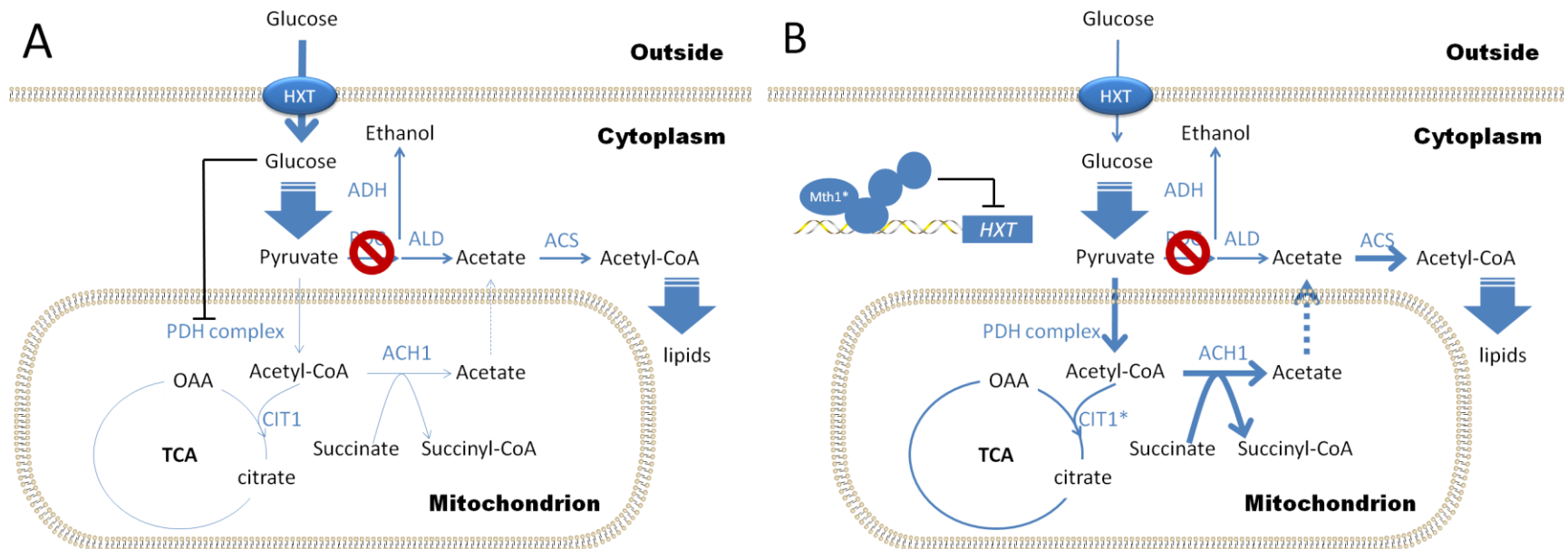


**Figure 4. Transcription analysis of HXTs (HXT1-7) in two M81 strains and wild type strain CEN.PK 113-11C.** Cells for transcription analysis were harvested at exponential phase ( $OD_{600}$  ~1). The expression levels of HXTs in wild type strain were set as 1.



1

2 **Figure 5. A simple illustration for possible roles of mutated proteins in the evolved Pdc negative strains.** The blue solid arrows represent the  
 3 reactions catalyzed by the enzymes, which are indicated in blue text. The blue dash line represents the transportation between different subcellular  
 4 organelles. The black lines with a bar at one end represent the repression or inhibition. The red circles represent the block due to Pdc deletions. . A)  
 5 Simplified acetyl-CoA metabolism in the parental Pdc negative strain. The PDH complex and TCA cycle enzymes are repressed by high glucose  
 6 uptake via hexose transporters (HXT). B) Simplified acetyl-CoA metabolism in evolved Pdc negative strain with point mutated Mth1 ( $Mth1^*$ ) and  
 7 Cit1 ( $Cit1^*$ ). Glucose uptake via HXT decreases in the presence of  $Mth1^*$ , resulting in derepression of the PDH complex and TCA cycle enzymes.  
 8  $Cit1^*$  with predicted decreased activity allows more mitochondria acetyl-CoA convert to acetate by Ach1, which can be transported to the cytosol  
 9 and converted to acetyl-CoA there.

19

## **Supplementary**

- **Analysis of mutations in Cit1 and their possible effects**

The alignment results of Cit1 from *S. cerevisiae* and other 378 homologous sequences from fungi, animals and plants revealed that M84V, H175R and P176Q mutations occurred at positions that are 79%, 99% and 98% conserved, respectively (Figure S5A). A homology model of Cit1 was generated using the crystal structure of the chicken citrate synthase with the aim of gaining insights into the function of M84, H175, and P176. As shown in Figure S5B, all three mutations are situated at the interface between the two polypeptides of the Cit1 homodimer. M84 is one of the highly conserved residues, which interact with the identical residue from the other polypeptide chain of the homodimer as shown in Figure S5C, and may serve structural and functionally important roles. Furthermore, R85 (R46 in chicken CS) hydrogen-bonds to the phosphate group of the substrate acetyl-CoA analogue, whereas R459 (R421 in chicken CS) to one carboxyl group of the substrate oxaloacetate. Therefore the M84V mutation might lead to a decreased Cit1 enzyme activity due to structural perturbations around the active sites, which in turn would lead to a decrease or loss of substrate binding affinity. As shown in Figure S5D, H175 forms a water bridge with Q317 (97% conserved) from an opposing alpha helix in the same polypeptide chain, which likely helps increasing the structural rigidity. The mutation H175R may therefore lead to incorrect or inefficient protein folding or interfere with interactions between the two monomers. P176 likely serves a structural role initiating an alpha helix (Figure S5D), and the mutation P176Q may therefore cause the alpha helix not to form or to form later in the primary sequence, which may cause structural perturbation of several amino acids, including H175.

- **Analysis of mutations in Hxt2 and their possible effects**

The alignment results of Hxt2 from *S. cerevisiae* and other 201 homologous sequences from unicellular fungi revealed that the mutations G75R and W466\* occurred at positions that are 100% and 93% conserved, respectively (Figure S4A). A homology model of Hxt2 was generated using the crystal structure of the human glucose transporter Glut1 with the aim of gaining insights into the function of G75 and W466 [50]. As shown in Figure S4B, G75 is positioned in the interface between the N-and C-terminal domains, and W466 and the residues thereafter comprise one and a half trans-membrane alpha helices situated on the outside of the protein. A close-up of the region surrounding G75 revealed it's positioned with the alpha carbon facing inwards in a bundle of four helices that form the substrate channel (Figure S4C). The mutation G75R at the 100% conserved residue could result in a very large change in side chain properties, since glycine has no side chain whereas arginine has the third largest side chain after tryptophan and tyrosine. Therefore, it is very likely that the G75R mutation completely disrupt the ability of this protein to mediate sugar transport due to steric hindrance. W466 is positioned at the middle of TM11, the second to last trans-membrane helix, which are structurally important and help in correctly positioning other helices with TM12 (Figure S5B&D). As shown in Figure S4D, the backbone of TM11 and the side chains of Y485 and Y489 on TM12 sterically push on residues Y333, F334, Y337 and I341 on TM7, causing a kink to form. The kink formed in TM7 brings it in contact with TM1 and together they represent the main constituents of the extracellular gate of the substrate

channel (Figure S4C). TM7 and TM1 form hydrogen-bonds in this region and mutations at these residues are known to cause Glut1 deficiency syndrome in humans [50]. However, it is hard to evaluate the effects of the mutation W466\* due to the very large changes resulting from a 76 amino acid deletion. We speculated that the mutation W466\* might relax the steric push on TM7, thus removing the kink and causing the substrate channel not form correctly, or may even cause complete misfolding of the protein.

- **Analysis of Rpd3 mutations and their possible effects**

The alignment results of Rpd3 from *S. cerevisiae* and other 265 homologous sequences from unicellular and multicellular fungi, plants, animals and a range of bacteria revealed that the mutations F85I and A196V occurred at positions that are 97% and 98% conserved, respectively (Figure S6A). A homology model of Rpd3 was generated using the crystal structure of the human histone deacetylase 2 protein (PDB ID: 4LXZ) with the aim of gaining insights into the function of F85 and A196 [5151](Figure S6B). F85 is buried in between two alpha helices and a loop in the N-terminal domain of the protein (Figure S6B&C). While F85 is highly conserved, the residues surrounding it are less so. There is a trend that the inward-facing hydrophobic amino acids of this region, such as Y82, L86, V89 and V106, are among the more conserved at 98%, 94%, 58% and 85% respectively. In contrast, the more outward-facing hydrophilic residues, such as R88, E100 and S101, are less conserved at 35%, 39% and 35% respectively (Figure S6C). The data therefore indicate that F85 is important for the hydrophobic packing of this region and thus serves a structural role in the protein. A196 is part of an alpha helix that is situated at the interface between the N- and C-terminal domains. The helix is also immediately adjacent to the bound  $\text{Ca}^{2+}$  and  $\text{Na}^+$  ions (Figure S6D). All of the amino acids on this helix are highly conserved (D191 100%, G192 100%, V193 99%, E194 90%, E195 100%, A196 98%, F197 100% and Y198 96%). V167 (98% conversed) is directly interacting with A196 across the domain interface. The very high degree of conservation in this region of the protein structure is astounding, especially when one considers how evolutionarily diverse the set of sequences is. The residues are obviously very sensitive to mutations. It's possible that the two extra methyl groups introduced by the A196V mutation sterically interfere with the side chain of V167, which may in turn cause a displacement of the conserved helix and result in decreased or abolished enzyme activity.

**Table S1. Primers used in this study and their sequences**

Primer #	Primer name	Sequence 5'→3'
1	pdc1-up-fw	TACTTGCTATCGTTCAACAC
2	pdc1-up-rev	CAGCGTACGAAGCTTCAGTGCCTGAGGGTTATGAGTAG
3	pdc1-dw-fw	GTGATATCAGATCCACTAGTACCAACGCTAACGAAATAAG
4	pdc1-dw-rev	CCTTGGTCCACTAATTCATC
5	pdc5-up-fw	TTAGGCATAATCACCGAAGA
6	pdc5-up-rev	CAGCGTACGAAGCTTCAGGAGAGGAAAGGACTTACTACA
7	pdc5-dw-fw	GTGATATCAGATCCACTAGTCTGTCCGTCTCCAG
8	pdc5-dw-rev	GGTGCCTACTGGTGATT
9	pdc6-up-fw	ACATCTCCAACGATCTCAT
10	pdc6-up-rev	CAGCGTACGAAGCTTCAGGAATCGCACCATATCCCTTA
11	pdc6-dw-fw	GTGATATCAGATCCACTAGCGTTATGCCGTGAATTAC
12	pdc6-dw-rev	TTGGTTGTAGATGGTGGTG
13	kanMX_1_fw	CTGAAGCTTACGCTG
14	kanMX_1_rev	TCACCATGAGTGACGACTGA
15	kanMX_2_fw	TTCCAACATGGATGCTGAT
16	kanMX_2_rev	CTAGTGGATCTGATATCAC
17	pdc1-up-check	GTGATGAGGCTCGTGGAA
18	pdc1-dw-check	CGAGGTGTCTAGTCTTCTATT
19	pdc5-up-check	ACTGCCATCACTAGAGAAGA
20	pdc5-dw-check	TTGTCGGAGTCCATTCT
21	pdc6-up_ck	TCGGTCCCTCATCATCTCT
22	pdc6-dw_ck	TCTTGTCCATTACGGTCTCT
23	mth_up_fw	GCTGCCTCAATCTCCATT
24	Mth1_81_rev	CTCATCTCTAtCTCTATCAGTGTACTCCGGA
25	Mth1_81_fw	CTGATAGAGaTAGAGATGAGATTTAAAAAG
26	mth1_dw_rev_n1	GTATTCTGGGCCTCCATGTCGCTGTGCTCAACTACCAA
27	mth1_in_fw2_n1	GAATGCTGGTCGCTATACTGATGCCTCGTCTTATCAATCA
28	mth_dw_rev	GCTGTGCTCAACTACCAA
29	amdS-F1	GACATGGAGGCCAGAATAC
30	amdS-R1	CAGTATAGCGACCAGCATT
31	amdS_in_F	TCTTGTTGGTCTTCTCT
32	amdS_in_R	GAGTGATTGGAGCGATGAT
33	mth1_up_fw1	CCGAGACTTACTGGACTT
34	mth1_dw_rev1	CATTGTTGTATTGTGCTGTG
35	MAT	AGTCACATCAAGATCGTTATGG
36	MAT a	ACTCCACTTCAAGTAAGAGTTG
37	MAT alpha	GCACGGAATATGGACTACTTCG
38	HXT1_fw_q	GGCCGTCGTAACTGTTGAT
39	HXT1_rv_q	AATTGGGGCCCAGGTAGTAG
40	HXT2_fw_q	TTGCCGAATCCTATCCTTG
41	HXT2_rv_q	ACCAAACAGCCATGAAGAC
42	HXT3_fw_q	GCTGACCTGCCTCGAATAG
43	HXT3_rv_q	ACCGAAGGCAACCATAACAC
44	HXT4_fw_q	GTTGCTTCGGTGGTTTG
45	HXT4_rv_q	AATGGCACAACCAATGTTGA
46	HXT5_fw_q	CAAGCGGTCCCTAGCAAGAG
47	HXT5_rv_q	ACCAACAGCCTGGAAAATTG
48	HXT6&7_fw_q	AAAGGTCCTTCAGCGTTGA
49	HXT6&7_rv_q	GCACCCCATAGCAAACAAGT

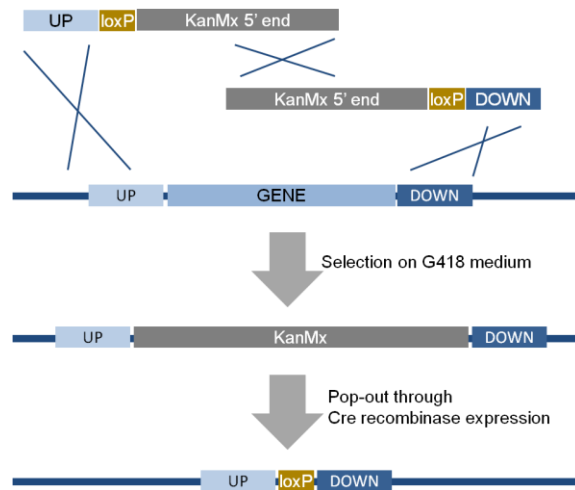


**Figure S1. Bipartite strategy for gene deletion**

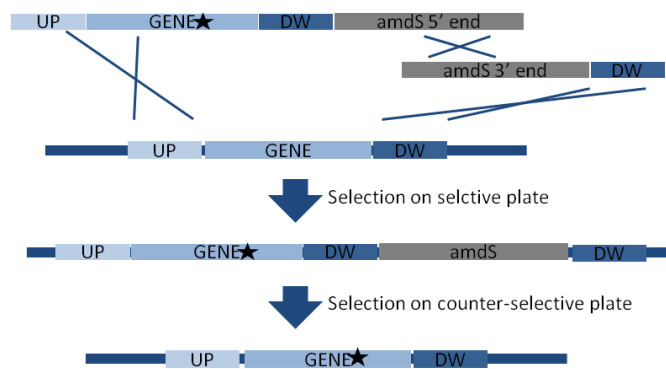


**Figure S2. Reverse engineering strategy for *MTH1*<sup>8ID</sup> integration into *MTH1* locus of E1 strain**

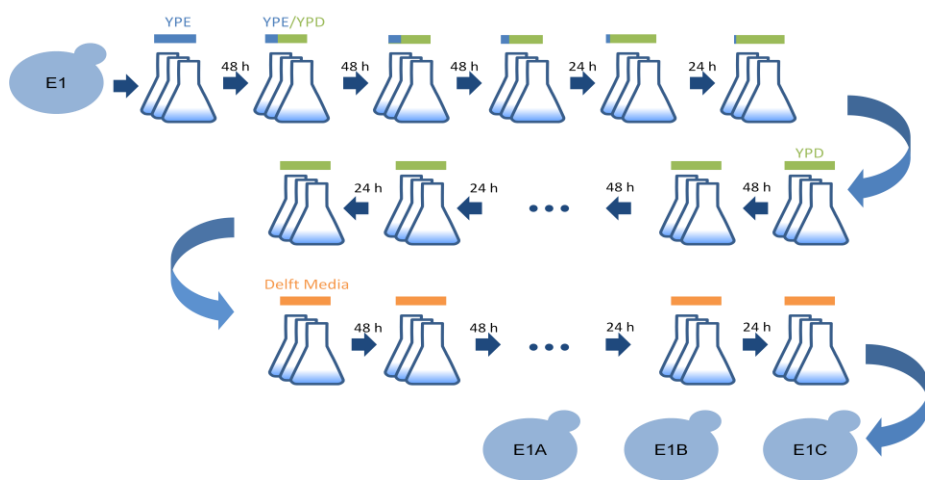


**Figure S3. Adaptive Evolution Process of the pdc negative strain E1**

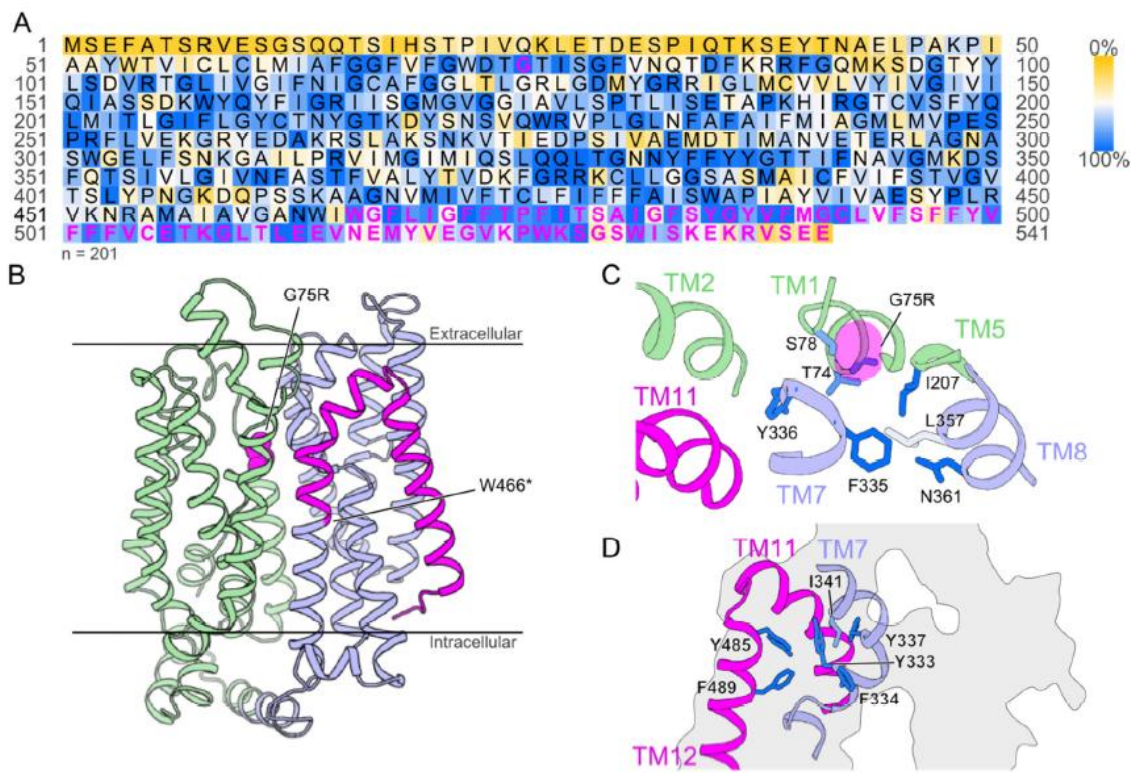


**Figure S4. Mapping and analysis of Hxt2 mutations.** A) Result of a multiple alignment using homologous sequences (n=201). The *S. cerevisiae* Hxt2 sequence is shown with colored conservation levels. Yellow indicates low conservation, white intermediate, and blue high. Magenta text indicates positions for the identified mutation and the amino acids missing due to the non-sense mutation. B) A cartoon representation of an Hxt2 homology model generated using a crystal structure of the human glucose transporter Glut1 (PDB ID: 4PYP). The N-terminal and C-terminal domain of the peptide are shown in pale green and purple, respectively. The global position of the mutation G75R is indicated by magenta sphere representation, and the mutation W466\* by magenta coloring for the deleted protein sequence. Lines indicate the approximate boundaries of the phospholipid bilayer in which the protein performs its function. C) A close-up of the region surrounding G75R. D) A close-up of the region surrounding W466\*. A protein cross-section is shown in grey with the substrate channel visible in white at the center of the protein. Amino acid sidechains are colored according their conservation using the same color as in A. The mutation is highlighted by a transparent magenta space-fill representation of the entire mutated amino acid. Hydrogen atoms in glycine are shown in order to visualize the residue position. The color-coded amino acid sequence was generated using custom software in Python and the structure was visualized using PyMol ([www.pymol.org](http://www.pymol.org)).

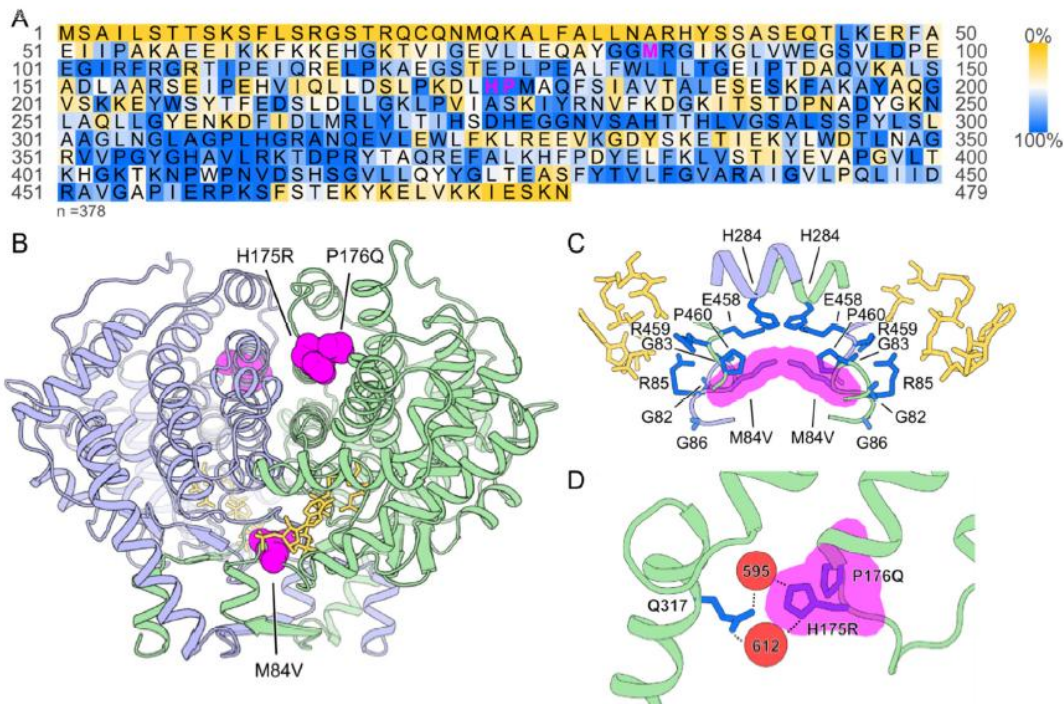


**Figure S5. Mapping and analysis of Cit1 mutations.** A) Result of a multiple alignment using homologous sequences (n=378). The *S. cerevisiae* Cit1 sequence is shown with colored conservation levels. Yellow indicates low conservation, white intermediate, and blue high. Magenta text indicates positions for non-synonymous mutations identified in this study. B) A cartoon representation of a Cit1 homology model generated using a crystal structure of chicken citrate synthase (PDB ID: 1AL6). The position of mutations is indicated by magenta sphere representations of the amino acids in the two polypeptides of Cit1 homodimer shown in pale purple and pale green respectively. The substrate oxaloacetate and the substrate analog N-hydroxyamido-CoA are shown in yellow. C) A close-up of the region surrounding M84V. Amino acid sidechains are colored according their conservation using the same color as in A. D) A close-up of the region surrounding H175R and P176Q. The mutation is highlighted by a transparent magenta space-fill representation of the entire mutated amino acid. Hydrogen atoms in glycine are shown in order to visualize the residue position. Water molecules are represented by red spheres and hydrogen bonds are indicated by dashed lines. The color-coded amino acid sequence was generated using custom software in Python and the structure was visualized using PyMol ([www.pymol.org](http://www.pymol.org)).

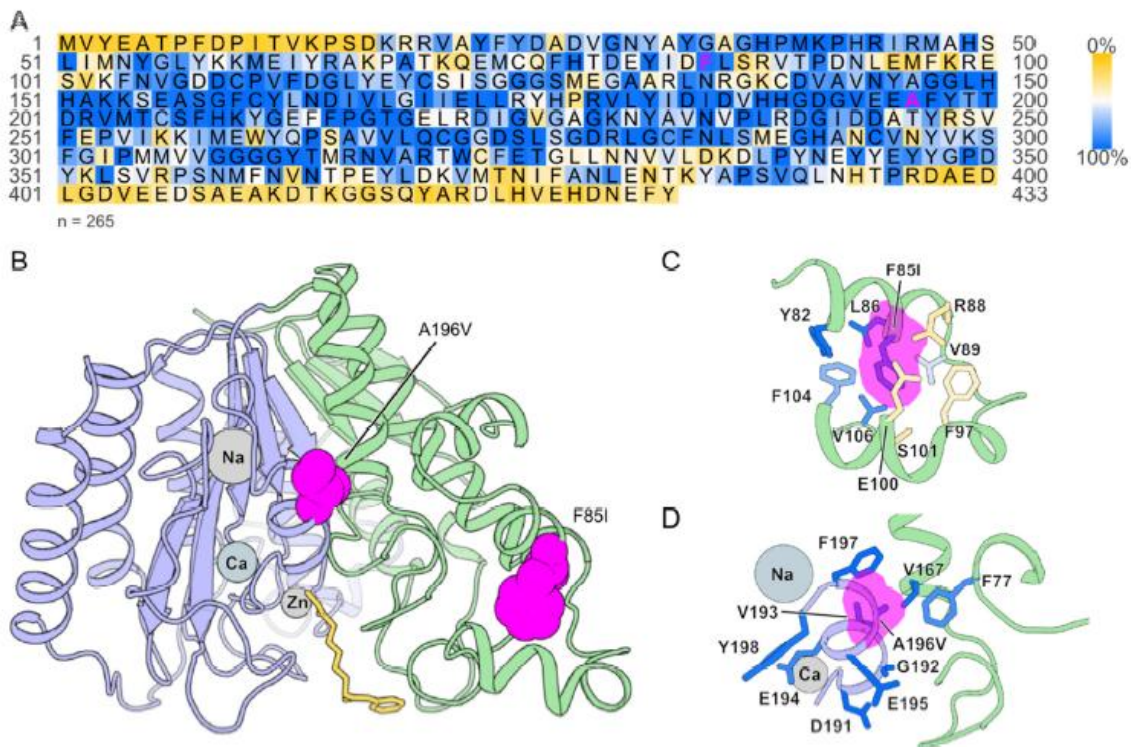


**Figure S6. Mapping and analysis of Rpd3 mutations.** A) Result of a multiple alignment using homologous sequences (n=265). The *S. cerevisiae* Rpd3 sequence is shown with colored conservation levels. Yellow indicates low conservation, white intermediate, and blue high. Magenta text indicates positions for non-synonymous mutations identified in this study. B) A cartoon representation of an Hxt2 homologous model generated using a crystal structure of the human histone deacetylase 2 protein (PDB: 4LXZ). The N-terminal and C-terminal domain of the polypeptide are shown in pale green and pale purple respectively. The global position of mutations is indicated by magenta sphere representations of the amino acids. The enzyme inhibitor Vorinostat co-crystallized with the enzyme is shown in yellow. Metal ions in the structure are shown in grey colors (Na: sodium ion, Ca: calcium ion; Zn: zinc ion.). C) A close up of the region surrounding F85I. D) A close-up of the region surrounding A196V. Amino acid sidechains are colored according their conservation using the same color as in A. The mutation is highlighted by a transparent magenta space-fill representation of the entire mutated amino acid. Hydrogen atoms in glycine are shown in order to visualize the residue position. The color-coded amino acid sequence was generated using custom software in Python and the structure was visualized using PyMol ([www.pymol.org](http://www.pymol.org)).

## **PAPER III**



1   **Title: Functional pyruvate formate lyase pathway expressed with its**  
2   **cofactors in *Saccharomyces cerevisiae* at aerobic growth**

3   Running title: Pyruvate formate lyase pathway functions  
4   aerobically in yeast

5   Yiming Zhang, Anastasia Krivoruchko, Yun Chen , Verena Siewers, Jens Nielsen\*

6   Department of Chemical and Biological Engineering, Chalmers University of Technology,  
7   Kemiv ägen 10, SE-412 96 Göteborg, Sweden

8   \*Corresponding author, Email: [nielsenj@chalmers.se](mailto:nielsenj@chalmers.se), Phone: +46 (0)31 772 3804, Fax: +46(0)31  
9   772 3801

10   **Abstract**

11   Pyruvate formate lyase (PFL) is characterized as an enzyme functional at anaerobic conditions,  
12   since the radical in the enzyme´s active form is sensitive to oxygen. In this study, pyruvate  
13   formate lyase and its activating enzyme from *Escherichia coli* were expressed in a  
14   *Saccharomyces cerevisiae* strain lacking pyruvate decarboxylase and having a reduced glucose  
15   uptake rate due to a mutation in the transcriptional regulator Mth1, IMI076 (Pdc<sup>-</sup> *MTH1-ΔT ura3-*  
16   52). PFL was expressed with two different cofactors as electron donors, reduced ferredoxin or  
17   reduced flavodoxin, respectively, and it was found that the co-expression either of these cofactors  
18   had a positive effect on growth under aerobic conditions, indicating increased activity of PFL.  
19   The positive effect on growth was manifested as a higher final biomass concentration and a  
20   significant increase in transcription of formate dehydrogenases (FDHs). Among the two cofactors  
21   reduced flavodoxin was found to be a better electron donor than reduced ferredoxin.

22   **Keywords:**

23   ferredoxin, flavodoxin, ferredoxin/flavodoxin NADP<sup>+</sup> reductase, aerobic growth, metabolic  
24   engineering, yeast

26    **Introduction**

27    In connection with establishing biobased production of fuels and chemicals it is necessary to  
28    engineer the metabolism of cell factories such that the raw material, typically sugars, are  
29    efficiently converted to the product of interest. Many industrially interesting products are  
30    biosynthesized from acetyl-CoA (Nielsen 2014) and there is therefore much interest in establish  
31    cell factory platforms for efficient conversion of sugars, e.g. glucose, to acetyl-CoA. In yeast, a  
32    key cell factory for production of a wide range of products (Kim *et al.* 2012; Chen *et al.* 2013),  
33    acetyl-CoA metabolism is compartmentalized into three main compartments, the mitochondria,  
34    the cytosol and the peroxisome (Chen *et al.* 2012). For efficient production of heterologous  
35    products it is generally preferred to biosynthesize these from cytosolic acetyl-CoA (Nielsen 2014).  
36    Naturally yeast convert pyruvate in the cytosol to acetaldehyde that is further converted to acetate  
37    and acetyl-CoA. This pathway requires consumption of ATP, which translates to a yield loss in  
38    the overall conversion of glucose to the product of interest, and there is therefore much interest in  
39    pathways that are more efficient than the endogenous pathway. Recently Kozak *et al.* expressed  
40    pyruvate dehydrogenase from *Enterococcus faecalis* in the cytosol with the objective to have  
41    more efficient acetyl-CoA biosynthesis in the cytosol (Kozak *et al.* 2014).

42    An alternative pathway is pyruvate formate lyase (PFL) and functional PFL has been expressed in  
43    *S. cerevisiae* under anaerobic conditions, by co-expressing *pflA* and *pflB* from *E. coli* and  
44    *Lactobacillus plantarum*, respectively (Waks *et al.* 2009; Kozak *et al.* 2014). Waks and Silver  
45    expressed *pflA* and *pflB* in a strain background with deletions in both formate dehydrogenase  
46    genes, *FDH1* and *FDH2*, which gave a 4.5 fold increase in formate production under anaerobic  
47    conditions (Waks *et al.* 2009). Kozak *et al.* found that *pflA* and *pflB* expression could restore  
48    anaerobic growth of an acetyl-CoA synthetase deficient (*acs1Δ acs2Δ*) mutant on glucose, by  
49    complementing cytosolic acetyl-CoA synthesis (Kozak *et al.* 2014). In these studies the cofactors  
50    (electron donor) were, however, not co-expressed even though it was speculated that there could  
51    be a cytosolic, single-electron donor replacing reduced flavodoxin to activate PFL (Waks *et al.*  
52    2009). While these previous studies serve as important demonstrations of functional PFL  
53    expression in yeast, the sole anaerobic functionality of this pathway could be restrictive for  
54    industrial use.

55    PFL was first found in *Escherichia coli* (Knappe *et al.* 1974), and later also in other facultative  
56    and obligate anaerobes (Sawers *et al.* 1998; Gelius-Dietrich *et al.* 2004). PFL plays an important  
57    role in pyruvate assimilation under anaerobic conditions, converting pyruvate to acetyl-CoA and  
58    formate. PFL exists in two forms, an inactive form and an active form. The active form of PFL is  
59    activated by pyruvate formate lyase activating enzyme (PFL-AE) with a radical formed at its  
60    active site, which is sensitive to oxygen and responsible for catalysis (Zhang *et al.* 2001). In *E.*  
61    *coli*, PFL functions as a homodimer and is encoded by *pflB*, while PFL-AE functions as a  
62    monomer encoded by *pflA*. PFL-AE utilizes S-adenosylmethionine (SAM) and reduced  
63    flavodoxin as the cosubstrates to generate a 5'-deoxyadenosyl radical (5'-dA·), which then  
64    activates PFL by abstracting a hydrogen atom from residue G734 (Wagner *et al.* 1992) generating  
65    the catalytically relevant glycyl radical. The radical formed in active PFL is anaerobically stable  
66    and can catalyze multiple reactions. Flavodoxin and ferredoxin are small proteins containing

67 flavin mononucleotide (FMN) and an iron-sulfur cluster, respectively. In *E. coli* they are encoded  
68 by *fldA/fldB* and *fdx*, respectively (Osborne *et al.* 1991; Ta *et al.* 1992; Gaudu *et al.* 2000), and  
69 they can transfer single electrons to an acceptor enzyme by inter-conversions between their  
70 oxidized forms and reduced forms. The reduced ferredoxin or flavodoxin can be formed by  
71 flavodoxin NADP<sup>+</sup> reductase (also called ferredoxin NADP<sup>+</sup> reductase), encoded by *fpr* in *E. coli*  
72 (Bianchi *et al.* 1993).

73 Here we demonstrated that the PFL pathway can be functional at aerobic growth conditions in  
74 yeast when co-expressed with appropriate co-factors. Furthermore, we demonstrate for the first  
75 time that a functional cytosolic pathway from pyruvate to acetyl-CoA can improve growth of a  
76 pyruvate decarboxylase negative strain with an internal deletion in *MTH1* (*Pdc<sup>-</sup> MTH1-ΔT*) (Oud  
77 *et al.* 2012). Thus, the reconstructed strain serves as a potential platform strain for production of  
78 acetyl-CoA derived products without production of ethanol as a by-product. Two cofactors and  
79 their reductase (*fdx-fpr*, *fldA-fpr*) were evaluated by expression individually together with the  
80 PFL pathway. We found that the co-expressed cofactors, especially *fldA-fpr*, facilitates PFL  
81 pathway function at aerobic growth conditions, which could be useful for application of the PFL  
82 pathway in yeast bioprocesses that have to be operated at aerobic conditions.

## 83 Materials and methods

### 84 • Plasmid Construction

85 The plasmids, strains and primers used in this study are shown in Table 1. *Escherichia coli* DH5a  
86 was used for general cloning procedures in this study.

87 All the plasmids were constructed based on the vector pSP-GM1 (Chen *et al.* 2012) with two sets  
88 of a constitutive promoter and a terminator, *P<sub>TEF1</sub>/T<sub>ADH1</sub>* and *P<sub>PGK1</sub>/T<sub>CYCI</sub>*, respectively. Codon-  
89 optimized *pflA* and *pflB* were synthesized by GenScript (GenScript USA Inc. Piscataway, USA),  
90 while *fdx*, *fldA* and *fpr* were amplified from *E. coli* genomic DNA.

91 In pPFL01, *pflA* was cloned downstream of the *PGK1* promoter using *Xho*I and *Xma*I, and *pflB*  
92 was cloned downstream of the *TEF1* promoter using *Not*I and *Sac*I. In pSP-GM1\_fdx/fldA\_fpr,  
93 *fpr* was cloned downstream of the *PGK1* promoter using *Xho*I and *Bam*HI, and either *fdx* or *fldA*  
94 was cloned downstream of the *TEF1* promoter using *Not*I and *Sac*I. A cassette *P<sub>TEF1</sub>-fdx/fldA-*  
95 *T<sub>ADH1</sub>*, amplified from pSP-GM1\_fdx/fldA\_fpr with primers 1-2, was cloned into pPFL01 using  
96 *Sse232I* and *Kpn*2I, and another cassette *P<sub>PGK1</sub>-fpr-T<sub>CYCI</sub>* amplified from pSP-GM1\_fdx/fldA\_fpr  
97 with primers 3-4 was cloned into the same plasmid using *Asc*I yielding pPFL06/pPFL07 (Figure  
98 1). All plasmids constructed in this study were sequenced for verification.

### 99 • *S. cerevisiae* strain construction

100 *S. cerevisiae* strain IMI076 (provided by Antonius J.A. van Maris, Delft University of  
101 Technology, The Netherlands) was used as the background strain. Strains YZ10, YZ11, YZ12  
102 and YZ13 were constructed by transforming IMI076 with the plasmids pSP-GM1, pPFL01,

103 pPFL06, and pPFL07, respectively. Transformation of *S. cerevisiae* was done according to the  
104 electroporation protocol described in (Suga *et al.* 2003). Transformants were selected on agar  
105 plates containing a synthetic medium consisting of Yeast nitrogen base (Formedium Ltd.,  
106 Hunstanton, England), complete supplement mixture w/o uracil (Formedium Ltd.), 1% (v/v)  
107 glucose and 0.75% (v/v) ethanol (SDE-ura). Single colony isolates were restreaked on selective  
108 plates and confirmed to have the correct plasmid DNA by colony PCR.

109 • **Cultivation procedures**

110 Pre-cultivation was performed at 30 °C with 200 rpm orbital shaking in SDE-ura liquid medium.  
111 Cells for inoculation were harvested at OD<sub>600</sub> between 1 and 2, and washed twice with sterile  
112 water.

113 Cultivation in 100-ml unbaffled shake flasks containing 40 ml medium was performed at 30 °C  
114 with the starting OD<sub>600</sub> of 0.05 and 200 rpm orbital shaking in triplicates. The defined minimal  
115 medium for cultivation was composed of 20 g/L glucose, 7.5 g/L (NH<sub>4</sub>)<sub>2</sub>SO<sub>4</sub>, 14.4 g/L KH<sub>2</sub>PO<sub>4</sub>,  
116 0.5 g/L MgSO<sub>4</sub>·7H<sub>2</sub>O, 2 ml/l trace metal solution, 1 ml/l vitamin solution, with pH adjusted to 6.5  
117 by adding 2 M NaOH. The final concentrations of trace metal elements and vitamins were  
118 previously described in (Verduyn *et al.* 1992).

119 Cultivation in Bioscreen C (Oy Growth Curves Ab Ltd, Finland) was performed in octuplicates at  
120 30 °C in a micro-plate (10x10 wells) with 200 µl minimal medium per well.

121 • **Determination of biomass and extracellular metabolites**

122 Biomass was determined by optical density (OD<sub>600</sub>) measurement at a wavelength of 600 nm with  
123 a GENESYS™ 20 Visible spectrophotometer (Thermo Electron Scientific, Madison, USA).  
124 Glucose, ethanol, glycerol, pyruvate and formate concentrations were determined in culture  
125 supernatants by high-performance liquid chromatography (Dionex-HPLC, Sunnyvale, CA, USA)  
126 equipped with UV detector and RI detector using a Bio-Rad HPX 87H column (Bio-Rad,  
127 Hercules, CA, USA). The HPLC was operated at 60 °C with 5 mM H<sub>2</sub>SO<sub>4</sub> as mobile phase at a  
128 flow rate of 0.6 ml min<sup>-1</sup>.

129 • **qRT-PCR procedures and gene expression analysis**

130 Cells for gene expression analysis were harvested by centrifugation at -20 °C, quenched by liquid  
131 nitrogen, and stored at -80 °C for use. Total RNA was isolated using RNeasy Mini Kit (QIAGEN,  
132 Germany), which was then processed to obtain fragmented cDNA using a QuantiTect Reverse  
133 Transcription Kit (QIAGEN, Germany). 2 µl of the synthesized cDNA (corresponding to 100 ng  
134 RNA) was used as the template for the qPCR reaction to a final reaction volume of 20 µl, using a  
135 DyNAamo Flash SYBR Green qPCR Kit (Thermo Scientific, USA). Quantitative RT-PCR was  
136 performed on Stratagene Mx3005P (Agilent Technologies, USA). The thermocycling program  
137 consisted of one hold at 95 °C for 15 min, followed by 40 cycles of 10 s at 95 °C and 20 s at 60 °C,  
138 and a final cycle of 1 min at 95 °C, 30 s at 55 °C and 30 s at 95 °C.

139 Primers for real-time PCR (Table 1) were designed using Primer3 (<http://bioinfo.ut.ee/primer3-0.4.0/>) with melting temperature ( $T_m$ ) around 60 °C. *ACT1*, a housekeeping gene, was selected as  
140 the reference gene (Teste *et al.* 2009). Final concentration of primers used was 0.5 mM in 20 µl  
141 qPCR reactions.  
142

143 **Results**

144 • **Introduction of the PFL pathway (*pflA* and *pflB*) into a non-ethanol producing *S.*  
145 *cerevisiae* strain**

146 The PFL encoding genes *pflA* and *pflB* from *E. coli* were codon-optimized for expression in *S.*  
147 *cerevisiae*, and cloned under the control of the constitutive promoters  $P_{PGK1}$  and  $P_{TEF1}$  respectively  
148 into the vector pSP-GM1, yielding pPFL01. Empty vector pSP-GM1 and pPFL01 were  
149 transformed into the background strain IMI076 (Pdc<sup>-</sup> *MTH1*-Δ*T ura3*) respectively, yielding two  
150 strains YZ10 and YZ11. Two transformants of each strains were picked and cultured in minimal  
151 medium to evaluate activity of the PFL pathway at aerobic growth conditions using Bioscreen C.  
152 Growth results revealed that, YZ11-1 and YZ11-2 (with the PFL pathway) reached a higher final  
153 biomass, compared with YZ10-1 and YZ10-2 (without the PFL pathway) (Figure 2). No major  
154 growth difference was observed between two different transformants for both strains. Also when  
155 YZ10-1 and YZ11-2 were cultured in shake flasks, a higher final biomass was also observed with  
156 strain YZ11-1 (with PFL pathway) (Figure 3).

157 • **Introduction of the PFL pathway with its cofactors into a non-ethanol producing *S.*  
158 *cerevisiae* strain**

159 As described before, the activation of PFL requires the activating enzyme PFL-AE, as well as two  
160 other cofactors (or co-substrates), reduced flavodoxin and S-adenosylmethionine (SAM) (Knappe  
161 *et al.* 1990). Reduced flavodoxin serves as an electron donor and SAM as a co-substrate for PFL-  
162 AE to generate a 5'-deoxyadenosyl radical (5'-dA<sup>·</sup>), which is responsible for PFL activation  
163 (Sawers *et al.* 1998). *In vitro*, other artificial one-electron reductants, for example, photo-reduced  
164 5-deazariboflavin or photo-reduced 5-deazaflavin, can replace reduced flavodoxin as the electron  
165 donor for PFL-AE (Frey *et al.* 1994). In a previous study, the PFL pathway was successfully  
166 introduced without any cofactor into *S. cerevisiae* for hydrogen production at anaerobic  
167 conditions (Waks *et al.* 2009), and it was speculated that there might be other cytosolic, single-  
168 electron donors for PFL activation in *S. cerevisiae*.

169 Here, two cofactors and their reductase were introduced together with the PFL pathway into *S.*  
170 *cerevisiae*, ferredoxin (encoded by *fdx*) and ferredoxin NADP<sup>+</sup> reductase (encoded by *fpr*), and  
171 flavodoxin (encoded by *fldA*) and flavodoxin NADP<sup>+</sup> reductase (encoded by *fpr*). *fdx* or *fldA* were  
172 cloned under the control of a *TEF1* promoter, and *fpr* was expressed under control of a *PGK1*  
173 promoter. The cassettes  $P_{TEF1}$ -*fdx*/*fldA*-*T<sub>ADH1</sub>*, and  $P_{PGK1}$ -*fpr*-*T<sub>CYCI</sub>* were cloned into pPFL01,  
174 yielding pPFL06 and pPFL07 respectively. pPFL06 and pPFL07 were transformed to the  
175 background strain IMI076 respectively, resulting in strain YZ12 and YZ13. The role of these two  
176 cofactors was evaluated by culturing YZ12 and YZ13 in minimal medium in shake flasks.

177 Three different transformants of YZ12 (with PFL pathway and ferredoxin) and YZ13 (with PFL  
178 pathway and flavodoxin) all reached a higher final biomass concentration, compared with YZ10  
179 and YZ11 (Figure 3A&B). However, three different transformants of YZ12 and YZ13,  
180 respectively, showed different growth behavior. As shown in Figure 3A, YZ12-1 and YZ12-4 had  
181 similar lag phases and maximum specific growth rates, while YZ12-2 had a longer lag phase and  
182 a lower maximum specific growth rate (Table 2). YZ12-1 and YZ12-2 reached similar final  
183 biomass concentrations, while YZ12-4 reached a higher final biomass concentration. For the three  
184 YZ13-2, YZ13-5 and YZ13-6 transformants there were growth differences both with respect to  
185 the lag phase and the maximum specific growth rate (Table 2), but all three strains reached a  
186 similar final biomass concentration (Figure 3B).

187 Overall, the YZ13 strains with *fldA-fpr* gave higher final biomass concentrations than those with  
188 *fdx-fpr*, and higher specific growth rates in the late growth phase. And they could completely  
189 consume the supplied glucose and no pyruvate accumulated in the culture, as shown in Table 2.  
190 Therefore, reduced flavodoxin seems more efficient as cofactor for the PFL pathway, compared  
191 to reduced ferredoxin.

192 We observed some differences in the growth behavior of the 3 transformants of each type. We  
193 therefore checked gene expression of the four introduced genes and found that the expression of  
194 *pflB* and *pflA* varied up to 2-fold between the three different YZ12 strains (Figure 3C), while it  
195 varied up to 5-fold between the three different YZ13 strains (Figure 3D). In YZ12-4 and YZ13-6,  
196 the two strains with highest final biomass concentrations, the expression levels of *pflA* and *pflB*  
197 were not the highest, which indicated that higher expression level of *pflA* and *pflB* might not be  
198 beneficial for obtaining a high final biomass concentration, especially expression of *pflB*.  
199 However, YZ13-5 had a relatively low expression of *fldA* and it showed delayed growth and had  
200 a higher glycerol yield on glucose. It therefore seems that the expression level of the cofactors  
201 might be crucial for optimal function of the PFL pathway under aerobic conditions.

## 202 • Induced expression of formate dehydrogenase

203 *S. cerevisiae* has two native formate dehydrogenases (FDH), encoded by *FDH1* and *FDH2*  
204 (Overkamp *et al.* 2002). Their expression is induced by methanol or formate, or with glycine as  
205 the sole nitrogen source. Furthermore, their transcription at aerobic and anaerobic conditions  
206 seems to be quite different, and no FDH transcript was found under anaerobic glucose limited  
207 chemostat conditions (ter Linde *et al.* 1999). However, when a functional PFL pathway was  
208 expressed in an *Acs<sup>-</sup>* mutant under anaerobic glucose-limited chemostat conditions, the transcript  
209 levels of *FDH1* and *FDH2* were over 25-fold higher than in the wild type (Kozak *et al.* 2014).

210 In previous studies performed at anaerobic conditions, formate was found as a byproduct of the  
211 PFL pathway in *S. cerevisiae* (Waks *et al.* 2009; Kozak *et al.* 2014). In our study, formate was not  
212 detectable in the culture supernatant for any of the constructed strains. One explanation could be  
213 that formate, produced by the PFL pathway, was converted to CO<sub>2</sub> by Fdh1 and/or Fdh2. We  
214 therefore measured the transcription levels of *FDH1* and *FDH2* in the different constructed  
215 strains (Figure 4). In the control strain YZ10-1, the expression of the *FDH* genes increased about

216 5-fold as OD<sub>600</sub> increased from 3.1 to 5.2. In the strain YZ11-1 with the PFL pathway, the  
217 expression of the genes increased about 3 fold when OD<sub>600</sub> increased from 3.6 to 5.2. In YZ13-2,  
218 the expression of FDHs did not show much increase when OD<sub>600</sub> increased from 1.2 to 2.3, but it  
219 increased more than 25 fold when OD<sub>600</sub> increased to 8.1. In YZ13-6, the expression of FDHs  
220 increased above 20 fold when the OD<sub>600</sub> increase from 1.7 to 4.6, and above 15 fold when OD<sub>600</sub>  
221 increased to 8.5. The 5-fold or 3-fold *FDH* transcription increase in YZ10-1 and YZ11-1 could be  
222 due to activity of some unknown reactions related with FDH (Overkamp et al. 2002), whereas the  
223 large increase in expression in the two YZ13 strains probably resulted from a direct response to  
224 formate production.

## 225 Discussion

226 Pdc negative strains can serve as platform strains for evaluation of heterologous pathways for  
227 cytosolic acetyl-CoA production, since such strains are unable to produce C<sub>2</sub> compounds in the  
228 cytosol. However, due to insufficient flux via the PFL pathway, or improper redox balancing, the  
229 introduction of the PFL pathway could not restore the growth of a Pdc negative strain on glucose,  
230 not even under anaerobic or semi-anaerobic conditions (data not shown). Although IMI076 (Pdc<sup>-</sup>  
231 *MTH1*-Δ*T*) grows on glucose, its capacity for glucose consumption is limited and pyruvate is  
232 accumulated when cultured in shake flasks without pH control, as shown in Table 2. Therefore  
233 IMI076 was used for PFL pathway evaluation in this study. When the PFL pathway was  
234 expressed alone, a small improvement in final biomass concentration was observed (Figure 2 and  
235 Figure 3). As previously reported by *in vitro* studies, the active form of pyruvate formate lyase is  
236 sensitive to oxygen due to cleavage of the protein into fragments at the activation site (Wagner et  
237 al. 1992). Therefore, even with constitutive expression in *S. cerevisiae*, the function of the PFL  
238 pathway was limited under aerobic conditions, which may explain the small improvement in the  
239 final biomass concentration in YZ11 strains, as shown in Figure 2.

240 When either ferredoxin or flavodoxin and the corresponding reductase were coexpressed with  
241 PFL there was clear improvement in the final biomass concentration (Figure 3). With flavodoxin  
242 and its reductase, the PFL pathway resulted in better glucose consumption and pyruvate  
243 dissimilation in the YZ13 strains (Table 2). However, no formate byproduct was detected at  
244 aerobic growth in our study, while formate was accumulated when PFL was expressed under  
245 anaerobic conditions. This might be due to different activities of FDHs under different conditions.  
246 In the study by Waks and Silver, it seemed that formate assimilation by FDHs was not as efficient  
247 under anaerobic conditions (Waks et al. 2009) as in aerobic conditions (Overkamp et al. 2002),  
248 probably due to inefficient recycling of NAD<sup>+</sup> resulting from the lack of electron transport chain  
249 and oxidative phosphorylation at anaerobic growth.

250 *FDH1/2* transcription data indicated that the PFL pathway may function at late growth phase  
251 (OD<sub>600</sub> above 4), since there was no major induction of FDH transcription during the exponential  
252 phase (Figure 3). This was consistent with the fact that the introduction of the PFL pathway with  
253 its cofactors mostly contributed to an increase in the final biomass concentration, but not in the  
254 maximum specific growth rate of all the strains (Figure. 2 and Table 2). These results could  
255 indicate that during the exponential growth phase an unknown native pathway provided the

256 cytosolic acetyl-CoA required for growth, and that the PFL pathway with cofactors supplied  
257 additional cytosolic acetyl-CoA via pyruvate assimilation. However, it is difficult to explain why  
258 the PFL pathway would mainly function during the late growth phase. One possible reason would  
259 be that a higher cell density may result in lower dissolved oxygen concentration, and then affect  
260 PFL activity - a hypothesis that would require additional investigations.

261 We found that co-expression of cofactors (*fdx-fpr* or *fldA-fpr*) was beneficial for the functionality  
262 of the PFL pathway, especially expression of *fldA-fpr*. Although ferredoxin and flavodoxin can  
263 both serve as single electron acceptors and donors and sometimes substitute for each other, some  
264 enzymes require either one or the other (Osborne *et al.* 1991; Sancho 2006). In *E. coli*, ferredoxin  
265 does not substitute for flavodoxin in the reaction catalyzed by PFL (Knoell *et al.* 1974), which  
266 probably explains why *fdx-fpr* co-expression did not contribute much to an increased biomass  
267 formation. Co-expression of *fldA-fpr* may continuously supply reduced flavodoxin as electron  
268 donors for PFL activating enzyme, which then could continuously activate PFL to convert  
269 pyruvate to acetyl-CoA, even though the active PFL is sensitive to aerobic conditions. Therefore,  
270 the functional PFL pathway may not behave as efficiently under aerobic conditions as under  
271 anaerobic conditions.

272 As members of iron-sulfur cluster (ISC) proteins, PFL activating enzyme and ferredoxin requires  
273 Fe-S assembly systems for their enzymatic activities. PFL-AE contains an essential 4Fe-4S  
274 cluster (Vey *et al.* 2008) while ferredoxin contains an 2Fe-2S cluster (Kakuta *et al.* 2001). 4Fe-4S  
275 and 2FeS-2S are two of the relatively simple iron-sulfur clusters, and more and more complex  
276 structures of ISCs have been found and identified (Lill *et al.* 2006). Yeast possesses a  
277 mitochondrial ISC assembly machinery, ISC export machinery and cytosolic iron-sulfur protein  
278 assembly (CIA) machinery (Lill *et al.* 2008). In mitochondria, iron-sulfur clusters (including 4Fe-  
279 4S and 2FeS-2S clusters) are transiently assembled on the scaffold proteins IscU1 and IscU2. For  
280 mitochondria ISC proteins, iron-sulfur clusters are then transferred to apoproteins with assistance  
281 of several components of the ISC assembly machinery (Lill *et al.* 2008). For cytosolic ISC  
282 proteins, ISC export machinery and CIA machinery are also required. ISC protein biosynthesis is  
283 known to play an important role in iron regulation in *S. cerevisiae* (Lill *et al.* 2008). In the  
284 previous study performed by Kozak *et al.*, transcriptome analysis of Acs<sup>-</sup> mutants with PFL  
285 pathway expression revealed that the upregulated genes were involved in the process of ion  
286 transport and cellular iron ion homestasis (Kozak *et al.* 2014). All these results suggested it was  
287 possible to express heterologous ISC proteins in the cytosol, although bacterial ISC protein  
288 expression in *S. cerevisiae* has often been challenging and not always successful (Partow *et al.*  
289 2012).

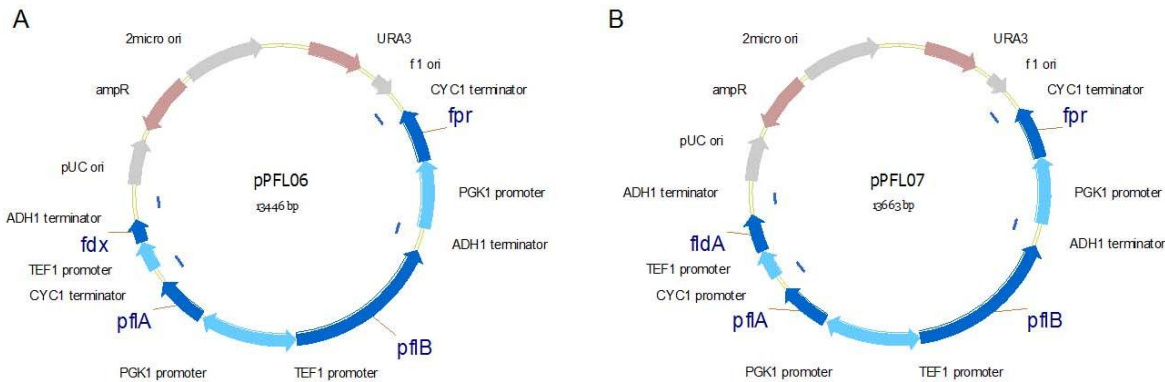
## 290 Acknowledgements

291 We are grateful to Klaas Buijs for providing the plasmids pSP-GM1\_fdx\_fpr and pSP-  
292 GM1\_fldA\_fpr, and Xin Chen for the help with RT-PCR. This work was performed in  
293 collaboration with Genomatica, Inc., and financially supported by Vetenskapsrådet, FORMAS  
294 and European Research Council (grant no. 247013).

295    **References**

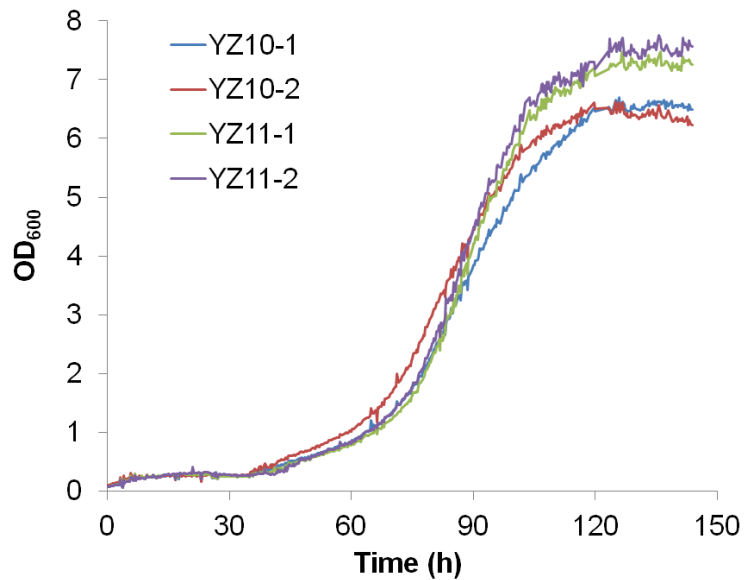
- 296    Bianchi V, Reichard P, Eliasson R, *et al.* Escherichia coli ferredoxin NADP+ reductase: activation  
297    of E. coli anaerobic ribonucleotide reduction, cloning of the gene (*fpr*), and overexpression of  
298    the protein. *Journal of Bacteriology* 1993, 175(6): 1590-1595.
- 299    Chen Y and Nielsen J. Advances in metabolic pathway and strain engineering paving the way for  
300    sustainable production of chemical building blocks. *Curr Opin Biotechnol* 2013, 24(6): 965-  
301    972.
- 302    Chen Y, Partow S, Scalcinati G, *et al.* Enhancing the copy number of episomal plasmids in  
303    *Saccharomyces cerevisiae* for improved protein production. *FEMS Yeast Res* 2012, 12(5): 598-  
304    607.
- 305    Chen Y, Siewers V and Nielsen J. Profiling of Cytosolic and Peroxisomal Acetyl-CoA Metabolism in  
306    *Saccharomyces cerevisiae*. *PLoS One* 2012, 7(8)
- 307    Frey M, Rothe M, Wagner A F, *et al.* Adenosylmethionine-dependent synthesis of the glycyl  
308    radical in pyruvate formate-lyase by abstraction of the glycine C-2 pro-S hydrogen atom.  
309    Studies of [2H]glycine-substituted enzyme and peptides homologous to the glycine 734 site. *J  
310    Biol Chem* 1994, 269(17): 12432-12437.
- 311    Gaudu P and Weiss B. Flavodoxin mutants of *Escherichia coli* K-12. *Journal of Bacteriology* 2000,  
312    182(7): 1788-1793.
- 313    Gelius-Dietrich G and Henze K. Pyruvate formate lyase (PFL) and PFL activating enzyme in the  
314    chytrid fungus *Neocallimastix frontalis*: a free-radical enzyme system conserved across  
315    divergent eukaryotic lineages. *J Eukaryot Microbiol* 2004, 51(4): 456-463.
- 316    Kakuta Y, Horio T, Takahashi Y, *et al.* Crystal structure of *Escherichia coli* Fdx, an adrenodoxin-  
317    type ferredoxin involved in the assembly of iron-sulfur clusters. *Biochemistry* 2001, 40(37):  
318    11007-11012.
- 319    Kim I K, Roldao A, Siewers V, *et al.* A systems-level approach for metabolic engineering of yeast  
320    cell factories. *FEMS Yeast Res* 2012, 12(2): 228-248.
- 321    Knappe J, Blaschkowski H P, Grobner P, *et al.* Pyruvate formate-lyase of *Escherichia coli*: the  
322    acetyl-enzyme intermediate. *Eur J Biochem* 1974, 50(1): 253-263.
- 323    Knappe J and Sawers G. A radical-chemical route to acetyl-CoA: the anaerobically induced  
324    pyruvate formate-lyase system of *Escherichia coli*. *FEMS Microbiol Rev* 1990, 6(4): 383-398.
- 325    Knoell H E and Knappe J. *Escherichia coli* ferredoxin, an iron-sulfur protein of the adrenodoxin  
326    type. *Eur J Biochem* 1974, 50(1): 245-252.
- 327    Kozak B U, van Rossum H M, Benjamin K R, *et al.* Replacement of the *Saccharomyces cerevisiae*  
328    acetyl-CoA synthetasases by alternative pathways for cytosolic acetyl-CoA synthesis. *Metab  
329    Eng* 2014, 21: 46-59.
- 330    Kozak B U, van Rossum H M, Luttik M A, *et al.* Engineering Acetyl Coenzyme A Supply: Functional  
331    Expression of a Bacterial Pyruvate Dehydrogenase Complex in the Cytosol of *Saccharomyces  
332    cerevisiae*. *MBio* 2014, 5(5)
- 333    Lill R, Dutkiewicz R, Elsasser H P, *et al.* Mechanisms of iron-sulfur protein maturation in  
334    mitochondria, cytosol and nucleus of eukaryotes. *Biochim Biophys Acta* 2006, 1763(7): 652-  
335    667.
- 336    Lill R and Muhlenhoff U. Maturation of iron-sulfur proteins in eukaryotes: mechanisms,  
337    connected processes, and diseases. *Annu Rev Biochem* 2008, 77: 669-700.
- 338    Nielsen J. Synthetic biology for engineering acetyl coenzyme a metabolism in yeast. *MBio* 2014,  
339    5(6)

- 340 Osborne C, Chen L M and Matthews R G. Isolation, cloning, mapping, and nucleotide sequencing  
341 of the gene encoding flavodoxin in Escherichia coli. *Journal of Bacteriology* 1991, 173(5):  
342 1729-1737.
- 343 Oud B, Flores C L, Gancedo C, *et al.* An internal deletion in MTH1 enables growth on glucose of  
344 pyruvate-decarboxylase negative, non-fermentative *Saccharomyces cerevisiae*. *Microb Cell*  
345 *Fact* 2012, 11(1): 131.
- 346 Overkamp K M, Kotter P, van der Hoek R, *et al.* Functional analysis of structural genes for  
347 NAD(+)-dependent formate dehydrogenase in *Saccharomyces cerevisiae*. *Yeast* 2002, 19(6):  
348 509-520.
- 349 Partow S, Siewers V, Daviet L, *et al.* Reconstruction and evaluation of the synthetic bacterial  
350 MEP pathway in *Saccharomyces cerevisiae*. *PLoS One* 2012, 7(12): e52498.
- 351 Sancho J. Flavodoxins: sequence, folding, binding, function and beyond. *Cell Mol Life Sci* 2006,  
352 63(7-8): 855-864.
- 353 Sawers G and Watson G. A glycyl radical solution: oxygen-dependent interconversion of  
354 pyruvate formate-lyase. *Mol Microbiol* 1998, 29(4): 945-954.
- 355 Suga M and Hatakeyama T. High-efficiency electroporation by freezing intact yeast cells with  
356 addition of calcium. *Curr Genet* 2003, 43(3): 206-211.
- 357 Ta D T and Vickery L E. Cloning, sequencing, and overexpression of a [2Fe-2S] ferredoxin gene  
358 from *Escherichia coli*. *J Biol Chem* 1992, 267(16): 11120-11125.
- 359 ter Linde J J, Liang H, Davis R W, *et al.* Genome-wide transcriptional analysis of aerobic and  
360 anaerobic chemostat cultures of *Saccharomyces cerevisiae*. *Journal of Bacteriology* 1999,  
361 181(24): 7409-7413.
- 362 Teste M A, Duquenne M, Francois J M, *et al.* Validation of reference genes for quantitative  
363 expression analysis by real-time RT-PCR in *Saccharomyces cerevisiae*. *BMC Mol Biol* 2009, 10:  
364 99.
- 365 Wagner A F, Frey M, Neugebauer F A, *et al.* The free radical in pyruvate formate-lyase is located  
366 on glycine-734. *Proc Natl Acad Sci U S A* 1992, 89(3): 996-1000.
- 367 Waks Z and Silver P A. Engineering a synthetic dual-organism system for hydrogen production.  
368 *Appl Environ Microbiol* 2009, 75(7): 1867-1875.
- 369 Verduyn C, Postma E, Scheffers W A, *et al.* Effect of benzoic acid on metabolic fluxes in yeasts: a  
370 continuous-culture study on the regulation of respiration and alcoholic fermentation. *Yeast*  
371 1992, 8(7): 501-517.
- 372 Vey J L, Yang J, Li M, *et al.* Structural basis for glycyl radical formation by pyruvate formate-lyase  
373 activating enzyme. *Proc Natl Acad Sci U S A* 2008, 105(42): 16137-16141.
- 374 Zhang W, Wong K K, Magliozzo R S, *et al.* Inactivation of pyruvate formate-lyase by dioxygen:  
375 defining the mechanistic interplay of glycine 734 and cysteine 419 by rapid freeze-quench  
376 EPR. *Biochemistry* 2001, 40(13): 4123-4130.
- 377
- 378



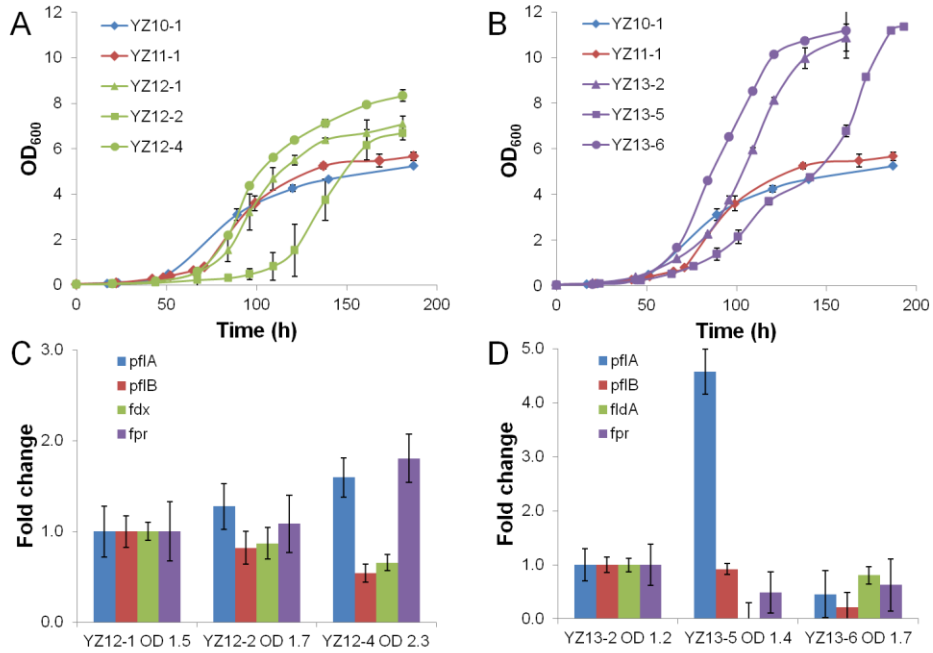
379

380 Figure 1. Plasmid maps of pPFL06 (A) and pPFL07 (B).



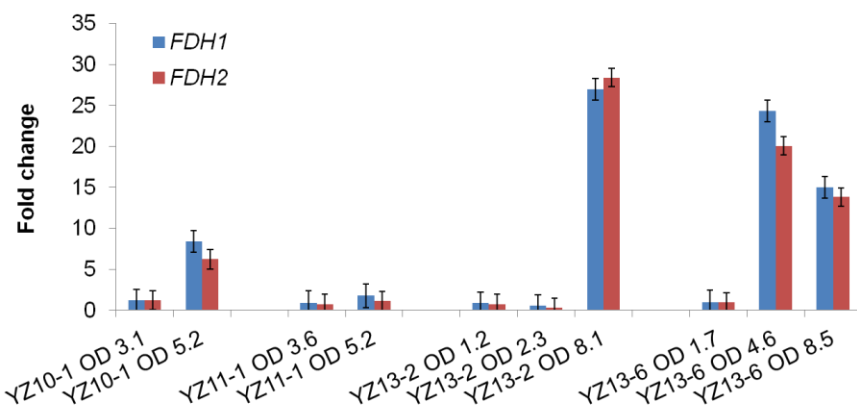
381

382 Figure 2. Growth comparision of the strains with and without the PFL pathway using Bioscreen C.  
 383 Two YZ10 transformants YZ10-1 and YZ10-2 (without PFL pathway), and two YZ11  
 384 transformants YZ11-1 and YZ11-2 (with PFL pathway) were cultured in minimal media in  
 385 octuplicate, and the standard deviations (not shown here) were within 5%.



386

387 Figure 3. Growth comparisons in shake flasks and gene expression analysis. (A) YZ10-1 (without  
388 PFL pathway), YZ11-1 (with PFL pathway), and three YZ12 transformants (YZ12-1, YZ12-2,  
389 YZ12-4, with PFL pathway and cofactor ferredoxin); (B) YZ10, YZ11 and three YZ13  
390 transformants (YZ13-2, YZ13-5, YZ13-6, with PFL pathway and cofactor flavodoxin). (C) Gene  
391 expression analysis of YZ12 strains. Samples were taken at OD<sub>600</sub> between 1-2.5 for the  
392 transcription analysis of 4 introduced genes (*pflA*, *pflB*, *fdx* and *fpr*). The gene expression levels  
393 of introduced genes in YZ12-1 were set as 1. (D) Gene expression analysis of YZ13 strains.  
394 Samples were taken at OD<sub>600</sub> between 1-2.5 for the transcription analysis of 4 introduced genes  
395 (*pflA*, *pflB*, *fldA* and *fpr*). The gene expression levels of introduced genes in YZ13-2 were set as 1.

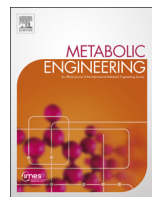


396

397 Figure 4. Expression analysis of *FDH1* and *FDH2* in constructed strains YZ10-1, YZ11-1, YZ13-  
398 2 and YZ13-6. *FDH1* and *FDH2* expression levels of YZ13-6 at OD<sub>600</sub> 1.7 were set to 1.

## **PAPER IV**





## Minireview

## Microbial acetyl-CoA metabolism and metabolic engineering



Anastasia Krivoruchko, Yiming Zhang, Verena Siewers, Yun Chen, Jens Nielsen\*

Department of Chemical and Biological Engineering, Chalmers University of Technology, Gothenburg, Sweden

## ARTICLE INFO

## Article history:

Received 16 August 2014

Received in revised form

25 November 2014

Accepted 26 November 2014

Available online 5 December 2014

## Keywords:

Yeast

Bacteria

Acetyl-CoA

Central carbon metabolism

Industrial biotechnology

## ABSTRACT

Recent concerns over the sustainability of petrochemical-based processes for production of desired chemicals have fueled research into alternative modes of production. Metabolic engineering of microbial cell factories such as *Saccharomyces cerevisiae* and *Escherichia coli* offers a sustainable and flexible alternative for the production of various molecules. Acetyl-CoA is a key molecule in microbial central carbon metabolism and is involved in a variety of cellular processes. In addition, it functions as a precursor for many molecules of biotechnological relevance. Therefore, much interest exists in engineering the metabolism around the acetyl-CoA pools in cells in order to increase product titers. Here we provide an overview of the acetyl-CoA metabolism in eukaryotic and prokaryotic microbes (with a focus on *S. cerevisiae* and *E. coli*), with an emphasis on reactions involved in the production and consumption of acetyl-CoA. In addition, we review various strategies that have been used to increase acetyl-CoA production in these microbes.

© 2014 International Metabolic Engineering Society. Published by Elsevier Inc. All rights reserved.

## 1. Introduction

In recent years, increasing concerns over the sustainability and environmental impact of petroleum-based fuels, as well as petroleum-based production processes of various chemicals, have stimulated research into alternative means of production. The rise of metabolic engineering and the use of microbial cell factories for production of desired molecules offer a flexible, sustainable and environmentally-friendly alternative to petroleum-based production. In addition, metabolic engineering offers the possibility to produce complex molecules that are difficult to synthesize using solely chemical means. Efforts in metabolic engineering often focus

on ensuring that the cell factory can meet required specifications for an economically viable production process, and this generally transfers into specific requirements for titers, rates and yields (TRY). In order to improve the TRY of a cell factory it is normally necessary to engineer the central carbon metabolism in order to ensure provision of adequate precursor levels for the synthesis of the compounds of interest. For this reason there has been much interest in engineering the central carbon metabolism of microbial cell factories for efficient conversion of sugars into acetyl-CoA as this metabolite serves as a precursor for many industrially relevant compounds.

Acetyl-CoA is a central molecule in the metabolism of the cell. It is composed of coenzyme A and acetic acid connected by a thioester bond and it functions as an intermediate molecule that can transfer acetyl groups between molecules for various chemical processes. Acetyl-CoA is a precursor molecule to a variety of biotechnology products, including fatty acids (used in dietary supplements, pharmaceuticals and biodiesel), 1-butanol, polyhydroxyalkanoates, polyketides (used as pharmaceuticals) and isoprenoids (used as flavours, fragrances, biofuels, dietary supplements, vitamins and pharmaceuticals). Introduction and/or overexpression of the pathways that form these products in microbial hosts usually results in drain of acetyl-CoA, potentially compromising cellular function. Therefore, a number of metabolic engineering studies have focused on increasing intracellular acetyl-CoA levels to serve as a precursor for a range of different products.

In this review we will present an overview of eukaryotic and prokaryotic acetyl-CoA metabolism with a focus on two key cell factories used as production platforms, *Saccharomyces cerevisiae*

**Abbreviations:** A-ALD, acetylating acetaldehyde dehydrogenase; ACC, acetyl-CoA carboxylase; acetyl-AMP, acetyladenylate; ACK, acetate kinase; ACL, ATP-citrate lyase; ACS, acetyl-CoA synthetase; ADH, alcohol dehydrogenase; ALD, acetaldehyde dehydrogenase; CAT, carnitine acetyltransferase; CS, citrate synthase; CSRE, carbon source responsive element; FAE, fatty acid ethyl esters; FBA, fructose-bisphosphate aldolase; FNR, fumarate and nitrate reductase; FPP, farnesyl pyrophosphate; HAP, heme activator protein; HAT, histone acetyltransferase; HDAC, histone deacetylase; HMGR, HMG-CoA reductase; ICRE, inositol/cholin-responsive element; MS, malate synthase; PDC, pyruvate decarboxylase; PDH, pyruvate dehydrogenase; PFOR, pyruvate:ferredoxin oxidoreductase; PK, phosphoketolase; PFL, pyruvate formate lyase; PFL-AE, PFL-activating enzyme; PHA, polyhydroxyalkanoate; PHB, poly-(R)-3-hydroxybutyrate; PNO, pyruvate:NADP<sup>+</sup> oxidoreductase; POX, pyruvate oxidase; PTA, phosphotransacetylase; RTG, retrograde; SDPADS, sirtuin-dependent protein acylation/deacylation system; TPI, triosephosphate isomerase; UAS, upstream activating site; URS, upstream repression site

\* Correspondence to: Department of Chemical and Biological Engineering, Chalmers University of Technology, Kemivagen 10, SE 412 96 Gothenburg, Sweden. Fax: +46 31 772 3801.

E-mail address: [nielsenj@chalmers.se](mailto:nielsenj@chalmers.se) (J. Nielsen).

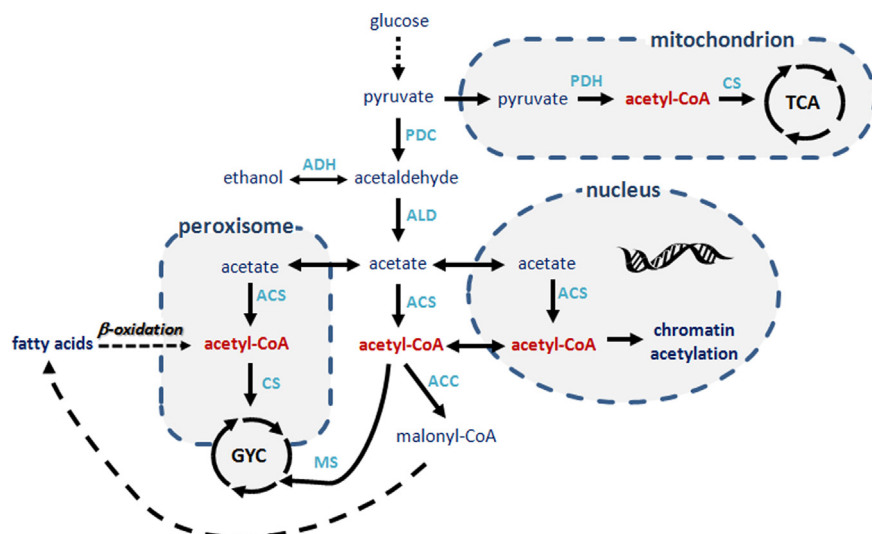


**Fig. 1.** Overview of the acetyl-CoA metabolism in *S. cerevisiae*. Acetyl-CoA metabolism in yeast is highly compartmentalized and occurs in the cytosol, mitochondrion, peroxisome and nucleus. Cytosolic acetyl-CoA is generated from pyruvate via acetaldehyde and acetate by the actions of PDC, ALD and ACS. ACC can convert cytosolic acetyl-CoA to malonyl-CoA, which is used as a substrate for fatty acid synthesis. Mitochondrial acetyl-CoA is generated from pyruvate by the actions of PDH and is then used in the TCA cycle. In the peroxisome, acetyl-CoA can be generated either from acetate via the actions of ACS or from  $\beta$ -oxidation of fatty acids. Peroxisomal acetyl-CoA can then be used as a substrate in the glyoxylate cycle. Nuclear acetyl-CoA is generated from acetate via the actions of ACS and is primarily used for acetylation of chromatin proteins.

and *Escherichia coli*. In addition, we summarize recent progress in the metabolic engineering of acetyl-CoA metabolism in these organisms for production of important biomolecules.

## 2. Acetyl-CoA metabolism in eukaryotic microbes

### 2.1. Acetyl-CoA metabolism in *S. cerevisiae*

As an activated form of acetate, acetyl-CoA serves as a crucial intermediate metabolite in the metabolic network of *S. cerevisiae* and is involved in metabolism in the cytosol, mitochondrion, peroxisome and nucleus (Fig. 1). It is the substrate for the TCA cycle that generates ATP and precursor metabolites for amino acids, nucleotide bases and porphyrins. Acetyl-CoA is also the building block for fatty acid synthesis and the end product of fatty acid degradation. In addition, acetyl-CoA is the substrate for protein acetylation, which plays a role in the regulation of enzyme function and DNA transcription.

#### 2.1.1. Acetyl-CoA in the central carbon metabolism

Under aerobic, glucose limited conditions, the TCA cycle plays a very important role in catabolism and acetyl-CoA generated by the pyruvate dehydrogenase (PDH) complex from pyruvate is the key substrate for this process. Pyruvate in the mitochondria derives from either cytosolic pyruvate generated via glycolysis from sugars or from malate via malic enzyme located in the mitochondria. Acetyl-CoA enters the TCA cycle in a step catalyzed by citrate synthase (CS). CS condenses acetyl-CoA with oxaloacetate, yielding citrate. There are 3 citrate synthase isoforms identified in *S. cerevisiae*, encoded by *CIT1* (Suissa et al., 1984), *CIT2* (Kim et al., 1986) and *CIT3* (Jia et al., 1997a). Cit1p and Cit3p are two mitochondrial isoforms, which catalyze the first and generally considered to be the flux controlling reaction of the TCA cycle, incorporating acetyl-CoA into the TCA cycle.

Similar to the TCA cycle, the glyoxylate cycle also begins with the condensation of acetyl-CoA, formed directly from acetate by acetyl-CoA synthetase (see below), and oxaloacetate to form citrate, catalyzed by Cit2p, which is located in the peroxisome in *S. cerevisiae*. Another reaction involving acetyl-CoA in the cycle is

catalyzed by malate synthase (MS), in which acetyl-CoA condenses with glyoxylate to form malate. In *S. cerevisiae*, Mls1p is responsible for this reaction.

PDH is one of the largest and most complicated protein complexes in *S. cerevisiae*, consisting of three main catalytic components termed E1 (pyruvate dehydrogenase, encoded by *PDA1* and *PDB1*), E2 (dihydrolipoamide acetyltransferase, encoded by *LAT1*), E3 (dihydrolipoamide dehydrogenase, encoded by *LPD1*) and a fourth component (protein X, encoded by *PDX1*) binding and positioning E3 to E2. The irreversible reaction catalyzed by the PDH complex converts pyruvate to acetyl-CoA,  $\text{CO}_2$  and NADH and requires the participation of five coenzymes (TPP, lipoic acid, FAD, CoA and  $\text{NAD}^+$ ). The regulation of the PDH complex occurs on several levels, e.g. on the transcriptional level, via the expression of *LPD1*, and post-transcriptional level, via the phosphorylation of Pda1 (Bowman et al., 1992; Gey et al., 2008; Pronk et al., 1996).

Cit1p is the major functional citrate synthase with an N-terminal mitochondrial targeting sequence and a C-terminal peroxisomal signal tripeptide SKN (Lee et al., 2000; Singh et al., 1992). Cit3p is a minor functional isoform also containing an N-terminal mitochondrial targeting sequence (Jia et al., 1997a). It has a dual specificity as both a citrate- and methylcitrate synthase, and catalyzes the condensation of acetyl-CoA and oxaloacetate to form citrate, as well as that of propionyl-CoA and oxaloacetate to form 2-methylcitrate (Graybill et al., 2007).

*CIT1* expression is repressed by glucose and further repressed by glucose and glutamate (Kim et al., 1986). Its expression is subjected to derepression by the heme activator protein (HAP) system (Rosenkrantz et al., 1994a), which is common for the enzymes of the TCA cycle and the electron transport chain. Besides a region responsible for glucose repression and one for derepression (Rosenkrantz et al., 1994b), an R box element is identified in the *CIT1* upstream sequence (Liu and Butow, 1999), which was first identified as a binding site for the retrograde (RTG) transcription complex Rtg1p–Rtg3p in a study of *CIT2* transcriptional regulation (Jia et al., 1997b). During detailed analysis of *CIT1* expression with different mutants in different carbon sources, it was observed that *CIT1* expression is dependent on HAP genes in cells with robust mitochondrial function and RTG genes in cells whose mitochondrial respiratory capacity has been compromised. It was proposed

that this ensures sufficient glutamate synthesis required for cell growth when the respiratory capacity is reduced (Liu and Butow, 1999).

Disruption of *CIT1* results in changes in the levels of TCA cycle metabolites, decrease in the activities or amounts of several enzymes (e.g. pyruvate and  $\alpha$ -ketoglutarate dehydrogenase complexes, which was proved not to be a result of repression by accumulated TCA cycle intermediates), reduced mitochondrial respiration of citrate and isocitrate, and inability to grow on acetate (Kispal et al., 1989, 1988). The growth ability of a *cit1 $\Delta$*  mutant on acetate could be restored by expressing an inactive but a structurally unchanged Cit1p mutant (Kispal et al., 1989), a native mitochondrial Cit1p, a mis-localized mitochondrial form of peroxisomal Cit2p (Velot et al., 1999), or additional copies of Cit3p (Jia et al., 1997a), but not by cytosolic Cit1p (Velot et al., 1999). One hypothesis for the growth inability on acetate was the dysfunction of the TCA cycle. It was proposed that Cit1p may have functions other than its catalytic activity, and the presence of a citrate synthase with normal conformation (even at an inactive state) permits the formation of a TCA cycle enzyme complex, in which the activity of the  $\alpha$ -ketoglutarate dehydrogenase complex is maintained.

*CIT2* encodes the peroxisomal isoform of citrate synthase (Lewin et al., 1990), with 81% and 74% identity with *CIT1* at the protein level and DNA level, respectively. Cit2p possesses a signaling tripeptide SKL at its C-terminus, which was found to be necessary and sufficient for directing it to the peroxisomes. Deletion of the peroxisomal targeting sequence (PTS) from Cit2p resulted in a mislocalized form of Cit2p to the mitochondria, which suggested Cit2p might contain additional signal sequences related to mitochondrial targeting (Singh et al., 1992). Using protein fusions, Lee et al. (2000) found that a 20 amino acid segment at the N-terminal of Cit2p contained a cryptic cleavable targeting signal for both the peroxisomes and mitochondria.

Similar to *CIT1*, expression of *CIT2* is repressed by glucose and reduced synergistically by glucose and exogenous glutamate (Kim et al., 1986). Elevated expression of *CIT2* was observed in cells with dysfunctional mitochondria, indicating its possible regulation by communication between mitochondria and nucleus (Liao et al., 1991). Rtg1p and Rtg3p were found to be together responsible for *CIT2* regulation by interacting with their two target sites in upstream sequences of *CIT2* (Chelstowska and Butow, 1995; Jia et al., 1997b), which appears to be activated in a Rtg2p-dependent fashion (Ferreira et al., 2005).

There are two functional isoforms of malate synthase reported in *S. cerevisiae*, encoded by *DAL7* (*MLS2*) and *MLS1*. *DAL7* was discovered in a study of allantoin catabolism in *S. cerevisiae* (Yoo et al., 1985), and its protein sequence was found to be nearly identical to the malate synthases from plants and bacteria. Using degenerate primers hybridizing to highly conserved regions in MS genes, *MLS1* was isolated, identified to be a second MS-encoding gene (Hartig et al., 1992), and demonstrated to be the one responsible for the reaction in the glyoxylate cycle.

Both MS proteins were putatively localized in the peroxisomes because of the tripeptide targeting sequence SKL at their C-termini. However, Kunze et al. found that Mls1p was localized in the cytosol when grown on ethanol, while advantageously being targeted to the peroxisomes when grown on oleic acid (Kunze et al., 2002). Chen et al. also revealed different distributions of Mls1p between the cytosol and peroxisomes in different mutants (Chen et al., 2012). Therefore, there might be some regulatory mechanisms for the subcellular distribution of Mls1p that are still unclear.

The repressed and derepressed expression of the *MLS1* gene is regulated by the carbon source according to the common response for genes involved in non-fermentative metabolism. Two sites in the upstream sequence of *MLS1* were identified as upstream activating sequences (UASs), UAS1 and UAS2 (Caspary et al.,

1997). These two UASs turned out to be functional Carbon Source Responsive Elements (CSREs), which were described also to function as UAS elements for *ACS1* expression (Kratzer and Schuller, 1997) as well as of genes involved in acetyl-CoA consumption (genes of the glyoxylate cycle and the subsequent gluconeogenesis such as *ICL1* (Scholer and Schuller, 1994), *MLS1* (Caspary et al., 1997), *FBP1* (Niederacher et al., 1992) and *PCK1* (Proft et al., 1995)).

Another important source for acetyl-CoA is acetyl-CoA synthetase (ACS). ACS forms part of the PDH bypass in *S. cerevisiae*, consisting of pyruvate decarboxylase (PDC), acetaldehyde dehydrogenase (ALD) and ACS. The reaction catalyzed by ACS consumes ATP to convert acetate to acetyl-CoA, forming AMP in two steps. In the first step, the enzyme binds ATP and then acetate, yielding enzyme-bound acetyl-AMP and releasing pyrophosphate (PPi). In the second step, ACS binds CoA and converts the intermediate to acetyl-CoA and AMP.

Two ACS isoforms were first identified as an 'aerobic' form and an 'anaerobic' form, which differed from each other in a number of ways, e.g. expression in certain culture conditions, enzymatic properties, cellular localizations, immunological properties and inhibition by long chain acyl-CoA (Satyanarayana and Klein, 1973, 1976; Satyanarayana et al., 1974). The 'aerobic' acetyl-CoA synthetase was identified to be encoded by *ACS1* (Devirgilio et al., 1992). As reported by Devirgilio et al., *ACS1* gene sequencing results revealed two start codons in-frame, which indicated that two proteins with different N-termini might be formed from the gene. This was consistent with the previous observation that the 'aerobic' ACS was either localized in the microsomal or in the mitochondrial fraction during different growth phases (Klein and Jahnke, 1971). The deduced Acs1p sequence ended with VKL at its C terminal suggesting its possible location in the peroxisome. Earlier enzyme assays have shown that ACS activity rose up to 19-fold upon entrance into the stationary phase from the exponential phase in YPD media, suggesting that Acs1p was under carbon catabolite repression or C<sub>2</sub> carbon induction (Devirgilio et al., 1992), similar to what was observed for the glyoxylate cycle enzyme isocitrate lyase. The strong derepression of *ACS1* transcripts revealed by Northern hybridization in a strain grown on non-fermentable carbon sources (Kratzer and Schuller, 1995), suggested that Acs1p was regulated at the transcriptional level by the carbon source, which was also observed in the filamentous fungus *Neurospora crassa* (Thomas et al., 1988).

The highly complex molecular mechanisms of *ACS1* transcriptional regulation have been mapped through studies of the *ACS1* upstream sequence (Kratzer and Schuller, 1995; Kratzer and Schuller, 1997), in which a CSRE, a binding site for the transcriptional factor Adr1p, two distinct upstream repression sites (URS) and three binding sites for the pleiotropic factor Abf1p were identified. The CSRE was responsible for about 45% of the *ACS1* activation under derepressed conditions. The Adr1p binding site was also identified as a UAS element and contributed to 35% of *ACS1* activation under derepressed conditions. Increased *ACS1* expression by over-expression of Adr1p under both repressed and derepressed conditions further confirmed Adr1p's activating function. The two upstream repression sites were identified as URS1 sequences. Although the negative influence of the two URS1 was not affected by the carbon source, the disruption of a URS1-binding transcriptional factor encoding gene *UME6* led to significant *ACS1* expression even under repressed conditions. In addition, it was found that in the *ume6* mutant glucose-insensitive expression of *ACS1* required at least one functional Abf1p binding site, which was found not to be required for the *ACS1* derepression. Thus, it was suggested that there is a functional balance between the pleiotropic factor Abf1p acting as an *ACS1* activator and the general repressor Ume6p. However under derepressed conditions, the positive control of two UAS elements overruled the negative

control of Ume6p, and Abf1p influence was negligible (Kratzer and Schuller, 1997).

A second acetyl-CoA synthetase was found to be encoded by ACS2 (van den Berg and Steensma, 1995). ACS2 was found to encode a putative protein of 683 amino acids (75.4 kDa) with 73.6% similarity and 57.0% identity to Acs1p (713 amino acids, 79 kDa). Van den Berg et al. (1996) found that ACS activity seemed to be encoded exclusively by ACS2 in anaerobic, glucose limited chemostat cultures, suggesting Acs2p could be the ‘anaerobic’ isoform reported earlier. They also found that the kinetic properties of Acs1p and Acs2p were consistent with those of the ‘aerobic’ isoform and ‘anaerobic’ isoforms. Therefore, it was concluded that the aerobic isoform is encoded by ACS1 and the anaerobic is encoded by ACS2.

The ACS2 gene was found expressed not only under anaerobic conditions but also at aerobic conditions (van den Berg et al., 1996). Under aerobic conditions, ACS2 expression did not show substantial differences on fermentable carbon sources (glucose) and non-fermentable carbon sources (ethanol) (Hiesinger et al., 1997; van den Berg et al., 1996). Thus, ACS2 was considered to be highly constitutively expressed. The analysis of the upstream sequences identified a sequence with significant similarity to the ICRE (inositol/cholin-responsive element) and three putative binding sites for Abf1p (Hiesinger et al., 1997). ICRES were previously described as UASs of structural genes required for membrane lipid biosynthesis, like FAS1, FAS2, INO1 (Schuller et al., 1992), interacting with transcriptional factors Ino2p/Ino4p (positive regulator) and Opi1p (negative regulator). With the ICRE obtained from ACS2 inserted upstream of the reporter gene lacZ, its expression increased about 12-fold under derepressed conditions compared with repressed conditions, and gene activation caused by the ICRE was completely abolished in an ino2Δ mutant, but no response was observed in an opi1Δ mutant. As mentioned above, Abf1p binding sites were also found in the ACS2 control region. Since Abf1p has been characterized as a pleiotropic factor required for the transcriptional activation of several housekeeping genes, the three Abf1p binding sites could contribute to the constitutive expression of ACS2.

The two ACS enzymes are members of the AMP-forming ACS family, which was found to be post-translationally regulated by acetylation of lysine in a conserved region (Starai et al., 2002, 2004; Starai and Escalante-Semerena, 2004). Amino acid alignments indicated that the reversible acetylation site is Lys675 in Acs1p and Lys637 in Acs2p. As reported in *Salmonella enterica*, acetylation of this lysine residue blocks the adenylating activity of ACS in the first step, but does not affect the thioester-forming activity in the second step, and activation of the acetylated enzyme requires the NAD<sup>+</sup>-dependent protein deacetylase activity of Sir2p. In *S. cerevisiae*, the Sir2p homologs Hst3p and Hst4p were found to be the most important for growth on acetate or propionate (Starai et al., 2003). However, the detailed regulatory signals and mechanisms for acetylation and deacetylation of ACS are still unclear.

Varying results have been reported for ACS1 disruptions. Chen et al. (2012) and van den Berg and Steensma (1995) reported ACS1 disruption to result in a prolonged lag phase in batch cultures with glucose. However, other studies have reported ACS1 to be subject to carbon catabolite repression by glucose (de Jong Gubbels et al., 1997; van den Berg et al., 1996). This suggests additional, yet uncharacterized functions for Acs1p, for example in chromatin regulation, since its nuclear localization has been reported (Huh et al., 2003). Another postulation has been that since Acs2p has a significantly lower affinity for acetate compared to Acs1p (van den Berg et al., 1996), acetate has to accumulate at higher than normal concentrations to allow growth of the ACS1 disruption mutants (van den Berg and Steensma, 1995). Acs1Δ mutants have also been

reported to completely fail to grow on non-fermentable carbon sources (Chen et al., 2012), indicating a key role for Acs1p in acetyl-CoA production under these conditions. ACS2 disruption in different strains caused an inability to grow in glucose media, but did not affect growth in acetate or ethanol media (Chen et al., 2012; van den Berg and Steensma, 1995). The growth inability of the *acs2Δ* mutant in glucose actually resulted from the ACS1 repression by glucose, since the *acs2Δ* mutant could grow in glucose limited chemostat cultures (van den Berg et al., 1996).

Acs2p has no obvious targeting sequences at the termini and is thought to be localized in the cytosol. The transcriptional regulation of ACS2 is similar to several genes in lipid biosynthesis, indicating that Acs2p is mainly involved in lipid biosynthesis. A study also supported its nucleocytosolic localization (Takahashi et al., 2006). The subcellular localization of Acs1p however seems quite complex and unclear, either mitochondrial (Kumar et al., 2002), peroxisomal, cytosolic or nuclear (Huh et al., 2003). The transcriptional regulation of Acs1p suggests that it plays a key function in C<sub>2</sub> carbon source (ethanol or acetate) assimilation related with the glyoxylate cycle, which supports a peroxisomal localization. The growth ability of the *acs2Δ* mutant in glucose limited culture on the other hand supported the possible cytosolic localization of Acs1p for lipid biosynthesis. Thus, Acs1p could be dually distributed in the cytosol and the peroxisome based on its known functions. The double deletion mutant *acs1Δacs2Δ* is not viable, suggesting that ACS is indispensable for cell survival.

### 2.1.2. Acetyl-CoA in fatty acid and sterol metabolism

Acetyl-CoA is converted to malonyl-CoA by acetyl-CoA carboxylase (ACC) in the first step of fatty acid biosynthesis, which is also the rate limiting step. Two ACCs have been identified in *S. cerevisiae*, a cytosolic isoform encoded by *ACC1* (or *FAS3*) (Al-Feel et al., 1992) and a mainly mitochondrial isoform encoded by *HFA1* (Hoja et al., 2004). The expression of *ACC1* is regulated by factors that control phospholipid metabolism (Hasslacher et al., 1993), e.g. Ino2p, Ino4p, Opi1p, as reviewed in (Tehlivets et al., 2007). In vitro, Acc1p can be phosphorylated and inactivated by the mammalian carboxylase kinases, such as AMPK, suggesting it could be regulated by Snf1p phosphorylation at the post-transcriptional level (Witters and Watts, 1990). A phosphorylation site at Ser1157 has been identified for Acc1p and suggested to be the target of Snf1p (Hofbauer et al., 2014). The first step in sterol biosynthesis is catalyzed by acetoacetyl-CoA thiolase, encoded by *ERG10* in *S. cerevisiae* (Hiser et al., 1994), which condenses two acetyl-CoA molecules into one acetoacetyl-CoA molecule.

### 2.1.3. Acetyl-CoA transport between subcellular organelles

Acetyl-CoA metabolism is highly compartmentalized in *S. cerevisiae*, as well as in other fungi, and it cannot travel freely between different subcellular organelles. Three transport systems have been proposed for acetyl-CoA transport between these organelles in fungi, which are the carnitine/acetyl-carnitine shuttle, C<sub>4</sub> dicarboxylic acid synthesis from acetyl-CoA via the glyoxylate shunt (as discussed above) and acetyl-CoA re-generation from citrate by cytosolic ATP citrate lyase. The first two have been identified in *S. cerevisiae*.

In *S. cerevisiae*, five enzymes have been identified to be involved in the carnitine/acetyl-carnitine shuttle, encoded by *YAT1*, *YAT2*, *CAT2* and *CRC1*. Carnitine cannot be synthesized *de novo* by *S. cerevisiae*, but extracellular carnitine can be transported into the cells by a plasma membrane transport protein Hnm1p (Aouida et al., 2013). Carnitine acetyltransferases (CATs) catalyze the reversible reactions of acetyl group transfer between coenzyme A and carnitine, with acetyl-carnitine as the transportable molecule across the membranes of the mitochondria or the peroxisomes. Mitochondrial and peroxisomal Cat2p (Elgersma et al., 1995) has been

identified as the main CAT, Yat1p (Schmalix and Bandlow, 1993) as a second CAT associated with the outer mitochondrial membrane, and Yat2p (Swiegers et al., 2001) as a third CAT which contributes significantly to total CAT activity when cells are grown on ethanol. Crc1p (Palmieri et al., 1999) is identified as a carnitine acetyl-carnitine translocase located in the inner mitochondrial membrane.

#### 2.1.4. Protein acetylation

Protein acetylation at  $\alpha$ - or  $\epsilon$ -amino groups during post-translational modification processes has been found to be important for regulation in both eukaryotes and prokaryotes (Jones and O'Connor, 2011; Soppa, 2010). Histone acetylation affects chromatin structure and regulates gene transcription via different interactions (Kurdustani et al., 2004). Non-histone protein acetylation modulates cellular signaling at multiple levels, e.g. mRNA stability, protein localization, protein interaction, protein degradation or protein function (Spange et al., 2009; Yang and Seto, 2008). A number of histone acetyltransferases (HATs) and histone deacetylases (HDACs) have been identified in *S. cerevisiae*, which are responsible for the acetylation and de-acetylation of histone and non-histone proteins, but for most of them, their functions as transcriptional regulators are still under investigation (Glozak et al., 2005).

Acetyl-CoA plays an important part in protein acetylation as acetyl donor. The nucleocytosolic acetyl-CoA abundance directly regulates the dynamic acetylation and deacetylation of proteins. Decreased activity of Acc1p, which consumes acetyl-CoA for *de novo* synthesis of fatty acids, has been shown to cause increased histone acetylation and altered transcriptional regulation (Galdieri and Vancura, 2012). Tu et al. found that acetyl-CoA drives the transcriptional growth program by promoting the acetylation of histones at growth related genes in yeast (Cai and Tu, 2011; Shi and Tu, 2013), and predicted that 'intracellular acetyl-CoA fluctuations might represent a distinctive gauge of cellular metabolic state that could be decoded by way of dynamic acetylation and deacetylation reactions' (Cai and Tu, 2011).

### 2.2. Alternative pathways for acetyl-CoA generation in other eukaryotes

In addition to the pathways for acetyl-CoA generation described above for yeast, some other eukaryotic organisms make use of additional pathways to generate acetyl-CoA.

#### 2.2.1. Oleaginous yeasts

ATP-citrate lyase (ACL) is a ubiquitous enzyme that uses citrate, an intermediate of the TCA cycle, as the substrate, and converts it to acetyl-CoA and oxaloacetate at the cost of one ATP (Zaidi et al., 2012). The enzyme is located in the cytosol, and as citrate can be transported across the mitochondrial membrane, this metabolite basically becomes a carrier of acetyl-CoA from the mitochondria to the cytosol. ACL is found in many different eukaryotic species, including fungi, plants and animals. Interestingly, while this enzyme is ubiquitous in oleaginous yeasts, it is not found in non-oleaginous yeasts such as *S. cerevisiae* (Vorapreeda et al., 2012), suggesting that this enzymes plays a role in supplying the precursor acetyl-CoA necessary for fatty acid and lipid biosynthesis. Indeed, it has been previously shown that ACL plays a crucial role in acetyl-CoA generation during the lipid accumulation phase in these organisms (Ratledge, 2002). Vorapreeda et al. (2012) conducted a comparative genomics analysis for various oleaginous and non-oleaginous species and identified putative routes that could potentially be involved in acetyl-CoA production in oleaginous species. They suggested that apart from ACL, enzymes in the oleaginous yeasts that are localized in the mitochondria might be

responsible for generating acetyl-CoA through degradation of branched-chain amino acids (leucine and lysine) and fatty acids. This acetyl-CoA could be transported to the cytosol via carnitine-dependent translocation and/or ACL (Strijbis and Distel, 2010).

#### 2.2.2. Phosphoketolase pathway

The phosphoketolase (PK) pathway is another pathway that has been suggested to have a role in acetyl-CoA generation. This pathway is used by some bacteria and filamentous fungi for sugar dissimilation as an alternative to the commonly used Embden–Meyerhof–Parnas pathway, and usually operates during growth on xylose. The PK pathway was first reported in heterofermentative and facultative homofermentative lactic acid bacteria, in bifidobacteria, as well as some xylose fermenting yeasts (Ratledge and Holdsworth, 1985). Phosphoketolase is an enzyme that generates acetyl phosphate from xylulose 5-phosphate or fructose 6-phosphate with concurrent formation of glyceraldehyde-3-phosphate or erythrose-4-phosphate, respectively. It has been found that in addition to PK, various fungal species contain acetate kinase (ACK), an enzyme that catalyzes conversion of acetyl-phosphate to acetate (Ingram-Smith et al., 2006). It is therefore possible that during growth on xylose, PK operates together with ACK and ACS to generate acetyl-CoA.

In addition, open-reading frames that encode phosphotransacetylase (PTA), an enzyme that catalyzes conversion of acetyl-phosphate to acetyl-CoA have been found e.g. in *Chlamydomonas reinhardtii* and *Phytophthora* species (Ingram-Smith et al., 2006). This enzyme could also serve as a source of acetyl-CoA via the PK pathway in these organisms.

#### 2.2.3. Anaerobic routes to acetyl-CoA production

While utilization of the PDH pathway to produce acetyl-CoA is widespread among eukaryotes, additional pathways for acetyl-CoA generation have been identified in other unicellular eukaryotes that experience anaerobic conditions, such as various protists. These include pyruvate formate lyase (PFL), pyruvate:ferredoxin oxidoreductase (PFOR) and pyruvate:NADP<sup>+</sup> oxidoreductase (PNO). These enzymes have been shown to localize in different compartments, depending on the organism, and substitute the role of PDH in the formation of acetyl-CoA under anaerobic conditions.

PFL catalyzes the conversion of pyruvate to acetyl-CoA and formate, and is activated by a PFL-activating enzyme (PFL-AE). Within eukaryotes, this pathway was first described in the hydrogenosomes of an anaerobic chytrid fungus, *Neocallimastix* sp (Akhamanova et al., 1999). The catalytic function of PFL is dependent on a radical, and oxygen destruction of the radical results in cleavage of PFL (Wagner et al., 1992). Since generation of acetyl-CoA via PFL does not produce CO<sub>2</sub>, this system has been hypothesized to function as an alternative to PFOR, when the latter is inhibited by high CO<sub>2</sub> levels in the organism's environment (Boxma et al., 2004). Besides *Neocallimastix* sp and its close relative *Promyces* sp E2 (Boxma et al., 2004), eukaryotic PFL activity was also described in the chloroplasts and mitochondria of the chlorophyte alga *C. reinhardtii* (Atteia et al., 2006; Hemschemeier et al., 2008). In addition, thorough mining of all publicly available EST projects for eukaryotes, Stairs et al. (2011) revealed a wide diversity of microbial eukaryotic lineages that possess PFL homologues and their activating enzymes. Many of these organisms are traditionally thought of as "aerobic" organisms and therefore the authors hypothesized that PFL is important for continued production of acetyl-CoA in organisms experiencing transient low oxygen conditions (Stairs et al., 2011).

PFOR catalyzes the anaerobic decarboxylation of pyruvate in a TPP-dependent reaction that produces acetyl-CoA and CO<sub>2</sub> (Charon et al., 1999), and releases 2 electrons. The electrons are then typically transferred to small low-redox-potential proteins,

either a ferredoxin or flavodoxin. PFOR contains several [4Fe–4S]-type iron–sulfur clusters and TPP as cofactors. While typically occurring in prokaryotes, PFOR has also been identified in the eukaryotic alga *C. reinhardtii* (Atteia et al., 2006).

Protists such as *Euglena gracilis* and apicomplexa such as *Cryptosporidium* and *Plasmodium* contain PNO. Recently, PNO homologs have been found to occur in many disparate eukaryotic lineages in EST sequencing projects (Hug et al., 2010), indicating this enzyme is far more widespread than previously thought. Like PFOR, this enzyme decarboxylates pyruvate to acetyl-CoA. It has an N-terminal domain similar to PFOR, but is fused to a C-terminal NADP-cytochrome P450 oxidoreductase domain (Rotte et al., 2001) and utilizes NADP<sup>+</sup> as an electron acceptor. In *E. gracilis* it is found in the mitochondrion, a facultative anaerobic organelle that produces ATP in both the presence and absence of O<sub>2</sub> (Buetow, 2011). This enzyme is oxygen-sensitive and functions under anaerobic conditions as a key enzyme of a unique wax ester fermentation where acetyl-CoA from PNO is used both as a primer and as C<sub>2</sub>-donor for fatty acid synthesis in the mitochondria (Inui et al., 1984). Fatty acids are reduced and esterified, yielding waxes that accumulate in the cytosol (Inui et al., 1984). Upon return to aerobic conditions, these waxes undergo β-oxidation and oxidative phosphorylation.

### 3. Prokaryotic acetyl-CoA metabolism

Since *E. coli* is often the preferred prokaryotic cell factory, we mainly focus on the metabolism of acetyl-CoA in *E. coli*, but relevant metabolism from other organisms will be discussed as well. An overview of the acetyl-CoA metabolism in *E. coli* is shown in Fig. 2.

#### 3.1. Acetyl-CoA production

##### 3.1.1. From pyruvate

Under aerobic conditions, one major route for acetyl-CoA production is the decarboxylation of pyruvate using PDH. In bacteria, PDH is an enzyme complex consisting of three enzymes: pyruvate dehydrogenase/decarboxylase (E1), dihydrolipoyl acetyltransferase (E2), and dehydrolipoamide dehydrogenase (E3). The PDH complex from Gram-negative bacteria possesses an octahedral (24 subunits) E2 core while the Gram-positive and eukaryotic PDH complexes are based on an icosahedral (60 subunits) core. In *E. coli*, genes encoding enzymes E1–E3 are organized in an operon in the order *aceE*, *aceF*, and *lpd* with small intergenic regions. Besides these essential components, additional genes are required for the attachment and activation of the lipoyl group, which belong either to the *de novo* pathway (*lipA* and *lipB*) or the salvage pathway (*lplA*) in *E. coli*. The reaction is catalyzed by each of the constituting enzymes in the sequence of: E1 using TPP to carry out the oxidative decarboxylation of the substrate with formation of a hydroxyethyl group, covalently attached to the lipoamide disulfide of E2, thereby being oxidized to an acetyl group, which is transferred to coenzyme A by the E2 component. The resulting dihydrolipoyl group is then reoxidized by E3 using NAD<sup>+</sup> as electron acceptor. It has been shown that expression of the PDH complex is regulated by the transcriptional repressor *PdhR*, whose coding sequence is included in the same operon in *E. coli* (Quail et al., 1994). Due to a lack of regulatory proteins, such as PDH phosphatase, the bacterial PDH complexes are normally regulated by allosteric mechanisms and product inhibition (de Kok et al., 1998).

Under anaerobic conditions, there are several oxygen-sensitive enzymes that can catalyze the formation of acetyl-CoA through either the non-oxidative conversion of pyruvate via PFL, or the oxidative decarboxylation of pyruvate via PFOR.

PFL is relatively widespread in facultative and obligate anaerobic eubacteria, as well as archaea (Sawers and Watson, 1998). It is essential for the anaerobic glucose metabolism in *E. coli* and the reaction is fully reversible with very high turnover numbers in both directions (Himo and Eriksson, 1998). PFL is interconverted between inactive and active forms. The active form is a homodimer and contains a glycyl radical, which is sensitive to oxygen. Thus, introduction of the radical into PFL only occurs anaerobically. The formation of the radical is catalyzed by PFL-AE, a monomeric iron–sulfur cluster protein, using S-adenosyl methionine as cofactor and reduced flavodoxin as reductant. Due to the oxygen sensitivity of the glycyl radical in vitro, PFL has been thought to function anaerobically only. However, it has been reported that PFL

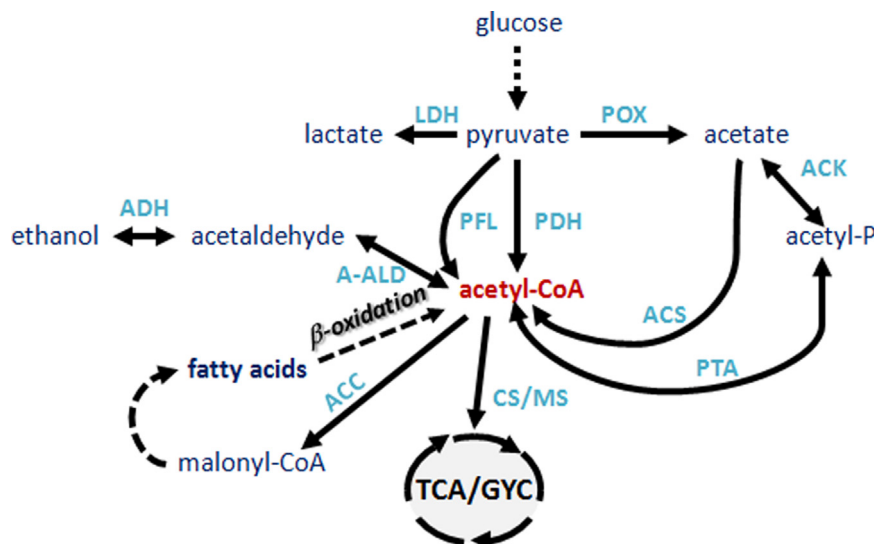


**Fig. 2.** Overview of the acetyl-CoA metabolism in *Escherichia coli*. Acetyl-CoA is generated directly from pyruvate via the actions of PDH under aerobic conditions, or PFL under anaerobic conditions. In addition, acetyl-CoA can be generated by conversion of pyruvate to acetate, acetyl-phosphate and finally acetyl-CoA by the actions of POX, ACK and PTA. Acetate can also be converted directly to acetyl-CoA via ACS. β-Oxidation of fatty acids also results in acetyl-CoA formation. Acetyl-CoA is used as a substrate for the TCA or glyoxylate cycles, or for fatty acid production via malonyl-CoA. Acetyl-CoA can also be converted back to acetate via acetyl-phosphate or reduced to ethanol via acetaldehyde, which are then excreted.

may also be functional in vivo under microaerobic conditions (Alexeeva et al., 2000). It is proposed that YfiD may act as a substitute for the glycyl radical domain to repair oxygen induced damage to the PFL glycyl radical (Wagner et al., 2001).

PFOR is widely distributed among bacteria and almost all members of archaea (Ragsdale, 2003). It has often been referred to as pyruvate synthase, as it catalyzes the reversible oxidation of pyruvate by ferredoxin to acetyl-CoA and CO<sub>2</sub>. Most bacterial PFORs are homodimeric, but can also be heterodimeric or heterotetrameric depending on the organism (Kletzin and Adams, 1996; Zhang et al., 1996). Iron-sulfur cluster numbers in PFORs can also vary from one to three. Like PDH, the PFOR reaction also uses TPP as a cofactor, but ferredoxin as the electron acceptor instead of NAD<sup>+</sup> in the case of PDH. As in the case of PFL, this reaction also involves the formation of a radical and the enzyme is sensitive to oxygen. One exception, however, is the *Desulfovibrio africanus* PFOR, which shows an unusual high stability towards oxygen (Pieulle et al., 1995).

### 3.1.2. From acetate

Prokaryotic cells have evolved three distinct pathways to activate acetate to acetyl-CoA. The first route involves reversible phosphotransacetylase-acetate kinase (Pta-Ack), which catalyzes the phosphorylation of acetate to form acetyl phosphate and subsequently convert this to acetyl-CoA. The second route depends on irreversible ACS (AMP forming), which transforms acetate and ATP to the enzyme-bound intermediate acetyladenylate (acetyl-AMP). Then, acetyl-AMP reacts with CoASH to form acetyl-CoA and releases AMP (Starai and Escalante-Semerena, 2004; Wolfe, 2005). The third route is composed of ADP forming ACS catalyzing the reversible activation of acetate to acetyl-CoA, which belongs to the class of ACSs that catalyze the synthesis of the product in a single step. This type of enzyme has been detected in the eukaryotic protist *Entamoeba histolytica* (Reeves et al., 1977) and the hyperthermophilic archaeon *Pyrococcus furiosus* (Schäfer and Schönheit, 1991).

In *E. coli*, the ACS route (AMP forming) is a high affinity pathway with a low *K<sub>m</sub>* of 200 μM for acetate, which primarily functions anabolically at low acetate concentrations (Kumari et al., 1995). The reversible Pta-Ack route can also assimilate acetate, but only in relatively high concentrations, as both enzymes in this pathway possess high *K<sub>m</sub>* values for their substrates (7–10 mM) (Brown et al., 1977). The regulation of ACS expression has been well studied in *E. coli* (Starai and Escalante-Semerena, 2004; Wolfe, 2005). The transcription of *acs* is repressed by glucose as it is activated by the Crp protein when cyclic AMP (cAMP) levels rise (Beatty et al., 2003). Its expression is triggered at mid-exponential phase, reaching a maximum when the cells enter the stationary phase. The activity of ACS is also regulated at the post-translational level by the sirtuin-dependent protein acylation/deacylation system (SDPADS). In *S. enterica*, ACS activity is post-translationally regulated via acetylation of residue Lys609, which results in blocking of the conversion of acetate to acetyl-AMP (Starai et al., 2002). The same group has identified the residue Leu641 as a critical amino acid for the acetylation of the *S. enterica* ACS and they have shown that mutations at Leu641 prevent acetylation and maintain the enzyme in its active state (Starai et al., 2005).

### 3.1.3. From fatty acids

Exogenous fatty acids can be used as carbon and energy source via the β-oxidation pathway coupled to the citric acid cycle. The final product of degradation of fatty acids is acetyl-CoA for fatty acids with an even number of carbons, and acetyl-CoA along with a single propionyl-CoA when fatty acids with odd numbers of

carbons are degraded. In *E. coli*, expression of the *fad* genes of the fatty acid degradation regulon is regulated by both the cyclic AMP-dependent catabolic repression system and the FadR transcriptional factor (Iram and Cronan, 2006). Since only long chains (>C<sub>12</sub>) coordinately induce *fad* gene expression, wild type *E. coli* can utilize long chain fatty acids, such as oleate, but not medium (C<sub>7</sub> to C<sub>11</sub>) and short-chain (C<sub>4</sub> to C<sub>6</sub>) fatty acids as a sole carbon source (Weeks et al., 1969). However, medium and short-chain fatty acids can be metabolized by *fadR* and *ato* mutants (Jenkins and Nunn, 1987; Overath et al., 1969). Although the fatty acid degradation enzymes of *E. coli* and *S. enterica* have high levels of similarity, the FadBA and FadE proteins of *S. enterica* are much more efficient at complete degradation of fatty acids than their homologs in *E. coli* (Iram and Cronan, 2006).

## 3.2. Acetyl-CoA consumption

### 3.2.1. Oxidation by TCA cycle

In the presence of sufficient oxygen, acetyl-CoA is mainly oxidized via the TCA cycle to generate energy. The condensation of acetyl-CoA with oxaloacetate to form citrate in *E. coli* is catalyzed by the *gltA* gene product, CS. As it is the first enzyme in the TCA cycle, this enzyme has been assumed to be an important control point for determining the flux through the cycle. The *E. coli* CS is a large enzyme consisting of six identical subunits and its activity is inhibited by NADH and ATP. Transcription of *gltA* is repressed by ArcA but independent of the fumarate and nitrate reductase (FNR) transcription factor (Park et al., 1994), unlike many other genes encoding enzymes of the TCA cycle. Nevertheless, the regulation of *gltA* gene expression, as many TCA cycle enzymes, is complex in meeting the different needs of the cell for biosynthesis and energy generation under different conditions (see review by Kern et al., 2007).

### 3.2.2. Excretion as acetate and ethanol

When cells grow on excess glucose or other carbon sources that are easily assimilated, respiration is inhibited in a behavior called the bacterial Crabtree effect (Luli and Strohl, 1990). As a consequence, up to 1/3 of the glucose could be excreted mainly as acetate via the reversible Pta-Ack pathway (Kern et al., 2007). Through the same enzymes that are used to activate acetate, acetyl-CoA is converted to acetyl phosphate and then sequentially to acetate, generating ATP without consuming reducing equivalents. Alternatively, the resultant acetyl-CoA can be reduced to ethanol by acetylating acetaldehyde dehydrogenase and alcohol dehydrogenase, which consumes reducing equivalents without ATP production.

### 3.2.3. Entry into the glyoxylate cycle

Under certain conditions, such as growth on acetate, fatty acids or aromatics as primary carbon source, whose degradation results in acetyl-CoA formation, the cell has to activate the glyoxylate cycle to allow the accumulation of four-carbon precursors, and also to activate gluconeogenesis pathways in order to provide sugar phosphates and other precursor metabolites required for biomass formation. The glyoxylate cycle uses isocitrate lyase and malate synthase to convert isocitrate to malate, by bypassing two oxidative steps of the TCA cycle. In addition to CS, MS also incorporates two-carbon units (in term of acetyl-CoA), permitting the cells a net biosynthesis of four-carbon metabolites from acetyl-CoA. The glyoxylate cycle is highly regulated in most organisms. Depending on the background, the transcription of *aceB* encoding MS is constitutive in the *E. coli* B strain which is a low acetate producer, whereas it is conditionally expressed in the *E. coli* K strain which is a high acetate producer (Phue and Shiloach, 2004).

### 3.2.4. Fatty acid biosynthesis

Acetyl-CoA is used for the *de novo* biosynthesis of fatty acids. In this process, the first committed step is conducted by acetyl-CoA carboxylase through condensation of bicarbonate with acetyl-CoA to form malonyl-CoA. The *E. coli* ACC is a heterotetramer which consist of four subunits, AccABCD. Having the key position in the formation of fatty acids, ACC is an important regulatory enzyme in fatty acid biosynthesis. It has been shown that ACC activity is subject to feedback inhibition by acyl-ACP (Davis and Cronan, 2001). The formed malonyl group is transferred from CoA to ACP by malonyl-CoA:ACP transacylase (FabD) to initiate the elongation cycle. This is carried out by  $\beta$ -ketoacyl-ACP synthase III (FabH) through condensation of acetyl-CoA with malonyl-ACP. Bacterial fatty acid biosynthesis has been reviewed by Rock and Jackowski (2002).

## 4. Engineering strategies for acetyl-CoA metabolism in yeast

The yeast *S. cerevisiae* is an attractive cell factory as it is robust, able to grow to high densities and at low pH. In addition, it is more resistant to phage contaminations compared to its bacterial counterparts. A lot of information is available on the physiology of *S. cerevisiae*, and many tools are available for its genetic manipulation. However, the production of acetyl-CoA-derived products in yeast often lags behind when compared to *E. coli*. This is likely due to the difference in acetyl-CoA metabolism between the two organisms, since acetyl-CoA metabolism in yeast is compartmentalized and acetyl-CoA cannot be readily transported across the different compartments. In the cytosol, ACS is a limiting step due to its low activity and high-energy input requirements (Shiba et al., 2007). This compartmentalization makes the acetyl-CoA metabolism in yeast more difficult to engineer. Indeed, it has been shown that the limited structural flexibility of the central carbon metabolism of *S. cerevisiae* could be a limiting factor in engineering it for higher alcohol production (Matsuda et al., 2011). Therefore, different strategies to enhance cytosolic acetyl-CoA production in yeast for increased biosynthesis of biotech products have been evaluated (Fig. 3).

### 4.1. PDH bypass

The first account of engineering the PDH bypass route to enhance acetyl-CoA levels was by Shiba et al. (2007) for production of amorphadiene, a sesquiterpene precursor to the anti-malarial drug artemisinin. This molecule is synthesized via the mevalonate pathway in yeast, using acetyl-CoA as a starting molecule. In this study, the native acetaldehyde dehydrogenase gene (*ALD6*), as well as a mutant acetyl-CoA synthetase from *S. enterica* (*ACS<sub>SE</sub><sup>L641P</sup>*) were over-expressed. Over-expression of these two enzymes resulted in increased production of amorphadiene of up to 4-fold. When these modifications were further combined with over-expression of the truncated form of HMG-CoA reductase (tHMGR), a flux controlling step in the mevalonate pathway, as well as overexpression of farnesyl pyrophosphate (FPP)-synthase, the highest amorphadiene levels were achieved, with the strain accumulating about 120 mg/L (Shiba et al., 2007).

A similar strategy was used by Chen and co-workers for production of  $\alpha$ -santalene, a sesquiterpene that acts as a perfume ingredient (Chen et al., 2013). In addition to over-expressing *ALD6* and *ACS<sub>SE</sub><sup>L641P</sup>*, the strategy also employed over-expression of the endogenous alcohol dehydrogenase 2 (*ADH2*) gene, which catalyzes the conversion of ethanol to acetaldehyde. A native thiolase gene, *ERG10*, was also over-expressed to ensure pulling of acetyl-CoA towards the product. Strains over-expressing these genes produced 3.65 mg/L of  $\alpha$ -santalene, compared to 2.08 mg/L produced by the reference

strain, representing a 75% increase. In contrast, strains over-expressing only the *ALD6* and *ACS<sub>SE</sub><sup>L641P</sup>* genes resulted in an only 25% increase in  $\alpha$ -santalene production demonstrating the importance of additional over-expression of *ADH2* and *ERG10*.

The above manipulations were further combined with strategies aimed at reducing carbon loss from the precursor acetyl-CoA pool through the deletion of one of two glyoxylate cycle genes, namely peroxisomal citrate synthase (*CIT2*) and cytosolic malate synthase (*MLS1*). It has been shown that cytosolic acetyl-CoA can be consumed by Mls1p and converted to C<sub>4</sub> organic acids that are transported into the mitochondrion for oxidation (Chen et al., 2012). In addition, it has been shown that acetyl-CoA formed by Acs1p from acetate is used by citrate synthase in the peroxisomes (Chen et al., 2012). Combining over-expression of the genes above with deletion in *CIT2* resulted in 4.98 mg/L of  $\alpha$ -santalene produced, while combining this strategy with *MLS1* deletion resulted in 8.29 mg/L, representing a 4-fold increase over the reference strain (Chen et al., 2013).

This strategy was also applied for production of poly-(R)-3-hydroxybutyrate (PHB) (Kocharin et al., 2012). PHB is a common type of polyhydroxyalkanoate (PHA), compounds that are synthesized and accumulated by some microorganisms as a carbon and energy storage material in response to conditions of physiological stress (Steinbuchel et al., 1993). PHB is a linear polyester that can be used as a biodegradable plastic. Applying the strategy above for production of PHB had somewhat different results when compared to  $\alpha$ -santalene production. While over-expression of *ADH2*, *ALD6*, *ACS<sub>SE</sub><sup>L641P</sup>* and *ERG10* resulted in a strong increase in PHB titers, this increase was significantly higher (18-fold) compared to  $\alpha$ -santalene. However, deletion of *CIT2* or *MLS1* had deleterious effects on PHB production as the majority of PHB was produced in the ethanol phase, which was compromised in the deletion mutants.

When applied for production of 1-butanol, an advanced biofuel derived from acetyl-CoA, over-expression of *ADH2*, *ALD6*, *ACS<sub>SE</sub><sup>L641P</sup>* and *ERG10* resulted in 10.3 mg/L of 1-butanol produced, representing a 4.9-fold increase over expression of the heterologous 1-butanol pathway alone and a 1.6-fold increase compared to over-expression of the 1-butanol pathway together with *ERG10* (Krivoruchko et al., 2013). When over-expression of these genes was combined with deletions in *MLS1* or *CIT2*, 1-butanol production was further increased to 14.0 and 16.3 mg/L, respectively (Krivoruchko et al., 2013).

### 4.2. PK pathway

Papini et al. (2012) described the effects of expression of the fungal PK pathway genes in *S. cerevisiae* during batch and chemostat cultivations. This involved reconstruction of the PK pathway in *S. cerevisiae* by expressing xylulose-5-phosphate phosphoketolase (XpkA) and acetate kinase (Ack) from *Aspergillus nidulans*. In addition, the cytosolic transhydrogenase gene *sth* was expressed to increase the drain of NADPH in order to increase flux through the pathway. <sup>13</sup>C labeling was used to resolve the intracellular flux distribution and determine if yeast actively used the heterologous pathway. The flux distribution showed an active role of this pathway, confirming the ability of yeast to use this pathway alongside glycolysis. In addition, the functionality of this pathway with the *Bacillus subtilis* phosphotransacetylase gene *pta* alternatively to the acetate kinase was also evaluated. However, in this case it was found that no flux went through the PK pathway during growth on glucose (Papini et al., 2012).

Kocharin et al. (2013) tested the use of the PK pathway for PHB production. This included over-expression of XpkA and Ack from *A. nidulans*, as well as *ACS<sub>SE</sub><sup>L641P</sup>* from *S. enterica* in yeast. In addition, genes coding for the PHB biosynthetic pathway were expressed. Since NADPH is required for PHB production, this strategy was also

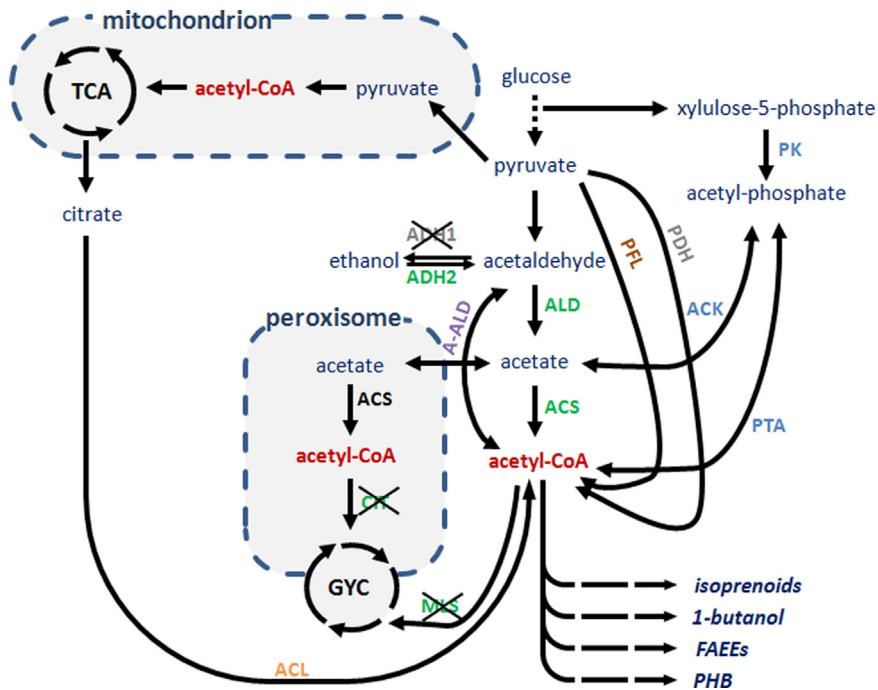


**Fig. 3.** Overview of different strategies employed for metabolic engineering of acetyl-CoA metabolism in yeast. Single colors denote proteins that were used together as part of the same strategy. The ethanol degradation strategy made use of ADH2, ALD and ACS to generate cytosolic acetyl-CoA from ethanol. This strategy was used in combination with CIT2 and MLS1 deletions. The PK pathway used PK, and either ACK/ACS or PTA to generate acetyl-CoA from the pentose phosphate pathway. A-ALD was used to convert acetaldehyde to acetyl-CoA, while PFL and PDH were used in separate strategies to convert pyruvate to acetyl-CoA. ACL was used to convert citrate from the TCA cycle to cytosolic acetyl-CoA. Several of these strategies have also been combined with production of compounds of commercial interest, including different isoprenoids, 1-butanol, FAEEs and PHB. (For interpretation of the references to color in this figure legend, the reader is referred to the web version of this article.)

evaluated with GapN, a non-phosphorylating, NADP<sup>+</sup>-dependent glyceraldehyde-3-phosphate dehydrogenase from *Streptococcus mutans*. The strain containing the PK pathway showed an improved PHB production not only compared with the reference strain but also compared with a strain that over-expressed the PDH bypass pathway described above. Over-expression of GapN did not improve yields in the PK-pathway-containing strains, but did when the PDH-bypass pathway was over-expressed. This is probably because excess NADPH is already generated when the PK pathway is utilized (Kocharin et al., 2013).

De Jong and co-workers (de Jong et al., 2014) examined the effects of PK pathway expression on production of fatty acid ethyl esters (FAEEs), which serve as biodiesel components. Expression of *xpkA* and *pta* in a strain containing multiple integrations of a wax ester synthase gene (*ws2*), resulted in 4670 µg/gCDW of FAEEs, which was 1.6-fold higher than the reference strain, while expression of *xpkA* and *ack* in this strain improved the final yield of FAEEs to 5100 µg/gCDW.

#### 4.3. Other heterologous pathways

Kozak et al. (2014a) evaluated the use of acetylating acetaldehyde dehydrogenase (A-ALD) and PFL as potential acetyl-CoA supply pathways in yeast. A-ALD catalyzes the ATP-independent conversion of acetaldehyde to acetyl-CoA (Pawlowski et al., 1993; Rudolph et al., 1968; Smith and Kaplan, 1980). The five genes encoding acetaldehyde dehydrogenase were deleted in this study and A-ALD genes from different sources were expressed. Expression of all tested A-ALD variants enabled fast growth of *ald2Δald3Δald4Δald5Δald6Δ* *S. cerevisiae* on synthetic medium containing 20 g/L glucose. The best strains (expressing *E. coli eutE* and *Listeria innocua lin1129*) showed the highest maximum specific growth rates, which were over 75% of that of the *ALD+* strain.

In addition, this study also evaluated the use of PFL as a potential acetyl-CoA source. To investigate functionality of PFL in yeast, an *acs2Δ* strain was used as a screening platform. Deletion of *ACS2* results in a strain unable to grow on glucose plates due to repression and glucose catabolite inactivation of *ACS1* and its gene product (de Jong Gubbels et al., 1997; van den Berg and Steensma, 1995). Genes encoding PFL from different organisms were expressed in this strain. Strains expressing PFL from *E. coli* or *Lactobacillus plantarum* were able to grow anaerobically on plates containing glucose as the sole carbon source. In addition, it was shown that expression of either PFL or A-ALD could restore growth in *acs1Δacs2Δ* mutants (Kozak et al., 2014a).

Lian et al. (2014) evaluated and compared a number of acetyl-CoA generating strategies. Since during glucose fermentation most of the metabolic flux from acetaldehyde goes towards ethanol rather than acetyl-CoA, they sought to disrupt ethanol production by deleting *ADH1* and *ADH4*. In addition, since previous reports indicated that decreased ADH activity led to increased production of glycerol (de Smidt et al., 2012), they also disrupted the glycerol pathway by deleting *GPD1* and *GPD2*. These modifications increased the acetyl-CoA levels by approximately 2-fold. When combined with a heterologous pathway for 1-butanol production, these modifications resulted in a 4-fold increase in 1-butanol titers when compared to a strain expressing the 1-butanol pathway but without these deletions. When this strategy was combined with overexpression of *ACS<sub>SE</sub><sup>1641P</sup>*, the 1-butanol titers were further improved.

In addition to overexpressing *ACS<sub>SE</sub><sup>1641P</sup>*, the authors of this study also examined the effect of expressing PDH on 1-butanol production. This was done by introducing either yeast PDH genes lacking the mitochondrial targeting sequence into a *adh1Δadh4Δgpd1Δgpd2Δ* strain, or *E. coli* PDH genes. These modifications resulted in a further increase in 1-butanol production. However, this study did not include co-expression of lipoylation genes for activation of the E2 subunit of

PDH, or addition of lipoate to the growth medium. It is therefore questionable if the PDH complex was actually functional and the effect on butanol production was caused by other routes being activated in the strain (Nielsen, 2014).

In a recent study, Kozak et al. (2014b) also evaluated the use of bacterial PDH as a strategy for the generation of cytosolic acetyl-CoA in yeast. In this publication, the PDH complex from *Enterococcus faecalis* was expressed in yeast. This PDH complex has been shown to be insensitive to high NADH/NAD<sup>+</sup> ratios, allowing it to function under both aerobic and anaerobic conditions (Snoep et al., 1993). Kozak et al. (2014b) have shown that this complex could be functionally expressed in yeast, with its expression fully replacing the ACS-dependent pathway for production of cytosolic acetyl-CoA.

The use of ACL for acetyl-CoA generation has also been reported. Tang et al. (2013) compared the effect of expression of mouse ACL on fatty acid production and composition in either wild-type strains, or strains containing deletions in *IDH1*, *IDH2*, or both. While slight changes in the levels of some fatty acids, as well as the fatty acid composition were observed between the different strains, these differences were fairly minor. In addition, Lian et al. (2014) have shown that co-expression of a *Yarrowia lipolytica* ACL with a 1-butanol pathway in an *adh1Δadh4Δgpd1Δgpd2Δ* strain resulted in approximately a 2-fold increase in 1-butanol production compared to the control strain. However, no positive effect on butanol production was observed when *Arabidopsis thaliana* ACL was used.

## 5. Engineering strategies for acetyl-CoA metabolism in *E. coli*

### 5.1. Deletion of competing pathways

While *E. coli* exhibits a mixed acid fermentation under anaerobic conditions, acetate resulting from overflow metabolism is the major by-product in aerobic fermentations at high specific growth rates. Acetate accumulation has a negative effect on cell growth and on recombinant protein production. In addition, it leads to a loss of carbon (De Mey et al., 2007). Early work on metabolic engineering of acetyl-CoA metabolism in *E. coli* therefore focused on minimizing acetate formation in recombinant protein production. Two pathways are mainly responsible for aerobic acetate formation: the Pta/AckA pathway, which dominates during exponential growth, and the pyruvate oxidase (PoxB) pathway dominant in the stationary phase (Dittrich et al., 2005a). Employment of a *ptaΔ* mutant was able to increase recombinant interleukin-2 and lipase production while reducing acetate formation (Bauer et al., 1990; Hahm et al., 1994).

In addition to recombinant protein production, deletion of *pta* and/or *ackA* was also applied in the production of acetyl-CoA derived metabolites. *Pta* deletion in an already engineered strain led to a 20% increase in fatty acid content (Lin et al., 2013). Isoamyl acetate, an important flavor compound, is produced from acetyl-CoA and isoamyl alcohol by an alcohol acetyl transferase (e.g. yeast *Atf2p*). Its formation in an *E. coli* strain expressing yeast *ATF2* and fed with isoamyl alcohol was doubled upon deletion of *pta-ackA* albeit only under anaerobic conditions (Vadali et al., 2004c). The same strategy was also successful in increasing PHB production up to 2.5-fold in strains harboring the PHB pathway from *Ralstonia eutropha* or *Azotobacter vinelandii* (Centeno-Leija et al., 2014; Chang et al., 1999; Miyake et al., 2000). Interestingly, Miyake et al. (2000) observed at the same time a substantial reduction in PHB synthase activity in the *pta-ackA* deletion strain. In some studies, inactivation of the Pta/AckA pathway was combined with deletion of *poxB*. Although this further reduced acetate formation, it had no additional effect on isoamylacetate accumulation (Dittrich et al., 2005b).

Under anaerobic conditions, deletion of the Pta/AckA pathway did not only lead to reduced acetate, formate and ethanol production, but also increased lactate secretion and reduced cell growth. In comparison to the wild-type strain, intracellular fluxes were shifted from pyruvate-formate lyase towards lactate dehydrogenase (Yang et al., 1999). However, when the lactate dehydrogenase encoding *ldhA* gene was additionally deleted, this further reduced growth and even led to a reduced isoamylacetate production in comparison to a *pta-ackAΔ* strain (Vadali et al., 2004c; Yang et al., 1999).

One reason for the growth reduction in strains with an inactive Pta/AckA pathway may be the loss of ATP production by acetate kinase. Furthermore, this strategy not only decreases acetate formation, but also the formation of acetyl-phosphate, which plays additional roles in cell metabolism (McCleary et al., 1993). To interfere in a less drastic way than with a pathway deletion, Kim and Cha (2003) instead reduced expression of the two enzymes using an antisense RNA strategy, which increased recombinant protein production up to 2-fold.

Nevertheless, optimization of *E. coli* for production of acetyl-CoA derived products under anaerobic or semi-anaerobic conditions usually involves the deletion of several of its fermentation pathways. Besides *pta-ackA*, *poxB* and *ldhA*, this includes the fumarate reductase complex (encoded by *frdABCD*), the alcohol/aldehyde dehydrogenase encoded by *adhE*, and sometimes PFL. In order to increase the formation of ethanol by *AdhE*, *ldhA*, *ackA* and *frdBC* were deleted, which led to a more than 2-fold improvement in the final product concentration, but also to reduced cell growth due to the creation of a redox imbalance (Zhou et al., 2008). Deletion of *ldhA*, *adhE* and *frdBC* doubled the production of 1-butanol in a strain carrying the clostridial butanol pathway. The additional deletion of *pta* however reduced 1-butanol formation and the subsequent knock-out of *pflB* nearly abolished it due to insufficient PDH activity under low-oxygen conditions (Atsumi et al., 2008). A modification of the butanol pathway by omitting the two ultimate dehydrogenase reactions and instead taking advantage of endogenous acyl-CoA thioesterase II (TesB) led to formation of butyrate, which was improved more than 10-fold under microaerobic conditions upon deletion of *frdA*, *ldhA*, *adhE* and *pta* (Baek et al., 2013). Deletion of these four fermentation pathways plus *poxB* and *pflB* was also able to increase PHB production by almost 3-fold, while at the same time increasing biomass formation (Jian et al., 2010).

Acetaldehyde is applied as a flavor ingredient in the food industry. Its production from acetyl-CoA in *E. coli* was established through expression of an acetyl-CoA reductase from *S. enterica*. While the primarily engineered strain only produced traces of the desired compound, deletion of *frdC*, *ldhH*, *pta-ackA* and *adhE* substantially increased its production (Zhu et al., 2011). Another group of platform chemicals are methyl ketones. In *E. coli*, they can be derived from 3-ketoacyl-ACPs, which are intermediates in fatty acid biosynthesis, via two heterologous enzymes, 3-ketoacyl-ACP thioesterase and beta-decarboxylase. Here, deletion of *adhE*, *ldhE*, *poxB* and *pta* resulted in a 5-fold increase in production (Park et al., 2012).

### 5.2. Modulation of acetyl-CoA generating enzymes

As mentioned above, the conversion of pyruvate to acetyl-CoA is mainly mediated by PDH under aerobic and by PFL under anaerobic conditions. Increasing the activity of PDH may have different benefits for the production of acetyl-CoA derived compounds. On the one hand, coordinated overexpression of the three PDH complex genes *lpdA*, *aceE* and *aceF* even under aerobic conditions can increase the acetyl-CoA supply, which was shown by an 80% enhanced isoamyl acetate production in a *poxBΔptaΔackAΔ* background strain (Dittrich et al., 2005b). An about 20% improved production of the flavanone

naringenin, a drug candidate derived from malonyl-CoA and *p*-coumarate through action of *p*-coumaroyl-CoA ligase, chalcone synthase and chalcone isomerase derived from plants, was seen in an already heavily engineered background strain (Xu et al., 2011). On the other hand, increasing PDH activity under anaerobic conditions to (entirely or partially) replace PFL may also improve redox balancing depending on the downstream pathways used since in contrast to PFL, PDH leads to NADH production. One potential approach was the inactivation of transcription factor FNR that is believed to repress PDH expression during anaerobic growth. While the individual deletion of either *fnr* or *pta* in an *adhEΔldhAΔfrdBCΔ* strain both decreased 1-butanol formation, the combination of both led to a 35% increase. Deletion of *fnr* was however not sufficient to restore 1-butanol production in a *pflB* deletion strain indicating insufficient PDH activity (Atsumi et al., 2008). Also elimination of another regulator involved in PDH repression (PdhR) did not lead to sufficient anaerobic PDH activity (Zhou et al., 2008). The authors therefore instead expressed the *aceEF-lpd* operon under control of the *pflB* promoter and its ribosome binding site, which together with a *pflB* deletion resulted in a 3-fold increase in ethanol formation in a *ldhAΔackAΔ frdBCΔ* background. Another approach to increase anaerobic PDH activity is the implementation of LPD mutants that render the PDH complex less sensitive to inhibition by NADH. These mutations were able to restore anaerobic growth of a *ldhAΔpflBΔ* strain and resulted in an about 15-fold higher ethanol production compared with the unmodified WT strain (Kim et al., 2008).

Many of the strategies described so far include the deletion of *pta-ackA* to inhibit acetate formation. An alternative way to reduce acetate formation and increase acetyl-CoA availability is the activation of acetate assimilation, i.e. actually the overexpression of the reversible Pta/AckA route or, as a second option, overexpression of ACS. Overexpression of ACS was shown to lead to reduced acetate formation and faster glucose consumption (Lin et al., 2006) and both overexpression of Pta/AckA and ACS were able to improve flavanone production with slightly better results using the ACS approach (Leonard et al., 2007).

In certain cases, pathway-specific approaches may be applied to increase acetyl-CoA regeneration. Matsumoto et al. (2013) constructed a new pathway for production of (*R*)-3-hydroxybutyrate through expression of  $\beta$ -ketothiolase and acetyl-CoA reductase from *R. eutropha* and a propionate CoA-transferase *Clostridium propionicum*, which converts 3-hydroxybutyryl-CoA to 3-hydroxybutyrate, while transferring the CoA moiety to acetate thus forming acetyl-CoA.

### 5.3. Increasing CoA levels

In addition to enhancing the efficiency of acetyl-CoA generating pathways, increasing the supply of coenzyme A can also be beneficial for the production of acetyl-CoA derived products. Although overexpression of the major rate-controlling enzyme of CoA biosynthesis, pantothenate kinase, did not result in an increase in CoA or acetyl-CoA levels, its combination with feeding pantothenate to the cells increased CoA levels 10-fold and acetyl-CoA levels 5-fold (Vadali et al., 2004a). This strategy was successfully applied to isoamyl acetate production leading to a 2-fold and 6-fold increase under aerobic and anaerobic cultivation conditions, respectively (Vadali et al., 2004b). Since the influence of this approach on the CoA content was higher than the influence on the acetyl-CoA content, the authors additionally overexpressed PDH (in a *ptaΔackAΔ* strain), increasing isoamyl acetate production by additional 2.5-fold (Vadali et al., 2004b).

### 5.4. Modulation of central carbon metabolic pathways

Strategies to increase acetyl-CoA supply do not only include enzymes close to the acetyl-CoA node, but also manipulation of

enzyme levels further up- and downstream in the central carbon metabolic pathways, i.e. the overexpression of enzymes in glycolysis and the pentose phosphate pathway as well as downregulation of the TCA cycle. Based on a previous study, which had identified triosephosphate isomerase (TpiA) and fructose-bisphosphate aldolase (FbaA) as being up-regulated in a PHB producing *E. coli* strain (Han et al., 2001), Lee et al. (2013) overexpressed *tpiA* and/or *fbaA* in different PHB producing background strains. Overexpression of either gene increased the acetyl-CoA content and PHB production was improved by up to 4-fold. Xu et al. (2011) used a computational modeling approach to increase the flux towards malonyl-CoA. The suggested interventions included overexpression of glyceraldehyde-3-phosphate dehydrogenase and phosphoglycerate kinase, which both resulted in an up to 60% increased flavanone production in already engineered background strains.

Overexpression of the pentose phosphate pathway genes *zwf* encoding glucose 6-phosphate dehydrogenase, *tktA* encoding transketolase and *talA* encoding transaldolase was addressed to improve PHB synthesis and all three approaches led to a higher PHB content (Jung et al., 2004; Lim et al., 2002; Song et al., 2006). It is however not clear whether this increase resulted mainly from an increased acetyl-CoA supply or actually from a higher amount of NADPH provided by an increased flux through this pathway. In fact, the acetyl-CoA content was reduced in the *zwf* overexpressing strain, while it was slightly increased in the *talA* overexpressing strain.

Computational modeling also predicted a positive influence of down-regulation of TCA cycle enzymes on the production of malonyl-CoA derived products. While deletion of some of the respective genes was detrimental for cell growth, deletion of either *fumB* or *fumC* both encoding fumarase or *sucC* encoding the  $\beta$ -subunit of succinyl-CoA synthetase was able to increase flavanone production by up to 30% without having a major impact on cell growth (Xu et al., 2011).

### 5.5. Efficient channeling of acetyl-CoA into downstream pathways

A variety of industrially interesting products are derived from malonyl-CoA. A crucial step is therefore the efficient conversion of acetyl-CoA to malonyl-CoA by ACC. This reaction is also considered the major flux controlling step in fatty acid biosynthesis in *E. coli* (Davis et al., 2000). Overexpression of all four subunits of *E. coli* ACC was shown to be able to increase the production of free fatty acids up to 6-fold (Cao et al., 2014; Davis et al., 2000; Xu et al., 2013). Results are however varying and seem to be especially dependent on the thioesterase used to release the fatty acids from the acyl carrier protein (Lennen et al., 2010; Lu et al., 2008). When implemented for the production of other malonyl-CoA derived compounds, overexpression of endogenous ACC increased e.g. flavanone production by up to 2-fold (Xu et al., 2011). When combined with overexpression of biotin ligase BirA required for cofactor attachment to ACC a 2.2-fold increase in 3-HP production via the malonyl-CoA pathway was achieved (Rathnasingh et al., 2012).

Since *E. coli* ACC is feedback inhibited by acyl-ACP (Davis and Cronan, 2001) and a negative effect on cell viability has been observed upon overexpression (Zha et al., 2009), several studies investigated the effect of expressing heterologous ACC enzymes on product formation. Expression of a 2-subunit ACC from *Corynebacterium glutamicum* resulted in an up to 4-fold increase in flavanone production (Miyahisa et al., 2005), expression of another 2-subunit ACC from *Nocardia farcinica* resulted in a 2.2-fold increase of the flavonoid-glycoside 7-O-methyl aromadendrin (Malla et al., 2012), while expression of a 4-subunit ACC from *Photorhabdus luminescens* increased flavanone production more

than 5-fold (Leonard et al., 2007). The additional expression of biotin ligase from *P. luminescens* or a chimeric *E. coli*/*P. luminescens* biotin ligase led to an additional 90% increase in the last study. Introduction of *C. glutamicum* ACC was also able to enhance production of phloroglucinol, a precursor of pharmaceuticals and explosives produced by a *Pseudomonas fluorescens* polyketide synthase, by 2.2-fold while increasing malonyl-CoA levels by 2.8-fold (Zha et al., 2009).

### 5.6. Construction of synthetic acetyl-CoA generating or consuming pathways

A disadvantage of the generation of acetyl-CoA ( $C_2$ ) via decarboxylation of pyruvate ( $C_3$ ) is the loss of carbon in this reaction, which limits the theoretical yield of acetyl-CoA derived compounds on glucose and other sugars. Mainguet et al. (2013) therefore designed a reversed version of the glyoxylate shunt to convert  $C_4$  TCA cycle intermediates into acetyl-CoA without carbon loss. This was established using a heterologous two-step pathway from malate to glyoxylate via malate thiokinase and malyl-CoA lyase (since the malate synthase reaction is irreversible), the reversible isocitrate lyase and aconitase reactions as well as heterologous ATP-citrate lyase (to revert the citrate synthase reaction). The pathway could theoretically be extended to allow for the production of three molecules of acetyl-CoA per molecule of glucose.

With the same intention, i.e. carbon conservation, also a synthetic non-oxidative glycolytic pathway was constructed. Here, fructose 6-phosphate is split into acetyl-phosphate and erythrose 4-phosphate by a phosphoketolase. Three erythrose 4-phosphate molecules can be converted back to two fructose 6-phosphate molecules via the transketolase and transaldolase of the non-oxidative pentose phosphate pathway (Bograd et al., 2013). Since no reducing equivalents are generated via this route, provision of other sources of reducing power would however be necessary to be able to replace glycolysis with this pathway.

While the above two pathways represent new routes to synthesize acetyl-CoA, an alternative way to channel acetyl-CoA into production of fatty acids and related products of different chain length is the reversal of the  $\beta$ -oxidation pathway (Clomburg et al., 2012; Dellomonaco et al., 2011). This was achieved by deregulation of pathway gene expression in combination with the deletion of native fermentation pathways. An advantage of this route is that acetyl-CoA is used for chain elongation instead of malonyl-CoA used in fatty acid biosynthesis. Since the synthesis of malonyl-CoA consumes ATP, this alternative route for fatty acid biosynthesis is energetically more favorable and therefore has a higher theoretical product yield.

## 6. Perspectives

Recent advances in genetic and metabolic engineering have allowed the design of 'tailor-made' microbial cell factories for the production of various compounds of interest. While such microbial production offers several advantages over traditional, chemical-based production processes, creating an organism capable of producing target compounds at industrially-relevant amounts remains a challenge. This is mainly due to the difficulties associated with engineering the central carbon metabolism of an organism. Through evolution, the central carbon metabolism has developed such that it can efficiently ensure cell growth, and the complex regulation resulting from evolution therefore typically prevents large redirection of carbon fluxes in this part of the metabolism. Several recent efforts have focused on increasing intracellular acetyl-CoA supplies to serve as a precursor for various

fuels and chemicals. These strategies included manipulation of the organisms' native central carbon metabolism, as well as introduction of heterologous routes for acetyl-CoA synthesis. Several of these appear promising, and have resulted in increased production of target compounds.

In addition to manipulation of structural genes directly involved in acetyl-CoA metabolism, recent studies have also shown that regulatory genes could also be potential targets for metabolic engineering. For example, it was shown that Snf1, the yeast ortholog of the mammalian AMP-activated protein kinase, is involved in the regulation of acetyl-CoA homeostasis and its inactivation resulted in a decrease in the pool of acetyl-CoA (Zhang et al., 2013). In addition, increased activation of the transcriptional regulator Mth1p through introduction of an internal deletion allowed the growth of *PDC* deletion strains on glucose without the additional supplementation of a  $C_2$  source (Oud et al., 2012). Since such mutants generally require supplementation of a  $C_2$  source to growth media due to their inability to synthesize cytosolic acetyl-CoA from pyruvate (Flikweert et al., 1999; Flikweert et al., 1996; van Maris et al., 2004), the ability of Mth1p to alleviate this auxotrophy could suggest a potential role for Mth1p in the regulation of cytosolic acetyl-CoA production. Therefore, manipulation of these, as well as additional regulatory genes could serve as another strategy for metabolic engineering.

Several challenges still exist with manipulation of acetyl-CoA metabolism, which includes achieving an appropriate balance between acetyl-CoA production and usage by heterologous pathways, maintaining adequate cellular growth, and achieving industrially relevant production of target compounds. This is particularly true for yeast, where compartmentalization of metabolism makes it inherently less flexible to manipulation, adding another dimension of difficulty in the creation of efficient cell factories. Therefore, additional research efforts must be focused on how to optimally increase metabolic flux towards acetyl-CoA production.

## Acknowledgments

Work in our lab is supported by the Knut and Alice Wallenberg Foundation, European Research Council project INSYSBIO (Grant no. 247013), the Novo Nordisk Foundation, Vetenskapsrådet and Ångpanneföreningens Forskningsstiftelse.

## References

- Akhmanova, A., Voncken, F.G., Hosea, K.M., Harhangi, H., Keltjens, J.T., op den Camp, H.J., Vogels, G.D., Hackstein, J.H., 1999. A hydrogenosome with pyruvate formate-lyase: anaerobic chytrid fungi use an alternative route for pyruvate catabolism. *Mol. Microbiol.* 32, 1103–1114.
- Al-Feel, W., Chirala, S.S., Wakil, S.J., 1992. Cloning of the yeast FAS3 gene and primary structure of yeast acetyl-CoA carboxylase. *Proc. Natl. Acad. Sci. U.S.A.* 89, 4534–4538.
- Alexeeva, S., De Kort, B., Sawers, G., Hellingwerf, K.J., De Mattos, M.J.T., 2000. Effects of limited aeration and of the ArcAB system on intermediary pyruvate catabolism in *Escherichia coli*. *J. Bacteriol.* 182, 4934–4940.
- Aouida, M., Rubio-Texeira, M., Thevelein, J.M., Poulin, R., Ramotar, D., 2013. Agp2, a member of the yeast amino acid permease family, positively regulates polyamine transport at the transcriptional level. *PLoS One* 8, e65717.
- Atsumi, S., Cann, A.F., Connor, M.R., Shen, C.R., Smith, K.M., Brynildsen, M.P., Chou, K.J., Hanai, T., Liao, J.C., 2008. Metabolic engineering of *Escherichia coli* for 1-butanol production. *Metab. Eng.* 10, 305–311.
- Atteia, A., van Lis, R., Gelius-Dietrich, G., Adrait, A., Garin, J., Joyard, J., Rolland, N., Martin, W., 2006. Pyruvate formate-lyase and a novel route of eukaryotic ATP synthesis in *Chlamydomonas* mitochondria. *J. Biol. Chem.* 281, 9909–9918.
- Baek, J.M., Mazumdar, S., Lee, S.W., Jung, M.Y., Lim, J.H., Seo, S.W., Jung, G.Y., Oh, M.K., 2013. Butyrate production in engineered *Escherichia coli* with synthetic scaffolds. *Biotechnol. Bioeng.* 110, 2790–2794.
- Bauer, K.A., Ben-Bassat, A., Dawson, M., de la Puente, V.T., Neway, J.O., 1990. Improved expression of human interleukin-2 in high-cell-density fermentor cultures of *Escherichia coli* K-12 by a phosphotransacetylase mutant. *Appl. Environ. Microbiol.* 56, 1296–1302.

- Beatty, C.M., Browning, D.F., Busby, S.J.W., Wolfe, A.J., 2003. Cyclic AMP receptor protein-dependent activation of the *Escherichia coli* *acsP2* promoter by a synergistic class III mechanism. *J. Bacteriol.* 185, 5148–5157.
- Bogorad, I.W., Lin, T.S., Liao, J.C., 2013. Synthetic non-oxidative glycolysis enables complete carbon conservation. *Nature* 502, 693–697.
- Bowman, S.B., Zaman, Z., Collinson, L.P., Brown, A.J.P., Dawes, I.W., 1992. Positive regulation of the *Lpd1* gene of *Saccharomyces cerevisiae* by the Hap2/Hap3/Hap4 activation system. *Mol. Gen. Genet.* 231, 296–303.
- Boxma, B., Voncken, F., Jannink, S., van Alen, T., Akhmanova, A., van Weelden, S.W., van Hellemont, J.J., Ricard, G., Huynen, M., Telens, A.G., Hackstein, J.H., 2004. The anaerobic chytridiomycete fungus *Piromyces* sp. E2 produces ethanol via pyruvate:formate lyase and an alcohol dehydrogenase. *E. Mol. Microbiol.* 51, 1389–1399.
- Brown, T.D.K., Jones-Mortimer, M.C., Kornberg, H.L., 1977. The enzymic interconversion of acetate and acetyl-coenzyme A in *Escherichia coli*. *J. Gen. Microbiol.* 102, 327–336.
- Buetow, D.E., 2011. *Euglena*. Encyclopedia of Life Sciences (ELS). John Wiley & Sons, Ltd., Chichester.
- Cai, L., Tu, B.P., 2011. Acetyl-CoA drives the transcriptional growth program in yeast. *Cell Cycle* 10, 3045–3046.
- Cao, Y., Liu, W., Xu, X., Zhang, H., Wang, J., Xian, M., 2014. Production of free monounsaturated fatty acids by metabolically engineered *Escherichia coli*. *Biotechnol. Biofuels* 7, 59.
- Caspary, F., Hartig, A., Schuller, H.J., 1997. Constitutive and carbon source-responsive promoter elements are involved in the regulated expression of the *Saccharomyces cerevisiae* malate synthase gene *MLS1*. *Mol. Gen. Genet.* 255, 619–627.
- Centeno-Leija, S., Huerta-Beristain, G., Giles-Gomez, M., Bolívar, F., Gosset, G., Martínez, A., 2014. Improving poly-3-hydroxybutyrate production in *Escherichia coli* by combining the increase in the NADPH pool and acetyl-CoA availability. *Antonie van Leeuwenhoek* 105, 687–696.
- Chang, D.E., Shin, S., Rhee, J.S., Pan, J.G., 1999. Acetate metabolism in a pta mutant of *Escherichia coli* W3110: importance of maintaining acetyl coenzyme A flux for growth and survival. *J. Bacteriol.* 181, 6656–6663.
- Charon, M.H., Volbeda, A., Chabrière, E., Pieulle, L., Fontecilla-Camps, J.C., 1999. Structure and electron transfer mechanism of pyruvate:ferredoxin oxidoreductase. *Curr. Opin. Struct. Biol.* 9, 663–669.
- Chelstowska, A., Butow, R.A., 1995. RTG genes in yeast that function in communication between mitochondria and the nucleus are also required for expression of genes encoding peroxisomal proteins. *J. Biol. Chem.* 270, 18141–18146.
- Chen, Y., Daviet, L., Schalk, M., Siewers, V., Nielsen, J., 2013. Establishing a platform cell factory through engineering of yeast acetyl-CoA metabolism. *Metab. Eng.* 15, 48–54.
- Chen, Y., Siewers, V., Nielsen, J., 2012. Profiling of cytosolic and peroxisomal acetyl-CoA metabolism in *Saccharomyces cerevisiae*. *PLoS One* 7, e42475.
- Clomburg, J.M., Vick, J.E., Blankschien, M.D., Rodriguez-Moya, M., Gonzalez, R., 2012. A synthetic biology approach to engineer a functional reversal of the beta-oxidation cycle. *ACS Synth. Biol.* 1, 541–554.
- Davis, M.S., Cronan Jr., J.E., 2001. Inhibition of *Escherichia coli* acetyl coenzyme A carboxylase by acyl-acyl carrier protein. *J. Bacteriol.* 183, 1499–1503.
- Davis, M.S., Solbiati, J., Cronan Jr., J.E., 2000. Overproduction of acetyl-CoA carboxylase activity increases the rate of fatty acid biosynthesis in *Escherichia coli*. *J. Biol. Chem.* 275, 28593–28598.
- de Jong, B.W., Shi, S., Siewers, V., Nielsen, J., 2014. Improved production of fatty acid ethyl esters in *Saccharomyces cerevisiae* through up-regulation of the ethanol degradation pathway and expression of the heterologous phosphoketolase pathway. *Microb. Cell Fact.* 13, 39.
- de Jong Gubbels, P., van den Berg, M.A., Steensma, H.Y., van Dijken, J.P., Pronk, J.T., 1997. The *Saccharomyces cerevisiae* acetyl-coenzyme A synthetase encoded by the *ACS1* gene, but not the *ACS2*-encoded enzyme, is subject to glucose catabolite inactivation. *FEMS Microbiol. Lett.* 153, 75–81.
- de Kok, A., Hengeveld, A.F., Martin, A., Westphal, A.H., 1998. The pyruvate dehydrogenase multi-enzyme complex from Gram-negative bacteria. *Biochim. Biophys. Acta* 1385, 353–366.
- De Mey, M., De Maeseneire, S., Soetaert, W., Vandamme, E., 2007. Minimizing acetate formation in *E. coli* fermentations. *J. Ind. Microbiol. Biotechnol.* 34, 689–700.
- de Smidt, O., du Preez, J.C., Albertyn, J., 2012. Molecular and physiological aspects of alcohol dehydrogenases in the ethanol metabolism of *Saccharomyces cerevisiae*. *FEMS Yeast Res.* 12, 33–47.
- Dellomonaco, C., Clomburg, J.M., Miller, E.N., Gonzalez, R., 2011. Engineered reversal of the beta-oxidation cycle for the synthesis of fuels and chemicals. *Nature* 476, 355–359.
- Devirgilio, C., Burckert, N., Barth, G., Neuhaus, J.M., Boller, T., Wiemken, A., 1992. Cloning and disruption of a gene required for growth on acetate but not on ethanol: the acetyl-coenzyme A synthetase gene of *Saccharomyces cerevisiae*. *Yeast* 8, 1043–1051.
- Dittrich, C.R., Bennett, G.N., San, K.Y., 2005a. Characterization of the acetate-producing pathways in *Escherichia coli*. *Biotechnol. Prog.* 21, 1062–1067.
- Dittrich, C.R., Vadali, R.V., Bennett, G.N., San, K.Y., 2005b. Redistribution of metabolic fluxes in the central aerobic metabolic pathway of *E. coli* mutant strains with deletion of the ackA-pta and *poxB* pathways for the synthesis of isoamyl acetate. *Biotechnol. Prog.* 21, 627–631.
- Elgersma, Y., Vanroermund, C.W.T., Wanders, R.J.A., Tabak, H.F., 1995. Peroxisomal and mitochondrial carnitine acetyltransferases of *Saccharomyces cerevisiae* are encoded by a single gene. *EMBO J.* 14, 3472–3479.
- Ferreira, J.R., Spirek, M., Liu, Z.C., Butow, R.A., 2005. Interaction between Rtg2p and Mks1p in the regulation of the RTG pathway of *Saccharomyces cerevisiae*. *Gene* 354, 2–8.
- Flikweert, M.T., de Swaaf, M., van Dijken, J.P., Pronk, J.T., 1999. Growth requirements of pyruvate-decarboxylase-negative *Saccharomyces cerevisiae*. *FEMS Microbiol. Lett.* 174, 73–79.
- Flikweert, M.T., Van Der Zanden, L., Janssen, W.M., Steensma, H.Y., Van Dijken, J.P., Pronk, J.T., 1996. Pyruvate decarboxylase: an indispensable enzyme for growth of *Saccharomyces cerevisiae* on glucose. *Yeast* 12, 247–257.
- Galdieri, L., Vancura, A., 2012. Acetyl-CoA carboxylase regulates global histone acetylation. *J. Biol. Chem.* 287, 23865–23876.
- Gey, U., Czupalla, C., Hoflack, B., Rodel, G., Krause-Buchholz, U., 2008. Yeast pyruvate dehydrogenase complex is regulated by a concerted activity of two kinases and two phosphatases. *J. Biol. Chem.* 283, 9759–9767.
- Glozak, M.A., Sengupta, N., Zhang, X., Seto, E., 2005. Acetylation and deacetylation of non-histone proteins. *Gene* 363, 15–23.
- Graybill, E.R., Rouhier, M.F., Kirby, C.E., Hawes, J.W., 2007. Functional comparison of citrate synthase isoforms from *S. cerevisiae*. *Arch. Biochem. Biophys.* 465, 26–37.
- Hahn, D.H., Pan, J., Rhee, J.S., 1994. Characterization and evaluation of a pta (phosphotransacetylase) negative mutant of *Escherichia coli* HB101 as production host of foreign lipase. *Appl. Microbiol. Biot.* 42, 100–107.
- Han, M.J., Yoon, S.S., Lee, S.Y., 2001. Proteome analysis of metabolically engineered *Escherichia coli* producing poly(3-hydroxybutyrate). *J. Bacteriol.* 183, 301–308.
- Hartig, A., Simon, M.M., Schuster, T., Daugherty, J.R., Yoo, H.S., Cooper, T.G., 1992. Differentially regulated malate synthase genes participate in carbon and nitrogen metabolism of *S. cerevisiae*. *Nucleic Acids Res.* 20, 5677–5686.
- Hasslacher, M., Ivessa, A.S., Paltauf, F., Kohlwein, S.D., 1993. Acetyl-CoA carboxylase from yeast is an essential enzyme and is regulated by factors that control phospholipid metabolism. *J. Biol. Chem.* 268, 10946–10952.
- Hemschemeier, A., Jacobs, J., Happe, T., 2008. Biochemical and physiological characterization of the pyruvate formate-lyase Pfl1 of *Chlamydomonas reinhardtii*, a typically bacterial enzyme in a eukaryotic alga. *Eukaryot. Cell* 7, 518–526.
- Hiesinger, M., Wagner, C., Schuller, H.J., 1997. The acetyl-CoA synthetase gene *ACS2* of the yeast *Saccharomyces cerevisiae* is coregulated with structural genes of fatty acid biosynthesis by the transcriptional activators *Ino2p* and *Ino4p*. *FEBS Lett.* 415, 16–20.
- Himo, F., Eriksson, L.A., 1998. Catalytic mechanism of pyruvate formate-lyase (PFL). A theoretical study. *J. Am. Chem. Soc.* 120, 11449–11455.
- Hiser, L., Basson, M.E., Rine, J., 1994. ERG10 from *Saccharomyces cerevisiae* encodes acetoacetyl-CoA thiolase. *J. Biol. Chem.* 269, 31383–31389.
- Hofbauer, H.F., Schopf, F.H., Schleifer, H., Knittel, O.L., Pieber, B., Rechberger, G.N., Wolinski, H., Gaspar, M.L., Kappe, C.O., Stadlmann, J., Mechtler, K., Zenz, A., Lohner, K., Tehlivets, O., Henry, S.A., Kohlwein, S.D., 2014. Regulation of gene expression through a transcriptional repressor that senses acyl-chain length in membrane phospholipids. *Dev. Cell* 29, 729–739.
- Hoja, U., Marthol, S., Hofmann, J., Stegner, S., Schulz, R., Meier, S., Greiner, E., Schweizer, E., 2004. HFA1 encoding an organelle-specific acetyl-CoA carboxylase controls mitochondrial fatty acid synthesis in *Saccharomyces cerevisiae*. *J. Biol. Chem.* 279, 21779–21786.
- Hug, L.A., Stechmann, A., Roger, A.J., 2010. Phylogenetic distributions and histories of proteins involved in anaerobic pyruvate metabolism in eukaryotes. *Mol. Biol. Evol.* 27, 311–324.
- Huh, W.K., Falvo, J.V., Gerke, L.C., Carroll, A.S., Howson, R.W., Weissman, J.S., O'Shea, E.K., 2003. Global analysis of protein localization in budding yeast. *Nature* 425, 686–691.
- Ingram-Smith, C., Martin, S.R., Smith, K.S., 2006. Acetate kinase: not just a bacterial enzyme. *Trends Microbiol.* 14, 249–253.
- Inui, H., Miyatake, K., Nakano, Y., Kitaoka, S., 1984. Fatty acid synthesis in mitochondria of *Euglena gracilis*. *Eur. J. Biochem.* 142, 121–126.
- Iram, S.H., Cronan, J.E., 2006. The beta-oxidation systems of *Escherichia coli* and *Salmonella enterica* are not functionally equivalent. *J. Bacteriol.* 188, 599–608.
- Jenkins, L.S., Nunn, W.D., 1987. Genetic and molecular characterization of the genes involved in short-chain fatty acid degradation in *Escherichia coli*: the ato system. *J. Bacteriol.* 169, 42–52.
- Jia, Y.K., Becam, A.M., Herbert, C.J., 1997a. The CIT3 gene of *Saccharomyces cerevisiae* encodes a second mitochondrial isoform of citrate synthase. *Mol. Microbiol.* 24, 53–59.
- Jia, Y.K., Rothermel, B., Thornton, J., Butow, R.A., 1997b. A basic helix-loop-helix-leucine zipper transcription complex in yeast functions in a signaling pathway from mitochondria to the nucleus. *Mol. Cell. Biol.* 17, 1110–1117.
- Jian, J., Zhang, S.Q., Shi, Z.Y., Wang, W., Chen, G.Q., Wu, Q., 2010. Production of polyhydroxyalkanoates by *Escherichia coli* mutants with defected mixed acid fermentation pathways. *Appl. Microbiol. Biot.* 87, 2247–2256.
- Jones, J.D., O'Connor, C.D., 2011. Protein acetylation in prokaryotes. *Proteomics* 11, 3012–3022.
- Jung, Y.M., Lee, J.N., Shin, H.D., Lee, Y.H., 2004. Role of *tktA* gene in pentose phosphate pathway on odd-ball biosynthesis of poly-beta-hydroxybutyrate in transformant *Escherichia coli* harboring *phbCAB* operon. *J. Biosci. Bioeng.* 98, 224–227.
- Kern, A., Tilley, E., Hunter, I.S., Legija, M., Glieder, A., 2007. Engineering primary metabolic pathways of industrial micro-organisms. *J. Biotechnol.* 129, 6–29.
- Kim, J.Y., Cha, H.J., 2003. Down-regulation of acetate pathway through antisense strategy in *Escherichia coli*: improved foreign protein production. *Biotechnol. Bioeng.* 83, 841–853.

- Kim, K.S., Rosenkrantz, M.S., Guarente, L., 1986. *Saccharomyces cerevisiae* contains two functional citrate synthase genes. *Mol. Cell. Biol.* 6, 1936–1942.
- Kim, Y., Ingram, L.O., Shamugam, K.T., 2008. Dihydrolipoamide dehydrogenase mutation alters the NADH sensitivity of pyruvate dehydrogenase complex of *Escherichia coli* K-12. *J. Bacteriol.* 190, 3851–3858.
- Kispal, G., Evans, C.T., Malloy, C., Srere, P.A., 1989. Metabolic studies on citrate synthase mutants of yeast. A change in phenotype following transformation with an inactive enzyme. *J. Biol. Chem.* 264, 11204–11210.
- Kispal, G., Rosenkrantz, M., Guarente, L., Srere, P.A., 1988. Metabolic changes in *Saccharomyces cerevisiae* strains lacking citrate synthases. *J. Biol. Chem.* 263, 11145–11149.
- Klein, H.P., Jahnke, L., 1971. Variations in the localization of acetyl-coenzyme A synthetase in aerobic yeast cells. *J. Bacteriol.* 106, 596–602.
- Kletzin, A., Adams, M.W.W., 1996. Molecular and phylogenetic characterization of pyruvate and 2-ketoisovalerate ferredoxin oxidoreductases from *Pyrococcus furiosus* and pyruvate ferredoxin oxidoreductase from *Thermotoga maritima*. *J. Bacteriol.* 178, 248–257.
- Kocharin, K., Chen, Y., Siewers, V., Nielsen, J., 2012. Engineering of acetyl-CoA metabolism for the improved production of polyhydroxybutyrate in *Saccharomyces cerevisiae*. *AMB Express* 2, 52.
- Kocharin, K., Siewers, V., Nielsen, J., 2013. Improved polyhydroxybutyrate production by *Saccharomyces cerevisiae* through the use of the phosphoketolase pathway. *Biotechnol. Bioeng.* 110, 2216–2224.
- Kozak, B.U., van Rossum, H.M., Benjamin, K.R., Wu, L., Daran, J.M., Pronk, J.T., van Maris, A.J., 2014a. Replacement of the *Saccharomyces cerevisiae* acetyl-CoA synthetases by alternative pathways for cytosolic acetyl-CoA synthesis. *Metab. Eng.* 21, 46–59.
- Kozak, B.U., van Rossum, H.M., Luttik, M.A., Akeroyd, M., Benjamin, K.R., Wu, L., de Vries, S., Daran, J.M., Pronk, J.T., van Maris, A.J., 2014b. Engineering acetyl coenzyme A supply: functional expression of a bacterial pyruvate dehydrogenase complex in the cytosol of *Saccharomyces cerevisiae*. *mBio* 5, e01696–14 (pii).
- Kratzer, S., Schuller, H.J., 1995. Carbon source-dependent regulation of the acetyl-coenzyme A synthetase-encoding gene ACS1 from *Saccharomyces cerevisiae*. *Gene* 161, 75–79.
- Kratzer, S., Schuller, H.J., 1997. Transcriptional control of the yeast acetyl-CoA synthetase gene, ACS1, by the positive regulators CAT8 and ADR1 and the pleiotropic repressor UME6. *Mol. Microbiol.* 26, 631–641.
- Krivoruchko, A., Serrano-Amatriain, C., Chen, Y., Siewers, V., Nielsen, J., 2013. Improving biobutanol production in engineered *Saccharomyces cerevisiae* by manipulation of acetyl-CoA metabolism. *J. Ind. Microbiol. Biotechnol.* 40, 1051–1056.
- Kumar, A., Agarwal, S., Heyman, J.A., Matson, S., Heidtman, M., Piccirillo, S., Umansky, L., Drawid, A., Jansen, R., Liu, Y., Cheung, K.H., Miller, P., Gerstein, M., Roeder, G.S., Snyder, M., 2002. Subcellular localization of the yeast proteome. *Genes Dev.* 16, 707–719.
- Kumari, S., Tishel, R., Eisenbach, M., Wolfe, A.J., 1995. Cloning, characterization, and functional expression of acs, the gene which encodes acetyl coenzyme A synthetase in *Escherichia coli*. *J. Bacteriol.* 177, 2878–2886.
- Kunze, M., Kragler, F., Binder, M., Hartig, A., Gurvitz, A., 2002. Targeting of malate synthase I to the peroxisomes of *Saccharomyces cerevisiae* cells depends on growth on oleic acid medium. *Eur. J. Biochem.* 269, 915–922.
- Kurdistani, S.K., Tavazoie, S., Grunstein, M., 2004. Mapping global histone acetylation patterns to gene expression. *Cell* 117, 721–733.
- Lee, J.G., Cho, S.P., Lee, H.S., Lee, C.H., Bae, K.S., Maeng, P.J., 2000. Identification of a cryptic N-terminal signal in *Saccharomyces cerevisiae* peroxisomal citrate synthase that functions in both peroxisomal and mitochondrial targeting. *J. Biochem.* 128, 1059–1072.
- Lee, S.H., Kang, K.H., Kim, E.Y., Chae, T.U., Oh, Y.H., Hong, S.H., Song, B.K., Jegals, J., Park, S.J., Lee, S.Y., 2013. Metabolic engineering of *Escherichia coli* for enhanced biosynthesis of poly(3-hydroxybutyrate) based on proteome analysis. *Biotechnol. Lett.* 35, 1631–1637.
- Lennen, R.M., Braden, D.J., West, R.A., Dumesic, J.A., Pfleger, B.F., 2010. A process for microbial hydrocarbon synthesis: overproduction of fatty acids in *Escherichia coli* and catalytic conversion to alkanes. *Biotechnol. Bioeng.* 106, 193–202.
- Leonard, E., Lim, K.H., Saw, P.N., Koffas, M.A., 2007. Engineering central metabolic pathways for high-level flavonoid production in *Escherichia coli*. *Appl. Environ. Microbiol.* 73, 3877–3886.
- Lewin, A.S., Hines, V., Small, G.M., 1990. Citrate synthase encoded by the CIT2 gene of *Saccharomyces cerevisiae* is peroxisomal. *Mol. Cell. Biol.* 10, 1399–1405.
- Lian, J., Si, T., Nair, N.U., Zhao, H., 2014. Design and construction of acetyl-CoA overproducing *Saccharomyces cerevisiae* strains. *Metab. Eng.* 24, 139–149.
- Liao, X.S., Small, W.C., Srere, P.A., Butow, R.A., 1991. Intramitochondrial functions regulate nonmitochondrial citrate synthase (CIT2) expression in *Saccharomyces cerevisiae*. *Mol. Cell. Biol.* 11, 38–46.
- Lim, S.J., Jung, Y.M., Shin, H.D., Lee, Y.H., 2002. Amplification of the NADPH-related genes zwf and gnd for the oddball biosynthesis of PHB in an *E. coli* transformant harboring a cloned phbCAB operon. *J. Biosci. Bioeng.* 93, 543–549.
- Lin, F., Chen, Y., Levine, R., Lee, K., Yuan, Y., Lin, X.N., 2013. Improving fatty acid availability for bio-hydrocarbon production in *Escherichia coli* by metabolic engineering. *PLoS One* 8, e78595.
- Lin, H., Castro, N.M., Bennett, G.N., San, K.Y., 2006. Acetyl-CoA synthetase overexpression in *Escherichia coli* demonstrates more efficient acetate assimilation and lower acetate accumulation: a potential tool in metabolic engineering. *Appl. Microbiol. Biot.* 71, 870–874.
- Liu, Z.C., Butow, R.A., 1999. A transcriptional switch in the expression of yeast tricarboxylic acid cycle genes in response to a reduction or loss of respiratory function. *Mol. Cell. Biol.* 19, 6720–6728.
- Lu, X., Vora, H., Khosla, C., 2008. Overproduction of free fatty acids in *E. coli*: implications for biodiesel production. *Metab. Eng.* 10, 333–339.
- Luli, G.W., Strohl, W.R., 1990. Comparison of growth, acetate production, and acetate inhibition of *Escherichia coli* strains in batch and fed-batch fermentations. *Appl. Environ. Microbiol.* 56, 1004–1011.
- Mainguet, S.E., Gronenberg, L.S., Wong, S.S., Liao, J.C., 2013. A reverse glyoxylate shunt to build a non-native route from C<sub>4</sub> to C<sub>2</sub> in *Escherichia coli*. *Metab. Eng.* 19, 116–127.
- Malla, S., Koffas, M.A., Kazlauskas, R.J., Kim, B.G., 2012. Production of 7-O-methyl aromadendrin, a medicinally valuable flavonoid, in *Escherichia coli*. *Appl. Environ. Microbiol.* 78, 684–694.
- Matsuda, F., Furusawa, C., Kondo, T., Ishii, J., Shimizu, H., Kondo, A., 2011. Engineering strategy of yeast metabolism for higher alcohol production. *Microb. Cell Fact.* 10, 70.
- Matsumoto, K., Okei, T., Honma, I., Ooi, T., Aoki, H., Taguchi, S., 2013. Efficient (R)-3-hydroxybutyrate production using acetyl CoA-regenerating pathway catalyzed by coenzyme A transferase. *Appl. Microbiol. Biot.* 97, 205–210.
- McCleary, W.R., Stock, J.B., Ninja, A.J., 1993. Is acetyl phosphate a global signal in *Escherichia coli*? *J. Bacteriol.* 175, 2793–2798.
- Miyahisa, I., Kaneko, M., Funa, N., Kawasaki, H., Kojima, H., Ohnishi, Y., Horinouchi, S., 2005. Efficient production of (2S)-flavanones by *Escherichia coli* containing an artificial biosynthetic gene cluster. *Appl. Microbiol. Bio.* 68, 498–504.
- Miyake, M., Miyamoto, C., Schnackenberg, J., Kurane, R., Asada, Y., 2000. Phosphotransacetylase as a key factor in biological production of polyhydroxybutyrate. *Appl. Biochem. Biotechnol.* 84–86, 1039–1044.
- Niederacher, D., Schuller, H.J., Grzeszita, D., Gutlich, H., Hauser, H.P., Wagner, T., Entian, K.D., 1992. Identification of UAS elements and binding proteins necessary for derepression of *Saccharomyces cerevisiae* fructose-1,6-bisphosphatase. *Curr. Genet.* 22, 363–370.
- Nielsen, J., 2014. Synthetic biology for engineering acetyl coenzyme a metabolism in yeast. *mBio* 5, e02153–14 (pii:).
- Oud, B., Flores, C.L., Gancedo, C., Zhang, X., Trueheart, J., Daran, J.M., Pronk, J.T., van Maris, A.J., 2012. An internal deletion in MTH1 enables growth on glucose of pyruvate-decarboxylase negative, non-fermentative *Saccharomyces cerevisiae*. *Microb. Cell Fact.* 11, 131.
- Overath, P., Pauli, G., Schairer, H.U., 1969. Fatty acid degradation in *Escherichia coli*. An inducible acyl-CoA synthetase, the mapping of old-mutations, and the isolation of regulatory mutants. *Eur. J. Biochem.* 7, 559–574.
- Palmieri, L., Lasorsa, F.M., Iacobazzi, V., Runswick, M.J., Palmieri, F., Walker, J.E., 1999. Identification of the mitochondrial carnitine carrier in *Saccharomyces cerevisiae*. *FEBS Lett.* 462, 472–476.
- Papini, M., Nookaew, I., Siewers, V., Nielsen, J., 2012. Physiological characterization of recombinant *Saccharomyces cerevisiae* expressing the *Aspergillus nidulans* phosphoketolase pathway: validation of activity through <sup>13</sup>C-based metabolic flux analysis. *Appl. Microbiol. Biot.* 95, 1001–1010.
- Park, J., Rodriguez-Moya, M., Li, M., Pichersky, E., San, K.Y., Gonzalez, R., 2012. Synthesis of methyl ketones by metabolically engineered *Escherichia coli*. *J. Ind. Microbiol. Biotechnol.* 39, 1703–1712.
- Park, S.J., McCabe, J., Turna, J., Gunsalus, R.P., 1994. Regulation of the citrate synthase (gltA) gene of *Escherichia coli* in response to anaerobiosis and carbon supply: role of the arcA gene product. *J. Bacteriol.* 176, 5086–5092.
- Phue, J.N., Shiloach, J., 2004. Transcription levels of key metabolic genes are the cause for different glucose utilization pathways in *E. coli* B (BL21) and *E. coli* K (JM109). *J. Biotechnol.* 109, 21–30.
- Pieulle, L., Guigliarelli, B., Asso, M., Dole, F., Bernadac, A., Hatchikian, E.C., 1995. Isolation and characterization of the pyruvate-ferredoxin oxidoreductase from the sulfate-reducing bacterium *Desulfovibrio africanus*. *Biochim. Biophys. Acta* 1250, 49–59.
- Pawlowski, J., Sahlman, L., Shingler, V., 1993. Purification and properties of the physically associated meta-cleavage pathway enzymes 4-hydroxy-2-ketovalerate aldolase and aldehyde dehydrogenase (acylating) from *Pseudomonas* sp. strain CF600. *J. Bacteriol.* 175, 377–385.
- Proft, M., Grzeszita, D., Entian, K.D., 1995. Identification and characterization of regulatory elements in the phosphoenolpyruvate carboxykinase gene PCK1 of *Saccharomyces cerevisiae*. *Mol. Gen. Genet.* 246, 367–373.
- Pronk, J.T., Steensma, H.Y., van Dijken, J.P., 1996. Pyruvate metabolism in *Saccharomyces cerevisiae*. *Yeast* 12, 1607–1633.
- Quail, M.A., Haydon, D.J., Guest, J.R., 1994. The pdhr-aceEF-lpd operon of *Escherichia coli* expresses the pyruvate dehydrogenase complex. *Mol. Microbiol.* 12, 95–104.
- Ragsdale, S.W., 2003. Pyruvate ferredoxin oxidoreductase and its radical intermediate. *Chem. Rev.* 103, 2333–2346.
- Rathnasingh, C., Raj, S.M., Lee, Y., Catherine, C., Ashok, S., Park, S., 2012. Production of 3-hydroxypropionic acid via malonyl-CoA pathway using recombinant *Escherichia coli* strains. *J. Biotechnol.* 157, 633–640.
- Ratledge, C., 2002. Regulation of lipid accumulation in oleaginous micro-organisms. *Biochem. Soc. Trans.* 30, 1047–1050.
- Ratledge, C., Holdsworth, J.E., 1985. Properties of a pentulose-5-phosphate phosphoketolase from yeasts grown on xylose. *Appl. Microbiol. Biot.* 22, 217–221.
- Reeves, R.E., Warren, L.G., Susskind, B., Lo, H.S., 1977. An energy conserving pyruvate to acetate pathway in *Entamoeba histolytica*. Pyruvate synthase and a new acetate thiokinase. *J. Biol. Chem.* 252, 726–731.

- Rock, C.O., Jackowski, S., 2002. Forty years of bacterial fatty acid synthesis. *Biochem. Biophys. Res. Commun.* 292, 1155–1166.
- Rosenkrantz, M., Kell, C.S., Pennell, E.A., Devenish, L.J., 1994a. The HAP2,3,4 transcriptional activator is required for derepression of the yeast citrate synthase gene, CIT1. *Mol. Microbiol.* 13, 119–131.
- Rosenkrantz, M., Kell, C.S., Pennell, E.A., Webster, M., Devenish, L.J., 1994b. Distinct upstream activation regions for glucose-repressed and derepressed expression of the yeast citrate synthase gene CIT1. *Curr. Genet.* 25, 185–195.
- Rotte, C., Stejskal, F., Zhu, G., Keithly, J.S., Martin, W., 2001. Pyruvate:NADP<sup>+</sup> oxidoreductase from the mitochondrion of *Euglena gracilis* and from the apicomplexan *Cryptosporidium parvum*: a biochemical relic linking pyruvate metabolism in mitochondrial and amitochondrial protists. *Mol. Biol. Evol.* 18, 710–720.
- Rudolph, F.B., Purich, D.L., Fromm, H.J., 1968. Coenzyme A-linked aldehyde dehydrogenase from *Escherichia coli*. I. Partial purification, properties, and kinetic studies of the enzyme. *J. Biol. Chem.* 243, 5539–5545.
- Satyanarayana, T., Klein, H.P., 1973. Studies on acetyl-coenzyme A synthetase of yeast: inhibition by long-chain acyl-coenzyme A esters. *J. Bacteriol.* 115, 600–606.
- Satyanarayana, T., Klein, H.P., 1976. Studies on the "aerobic" acetyl-coenzyme A synthetase of *Saccharomyces cerevisiae*: purification, crystallization, and physical properties of the enzyme. *Arch. Biochem. Biophys.* 174, 480–490.
- Satyanarayana, T., Mandel, A.D., Klein, H.P., 1974. Evidence for two immunologically distinct acyl-co-enzyme A synthetase in yeast. *Biochim. Biophys. Acta* 341, 396–401.
- Sawers, G., Watson, G., 1998. A glycol radical solution: oxygen-dependent interconversion of pyruvate formate-lyase. *Mol. Microbiol.* 29, 945–954.
- Schäfer, T., Schönheit, P., 1991. Pyruvate metabolism of the hyperthermophilic archaeabacterium *Pyrococcus furiosus*—acetate formation from acetyl-CoA and ATP synthesis are catalyzed by an acetyl-CoA synthetase (ADP forming). *Arch. Microbiol.* 155, 366–377.
- Schmalix, W., Bandlow, W., 1993. The ethanol-inducible YAT1 gene from yeast encodes a presumptive mitochondrial outer carnitine acetyltransferase. *J. Biol. Chem.* 268, 27428–27439.
- Scholer, A., Schuller, H.J., 1994. A carbon source-responsive promoter element necessary for activation of the isocitrate lyase gene ICL1 is common to genes of the gluconeogenic pathway in the yeast *Saccharomyces cerevisiae*. *Mol. Cell. Biol.* 14, 3613–3622.
- Schuller, H.J., Hahn, A., Troster, F., Schutz, A., Schweizer, E., 1992. Coordinate genetic control of yeast fatty acid synthase genes FAS1 and FAS2 by an upstream activation site common to genes involved in membrane lipid biosynthesis. *EMBO J.* 11, 107–114.
- Shi, L., Tu, B.P., 2013. Acetyl-CoA induces transcription of the key G1 cyclin CLN3 to promote entry into the cell division cycle in *Saccharomyces cerevisiae*. *Proc. Natl. Acad. Sci. U.S.A.* 110, 7318–7323.
- Shiba, Y., Paradise, E.M., Kirby, J., Ro, D.K., Keasling, J.D., 2007. Engineering of the pyruvate dehydrogenase bypass in *Saccharomyces cerevisiae* for high-level production of isoprenoids. *Metab. Eng.* 9, 160–168.
- Singh, K.K., Small, G.M., Lewin, A.S., 1992. Alternative topogenic signals in peroxisomal citrate synthase of *Saccharomyces cerevisiae*. *Mol. Cell. Biol.* 12, 5593–5599.
- Smith, L.T., Kaplan, N.O., 1980. Purification, properties, and kinetic mechanism of coenzyme A-linked aldehyde dehydrogenase from *Clostridium kluyveri*. *Arch. Biochem. Biophys.* 203, 663–675.
- Snoep, J.L., de Graaf, M.R., Westphal, A.H., de Kok, A., Teixeira de Mattos, M.J., Neijssel, O.M., 1993. Differences in sensitivity to NADH of purified pyruvate dehydrogenase complexes of *Enterococcus faecalis*, *Lactococcus lactis*, *Azotobacter vinelandii* and *Escherichia coli*: implications for their activity in vivo. *FEMS Microbiol. Lett.* 114, 279–283.
- Song, B.G., Kim, T.K., Jung, Y.M., Lee, Y.H., 2006. Modulation of talA gene in pentose phosphate pathway for overproduction of poly-beta-hydroxybutyrate in transformant *Escherichia coli* harboring phbCAB operon. *J. Biosci. Bioeng.* 102, 237–240.
- Soppa, J., 2010. Protein acetylation in archaea, bacteria, and eukaryotes. *Archaea* 2010, 820681 (pii:).
- Spange, S., Wagner, T., Heinzel, T., Kramer, O.H., 2009. Acetylation of non-histone proteins modulates cellular signalling at multiple levels. *Int. J. Biochem. Cell B* 41, 185–198.
- Stairs, C.W., Roger, A.J., Hampl, V., 2011. Eukaryotic pyruvate formate lyase and its activating enzyme were acquired laterally from a Firmicute. *Mol. Biol. Evol.* 28, 2087–2099.
- Starai, V.J., Celic, I., Cole, R.N., Boeke, J.D., Escalante-Semerena, J.C., 2002. Sir2-dependent activation of acetyl-CoA synthetase by deacetylation of active lysine. *Science* 298, 2390–2392.
- Starai, V.J., Escalante-Semerena, J.C., 2004. Acetyl-coenzyme A synthetase (AMP forming). *Cell Mol. Life Sci.* 61, 2020–2030.
- Starai, V.J., Gardner, J.G., Escalante-Semerena, J.C., 2005. Residue Leu-641 of acetyl-CoA synthetase is critical for the acetylation of residue Lys-609 by the protein acetyltransferase enzyme of *Salmonella enterica*. *J. Biol. Chem.* 280, 26200–26205.
- Starai, V.J., Takahashi, H., Boeke, J.D., Escalante-Semerena, J.C., 2003. Short-chain fatty acid activation by acyl-coenzyme A synthetases requires Sir2 protein function in *Salmonella enterica* and *Saccharomyces cerevisiae*. *Genetics* 163, 545–555.
- Starai, V.J., Takahashi, H., Boeke, J.D., Escalante-Semerena, J.C., 2004. A link between transcription and intermediary metabolism: a role for Sir2 in the control of acetyl-coenzyme A synthetase. *Curr. Opin. Microbiol.* 7, 115–119.
- Steinbuchel, A., Hustede, E., Liebergesell, M., Pieper, U., Timm, A., Valentini, H., 1993. Molecular basis for biosynthesis and accumulation of polyhydroxylalkanoic acids in bacteria. *FEMS Microbiol. Rev.* 10, 347–350.
- Strijbis, K., Distel, B., 2010. Intracellular acetyl unit transport in fungal carbon metabolism. *Eukaryot. Cell* 9, 1809–1815.
- Suissa, M., Suda, K., Schatz, G., 1984. Isolation of the nuclear yeast genes for citrate synthase and fifteen other mitochondrial proteins by a new screening method. *EMBO J.* 3, 1773–1781.
- Swiegers, J.H., Dippenaar, N., Pretorius, I.S., Bauer, F.F., 2001. Carnitine-dependent metabolic activities in *Saccharomyces cerevisiae*: three carnitine acetyltransferases are essential in a carnitine-dependent strain. *Yeast* 18, 585–595.
- Takahashi, H., McCaffery, J.M., Irizarry, R.A., Boeke, J.D., 2006. Nucleocytosolic acetyl-coenzyme A synthetase is required for histone acetylation and global transcription. *Mol. Cell* 23, 207–217.
- Tang, X., Feng, H., Chen, W.N., 2013. Metabolic engineering for enhanced fatty acids synthesis in *Saccharomyces cerevisiae*. *Metab. Eng.* 16, 95–102.
- Tehlivets, O., Scheuringer, K., Kohlwein, S.D., 2007. Fatty acid synthesis and elongation in yeast. *Biochim. Biophys. Acta* 1771, 255–270.
- Thomas, G.H., Connerton, I.F., Fincham, J.R., 1988. Molecular cloning, identification and transcriptional analysis of genes involved in acetate utilization in *Neurospora crassa*. *Mol. Microbiol.* 2, 599–606.
- Vadali, R.V., Bennett, G.N., San, K.Y., 2004a. Applicability of CoA/acetyl-CoA manipulation system to enhance isoamyl acetate production in *Escherichia coli*. *Metab. Eng.* 6, 294–299.
- Vadali, R.V., Bennett, G.N., San, K.Y., 2004b. Enhanced isoamyl acetate production upon manipulation of the acetyl-CoA node in *Escherichia coli*. *Biotechnol. Prog.* 20, 692–697.
- Vadali, R.V., Horton, C.E., Rudolph, F.B., Bennett, G.N., San, K.Y., 2004c. Production of isoamyl acetate in ackA-pta and/or ldh mutants of *Escherichia coli* with overexpression of yeast ATF2. *Appl. Microbiol. Biot.* 63, 698–704.
- van den Berg, M.A., de Jong-Gubbel, P., Kortland, C.J., van Dijken, J.P., Pronk, J.T., Steensma, H.Y., 1996. The two acetyl-coenzyme A synthetases of *Saccharomyces cerevisiae* differ with respect to kinetic properties and transcriptional regulation. *J. Biol. Chem.* 271, 28953–28959.
- van den Berg, M.A., Steensma, H.Y., 1995. ACS2, a *Saccharomyces cerevisiae* gene encoding acetyl-coenzyme A synthetase, essential for growth on glucose. *Eur. J. Biochem.* 231, 704–713.
- van Maris, A.J., Geertman, J.M., Vermeulen, A., Groothuizen, M.K., Winkler, A.A., Piper, M.D., van Dijken, J.P., Pronk, J.T., 2004. Directed evolution of pyruvate decarboxylase-negative *Saccharomyces cerevisiae*, yielding a C<sub>2</sub>-independent, glucose-tolerant, and pyruvate-hyperproducing yeast. *Appl. Environ. Microbiol.* 70, 159–166.
- Velot, C., Lebreton, S., Morgunov, I., Usher, K.C., Srere, P.A., 1999. Metabolic effects of mislocalized mitochondrial and peroxisomal citrate synthases in yeast *Saccharomyces cerevisiae*. *Biochemistry* 38, 16195–16204.
- Vorapreeda, T., Thammarongtham, C., Cheevadhanarak, S., Laoteng, K., 2012. Alternative routes of acetyl-CoA synthesis identified by comparative genomic analysis: involvement in the lipid production of oleaginous yeast and fungi. *Microbiology* 158, 217–228.
- Wagner, A.F., Frey, M., Neugebauer, F.A., Schafer, W., Knappe, J., 1992. The free radical in pyruvate formate-lyase is located on glycine-734. *Proc. Natl. Acad. Sci. U.S.A.* 89, 996–1000.
- Wagner, A.F.V., Schultz, S., Bomke, J., Pils, T., Lehmann, W.D., Knappe, J., 2001. YfiD of *Escherichia coli* and Y061 of bacteriophage T4 as autonomous glycyl radical cofactors reconstituting the catalytic center of oxygen-fragmented pyruvate formate-lyase. *Biochem. Biophys. Res. Commun.* 285, 456–462.
- Weeks, G., Shapiro, M., Burns, R.O., Wakil, S.J., 1969. Control of fatty acid metabolism. I. Induction of the enzymes of fatty acid oxidation in *Escherichia coli*. *J. Bacteriol.* 97, 827–836.
- Witters, L.A., Watts, T.D., 1990. Yeast acetyl-CoA carboxylase: in vitro phosphorylation by mammalian and yeast protein kinases. *Biochem. Biophys. Res. Commun.* 169, 369–376.
- Wolfe, A.J., 2005. The acetate switch. *Microbiol. Mol. Biol. Rev.* 69, 12–50.
- Xu, P., Gu, Q., Wang, W., Wong, L., Bower, A.G., Collins, C.H., Koffas, M.A., 2013. Modular optimization of multi-gene pathways for fatty acids production in *E. coli*. *Nat. Commun.* 4, 1409.
- Xu, P., Ranganathan, S., Fowler, Z.L., Maranas, C.D., Koffas, M.A., 2011. Genome-scale metabolic network modeling results in minimal interventions that cooperatively force carbon flux towards malonyl-CoA. *Metab. Eng.* 13, 578–587.
- Yang, X.J., Seto, E., 2008. Lysine acetylation: codified crosstalk with other post-translational modifications. *Mol. Cell* 31, 449–461.
- Yang, Y.T., San, K.Y., Bennett, G.N., 1999. Redistribution of metabolic fluxes in *Escherichia coli* with fermentative lactate dehydrogenase overexpression and deletion. *Metab. Eng.* 1, 141–152.
- Yoo, H.S., Genbauffe, F.S., Cooper, T.G., 1985. Identification of the ureidoglycolate hydrolase gene in the DAL gene cluster of *Saccharomyces cerevisiae*. *Mol. Cell. Biol.* 5, 2279–2288.
- Zaidi, N., Swinnen, J.V., Smans, K., 2012. ATP-citrate lyase: a key player in cancer metabolism. *Cancer Res.* 72, 3709–3714.
- Zha, W., Rubin-Pitel, S.B., Shao, Z., Zhao, H., 2009. Improving cellular malonyl-CoA level in *Escherichia coli* via metabolic engineering. *Metab. Eng.* 11, 192–198.
- Zhang, M., Galdieri, L., Vancura, A., 2013. The yeast AMPK homolog SNF1 regulates acetyl coenzyme A homeostasis and histone acetylation. *Mol. Cell. Biol.* 33, 4701–4717.
- Zhang, Q., Iwasaki, T., Wakagi, T., Oshima, T., 1996. 2-oxoacid:ferredoxin oxidoreductase from the thermoacidophilic archaeon, *Sulfolobus sp.* strain. *J. Biochem.* 120, 587–599.
- Zhou, S., Iverson, A.G., Grayburn, W.S., 2008. Engineering a native homoethanol pathway in *Escherichia coli* B for ethanol production. *Biotechnol. Lett.* 30, 335–342.
- Zhu, H., Gonzalez, R., Bobik, T.A., 2011. Coproduction of acetaldehyde and hydrogen during glucose fermentation by *Escherichia coli*. *Appl. Environ. Microbiol.* 77, 6441–6450.